

**Population genetic and morphological
studies in a hybrid zone between two
subspecies of *Tephroseris helenitis* (L.) B.
NORD. (Asteraceae) at the northern fringe
of the Alps**

Masterarbeit

Zur Erlangung des Mastergrades
an der Naturwissenschaftlichen Fakultät
der Paris-Lodron-Universität Salzburg

eingereicht von
Georg Pflugbeil

Gutachter:
Univ.-Prof. Dr.rer.nat. Hans-Peter Comes

Fachbereich:
Organismische Biologie

Salzburg, November 2012

“Is it all ready? Right. Come on then. Back to creation. We mustn't waste any more time. They'll think I've lost control again and put it all down to evolution.”

Supreme Being in “Time Bandits” (1981)



Contents

Abstract.....	ix
Zusammenfassung	xi
1. Introduction	1
1.1. General introduction.....	1
1.2. Aims of the study	4
2. Material and methods.....	6
2.1. Study system	6
2.2. Plant material.....	13
2.3. Genetic analyses	15
2.3.1. DNA-Extraction.....	15
2.3.2. Generating AFLPs	16
2.3.3. Data scoring.....	18
2.3.4. Quantifying the error rate.....	18
2.3.5. Pruning the binary matrix	18
2.4. Genetic data analyses	19
2.4.1. Genetic differentiation.....	19
2.4.2. Genetic relationships	20
2.4.3. Principal coordinates analysis (PCoA)	20
2.4.4. Analyses of molecular variance (AMOVAs).....	21
2.4.5. AMOVA-derived F_{ST} values (Φ_{ST}) and patterns of isolation by distance (IBD)	21
2.4.6. Genetic diversity and rarity.....	22
2.4.7. Detection of F_{ST} outlier loci and clinal distribution of allele frequencies at single AFLP loci	22
2.5. Morphological analyses	23
2.6. Vegetation data analyses	24
2.7. Correlations of genetic, morphological and vegetation data	25
2.8. Self-incompatibility tests.....	25
3. Results	28
3.1. AFLP data set and error rate	28
3.2. Genetic differentiation.....	28
3.2.1. STRUCTURE assignment tests using independent allele frequencies.....	28
3.2.2. STRUCTURE assignment tests using correlated allele frequencies.....	35

3.2.3.	BAPS non-spatial clustering.....	38
3.2.4.	BAPS spatial clustering	41
3.3.	Genetic relationships.....	43
3.3.1.	Individual-based relationships	43
3.3.2.	Population-based relationships.....	46
3.4.	Principal coordinates analysis (PCoA)	49
3.5.	Analyses of molecular variance (AMOVAs)	52
3.5.1.	Non-hierarchical AMOVAs.....	52
3.5.2.	Hierarchical AMOVAs	54
3.6.	Genetic diversity and rarity	55
3.7.	AMOVA-derived F_{ST} values (Φ_{ST}) and patterns of isolation by distance (IBD).....	62
3.8.	Detection of F_{ST} outlier loci and clinal distribution of allele frequencies at single AFLP loci	65
3.9.	Morphological analyses.....	69
3.10.	Vegetation data analyses	75
3.11.	Association of morphological characters and vegetation data with genetic data..	79
3.11.1.	Mapping of morphological characters onto the genetic data.....	79
3.11.2.	Mapping of vegetation data onto the genetic data	83
3.12.	Self-incompatibility tests	86
4.	Discussion.....	87
4.1.	Taxonomical aspects	87
4.1.1.	Distribution patterns of <i>Tephroseris helenitis</i> subsp. <i>helenitis</i> and <i>salisburgensis</i> at the northern fringe of the Alps	87
4.1.2.	Association of achene type with genetic, morphological and vegetation data ..	88
4.1.3.	Is the taxonomic rank of “subspecies” for individuals with glabrous achenes justifiable?	90
4.2.	Population history of <i>Tephroseris helenitis</i> at the northern fringe of the Alps	91
4.3.	Hybrid zone between subsp. <i>helenitis</i> and <i>salisburgensis</i>	93
4.3.1.	Do the two subspecies form a hybrid zone?	93
4.3.2.	Is the hybrid zone a primary or secondary one?	95
4.3.3.	Origin and maintenance of characters varying along the cline.....	97
4.4.	Miscellaneous aspects.....	98
4.4.1.	Red bract/stem color and anthocyanin synthesis	98
4.4.2.	Replacement of “glabrous individuals” by “pubescent” ones	98
4.4.3.	Conservation aspects	99
4.4.4.	Self-incompatibility tests.....	100

4.5. Outlook.....	100
Conclusions	101
Acknowledgements.....	103
References.....	105
A. Appendix	114

Abstract

This study has three major aims. First, the distribution of *Tephrosieris helenitis* subsp. *helenitis* and *salisburgensis* at the northern fringe of the Alps was explored according to their achene type as character of subspecies designation. It was tested whether achene type is associated with other morphological characters, which therefore could be used for subspecies designation, too. Genetic data were used to test if there is differentiation between the subspecies and a potential association with morphological characters and/or vegetation data (viz. microhabitat differences). Second, the population genetic history of *T. helenitis* was inferred using genetic diversity measures in order to test two alternative but mutually non-exclusive hypotheses: populations in formerly glaciated regions at the (south-) eastern part of the species' range might have recolonized through immigration from the west, or *T. helenitis* outlasted the Ice Ages in at least one refugium close to the glacier borders. As a third aim, the existence of a putative primary or secondary hybrid zone between subsp. *helenitis* and *salisburgensis* was investigated.

The study area is located at the northern fringe of the Alps, ranging from the Swabian Jura (Baden-Wuerttemberg) in the west to the easternmost populations of *T. helenitis* at the Attersee (Upper Austria) in the east. Amplified fragment length polymorphisms (AFLPs) were performed to assess genetic variation in 30 *T. helenitis* populations. Morphological characters were recorded as present/absent in 27 populations (achene type) and six populations (capitulum type, stem color, bract tip color, basal leaf shape, basal leaf indumentum and rosette leaf margin), respectively. Vegetation surveys of vascular plant species were performed within a diameter of one meter around 13 to 20 *T. helenitis* individuals in four populations, including one pure population of each subspecies and two mixed stands.

Individuals showing pubescent achenes (ssp. *helenitis*) were found throughout the whole study area, while individuals with glabrous or sparsely hairy achenes (ssp. *salisburgensis*) were distributed only east of the Munich area, which is generally concordant with the literature. None of the other surveyed morphological characters were clearly associated with achene type and can thence be treated as unsuitable for subspecies diagnosis. Also, individual-based AFLP data failed to separate the two subspecies, regardless of whether classified by their achene type or other morphological characters. Microhabitat differences among the two subspecies also could not be found.

Intra-population genetic diversity varied in a mosaic-like pattern, albeit with a tendency of populations with high diversities being located within the same area. Clinally varying diversities along a longitudinal gradient were not found, as would be expected, if western populations had served as sources for postglacial recolonization of formerly glaciated areas. Therefore, it can be supposed that *T. helenitis* outlasted the Ice Ages in local refugia close to the glaciers.

Populations of *T. helenitis* showed only low levels of genetic differentiation, but up to three population clusters were found by Bayesian clustering algorithms. Individuals in the central and eastern part of the study area were highly admixed and had a higher frequency of intermediate achene types (sparsely hairy). Therefore, a hybrid zone between subsp. *helenitis* and *salisburgensis* can be presumed in a broad area, ranging from the Ammersee region (southern Bavaria) in the west to the Attersee region (Upper Austria) in the east. Significant sigmoid clines along a longitudinal gradient were found at three F_{ST} outlier loci, whereas the

inflection points of the regression lines were distributed at a range of about 90 km (1.20°), indicating a primary hybrid zone. Peaks of genetic diversities were found in the Ammersee region and the Untersberg region, which could indicate a secondary hybrid zone. However, the Ammersee region is outside the hybrid zone's center and the Untersberg region does not show a clear peak. Therefore, a primary hybrid zone seems more probable.

Zusammenfassung

Diese Studie beinhaltet drei übergeordnete Ziele. Erstens wurde die Verbreitung von *Tephrosieris helenitis* subsp. *helenitis* und *salisburgensis* am Nordrand der Alpen anhand des Achärentyps als Unterscheidungsmerkmal zwischen den Unterarten untersucht. Hierbei wurde getestet, ob der Achärentyp mit anderen morphologischen Merkmalen assoziiert ist, welche dadurch ebenfalls für die Unterartunterscheidung verwendet werden könnten. Zusätzlich wurden genetische Daten genutzt, um eine mögliche Differenzierung zwischen den beiden Unterarten bzw. eine potenzielle Assoziation mit morphologischen Merkmalen und/oder Vegetationsdaten (welche Mikrohabitatunterschiede zeigen) zu ermitteln. Zweitens wurde die populations-genetische Geschichte von *T. helenitis* mit Hilfe von genetischen Diversitätsmaßen untersucht, um zwei alternative, aber sich nicht unbedingt ausschließende, Hypothesen zu testen: (i) die Populationen im (süd-) östlichen und ehemals vergletscherten Arealbereich wurden durch Einwanderung von Westen her neu besiedelt, und/oder (ii) *T. helenitis* hat die Eiszeiten in mindestens einem Refugium nahe der Gletschergrenzen überdauert. Drittens wurde versucht, eine eventuell vorhandene primäre oder sekundäre Hybridzone zwischen subsp. *helenitis* und *salisburgensis* festzustellen und genauer zu untersuchen.

Das Untersuchungsgebiet befindet sich am Nordrand der Alpen und reicht von der Schwäbischen Alb (Baden-Württemberg) im Westen bis zu den östlichsten Populationen von *T. helenitis* am Attersee (Oberösterreich). Um die genetische Variation in/zwischen 30 *T. helenitis*-Populationen zu erfassen, wurde die AFLP-(Amplified fragment length polymorphisms)-Fingerprinting-Methode verwendet. Morphologische Merkmale wurden als „vorhanden“ oder „fehlend“ in 27 Populationen (Achärentyp) bzw. sechs Populationen (Köpfchentyp, Stängelfarbe, Hüllblattspitzen-Farbe, Grundblattform, -behaarung und -rand) aufgenommen. Begleitende Gefäßpflanzenarten wurden als „vorhanden“ oder „fehlend“ in einem Durchmesser von einem Meter um 13 bis 20 *T. helenitis*-Individuen in vier Populationen (je eine „reine“ Population von subsp. *helenitis* und *salisburgensis*, sowie zwei gemischte Populationen) aufgenommen.

Individuen mit behaarten Achänen (ssp. *helenitis*) wurden im gesamten Untersuchungsgebiet gefunden, während Individuen mit kahlen bzw. spärlich behaarten Achänen (ssp. *salisburgensis*) nur östlich der Gegend um München gefunden wurden. Dies ist generell übereinstimmend mit den Angaben aus der Literatur. Die weiteren untersuchten morphologischen Merkmale waren nicht deutlich mit der Achänenbehaarung assoziiert und erwiesen sich daher als ungeeignet zur Unterart-Unterscheidung. Auch Individuen-basierte AFLP-Daten konnten die Unterarten nicht trennen, auch wenn diese durch Achänenbehaarung oder ein anderes morphologisches Merkmal zugeordnet wurden. Mikrohabitatunterschiede zwischen beiden Unterarten, welche durch die Begleitvegetation einzelner *T. helenitis*-Individuen untersucht wurden, konnten ebenfalls nicht gefunden werden.

Die genetische Diversität der Populationen zeigte ein Mosaik-ähnliches Muster auf geographischem Raum, wobei sich Populationen mit höheren Diversitäten auf kleinere Gebiete konzentrieren. Entlang des Längengrades von West nach Ost konnte keine Verringerung der genetischen Variation detektiert werden, was im Falle einer Wiederbesiedelung der ehemals vergletscherten Gebiete durch Ausgangspopulationen vom Westen nach Osten erwartet

worden wäre. Daher kann angenommen werden, dass *T. helenitis* die Eiszeiten in Refugien nahe den Gletschergrenzen überdauerte.

Die Populationen von *T. helenitis* zeigten nur eine geringe genetische Differenzierung, jedoch konnten durch Bayes'sche Clusteranalysen bis zu drei Populationscluster gefunden werden. Individuen im zentralen und östlichen Bereich des Untersuchungsgebietes umfassten stark gemischte Genotypen und einen höheren Anteil an intermediären Achämentypen (spärlich behaart). Dies deutet auf eine Hybridzone zwischen *ssp. helenitis* und *salisburgensis* hin, die sich in einer breiten Zone von der Gegend um den Ammersee (südliches Bayern) im Westen bis zum Attersee (Oberösterreich) im Osten erstreckt. Signifikante sigmoide Gradienten entlang des Längengrades wurden in drei „ F_{ST} outlier loci“ gefunden, wobei die Wendepunkte der Regressionskurven etwa 90 km ($1,20^\circ$) voneinander entfernt waren, was auf eine primäre Hybridzone hinweist. Erhöhte genetische Diversität in den Populationen um den Ammersee und den Untersberg könnten eine sekundäre Hybridzone anzeigen, jedoch befindet sich die Gegend um den Ammersee außerhalb des Zentrums der Hybridzone und die Populationen der Untersberg-Region zeigen keinen deutlichen Diversitäts-Peak, der zu den benachbarten Populationen hin deutlich abfällt. Somit erscheint eine primäre Hybridzone viel wahrscheinlicher als eine sekundäre Hybridzone.

1. Introduction

1.1. General introduction

Speciation is still a hotly discussed topic, even though discussions mainly started when DARWIN (1859) presented his theory of the origin of species more than 150 years ago. At first it is necessary to define the term “species”, which is tightly linked to “speciation”. Its definition is rather ambiguous as reflected in numerous “species concepts”. One of the most common species concepts is the “biological species concept” (MAYR 1942), referring to species as “groups of actually or potentially interbreeding natural populations that are reproductively isolated from other such groups” (FUTUYMA 2005). But if there were “absolute reproductive isolation” between two species, this would imply they cannot interbreed. And this would exclude the possibility of hybrids, the emergence of which necessitates a certain amount of genetic “leakage”. Many mechanisms are responsible for reproductive isolation, which are generally classified as prezygotic or postzygotic mechanisms (DOBZHANSKY 1970, MAYR 1970). When genetic reproductive barriers arose through geographic separation of populations, the mode of speciation will be called “allopatric speciation” (FUTUYMA 2005). When these separated groups meet again it is probable that genetic differences have arisen meanwhile, whereby the degree of genetic differentiation mainly depends on the duration of separation. These groups may interbreed at “contact zones”, if the differentiation between these groups is not too strong, and “secondary hybrid zones” will be formed (BARTON & HEWITT 1985, COYNE & ORR 2004). Hybrid zones can also be formed along a geographic and ecological cline, where clinal genetic differences often lead to “parapatric speciation” (COYNE & ORR 2004, FUTUYMA 2005, JOHANNESSEN et al. 2010). These zones of gradual differentiation along a gradient are often termed “primary hybrid zones” (ENDLER 1977). Distinction between primary and secondary hybrid zones is difficult, especially when historical evidence is missing (ENDLER 1977, BARTON & HEWITT 1985). Nonetheless, as shown in FUTUYMA (2005), a distinction can be made by plotting allele frequencies of single loci against geographic positions of populations along the cline. In primary hybrid zones, genetic clines are expected to have different centers in relation to their geographical positions (non-concordant). Selection pressures may vary among non-neutral loci under selection (JOHANNESSEN et al. 2010), i.e. the clines are at different geographic positions because they are affected discriminatively by selective environmental gradients. In contrast, genetic clines of secondary hybrid zones have a common center in relation to their geographic position (concordant) and often show different degrees of steepness.

Populations at the margin of the species distribution are often geographically and ecologically isolated (“peripheral isolates”) from populations in the distribution center. In consequence, such peripheral populations might be under extreme selection pressures. Moreover, in combination with reduced gene flow and small effective population sizes, genetic drift may have a strong effect and therefore allele frequencies may differ strongly from central populations. Peripheral populations are also expected to have lower genetic variation due to genetic drift (LESICA & ALLENDORF 1995, SCHWARTZ et al. 2003, PARISOD & BONVIN 2008). Potentially, these processes promote “(incipient) speciation on the edge”. If the peripheral isolates were geographically fully isolated from the center of distribution, e.g., resulting from a founder event, this could exemplify a case of “peripatric speciation”, while populations along a

“central-marginal” cline may undergo “parapatric speciation” and show genetic patterns as in primary hybrid zones (see above). A very particular review including the comparison of 134 studies concerning the central-marginal hypothesis has been made by ECKERT et al. (2008). The compared studies, representing 115 species, have been “tested for declines in within-population genetic diversity and/or increases in among-population differentiation towards range margins using molecular genetic markers”. On average, 64.2% of the studies have shown the expected decline in diversity and 70.2% an increased differentiation, whereas these trends were positively associated. A further review concerning this topic was done by JOHANNESSON & ANDRÉ (2006), which present patterns of genetic isolation and genetic diversity between the Baltic Sea and Atlantic regions, where 29 species have been compared.

The literature on hybrid zones abounds with examples from animals (SZYMURA & FARANA 1978, GOLLMANN 1984, EASTWOOD & HUGHES 2003, CRUZ et al. 2004, MURRAY & HARE 2006, GOMPERT et al. 2010, JOHANNESEN et al. 2010) and – to a slightly lesser extent - plants (MILLAR 1983, ARAFEH et al. 2002, STREISFELD & KOHN 2005, BRENNAN et al. 2009, KOLAR et al. 2009). Nearly all of the discussed hybrid zones in the literature are secondary hybrid zones (STREISFELD & KOHN 2005, MURRAY & HARE 2006, GOMPERT et al. 2010), while only a few are primary (ARAFEH et al. 2002, CRUZ et al. 2004). Some few publications deal with primary as well as secondary hybrid zones (KOLAR et al. 2009, JOHANNESEN et al. 2010). In their review on hybrid zones, BARTON & HEWITT (1985) postulated that 37% of all hybrid zones could be clearly ascribed to secondary contacts. TABERLET et al. (1998) and HEWITT (2000) mention that central Europe is part of a so called “suture zone” (REMINGTON 1968), which is “a band, whether narrow or broad, of geographical overlap between major biotic assemblages, including some pairs of species or semispecies, which hybridize in the zone”. A secondary hybrid zone in this suture zone (at the northern edge of the Alps) is exemplified by the two diploid taxa *Arabidopsis arenosa* and *A. lyrata* ssp. *petraea*, which are sympatrically distributed at the foothills of the eastern Austrian Alps (SCHMICKL & KOCH 2011). In this hybrid zone, a tetraploid cytotype of *A. lyrata* arose through unidirectional gene flow from *A. arenosa* to *A. lyrata* ssp. *petraea*. This cytotype spread northwards into silicious areas, whereas the diploid cytotype remained restricted to limestone. An intraspecific contact zone north of the Alps is also known from populations of *Hippophae rhamnoides* (BARTISH et al. 2006). Lineages from the north (“east/central European-Scandinavian lineage”) and south (“Alps”) form narrow contact zones in the Alpine foothills of southeastern Bavaria and in Northern Tyrol. Another notable example of a secondary contact zone at the northern edge of the Alps is the orchid *Himantoglossum hircinum*. Molecular studies (PFEIFER et al. 2009) showed that genetic diversity decreases from central populations in France to peripheral populations in central and south-western Germany. It can be described as a primary hybrid zone along an ecological gradient following range expansion.

There are only a few plant taxa, which are endemic to the foothill areas of the northern Alps. For example, *Tephrosieris integrifolia* ssp. *vindellicorum* occurs exclusively in a small region south of Augsburg in Bavaria, the Lechfeld (KRACH 1988), and has been studied using molecular methods (MEINDL 2006, MEINDL & POSCHLOD 2007). Another endemic is *Cochlearia bavarica*, which is found in southern and southeastern Bavaria. This allohexaploid species evolved via hybridization between the diploid *C. pyrenaica* and the tetraploid *C. officinalis*. It has been suggested that *C. bavarica* was once more widely distributed and that the remaining populations are remnants rather than recent immigrants or of polytopic origin (KOCH 2002). A further endemic taxon at the northern edge of the Alps is *Armeria maritima* ssp. *purpurea*,

which is a relict that is currently distributed exclusively in the Benninger Ried next to Memmingen in Bavaria, where it grows in calcareous petrifying springs with contact to wet meadows (FLORAWEB 2011). Furthermore there are three Bodensee (lake Constance) endemics, *Myosotis rehsteineri*, *Deschampsia littoralis* and *Saxifraga oppositifolia* ssp. *amphibia*, which grow at the shores of this nutrient-poor lake (FLORAWEB 2011).

Another example of the few endemics of the northern foothill areas of the Alps is comprised within the focal taxon of my study, *Tephroseris helenitis* (L.) B. NORD. This short-lived perennial (Asteraceae) is distributed broadly throughout western and central Europe, i.e. from the French Armorican region in the northwest to the Austrian Salzkammergut region in the southeast. However, more or less disjunct distribution areas are found in the Auvergne region, the Pyrenees and Galicia (MEUSEL & JÄGER 1992). Thus, in Central Europe, the species reaches its southern limit of distribution in the foothill areas of the Alps. *Tephroseris helenitis* is separated into several subspecies of which the taxonomy remains partly controversial (see section 2.1 for details). At the easternmost part of the species' distribution, two subspecies are para-/sympatrically distributed and even form mixed stands there, ssp. *helenitis*, which is distributed almost throughout the whole species' range, reaches its eastern limit of distribution and comes into contact with ssp. *salisburgensis* (CUF.) B. NORD, an endemic of southeastern Bavaria and the Flach- and Tennengau regions of the Salzburg province, as well as adjacent areas in southwestern Upper Austria (HEGI 1928, CUFODONTIS 1933, KRACH 2000). The main character differentiating the two subspecies is the achene indumentum, which is pubescent in ssp. *helenitis* and glabrous or sparsely hairy in ssp. *salisburgensis* (further morphological differences are mentioned in section 2.1). Both subspecies generally grow in wet base-rich meadows and fens, especially in those of the "Molinion alliance", for which *T. helenitis* is a character species. Little is known about differences in ecological conditions or in associated vegetation between the two subspecies. However, in contrast to ssp. *salisburgensis*, ssp. *helenitis* is also reported for semi-dry deciduous forests and shrubberies (HEGI 1918, HEB et al. 1972, OBERDORFER 1983, SCHUBERT & VENT 1988). Wet meadows and fens were common in the alpine foothills until the second half of the 20th century. The raw fiber rich plants ("bedding meadows") were used to compensate the lack of litter in dairy farms, which emerged when fields (yield in raw fiber rich straw) were converted into meadows (KONOLD & HACKEL 1990, ZELESNY 1991). However, stables without litter were increasingly used, or straw was bought in addition, and wet meadows were not needed any longer and therefore drained, afforested or turned into fallow grounds. In consequence, these wet habitats became rare and increasingly fragmented. In the last decades, the importance of wet meadows as a (secondary) habitat for rare plants and animals has been recognized, resulting in the protection of those habitats (STÖHR 2003).

The above mentioned para-/sympatric distribution of subspp. *helenitis* and *salisburgensis* makes these taxa interesting objects for the study of (incipient) speciation and hybrid zones. A further advantage is that the main character supposedly differentiating the two subspecies, the achene indumentum, is easy to prospect and ensures a preliminary assignment of plants to each taxon. Another interesting aspect is the fact that the glaciers of the last Ice Ages covered extensive parts of the extant distributional range of the species at the northern fringe of the Alps. A map presenting the extent of the glaciers is shown in VAN HUSEN (1987). The whole distribution range of ssp. *salisburgensis* was glaciated at the LGM (last glacial maximum, about 18,000 years ago) of the Wuermian. Hence, populations can be expected to have been founded by recolonization following the melting of the glaciers after the LGM. The direction of

recolonization or potential refugia can be inferred by using molecular methods (described in the aims of this study, see section 1.2). For example, COMES & KADEREIT (1998) reviewed the consequences of the climatic changes in the Quaternary for plant species, and major recolonization routes in Europe are presented in TABERLET et al. (1998). SCHÖNSWETTER et al. (2005) show a map of potential refugia for plants at the periphery of the Alps during the LGM, which focuses on alpine plants and cannot be used for plants of the foothills absolutely.

1.2. Aims of the study

There are three major aims of this study, whereby taxonomical aspects will be treated at the beginning. First, I want to clarify the geographical distribution of the two subspecies *salisburgensis* and *helenitis* at the northern edge of the Alps. In the literature (HEGI 1928, CUFODONTIS 1933, CHATER & WALTERS 1976, MEUSEL & JÄGER 1992) ssp. *helenitis* is assumed to be present in the whole sampling area, but in Salzburg the data from herbaria and databases mainly refer to just ssp. *salisburgensis* for several populations. Is this an artifact and ssp. *helenitis* was simply overlooked or does it rarely exist in Salzburg, indeed? Another explanation could be that other characters than achene indumentum were used for taxonomical assignment or ssp. *salisburgensis* was considered merely as “*T. helenitis*”, which grows around Salzburg, whereas the other subspecies does not exist there. On the other hand, ssp. *salisburgensis* is not mentioned for regions more western than Munich (CUFODONTIS 1933, SCHUBERT & VENT 1988, KRACH 2000, BIB 2010, FLORAWEB 2010). This distribution pattern will be critically evaluated by own observations. Due to the controversial taxonomical separation of subspp. *helenitis* and *salisburgensis* I examined other presumably differentiating morphological characters. The main character, achene indumentum, was recorded in 561 individuals (27 populations) throughout the sampling area, while further six morphological characters (capitulum type, stem color, bract tip color, basal leaf shape, basal leaf indumentum and basal leaf margin) were surveyed in 105 individuals (6 populations). Achene type was compared with morphological, genetic and vegetation data. The comparison of achene type with further morphological characters was used to determine, which of them could be used for subspecies differentiation. Amplified fragment length polymorphisms (AFLPs) were surveyed in 338 individuals (34 populations, including 20 samples of four outgroup populations). The advantages of AFLPs compared to other genetic analyses are the time and cost efficiency and the high number of markers (loci). Nevertheless, the main disadvantage is that only dominant markers could be produced (MUELLER & WOLFENBARGER 1999). After the lab procedure 250 individuals (including 17 individuals of outgroups) were used for further statistical analyses. I tried to unravel the association of genetic data with achene type and further morphological characters to obtain an overall picture of the genetic and phenotypic differentiation between the two subspecies. Vascular plant species were recorded in 68 plots (four populations) to obtain possible differences in associated vegetation within one meter diameter around *T. helenitis* individuals. This data set was compared with achene type to infer possible microhabitat differences between the subspecies. The obtained analyses will be used to discuss whether or not the taxonomic rank of “subspecies” is justifiable for ssp. *salisburgensis*.

As to the second major aim of this study, the population genetic history of *T. helenitis* at the northern edge of the Alps was inferred by intra-population genetic diversity measures. The Ice Ages of the Pleistocene caused huge glaciated areas in the (south-) eastern parts of the distribution area of ssp. *helenitis* and the whole range of ssp. *salisburgensis*. Thus, extant populations might have recolonized previously glaciated areas after the LGM. Another mutually non-exclusive possibility is that *T. helenitis* outlasted the Ice Ages at least in one refugium close to the glaciers, which then might have served as source(s) for recolonization.

The third major aim of the study concerns the observation and distinction of a putative hybrid zone between subspp. *helenitis* and *salisburgensis*. Patterns of genetic differentiation and diversity can primarily be used to differentiate the origin of hybrid zones. Genetic differentiation will be obtained by programs inferring population structure using clustering algorithms, implemented in the programs STRUCTURE (PRITCHARD et al. 2000) and BAPS (CORANDER & MARTTINEN 2006, CORANDER et al. 2006, CORANDER et al. 2008a, CORANDER et al. 2008b), or by distance-based analyses of genetic relationships, using TREECON (VAN DE PEER 1994) and SPLITSTREE (HUSON & BRYANT 2006). For example, when two more or three more or less distinct but partially admixed population genetic clusters are revealed by such a dataset, a potential hybrid zone might be inferred. However, it will be not feasible to distinguish primary or secondary hybrid zones with this data. The usage of genetic diversity measures refines the distinction of hybrid zones and provides further hints regarding their nature. If there is a clinal difference in diversity of western and eastern populations, a primary hybrid zone could be taken into account, while a peak of diversity at the center of the hybrid zone and decreasing diversities to the marginal parts of the sampling area accords with a secondary hybrid zone (PETIT et al. 2003). If there is no clinal variation panmictic populations and a high amount of gene flow is expected. Another method, which is commonly used in the literature to distinguish primary and secondary hybrid zones (BEAUMONT & BALDING 2004, MURRAY & HARE 2006, MINDER & WIDMER 2008, GAGNAIRE et al. 2009, PEREZ-FIGUEROA et al. 2010) makes use of F_{ST} outlier loci. If the calculated F_{ST} outliers, which will be expected to be under selection or be linked to loci under selection, show a clinal pattern of allele frequencies, a further distinction of primary vs. secondary hybrid zones might be feasible. As shown in FUTUYMA (2005) primary hybrid zones present a steep decrease in allele frequencies of different loci at several locations across the hybrid zone, while secondary hybrid zones show steepest clines at the same location at several loci. A further point of interest concerns the maintenance of different and fixed characters between the two subspecies and the question of whether there are any selection pressures acting on these character.

2. Material and methods

2.1. Study system

Tephrosieris helenitis (L.) B. NORD. is a member of the angiosperm family Asteraceae, which is ascribed to the order Asterales within the core eudicots (STEVENS 2001 onwards). The genus *Tephrosieris* (RCHB.) RCHB. is morphologically closely related to the genus *Senecio* L. and is alternatively described as its section *Tephrosieris* (RCHB.) HALL. (CUFODONTIS 1933, CHATER & WALTERS 1976, MEUSEL & JÄGER 1992). Recent phylogenetic analyses by PELSNER et al. (2007), based on ITS data, supported that *Tephrosieris* should be regarded as genus (*Tephrosieris* is part of the subtribe Tussilaginatae, while *Senecio* s.str. is part of the Senecioninae). *Tephrosieris* consists of 50 (NORDENSTAM 1978) or 15 (CUFODONTIS 1933) species, respectively, which are perennial herbs, usually more or less arachnoid-lanate and have undivided and often entire leaves. Supplementary bracts are absent in involucre of *Tephrosieris* (in contrast to *Senecio* s.str.; CHATER & WALTERS 1976). *Tephrosieris helenitis* is distributed throughout western and central Europe and is described as a western spinoff of the Eurasian-continental genus/section. As shown in Fig. 1a the distribution area extends from the Armorican region in the northwest through Belgium, central and southern Germany to the Salzkammergut region in Upper Austria as the eastern edge. The southern border of the species' distribution coincides with the northern edge of the Alps (the distribution in central Europe is presented as a raster map in Fig. 1b). In the Auvergne region, the Pyrenees and Galicia *T. helenitis* is distributed in more or less separated patches from the main area in the north (MEUSEL & JÄGER 1992).

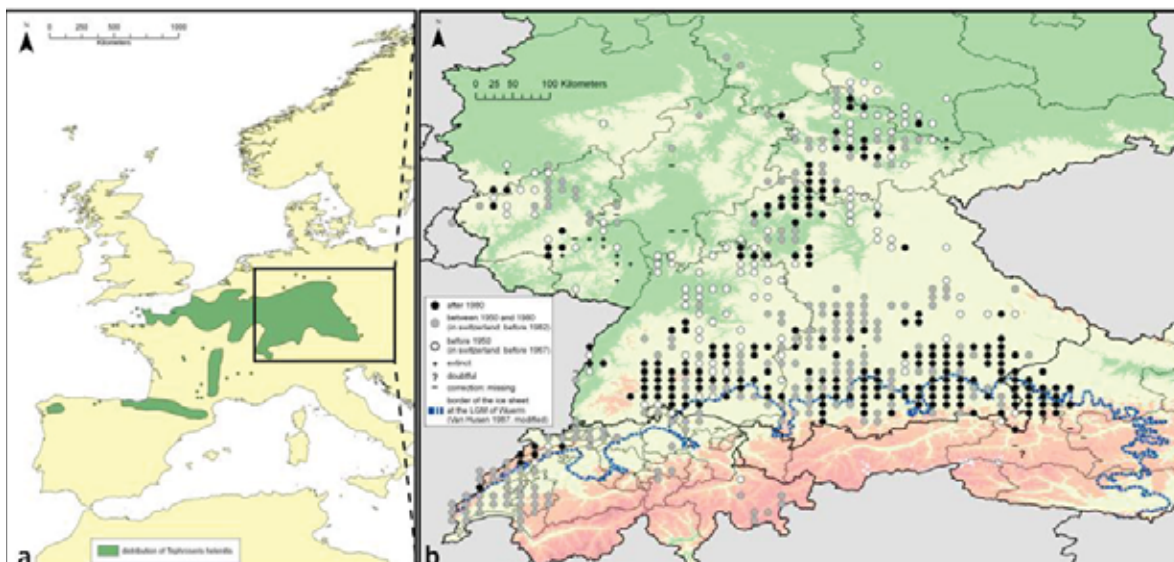


Figure 1. Distribution range of *Tephrosieris helenitis* (a; MEUSEL & JÄGER 1992) and its distribution in central Europe as a raster map displaying the time period of the latest records as well as extinct and doubtful records (b; BIB 2010, FLORAWEB 2010, FLORISTISCHE KARTIERUNG ÖSTERREICHS unpubl. data, GBIF 2009, KRACH 2000, PILSL et al. 2002, POLATSCHKE 1997, SABOTAG unpubl. data, ZDSF 2010, own observations). Graphic created with ArcMap (version 9.2, ESRI Inc. 2006).

Cytological data for this species is very scarce. Chromosome counts in the literature refer to one source (AFZELIUS 1949), where only material of botanical gardens was used. Based on this, the chromosome number of *T. helenitis* was measured as $2n=48$. HOLUB (1973) mentions that the basic chromosome number of *Tephrosieris* sp. seems to be $x=8$, but that a revision would be necessary. Since no revisions were found in the literature this basic number is cautiously adopted here for *T. helenitis*, suggesting that the species is hexaploid. However, KLOTZ et al. (2002) mention that *T. helenitis* is diploid ($2n = 48$, $x = 24$) and refer to OBERDORFER (1983). Therein, however, only the chromosome number ($2n = 48$ (50)) was found without a citation of the basic chromosome number. Genome sizes were measured by SCHISTEK (unpubl. data) using four samples of *T. helenitis* s.l. from the Untersberg region (Salzburg, Austria). The genome size was measured as 7.57 ± 0.04 pg.

Tephrosieris helenitis is described in HEGI (1928) and CHATER & WALTERS (1976) as perennial plant with slender, erect stems and short, vertical rhizomes, which reaches heights of 20-70 cm. Aerial organs are more or less lanate due to thin arachnoid hairs (the plants are only seldomly nearly glabrous). The stem base and the indumentum are often reddish colored, whereas CUFODONTIS (1933) assumed that the indumentum could utilize this as heat absorber and reservoir.

Cauline leaves are densely distributed at the basal part of the stem and are thinning out to the upper parts. The shape of the lamina is oblanceolate to linear and the leaf base is sessile, scarcely petiolate or subamplexicaul. Lower leaf surface is grey to white arachnoid-lanate and becomes more or less glabrous in older plants. Basal leaves are ovate to elliptic oblong with mostly crenate leaf margins. The lamina is narrowed gradually to abruptly into the clearly longer petiole. The basal leaves are not appressed to the ground and more or less erect.

The (3-) 6-12 (-20) capitula, which are 2 -2.5 cm in diameter, are in rather lax corymbs, with rather long peduncles. Involucres are 8-12 mm long and consist of 21 linear bracts with red tips. Ligules are yellow to golden yellow (very rarely orange) and 1-2 x 8-10 mm long, or rarely to frequent absent. Figure 2 shows aerial organs of *T. helenitis* with either present (a) or absent (b) ligules. Achenes are 3 mm long, serrated and pubescent to glabrous. The pappus is 2 – 2.5 times longer than the nut-brown mature achene (CUFODONTIS 1933).

Habitats of subspp. *helenitis* and *salisburgensis* are wet meadows (Fig. 3a) and fens, which are wet-dry, deficient in lime, rich in bases and neutral to moderate acidic. The soil type is limy and peaty. *Tephrosieris helenitis* is a character species for the “Molinion alliance” and for wet-dry conditions. The species also occurs in semi-dry deciduous forests (Fig. 3b) and shrubberies (HEGI 1928, HEß et al. 1972, OBERDORFER 1983, SCHUBERT & VENT 1988). In Franconia it is also known in “coppices with standards”, where some scattered stems are omitted from coppicing (MEIEROTT pers. comm). The altitudinal distribution of *T. helenitis* subspp. *helenitis* and *salisburgensis* comprises foothills as well as submontane and montane regions (HEGI 1928, HEß et al. 1972, FISCHER et al. 2008).

Blooming time in the uplands (between 300 – 800 m) is from beginning of May to mid-June. The peak is between May 20th and the beginning of June. At higher altitudes, the blooming time is delayed for one month (CUFODONTIS 1933). *Tephrosieris helenitis* is described as a short-lived species, which generates one or a few new rosettes. These could bloom in the next year under optimal circumstances. When conditions are suboptimal, it will be necessary to provide open spaces for germinating achenes to maintain the population (KRACH 2000). Seeds are produced sexually and exclusively amphimictic, which means that they are not produced through apomixis (KLOTZ et al. 2002), whereas this refers to the fact that no apomicts are

known in the genus *Tephroseris*. The literature regarding the compatibility system of *T. helenitis* is contradictory (KLOTZ et al. 2002: self-compatible; KRACH 2000: self-incompatible). KNUTH (1898) describes the flowers as gynomonoeious and protandric. Pollination vectors are rarely described in the literature, but *T. helenitis* tends to be pollinated by various insects, which are not mentioned in detail (Fig. 4a-c), and is wind-dispersed (STÖHR 2009). Own observations (Fig. 4a-c) have shown that *Malachius* sp., Diptera and small beetles were found on capitula or within disc flowers.



Figure 2. Aerial organs of *Tephroseris helenitis* with present (a) and absent (b) ray flowers. Photos by Andreas Tribsch.



Figure 3. Habitats of *Tephroseris helenitis*: a wet meadow in Koegelsberg/ Bavaria, pop. KOE1 (a) and a steep, rocky deciduous wood in Hayingen/ Baden-Wuerttemberg, pop. HAY1 (b). Photos by Georg Pflugbeil.

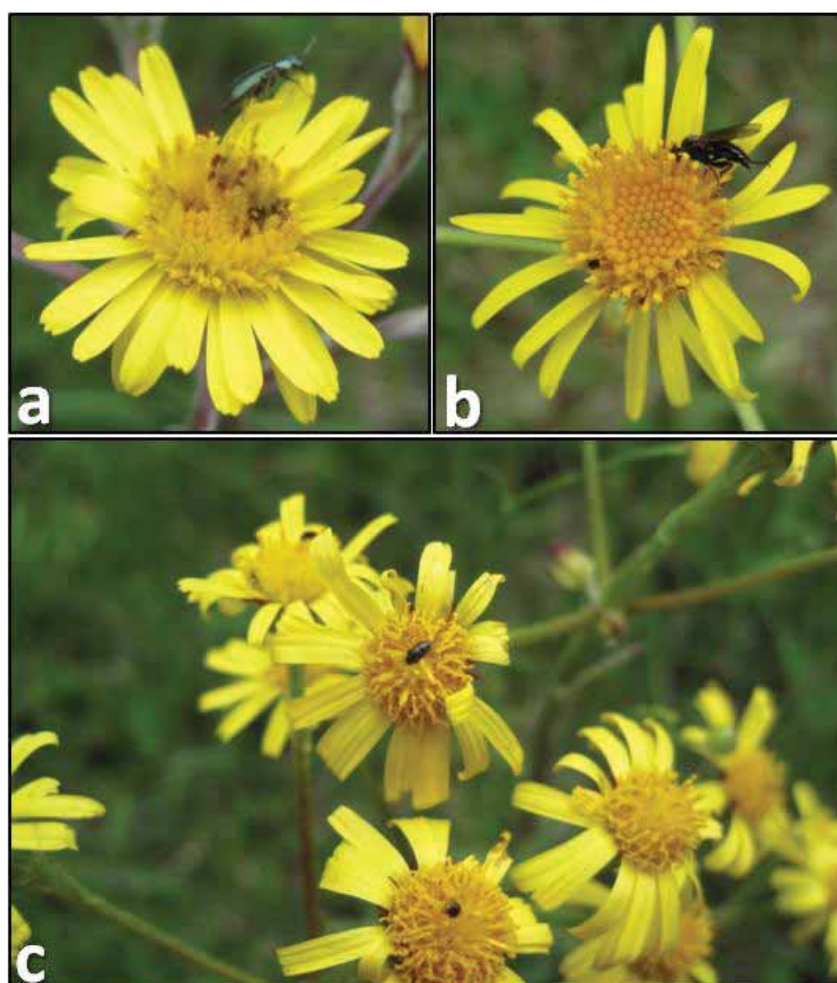


Figure 4. Pollinators of *Tephroseris helenitis* in the Gerlhamer Moor/ Upper Austria (pop. GER1) including beetles (a and c) and a Diptera (b). Figure 4a shows a member of the genus *Malachius* (det. Patrick Gros). Photos by Ursula Jaros.

The taxonomy of *T. helenitis* is not fully settled in the literature, so mainly the taxonomy of the Global Compositae Checklist (FLANN 2009 onwards) will be followed here with modifications of KERGUELEN (1987). The major part of the species' range is occupied by a type, which is not differentiated in FLANN (2009 onwards), but described as ssp. *helenitis* in KERGUELEN (1978). The latter one characterizes plants at higher altitudes in the Pyrenees, which lack ligules and show oblong to ovate-oblong leaves as var. *discoidea* (DC.) KERGUELEN (synonym: *Tephroseris pyrenaica* HOLUB), while the remaining forms of ssp. *helenitis* are characterized as var. *helenitis*. On clayey soils of the Pyrenees ssp. *macrochaeta* (WILLK.) B. NORD. occurs, which has rhizomatous and branched stocks with several non-flowering rosettes and finely dentate basal leaves. Plants of the Armorican region with fleshy leaves are described as ssp. *candida* (CORB.) B. NORD., subalpine forms of the Auvergne region are described as ssp. *arvernensis* (ROUY) B. NORD.

At the easternmost part of the distribution range ssp. *helenitis* occurs para-/sympatrically with ssp. *salisburgensis*, which is endemic to Salzburg province and adjacent areas in Bavaria and Upper Austria (Fig. 5).

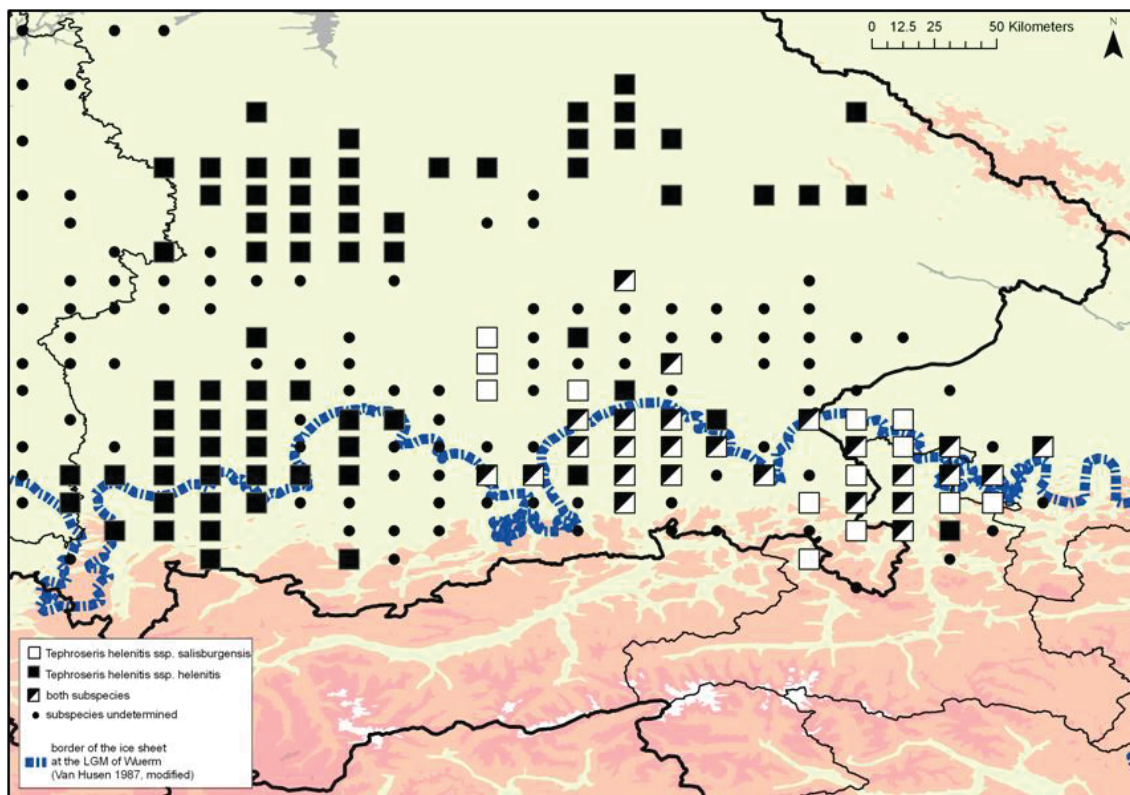


Figure 5. Distribution of the two subspecies of *Tephroseris helenitis* at the northern edge of the Alps (BIB 2010, FLORAWEB 2010, FLORISTISCHE KARTIERUNG ÖSTERREICHS unpubl. data, GBIF 2009, KRACH 2000, PILSL et al. 2002, POLATSCHEK 1997, SABOTAG unpubl. data, own observations). Graphic created with ArcGis (version 9.2).

Morphological differences of *T. helenitis* subspp. *salisburgensis* and *helenitis* will be regarded in more detail as a major aim of this study. Subspecies *salisburgensis* is mainly characterized by glabrous or sparsely hairy achenes, while those of ssp. *helenitis* are pubescent (Fig. 6a-c). Transitional forms of the two subspecies are mentioned in HEGI (1928) and KRACH (2000). According to the latter, ssp. *salisburgensis* is a “nascent form” always associated with individuals showing pubescent achenes. There are additional characters (also listed in Table 2),

which are thought to differentiate the two subspecies. CUFODONTIS (1933) mentions frequent reddened stem bases and bract tips (also in FISCHER et al. 2008) in ssp. *salisburgensis* (Fig. 6f-g). The latter character state only occurs when the bracts are sparsely hairy. According to numerous authors (OBERDORFER 1983, SCHUBERT & VENT 1988, SEYBOLD 2006, FISCHER et al. 2008), ssp. *salisburgensis* is frequently lacking ray flowers, a condition only rarely observed in ssp. *helenitis*. The shape of the basal leaves is also mentioned as a character differentiating the two subspecies by OBERDORFER (1983) and SCHUBERT & VENT (1988). In addition, subspecies *helenitis* is thought to have a crenate to dentate lamina, which is abruptly narrowed to the petiole (Fig. 6d), while ssp. *salisburgensis* has an entire to slightly crenate lamina, which is gradually narrowed to the petiole (Fig. 6e). CHATER & WALTERS (1978) and FISCHER et al. (2008) describe ssp. *helenitis* as showing 13 and ssp. *salisburgensis* 15-18 ligules.

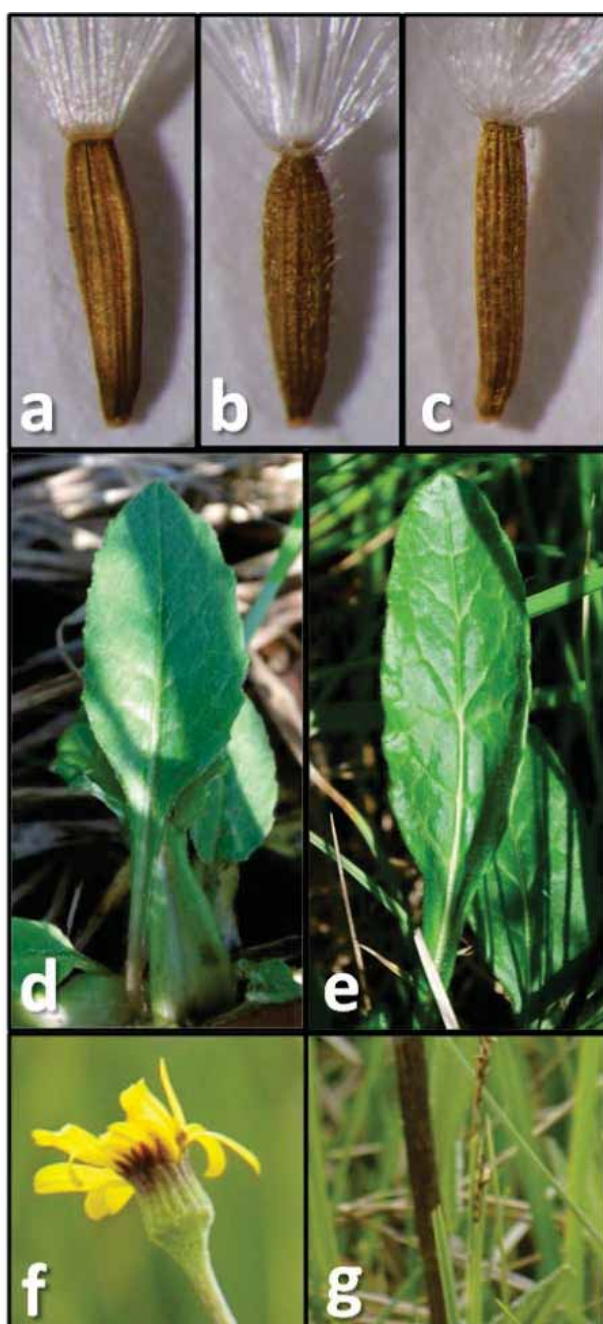


Figure 6. Morphological characters of *Tephrosia helenitis*. The upper row shows glabrous achenes viz. ssp. *salisburgensis* (a), pubescent achenes viz. ssp. *helenitis* (b) and sparsely hairy achenes viz. ssp. *salisburgensis* (c). The lower row displays slightly dentate leaves with a weak arachnoid upper surface, where the lamina is abruptly narrowed to the petiole as described for ssp. *helenitis* (d) and nearly entire leaves with a glabrous upper surface, where leaves are gradually narrowed to the petiole as described for ssp. *salisburgensis* (e). Photos by Georg Pflugbeil (a-c), Martin Kletzander (d-e) and Günther Nowotny (f-g) at population EST2.

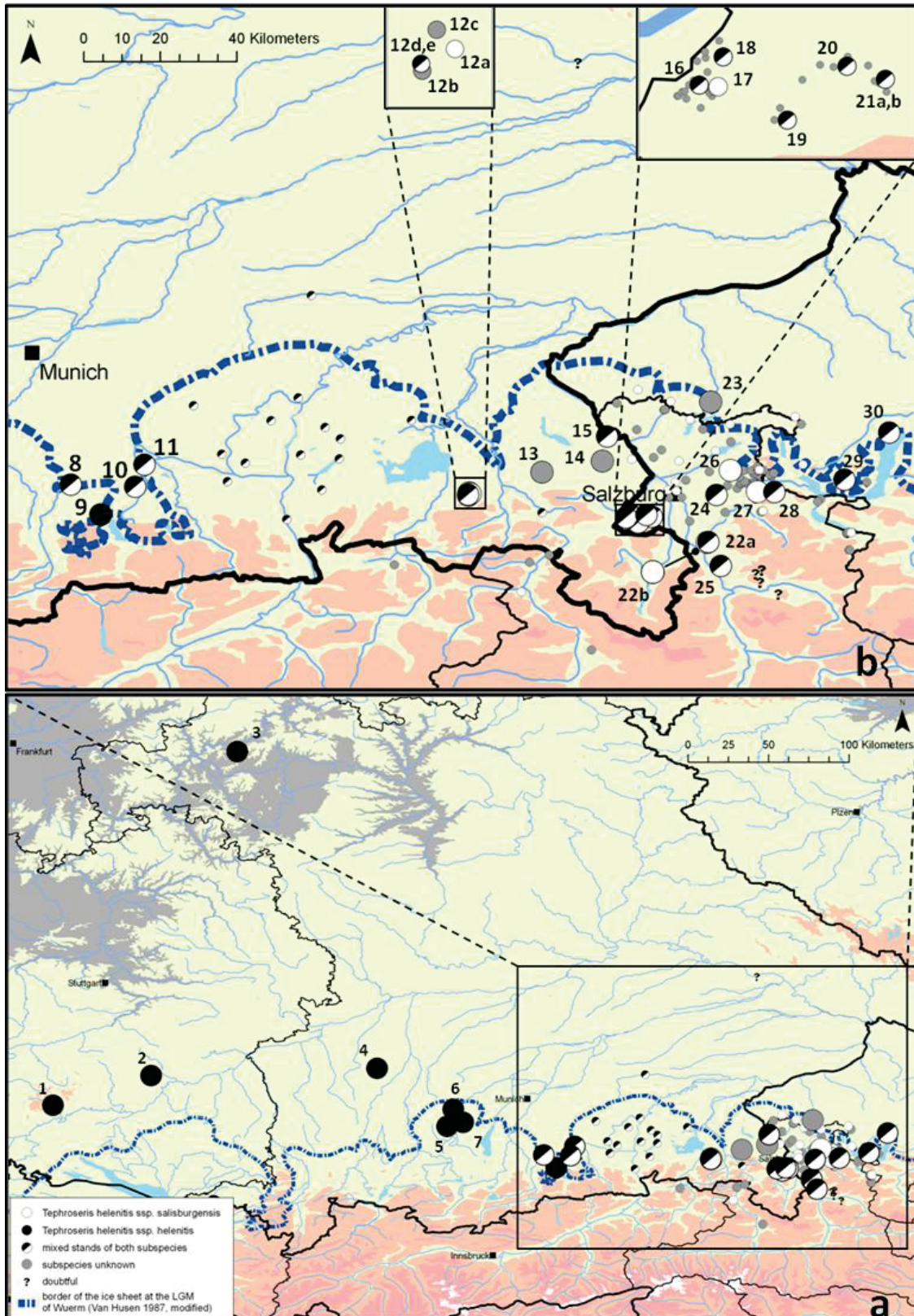


Figure 7. Sampled populations of *Tephrosieris helenitis* (large circles) and further recorded, but not surveyed populations of this taxon at the northern edge of the Alps (small circles; GBIF 2009, KRACH 2000, PILSL et al. 2002, POLATSCHEK 1997, SABOTAG unpubl. data). Population numbers are displayed next to the populations. Pure ssp. *helenitis*, pure ssp. *salisburgensis* and mixed stands are distinguished. Graphic created with ArcGIS (version 9.2).

2.2. Plant material

Leaf samples for genetic analyses were collected from 30 *T. helenitis* populations (675 individuals, in total; 23 individuals on average per population) in 2006, 2009 and 2010 in Salzburg, Upper Austria, Bavaria and Baden-Wuerttemberg (Table 1 and Fig. 7; detailed population table in Appendix: Table 26), whereas populations BER1-BER5 are considered as five subpopulations and populations ADN1-ADN2 and EST1-EST2 each as two subpopulations. Seven of these populations (located in the western and northern part of the sampling area) consisted of individuals with pubescent achenes viz. ssp. *helenitis* (AMM1, AMM2, AMM3, GEO1, HAY1, MAR1 and NUS1). The latter three populations (the most western ones) were only sporadically checked for achene indumentum type, because only individuals with pubescent achenes were expected. Individuals of five populations in the eastern sampling area exclusively showed glabrous or sparsely hairy achenes viz. ssp. *salisburgensis* (ADN2, BER1, FUS1, UNT2 and WOE1). In population BER1 only old achenes of two individuals were available, so the determination of achene indumentum type is uncertain here. Most of the populations in the central and eastern part of the sampling area (18 populations) were mixed stands consisting of individuals showing either pubescent, sparsely hairy or glabrous achenes viz. both subspecies. Achene type of five populations (BER2, BER3, HAM1, PAL1, SCH1 and SUR1) could not be determined, because of the lack of achenes. Population HAM1 was expected to show only individuals with pubescent achenes, because it is the northernmost population and ssp. *salisburgensis* could be excluded there. Individuals were sampled randomly trying to cover the entire population.

Additionally, leaf samples for genetic analysis were collected from four populations of further *Tephroses* species (20 individuals in total, five individuals per population) in 2006, 2007 and 2009. As displayed in Table 1 there is each one population of *Tephroses* cf. *tenuifolia* (GAUD.) HOLUB, *Tephroses integrifolia* (L.) HOLUB, *Tephroses* cf. *longifolia* (JACQ.) GRISEB. & SCHENK and *Tephroses crispa* (JACQ.) RCHB.

One or two leaves (rosette leaves were preferred, because of the lower content of secondary plant compounds) were carefully cut off the plant and immediately put into bags containing silica-gel (Roth, Karlsruhe, Germany). Silica-gel dried the leaves quickly and avoided a biological degradation of DNA in the plant cells. If necessary, i.e. when the silica-gel was saturated with water, it was exchanged with fresh one.

Table 1. Population number, taxon designation, population codes and sampling sites for populations of *Tephroses helenitis* at the study area. Abbreviations: A, Austria; ach., achenes recorded for indumentum; AFLP prof., number of AFLP profiles used for genetic data analyses; AT, Andreas Tribsch; B, Bavaria; BW, Baden-Wuerttemberg; DNA, samples for DNA Extraction; CE, Christian Eichberger; CN, Christian Niederbichler; FH, Franz Höglinger; G, Germany; GP, Georg Pflugbeil; GPa, Georg Pangerl; HPC, Hans Peter Comes; I, Italy; L, Lower Austria; LM, Lenz Meierott; mor., morphological traits observed; N, total number of individuals for DNA samples and recorded for achene indumentum; P, Piedmont; S, Salzburg; SV, Slovenia; Tc, *Tephroses crispa*, Ti, *T. integrifolia*, Th, *T. helenitis*; Thh, *T. helenitis* ssp. *helenitis*; Ths, *T. helenitis* ssp. *salisburgensis*; TM, Thomas Meyer; To, *Tephroses* cf. *longifolia*; Tt, *T. cf. tenuifolia*; U, Upper Austria; UC, Upper Carniola; UJ, Ursula Jaros; veg., vegetation plots performed; WR, Wolfgang Riedel; X, longitude; Y, latitude.

Pop Nr.	Taxon	Code	DNA	Ach.	Mor.	Veg.	N	AFLP prof.	Locality	X (E)	Y (N)	Collectors	Date
1	Thh	NUS1	X				21	10	G, BW, Nusplingen	8.8903	48.1072	AT + GP	2010
2	Thh	HAY1	X				10	9	G, BW, Hayingen	9.4392	48.2733	AT, GP, WR + GPa	2010

2. Material and methods

3	Thh	HAM1	X				5	5	G, B, Hammelburg	9.9214	50.0853	LM	2010
4	Thh	MAR1	X				20	8	G, B, Margertshausen	10.7033	48.3133	AT, GP + TM	2010
5	Thh	AMM1	X	X			20	8	G, B, Ammersee	11.0943	47.9885	CN	2009
6	Thh	AMM2	X	X			17	4	G, B, Ammersee	11.1288	48.085	CN	2009
7	Thh	AMM3	X	X			20	4	G, B, Ammersee	11.1837	48.0116	CN	2009
8	Thh + Ths	KOE1	X	X			21	5	G, B, Koegelsberg	11.6338	47.8293	GP	2009
9	Thh	GEO1	X	X	X	X	15	11	G, B, Georgenried	11.7043	47.759	GP	2009
10	Thh + Ths	MOO1	X	X			20	6	G, B, Moosbachtal	11.7849	47.824	GP	2009
11	Thh + Ths	FEN1	X	X			22	5	G, B, Fentbachmoos	11.8072	47.8764	GP	2009
12d	Thh + Ths	BER4	X	X			6	1	G, B, Bergener Moos	12.5624	47.8009	CN	2006
12e	Thh + Ths	BER5	X	X			18	4	G, B, Bergener Moos	12.5676	47.8058	CN	2009
12b	Th	BER2	X				20	-	G, B, Bergener Moos	12.5678	47.8047	AT	2006
12c	Th	BER3	X				2	-	G, B, Bergener Moos	12.57	47.8112	CN	2006
12a	Ths	BER1	X	X			8	-	G, B, Bergener Moos	12.5728	47.8081	AT	2006
13	Th	SUR1	X				6	-	G, B, Surtal	12.7415	47.8591	GP	2009
14	Th	SCH1	X				14	8	G, B, Schönramer Filz	12.883	47.8856	GP	2009
15	Thh + Ths	LAU1	X	X	X	X	20	18	G, B, Laufen	12.8943	47.9429	GP	2009
16	Thh + Ths	UNT3	X	X			14	8	A, S, Großmain	12.9389	47.7514	HPC + AT	2006
17	Ths	UNT2	X	X			7	4	A, S, Großmain	12.945	47.7508	HPC + AT	2006
18	Thh + Ths	UNT1	X	X			31	7	A, S, Großmain	12.9467	47.7606	HPC + AT	2006
19	Thh + Ths	LAN1	X	X			20	8	A, S, Langwiesen	12.9675	47.74	HPC	2006
20	Thh + Ths	VIE1	X	X			35	9	A, S, Viehausen	12.9869	47.7575	HPC	2006
21a	Thh + Ths	EST1	X	X			30	-	A, S, Fuerstenbrunn	12.9994	47.7539	HPC + AT	2006
21b	Thh + Ths	EST2	X	X	X	X	20	15	A, S, Fuerstenbrunn	12.9994	47.7533	GP	2009
22a	Thh + Ths	ADN1	X	X			31	9	A, S, Adnet	13.132	47.6941	HPC + CE	2006
22b	Ths	ADN2	X	X	X	X	20	17	A, S, Adnet	13.129	47.6942	GP	2009
23	Th	PAL1	X				2	2	A, U, Imsee	13.1377	48.0245	GP	2009
24	Thh + Ths	KOP1	X	X			32	7	A, S, Koppler Moor	13.1511	47.8044	CE	2006
25	Thh + Ths	KUC1	X	X			33	4	A, S, Freimoos	13.1617	47.6375	HPC + CE	2006
26	Ths	WOE1	X	X			20	5	A, S, Woerlemoos	13.1839	47.8633	CE	2006
27	Ths	FUS1	X	X			33	3	A, S, Fuschlsee	13.2475	47.8133	AT	2006
28	Thh + Ths	STI1	X	X			32	10	A, S, Stilles Tal	13.2875	47.8117	CE	2006
29	Thh + Ths	HAS1	X	X	X		10	7	A, U, Haslau-Moos	13.4517	47.8411	GP, UJ + FH	2010
30	Thh + Ths	GER1	X	X	X		20	12	A, U, Gerlhamer Moor	13.5578	47.9522	GP, UJ + FH	2010
31	Tt	ORM1	X				15	5	I, P, Ormea	7.9327	44.1286	GP	2009
32	Ti	PER1	X				10	2	A, L, Perchtoldsd. Heide	16.2519	48.1222	AT	2007
33	TI	KAR1	X				5	5	SV, UC, Preddvor	14.4417	46.3333	AT	2006
34	Tc	STK1	X				5	5	A, S, St. Koloman	13.2325	47.6367	AT	2007

2.3. Genetic analyses

2.3.1. DNA-Extraction

Silica-dried leaf samples of ca. 0.5 cm² were put into 2 ml reaction tubes including two sterile steel beads. These reaction tubes were put into a mixer mill (Retsch MM 301, Haan, Germany) and grinded for 2 minutes at 30 Hz. As the leaf samples of *T. helenitis* have densely hairy lower surfaces, the steel beads were sometimes caught within these and the leaves could not be grinded. In that case the hairs were removed and the grinding procedure was repeated.

Isolation of genomic DNA was first attempted using the Wizard Genomic DNA Purification Kit (Promega, Madison, USA). DNA could be extracted in adequate amounts, but the samples were too contaminated with secondary plant compounds and the following AFLP procedure did not work.

Using the DNeasy Plant Mini Kit (Qiagen, Venlo, Netherlands) the DNA extractions contained an adequate amount of DNA and less contaminations. So, this Kit was chosen for extracting DNA of 338 *T. helenitis* samples (ten individuals per population, when available, as well as all individuals of population ADN2, EST2, GEO1 and LAU1, from which morphological and vegetation data were available, and 10-15 individuals of population GER1 and HAS1, from which morphological data was available) and 20 samples of the four additional *Tephrosia* species (see Table 1) following the manufacturers protocol with minor modifications. Twelve samples of the four populations, from which morphological and vegetation data were available (ADN2, EST2, GEO1 and LAU1) were extracted a second time because the AFLPs did not work. Quickly after the 24 leaf samples of the batch had been grinded, 400 µl "Buffer AP1" and 4 µl "RNase A" were added to the reaction tubes and vortexed vigorously. After a brief centrifugation step, to get most of the plant material into the suspension, the samples were incubated for 10 minutes on a heating block at 65°C. During incubation the samples were inverted 2-3 times. After the addition of 130 µl "Buffer AP2" the reaction tubes were inverted 2-3 times and incubated for 5 minutes on ice. An additional centrifugation step (5 minutes at 20,000 g) was performed to precipitate substances, which were not in suspension. The lysate (about 460 µl) was transferred into a QIAshredder Mini spin column, which was attached on a 2 ml collection tube, and centrifuged for 2 minutes at 20,000 g. The volume of the flow-through was measured and put into a new reaction tube. 1.5 volumes of "Buffer AP3/E" were added and mixed by pipetting. 650 µl of the sample were transferred into a DNeasy Mini spin column, which was attached on a 2 ml collection tube, and centrifuged for 1 minute at 6,000 g. The flow-through was discarded and the remaining sample transferred into the spin column. The centrifugation step was repeated and the 2 ml collection tube discarded. The spin column was placed into a new 2 ml collection tube. 500 µl "Buffer AW" were added to the spin column and centrifuged for 1 minute at 6,000 g. The flow-through was discarded and another 500 µl were added to the spin column. The sample was centrifuged for 2 minutes at 20,000 g and the spin column put into an autoclaved 2 ml reaction tube. 50 µl of "Buffer AE" were added to the membrane of the spin column and centrifuged for 1 min at 6,000 g. The flow-through was transferred to the membrane of the spin column again and centrifuged for 1 min at 6,000 g. The spin columns were discarded and the reaction tubes put on ice or frozen at -20°C.

Quality checks were performed for all DNA extracts on a 1% w/w agarose gel (UltraPure™ Agarose, Invitrogen, Carlsbad, USA) at 100 V for 25 minutes.

DNA concentration was measured for 34 samples of the first and second batch of DNA extraction at a micro-volume UV-Vis Spectrophotometer (Nanodrop ND-1000, Thermo Fisher Scientific, Waltham, USA). Average DNA concentration was between 20 and 40 ng / μl , while a few samples reached concentrations up to 71 ng / μl . Higher values often had an absorbance spectrum suggesting contamination with polysaccharides and/or phenols.

Twenty-four of those samples showing low DNA concentrations were concentrated using the following protocol: 5 μl sodium acetate (3M) were added to 50 μl DNA extract and mixed carefully by inverting. Further on 33 μl isopropyl alcohol were added and centrifuged for 15 minutes at 16,300 g. The lysate was discarded and 150 μl ethanol (70%) were added. The reaction tube was centrifuged for 5 minutes at 16,300 g. After centrifugation the lysate was soaked up and discarded as far as possible and the reaction tube was dried at 50°C on a heating block for 5-7 minutes with opened caps. Finally the DNA pellet was resuspended in 10 μl ddH₂O. Measuring the DNA concentration with the spectrophotometer showed a 2-3 times higher concentration.

2.3.2. Generating AFLPs

The AFLP procedure followed the protocol of Vos et al. (1995) with some modifications (HAZEN et al. 2002; TREMETSBERGER et al. 2003). For each run the samples were arranged in 48-well PCR plates (an example is shown in the Appendix: Table 27).

Genomic DNA was cut with restriction enzymes at the restriction/ligation (RL) step, while at the same time DNA adaptors, including primer sites for the following DNA amplification steps, were ligated to the restriction sites. First, the adaptors (Appendix: Table 28) had to be denatured in a MyCycler™ thermal cycler (Bio-Rad, Hercules, USA) for each 10 minutes at 65°C, 37°C and 25°C. Eight μl of the reaction mix containing the adaptors, restriction enzymes and the DNA ligase (Appendix: Table 29) were added to 3 μl of undiluted genomic DNA (about 60-120 ng) and incubated for two hours at 37°C in a GeneAmp® PCR System 9700 thermocycler (Applied Biosystems, Foster City, USA). The success of the RL step was checked on an 1% w/w agarose gel (100V for 30 minutes), expecting a smear of DNA fragments with different lengths.

The next step was the preselective amplification (presel) of the RL products. A polymerase chain reaction (PCR) reduced the number of different RL-fragments by designing primers with the restriction sites and one (or two: only at the primer-trials) selective base. The RL product was diluted 10 times with ddH₂O. Two μl of this dilution were transferred into a well of a 96-well PCR plate (Thermo-Fast® 96 Non-skirted, Thermo Fisher Scientific) containing 8 μl of a reaction mix (Appendix: Table 30) including GoTaq® DNA polymerase, dNTPs and the DNA primers 5'-EcoRI+A-3' and 5'-MseI+C-3' (Appendix: Table 31). The PCR was performed (PCR program: Appendix: Table 32) in the GeneAmp® PCR System 9700 thermocycler. Amplification products were checked on an 1% w/w agarose gel (100V for 30 minutes), expecting broad bands up to 1500 bp.

The presel was followed by a selective amplification step (sel), which reduces the number of DNA fragments again by adding three selective bases to three different primer pairs. Each primer with an EcoRI restriction site was labeled with a fluorescent color, while the MseI primers were unlabeled. To find out, which primer-pairs show the most suitable patterns for further analyses, primer-trials were performed for 24 primer-pairs (see Appendix: Table 33) in

8 individuals of *T. helenitis*. The following three primer-pairs were chosen, each one primer-pair per label (VIC-5'-EcoRI+ACG-3' / 5'-MseI+CAT-3'; 6-FAM-5'-EcoRI+AGA-3' / 5'-MseI+CAC-3'; NED-5'-EcoRI+AGC-3' / 5'-MseI+CAG-3'; see also Appendix: Table 34). The pre-sel products were diluted 20 times with ddH₂O. Two µl of the diluted sample were transferred into a well of a 96-well PCR plate containing the reaction mix including GoTaq® DNA polymerase, dNTPs and the DNA primers (Appendix: Table 35). The selective PCR was performed in the GeneAmp® PCR System 9700 thermocycler (PCR program: Appendix: Table 36).

To reduce the concentration of ions in the samples, a DNA purification step was performed before running the samples in the gel electrophoresis. Therefore, Sephadex® G-50 Superfine Resin (GE Healthcare Bio-Sciences, Uppsala, Sweden) was used following the manufacturers protocol. The Sephadex® resin was filled into MultiScreen filtration plates (MAHVN45, Millipore, Molsheim, France) and swollen with 300 µl ddH₂O for two hours at room temperature. After centrifugation (910 g for 5 minutes) another 150 µl ddH₂O were added and centrifuged at 910 g for 5 minutes again. Afterwards the MultiScreen filtration plate was put onto a sterile 96-well PCR plate. Three µl of the FAM-labeled, three µl of the VIC-labeled and six µl of the NED-labeled sel products were added onto the swollen Sephadex® resin using a multi-channel pipette. The MultiScreen filtration plate was fixated with the PCR plate and centrifuged at 910 g for 5 minutes receiving the purified sel products in the PCR plate. Two µl of each sample were transferred into a 96-well PCR Cycleplate® (Thermo Fisher Scientific) containing 13 µl ET550-R-ROX-MegaBace™-Standard dilution (Appendix: Table 37) and put onto ice.

Before loading onto the sequencer, the samples were denatured at 95°C for 3 minutes and quickly cooled down in the GeneAmp® PCR System 9700 thermocycler. The PCR plates were centrifuged shortly and put on ice. Within 30 minutes the denatured PCR products were loaded onto the MegaBace™ 1000 DNA Analysis System (GE Healthcare Bio-Sciences) following the manufacturers manual. The settings are shown in the Appendix: Table 38.

In total, 532 samples (including the 338 *T. helenitis* individuals, the 20 *Tephroses* spp. individuals and the individuals, where the AFLPs were repeated one or more times) were examined in batches (runs) of 45 samples each. To check the quality of the AFLP patterns within and/or between the runs, three wells were used per plate. In one well a sample, which had shown a positive AFLP pattern in former tests, was used as a positive control (“between-run-replicate”). A second well was used as a “within-plate-replicate”. Therefore, the extracted DNA of one examined individual was transferred into two wells of the same batch. Similar AFLP patterns of the replicates indicate a high reproducibility within the run. The third well was used as a blind sample. Instead of a DNA sample ddH₂O was used in the RL step. The blind sample indicates contaminations with foreign DNAs.

After analyzing all 358 individuals, the ones which did not show a reliable AFLP pattern (156 individuals) were examined a second time. 17 samples were analyzed with the same protocol, while for 139 samples the RL step was modified. Instead of using three µl genomic DNA, one µl genomic DNA + two µl ddH₂O were used. For 18 samples a third attempt was performed. In total, 54 individuals did not show a useable AFLP electropherogram in one or more primer-pairs and thus were excluded from any further analysis.

2.3.3. Data scoring

Based on the AFLP electropherograms a binary matrix was produced using the program DAX (version 8.0; VAN MIERLO 2006). As a first step the three different primer-pairs (VIC-labeled, 6-FAM-labeled, NED-labeled) were separated by their fluorescence. Therefore, a color separation matrix was created (see Appendix: Table 39) and imported into the program. ET-ROX-550-Standard was used to calibrate the size of different samples and for the conversion of the horizontal axis from migration time into length of fragments (in base-pairs). A baseline was automatically constructed and subtracted by the program to avoid the influence of noise signals from the electropherograms. A binning sheet was created, setting bins as “user defined”. The peak search was performed automatically by the program (settings: Appendix: Table 40). Each peak was checked manually and, if necessary, erroneously marked peaks were removed or missing peaks were set, respectively. Finally, the binary matrix was created for each primer-pair by listing only the presence/absence of peaks in the bins (also called markers or loci). The three matrices were imported into Excel 2007 (Microsoft, Redmont, USA) and merged.

2.3.4. Quantifying the error rate

The sums of mismatches of five within-run-replicates were calculated for each bin. Additionally, the number of mismatches for the four positive controls was calculated. Even if only one of the positive controls showed a mismatch, it was counted as a full mismatch. Markers with mismatches in two or more replicates (58, in total) were removed.

The error rate was calculated as the total number of mismatches across all loci divided by the total number of loci (BONIN et al. 2004).

2.3.5. Pruning the binary matrix

Individuals were checked for having too few or too many loci, whereas too few loci indicate a poorly functioning restriction of the DNA according to, e.g., bad DNA quality and too many loci potentially indicate contamination with foreign DNAs. The total number of present loci in each of the three primer-pairs was calculated for each individual. The mean number of loci and its standard deviation (SD) was calculated for each primer-pair and the total dataset. Individuals with lower or higher numbers of loci than the mean \pm SD in two or more primer-pairs or at least one primer-pair and the total dataset were removed (48, in total). In five cases (ADN2_04, AMM1_09, EST2_16, LAN1_12 and WOE1_11) the individuals were not removed, because of having either a generally lower/higher number of loci or only slightly lower/higher numbers of loci, respectively.

Additionally, loci which were only present in one individual were removed (3 loci, in total). For the matrix without the outgroup species ten further loci were removed, because they were present in none or one of the remaining individuals.

The NJ analysis (see section 2.4.2, results not shown) for 314 individuals showed seven individuals (GEO1_14, KUC1_08, KUC1_09, MOO1_07, SCH1_04, SUR1_05 and UNT2_03) with long branches in the NJ tree and were removed from the dataset.

2.4. Genetic data analyses

2.4.1. Genetic differentiation

STRUCTURE (version 2.1; PRITCHARD et al. 2000) was used to infer the genetic structure of the dataset. This model-based program uses a Bayesian clustering algorithm, which calculates the probability $P(X|K)$ for different numbers of groups (K) and assigns the individuals with calculated proportions (Q -values: estimated membership coefficient for each individuals to each cluster) to these groups. The admixture model was performed, because the current approach is an intraspecific one and the species is strictly outcrossing (see section 3.12). Regarding model choice for allele frequencies, both models available (independent and correlated, respectively, see FALUSH et al. 2003). The analysis was computed for $K=1$ to $K=9$ (10 replicates for each K ; length of burnin period: 200,000; MCMC replicates: 500,000; recessive alleles) at the Bioportal at the University of Oslo (KUMAR & SKJAEVELAND 2009). To estimate the most probable number of groups, the R-script STRUCTURE-SUM (version 2009; EHRICH et al. 2007) was utilized. The function "Structure.table" was used to create a diagram plotting the probabilities of each STRUCTURE-run, $\ln P(D)$, against the number of groups (K). "Structure.simil" calculates a similarity coefficient among each pair of STRUCTURE-runs according to NORDBORG et al. (2005). The average of the similarities and the standard deviations of each K were plotted against the number of K . "Structure.DeltaK" is a function to estimate the most probable number of K using the method of EVANNO et al. (2005). The most probable K -value was chosen as follows: it is showing a high probability in the plot of "Structure.table", the probabilities of the single replications do not scatter, the similarities are high in "Structure.simil" and the plot of "Structure.DeltaK" shows a peak in the "mean DeltaK".

The program BAPS (Bayesian Analysis of Population Structure, version 5.4) was used as an alternative to STRUCTURE, which estimates the population structure using a Bayesian clustering algorithm. Four computations were done, using spatial- and non-spatial analyses each with and without admixture. First, a non-spatial genetic mixture analysis of individuals (CORANDER et al. 2006; CORANDER et al. 2008b) was performed for $K=1$ to $K=9$ (5 replications for each K). This method computes the optimal number of groups and ascribes each individual to one of these groups. Second, an admixture analysis of individuals (CORANDER & MARTTINEN 2006; CORANDER et al. 2008b) based on the mixture analysis was performed (using 100 iterations to estimate the admixture coefficient, 200 reference individuals from each population, and 50 iterations to estimate the admixture coefficient for the reference individuals). In the admixture analysis individuals can be admixed among the groups. Third, a spatial genetic mixture analysis was performed (CORANDER et al. 2008a) to produce Voronoi tessellations of the populations. Fourth, an admixture analysis based on the spatial genetic mixture analysis was performed. The settings for the latter two computations were the same as for the non-spatial analyses.

The mean Q -values of the STRUCTURE clusters, as well as the mean values of the "changes in $\log(\text{marginal likelihood})$ if individual i is moved to group j " of the BAPS clusters in each population were correlated with the longitude using SPEARMAN'S (1904) rank correlation coefficient in SPSS (version 16.0.2, SPSS INC. 2008). This program was also used to compute linear regressions. Longitude and achene indumentum, respectively, were set as independent variables and the mean values of STRUCTURE/ BAPS clusters as dependent variables (as well as achene indumentum, when longitude was an independent variable).

2.4.2. Genetic relationships

A neighbor-joining (NJ) analysis based on NEI & LI's (1979) genetic distance measure was performed in TREECON FOR WINDOWS (Version 1.3b; VAN DE PEER 1994). NJ analyses with bootstrap values (1000 permutations) were performed for 261 individuals in total and without the replicates (9 individuals) and/or the outgroups (17 individuals), respectively. The resulting bootstrap values were mapped onto a NJ-tree, which was rooted with the outgroups.

A Neighbor-Net analysis was computed by the program SPLITSTREE (vers. 4.10; HUSON & BRYANT 2006). It was performed for 250 individuals (including the 17 outgroup samples, but without the nine replicates) and for 233 individuals (without the 17 outgroup samples and the nine replicates).

The matrix for population-based NJ trees was generated in R (version 2.9.2; R DEVELOPMENT CORE TEAM 2009), using the "Presence" function of the script AFLPDAT (modification of 20.10.2010; EHRICH 2006). Here, a locus which is present in at least one individual of the population is counted as present for the population. A rooted NJ analysis was performed in TREECON FOR WINDOWS and a Neighbor-Net analysis was computed in SPLITSTREE for 33 populations and 29 populations (without the outgroups). The unrooted NJ-tree was calculated using PHYLIP (version 3.69; FELSENSTEIN 2005). Before using the program the allele frequencies were estimated by GENALEX (Genetic Analysis in Excel; version 6.41; PEAKALL & SMOUSE 2006), assuming complete outcrossing and following LYNCH & MILLIGAN (1994). The "Frequency" function was chosen for "binary (diploid)" data. Afterwards, the input file for PHYLIP was built manually and loaded into GENDIST (implemented in PHYLIP) to calculate NEI's (1972) genetic distances. The output file of GENDIST was imported into NEIGHBOUR (implemented in PHYLIP) to estimate an unrooted NJ tree (clustering algorithm of SAITOU & NEI 1987), visualized using the program TREEVIEW (version 1.6.6; PAGE 1996). A bootstrap analysis was performed to show the support for each node of the NJ tree. Therefore, the program SEQBOOT (implemented in PHYLIP) was used to calculate 1,000 replicates of the allele frequency matrix. Distance matrices of these 1,000 replicates were calculated in GENDIST and NJ trees were constructed afterwards in NEIGHBOUR. A consensus tree out of the 1,000 NJ-trees was obtained using the program CONSENSE (implemented in PHYLIP). The bootstrap values were mapped onto the original NJ-tree and displayed by TREEVIEW.

2.4.3. Principal coordinates analysis (PCoA)

This ordination method was applied to the whole individual-based dataset of *T. helenitis* in the program PAST (PAleontological STatistics; version 1.93; HAMMER et al. 2001) using the algorithm of DAVIS (1986) and the Dice similarity coefficient (DICE 1945). Eigenvectors (coordinates) and Eigenvalues (given for the four most important coordinates) were computed in this analysis. The coordinates of the first two axes were imported into SPSS and displayed as a scatter plot.

As a matrix for the population-based PCoA the presence matrix was used, which was computed with AFLPDAT as mentioned section 2.4.2. The PCoA again, was performed in PAST. For the graphical presentation of the coordinates the program SPSS was used as for the individual-based PCoA.

The scores of the individual- and population-based PCoA axis 1 were correlated with the longitude of the populations using SPEARMAN's (1904) rank correlation coefficient in SPSS (version 16.0.2, SPSS INC. 2008).

2.4.4. Analyses of molecular variance (AMOVAs)

The partitioning of genetic variance within and among populations (non-hierarchical AMOVAs; 2-level-AMOVAs) and/or among user-defined groups of populations (hierarchical AMOVAs; 3-level-AMOVAs) in the AFLP data were estimated in the program ARLEQUIN (version 3.11; EXCOFFIER et al. 2005). AMOVAs are described in EXCOFFIER et al. (1992). Input files were created with the R-script AFLPDAT using the "Arlequin" command.

Non-hierarchical AMOVAs were performed for the entire dataset of *T. helenitis* (29 populations). First, based on the results of the program STRUCTURE (see section 3.2), non-hierarchical AMOVAs were calculated for each STRUCTURE cluster. The highest proportion of the mean Q-values in each population was used to ascribe the populations to different groups. Second, populations were ascribed to AMOVA groups due to their geographic position. These were concordant with STRUCTURE results, only the two populations GEO1 and KUC1 were ascribed to a STRUCTURE-cluster, which was not predominant in the geographical region. Third, to test for significant genetic variance between individuals with glabrous/sparsely hairy achenes (viz. ssp. *salisburgensis*) and pubescent achenes (viz. ssp. *helenitis*) a non-hierarchical AMOVA was performed ascribing them to two populations (in fact: types viz. the two subspecies).

A hierarchical AMOVA approach was performed, whereas the populations were grouped as in the non-hierarchical AMOVAs. First, groups were formed due to the highest proportion of the mean Q-values of STRUCTURE in each population. Second, populations were ascribed according to their geographic position.

Permutations were performed in the program ARLEQUIN (1023 permutations) to calculate the significances of all computed variance components.

2.4.5. AMOVA-derived F_{ST} values (Φ_{ST}) and patterns of isolation by distance (IBD)

The program ARLEQUIN (version 3.11; EXCOFFIER et al. 2005) was used to calculate pairwise Φ_{ST} values among the 29 populations based on their AFLP data. Input files for ARLEQUIN were created utilizing the R-script AFLPDAT.

To test for a pattern of isolation by distance, a correlation between two symmetric matrices was also performed in ARLEQUIN computing a Mantel test (MANTEL 1967) with 1,000 permutations. Therefore, the abovementioned pairwise Φ_{ST} matrix was correlated with geographical distances among the 29 *T. helenitis* populations. These geographical distances were created with AFLPDAT using the "Geodist" function and merged with the pairwise Φ_{ST} matrix using the "PlotIBD" function. This matrix was used to perform a Mantel test. Isolation by distance was tested also within each STRUCTURE cluster.

2.4.6. Genetic diversity and rarity

There are many indices to describe the genetic diversity within populations. For this study three measures of genetic diversity were taken into account. The first index is the proportion of polymorphic loci (%PLP). It relates the number of loci, which are not present in every individual (polymorphic), to the total number of loci. The %PLP was computed in the program GENALEX. As a second measure NEI's (1987) genetic diversity (H_E) was calculated in AFLPDAT utilizing the function "Diversity.boot". This function uses bootstrap replicates for the computation of confidence intervals. In this study 1,000 bootstrap replicates were performed. As a third diversity measure SHANNON's (1948) information index based on SHERWIN et al. (2006) was estimated in GENALEX.

A method to identify rare markers in populations is presented in SCHÖNSWETTER & TRIBSCH (2005). The functions "Rarity" and "Rarity.permut" (TRIBSCH & EHRICH unpubl. data) in AFLPDAT calculate rarity measures corresponding to the frequency down weighted marker values referred to the latter publication. Seventy-five % and 95% confidence intervals of rarity values were calculated using the "Rarity.permut" function with 1,000 permutations each. Numbers of private markers for single populations and numbers of bands (with a frequency >5%), which occur in max. 25% and 50% of the populations, respectively, were computed in the program GENALEX.

The abovementioned diversity and rarity measures were also calculated for groups identified by STRUCTURE (see section 3.2). Estimates of genetic diversity and rarity of populations were correlated with their longitude, sample size using SPEARMAN's (1904) rank correlation coefficient in SPSS (version 16.0.2, SPSS INC. 2008). The program was also used to calculate linear regressions setting longitude and sample size as independent variables and genetic diversity and rarity as dependent variables. Regressions were also performed with genetic diversity as dependent variable and rarity as independent variable.

2.4.7. Detection of F_{ST} outlier loci and clinal distribution of allele frequencies at single AFLP loci

F_{ST} outlier loci are single (AFLP) markers, which are thought to be under divergent selection (candidate loci). I identified the outlier loci using two programs. MCHEZA (ANTAO & BEAUMONT 2011) is based on the algorithm of DFDIST, a modification of FDIST (BEAUMONT & NICHOLS 1996) for the usability of dominant markers. BAYESCAN (version 2.01; FOLL & GAGGIOTTI 2008) is based on the multinomial-Dirichlet model and calculates a "posterior probability" for the model including selection for each locus, which can not directly be compared to the p-value of FDIST. The "False Discovery Rate" (BENJAMINI & HOCHBERG 1995) is "the expected proportion of false positives among outlier loci" (FOLL 2010) and is set to 0.05 in both programs. MCHEZA was performed with a theta of 0.06, beta-a and beta-b of 0.25, subsample size of 8, critical frequency of 0.99 and a confidence interval of 95% for 50,000 simulations. The standard settings were used in BAYESCAN (sample size of 5,000 with a thinning interval of 10, 20 pilot runs with a length of 5,000, additional burn-in of 50,000, prior odds for neutral model: 10, F_{IS} prior uniform between 0.0 and 1.0). In the Bayesian analysis, the density of the F_{ST} posterior

distribution was calculated with R (version 2.9.2; R DEVELOPMENT CORE TEAM 2009) using the script “plot_R”, which is implemented in BAYESCAN and described in FOLL (2010).

The allele frequency clines of these potential F_{ST} outlier loci were computed using the program R. To detect clines showing a significant sigmoid curve, the Huisman-Olff-Fresco or HOF models II and III (HUISMAN et al. 1993) were implemented in R. OKSANEN & MINCHIN (2002) developed the fitting procedure presented by HUISMAN et al. (1993) and used maximum likelihood estimation instead of the original least-squares method. Maximum likelihood fitting of non-linear HOF models were performed with non-linear minimization (function “HOF”) in the package “gravy” (OKSANEN 2011), which is part of the “vegan” project (OKSANEN et al. 2011). The computational procedure first searches for loci that show a significant trend along the spatial gradient (longitude) and fit them to HOF models. The procedure is performed again, but dismisses model I (no trend). Afterwards, it is run on a subset of loci that best fit model II and then model III.

The inflection points of the curves showing significant clines in model II or III were calculated with the nonlinear least squares model to compare these clines relative to their longitudinal location. The comparison of the locations can be used to distinguish between a primary and a secondary hybrid zone (see section 4.3.2). “Non linear least squares” was used to determine the nonlinear least-squares estimates of the parameters of a logistic function and its gradient. Models were fitted using function “nls” in package “nlme” (PINHEIRO et al. 2012). At first it was attempted to fit the logistic regression for all loci. This was then repeated for those loci that fitted to a logistic model. Loci, which showed a significant ($P \leq 0.05$) model fit, were selected. The slope inflection points and their standard errors were extracted and confidence intervals of the regression fit were computed by linear approximation. Afterwards, the kernel density of all slope inflection points was estimated.

2.5. Morphological analyses

The two subspecies at the northern edge of the Alps (*ssp. helenitis* and *ssp. salisburgensis*) are supposed to be differentiated by a couple of morphological traits (CUFODONTIS 1933, OBERDORFER 1983, SCHUBERT & VENT 1988, SEYBOLD 2006, FISCHER et al. 2008), including, as a presumably diagnostic trait, the indumentum of the achenes. This character and six additional morphological traits (capitulum and vegetative traits) were further analyzed. The seven characters, their states and assignment to the two subspecies, are summarized in Table 2. Achenes were harvested from 27 populations (25 populations, which also were surveyed for AFLPs and two additional populations, BER1 and EST1; Table 1) and 561 individuals, in total. Indumentum of achenes was observed with a magnifying glass or a stereo microscope. The following character states were distinguished: achenes pubescent, achenes sparsely hairy and achenes glabrous. The six additional morphological traits were observed for 105 individuals of six populations (ADN2, EST2, GEO1, GER1, HAS1 and LAU1; all of these were surveyed for AFLPs and achene indumentum, too; Table 1). Character states of these traits were recorded as present (1) or absent (0).

A correlation of achene pubescence with longitude was computed for 561 individuals, using SPEARMAN’S (1904) rank correlation coefficient (mentioned in section 2.4.1), while a

comparison of all seven morphological traits was performed for the abovementioned 105 individuals performing a cross tabulation in SPSS.

Table 2. Recorded morphological traits and their assignment to the two *Tephrosia helenitis* subspecies *helenitis* and *salisburgensis*. Abbreviations: C, CUFODONTIS (1933); F, FISCHER et al. (2008); O, OBERDORFER (1983); S, SEYBOLD (2006); SV, SCHUBERT & VENT (1988).

Character state: present (1)	Character state: absent (0)	Assigned to subspecies	Literature
Achenes pubescent	Achenes glabrous or sparsely hairy	<i>helenitis</i>	C, F, O, S, SV
Ray flowers present	Ray flowers absent	-	F, O, S, SV
Stem red colored	Stem green or brownish colored	<i>salisburgensis</i>	C
Bract tips red colored	Bract tips green or brown colored	<i>salisburgensis</i>	C, F
Rosette leaf lamina abruptly narrowed to the petiole	Rosette leaf lamina gradually narrowed to the petiole	<i>helenitis</i>	O, SV
Upper surface of rosette leaves glabrous or with short hairs	Upper surface of rosette leaves arachnoid	<i>salisburgensis</i>	O
Rosette leaves crenate to dentate	Rosette leaves entire or slightly crenate	<i>helenitis</i>	O, SV

2.6. Vegetation data analyses

Vegetation plots were obtained in four populations (ADN2, EST2, GEO1 and LAU1; these were also surveyed for AFLPs and morphological traits) in 2009 to observe a possible correlation of genetic variation with species assemblages or with single plant species. Community samples of vascular plants were recorded as present (1) or absent (0) within a diameter of one meter around 13 to 20 randomly selected *T. helenitis* individuals per population. Species richness of populations ranged from 36 to 64 species. The combined dataset consisted of 105 species and 68 plots.

The resulting binary matrix was used to perform a principal component analysis (PCA) in PAST. The resulting scatter plot was displayed using in SPSS. Overall variation in the vegetation data should be indicated, as well as single by species showing higher loading values. The latter ones could be potentially used as indicator species for different plant communities.

Additionally, average ELLENBERG (1992) indicator values adapted by G. KARRER (in the program HITAB 5; WIEDERMANN 1995) were calculated for each plot. Six indicator values were surveyed: light, temperature, continentality, soil humidity, soil acidity and nutrients. Therefore, the value for present species in the binary matrix (1) was replaced by all of their indicator values in a separate matrix. If the species was absent (0) in a plot, no indicator value was inserted and the data was treated as missing. Also, indicator values, which are given as

“indifferent” were treated as missing. Furthermore, the average of each indicator value was calculated per plot and population, respectively, and displayed as a box plot diagram in SPSS.

2.7. Correlations of genetic, morphological and vegetation data

To estimate a potential interrelation of the three types of observed data (genetic, morphological and vegetational data) correlations were performed using the program CANOCO FOR WINDOWS (version 4.55; TER BRAAK & ŠMILAUER 2002). Input files have been created with the supplied program of the CANOCO package, WCANOIMP. In four populations (ADN2, EST2, GEO1 and LAU1; Table 1) genetic data, morphological data and vegetation data of single individuals were analyzed. In two additional populations (GER1 and HAS1) genetic data and morphological data of single individuals were recorded. Therefore, it was possible to correlate the abovementioned dataset for single individuals viz. samples or plots, using AFLP loci, plant species composition and morphological traits as variables. Genetic data was used for all analyses as the primary matrix (this is called “species data” in CANOCO). This primary matrix was used as the dataset for the computation of a PCA. A secondary matrix (this is called “environmental data” in CANOCO) was used to correlate morphological and vegetation variables with the axes of the PCA. Additionally, the matrix of indicator values (based on the vegetation data) was used as a secondary matrix (to represent the 105 recorded species, which have been reduced to six indicators). It was necessary to compare the same amount of samples of primary and secondary matrix. In fact, that data was not always present for all samples (i.e. AFLPs did not work or morphological traits could not be observed in some individuals). For the correlation of genetic data with morphological data 68 samples were used, while for the correlation with vegetation data and indicator values only 56 samples were available. Originally, 80 samples of genetic data, 105 samples of morphological data and 68 samples of vegetation data were recorded.

Genetic data and vegetation data were also compared by the pairwise Euclidian distances between vegetation plots and genetic samples (calculated in PCORD; version 5.10; McCUNE & MEFFORD 2006). The distances between vegetation plots and genetic samples were correlated using SPEARMAN’S (1904) rank correlation coefficient in SPSS. Linear regressions were performed setting Euclidian distances between vegetation plots as independent variables and Euclidian distances between genetic samples as dependent variables. To compare the scores of the individual-based PCoA-Ax1 (representing “genetic data”) and longitude with achene indumentum and the further six morphological characters a binary logistic regression was performed in SPSS, setting the morphological characters as dependent variables and PCoA-scores and longitude as covariates.

2.8. Self-incompatibility tests

Regarding the missing references of the breeding system in *T. helenitis*, self-incompatibility tests were performed at two sites. One site was in the field (population VIE1), while the second site was at the outdoor flower bed of the Salzburg Botanical Garden (SBG). At each

sites, entire inflorescences or single capitula of 11 and 8 *T. helenitis* plants, respectively, were bagged with nylon (Fig. 8a), lens tissue paper, plastic tea bags (both in Fig. 8b), paper tea bags (Fig. 8c) or paper bags (Fig. 8d). For each setting, open-pollinated plants nearby (only VIE1) or non-bagged capitula of the same plant (only SBG) served as controls. Three plants of the field site and three plants of the Botanical Garden could be identified as ssp. *helenitis* due to their achenes being pubescent. Subspecies *salisburgensis* was determined in 8 and 6 individuals, respectively, including one individual with sparsely hairy achenes at the field site, while the remaining individuals showed glabrous achenes. Table 3 shows the settings used for the bagging-test at the two sites.

Table 3. Settings of the self-incompatibility test.

Ind.	Bagged plant organs	Bagging material	Achene pubescence viz. subspecies
Field site (population VIE1)			
1	One capitulum	Nylon	Achenes pubescent (ssp. <i>helenitis</i>)
2	Entire inflorescence	Paper tea bag	Achenes glabrous (ssp. <i>salisburgensis</i>)
3	Entire inflorescence	Paper bag	Achenes pubescent (ssp. <i>helenitis</i>)
4	Entire inflorescence	Nylon	Achenes pubescent (ssp. <i>helenitis</i>)
5	Entire inflorescence	Nylon	Achenes glabrous (ssp. <i>salisburgensis</i>)
6	Entire inflorescence	Nylon	Achenes glabrous (ssp. <i>salisburgensis</i>)
7	Entire inflorescence	Paper bag	Achenes glabrous (ssp. <i>salisburgensis</i>)
8	Control	-	Achenes glabrous (ssp. <i>salisburgensis</i>)
9	Control	-	Achenes glabrous (ssp. <i>salisburgensis</i>)
10	Control	-	Achenes glabrous (ssp. <i>salisburgensis</i>)
11	Control	-	Achenes sparsely hairy (ssp. <i>salisburgensis</i>)
Salzburg Botanical Garden			
1	Three capitula bagged + one capitulum as control	Lens tissue paper	Achenes glabrous (ssp. <i>salisburgensis</i>)
2	One capitulum	Plastic tea bag	Achenes glabrous (ssp. <i>salisburgensis</i>)
3	Two capitula bagged + one capitulum as control	Plastic tea bag	Achenes glabrous (ssp. <i>salisburgensis</i>)
4	One capitulum	Plastic tea bag	Achenes glabrous (ssp. <i>salisburgensis</i>)
5	Entire inflorescence	Plastic tea bag	Achenes pubescent (ssp. <i>helenitis</i>)
6	Two capitula	Lens tissue paper	Achenes glabrous (ssp. <i>salisburgensis</i>)
7	One capitulum	Plastic tea bag	Achenes glabrous (ssp. <i>salisburgensis</i>)
8	Two capitula	Lens tissue paper	Achenes pubescent (ssp. <i>helenitis</i>)

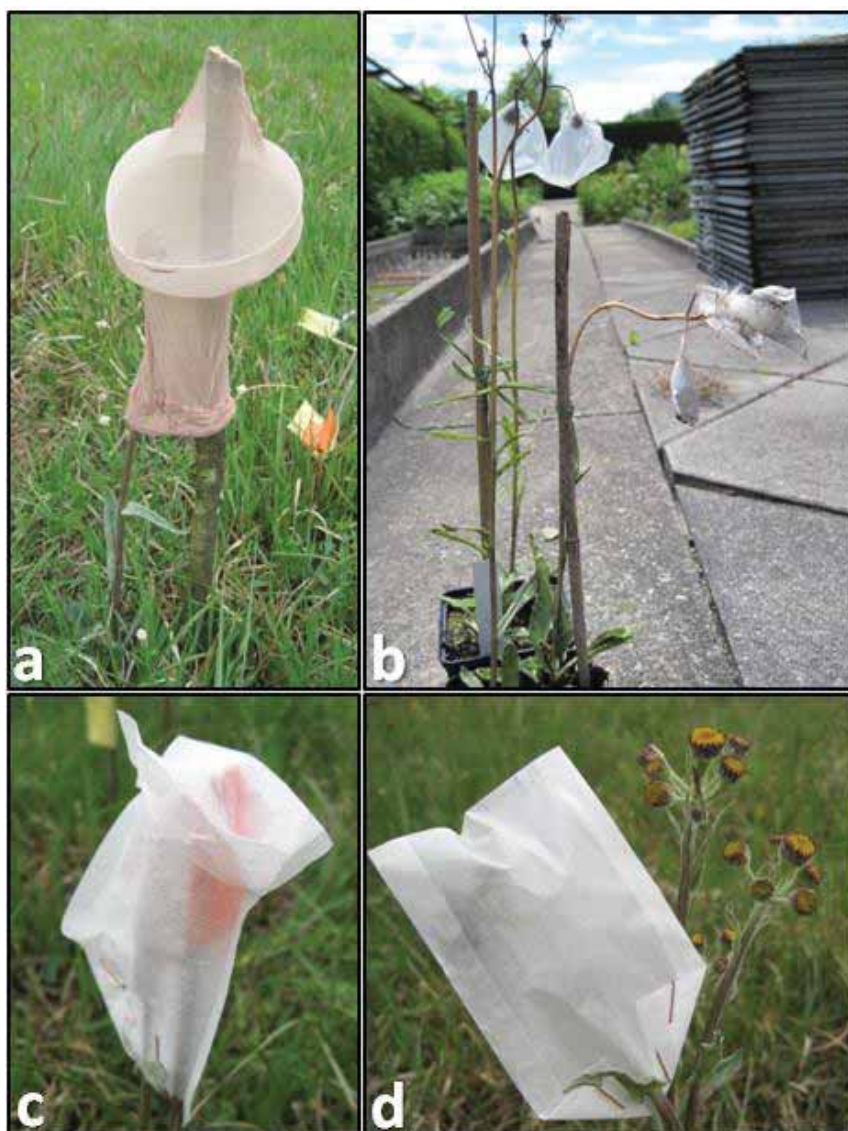


Figure 8. Bagging material used for the self-incompatibility tests. Entire inflorescences bagged with nylon (a), single capitula bagged with plastic tea bags (b; left top) and lens tissue paper (b; right middle), entire inflorescences bagged with paper tea bags (c) and paper bags (d). Photos by Georg Pflugbeil.

3. Results

3.1. AFLP data set and error rate

Altogether, 338 individuals of *Tephrosia helenitis* and 20 individuals of four further *Tephrosia* species, which served as outgroups, were examined for AFLPs. In total, 54 *T. helenitis* individuals did not show satisfying AFLP fragments in one or two repetitions of the AFLP procedure and were removed from the dataset. The remaining 314 samples (including five between-run-replicates and five within-run-replicates) were used for AFLP scoring. After the matrix was pruned (samples with too few/many loci were removed; see section 2.3.5) and samples with long branches in the NJ tree (55 samples in total, including one between-run-replicate) had been removed, as well, 259 samples (including 233 *T. helenitis* samples with four between-run-replicates and five within-run-replicates, as well as 17 outgroup samples) remained for genetic data analyses.

The three primer combinations yielded 462 markers (211 FAM-loci, 100 NED-loci and 151 VIC-loci). Eleven loci (8, 2 and 1 loci of FAM, NED and VIC, respectively) were exclusively found in outgroup samples. Fragment lengths of loci ranged from 109.4 – 582.1 bp in FAM, 83.3 – 560.3 bp in NED and 77.0 – 571.5 bp in VIC. The mean number of fragments was 131.16 ± 15.55 (FAM: 53.73 ± 7.62 , NED: 22.21 ± 3.88 , VIC: 55.22 ± 7.34). The proportion of present loci (number of present loci divided by the number of absent loci) in the data set was 28.39% (FAM: 25.46%, NED: 22.21%, VIC: 36.56%).

The error rate (total number of mismatches divided by the total number of markers over the five within-run-replicates) was 3.58% (FAM: 3.41%, NED: 3.00%, VIC: 5.03%). Typical error rates are between 2-5% and should not be higher than 10% (BONIN et al. 2007).

3.2. Genetic differentiation

3.2.1. STRUCTURE assignment tests using independent allele frequencies

All 233 individuals of 29 *T. helenitis* populations were analyzed in STRUCTURE assuming the admixture model with independent allele frequencies. As shown in Fig. 9a the likelihoods ($\ln P$) from K=3 to K=9 were very similar. The likelihood at K=1 was slightly lower as the latter mentioned, the likelihood at K=2 was obviously lower and the replications scattered clearly. Also the similarity coefficients (Fig. 9b) were more or less equal at K=3 to K=9. Estimations of mean ΔK (Fig. 9c) showed a clear peak at K=3, so this number of groups was chosen to be the most probable.

However, examinations of bar plots, which presented the Q-values of each cluster in single individuals, showed that only two of the three clusters were largely present in the dataset. The third cluster was represented in individuals with proportions <6% only. The bar plots at K=2 showed great admixture of the two clusters in all individuals. The two clusters were represented in the individuals at a minimum of 30% and a maximum of 70%. Bar plots at K=4

to $K=9$ were nearly identical to $K=3$. Each new K represented only a minor group of generally $<2.5\%$. These results strengthened the choice of $K=3$ as the most probable number of groups, even though the third cluster was only negligibly present.

As shown in the bar plots of single individuals (Fig. 10a), the line charts showing the Q -values of STRUCTURE clusters plotted against longitude (Fig. 11) and the map (Fig. 12), cluster 1 predominated in the individuals of the westernmost populations and in population AMM1 of the Ammersee region. The individuals of the remaining two populations of the Ammersee region (AMM2 and AMM3) comprised higher proportions of cluster 2, but nonetheless could be ascribed more likely to cluster 1, which predominated in these populations. In the more eastern Miesbach region, population GEO1 was admixed between the two clusters and was treated as intermediate. About half of the individuals were admixed (ascribed to the clusters with $<75\%$), the second half was ascribed to one of the two clusters ($>75\%$). Two and three individuals were ascribed to cluster 1 and 2, respectively. The remaining three populations of the Miesbach region (FEN1, KOE1 and MOO1) were mainly ascribed to cluster 2, but still showed high proportions of cluster 1 (29-38%). In populations from the Chiemsee region eastwards, the proportion of cluster 2 rose up to 71-99% and was highest in the eastern Flachgau/Attersee region. The geographical break between the two clusters could be cautiously located between the Ammersee and Miesbach regions, excluding the intermediate population GEO1 (see above). Table 4 shows the affiliation of *T. helenitis* populations to the STRUCTURE clusters and the geographic region. As shown in Figure 11a there was an overlap of standard deviations in proportions of STRUCTURE clusters in populations from the Ammersee region (AMM2 and AMM3) and the Miesbach region. Exclusion of admixed individuals (Fig. 11b-c) resulted in the loss of the whole population AMM3 and the ascribing of population AMM2 to cluster 1, while populations of the Miesbach region remained admixed. Nine individuals (Table 5) were identified as putative migrants between the two clusters. Three of them were also found in the NJ-analysis (AMM2_10, KOE1_15 and LAU1_18).

Correlations of mean proportions of the STRUCTURE clusters in populations with longitude or mean proportion of pubescent achenes of populations using SPEARMAN'S (1904) rho showed high correlation coefficients $>80\%$ and high significance (Table 6). Linear regressions resulted in a high regression coefficient when longitude was used as an independent variable (about 0.87) and a moderately high coefficient in the case of mean proportion of pubescent achenes (about 0.66).

Table 4. Populations of *Tephrosia helenitis* used for AFLP analyses and their affiliation to clusters formed by the program STRUCTURE and the geographic region, where populations are located.

population	STRUCTURE cluster	geographical region
ADN1+2	east	Salzach valley region
AMM1	west	Ammersee
AMM2	west	Ammersee
AMM3	west	Ammersee
BER4+5	east	Chiemsee
EST2	east	Salzach valley region
FEN1	east	Miesbach
FUS1	east	Eastern Flachgau/Attersee
GEO1	intermediate	Miesbach
GER1	east	Eastern Flachgau/Attersee
HAM1	west	Westernmost populations
HAS1	east	Eastern Flachgau/ Attersee
HAY1	west	Westernmost populations
KOE1	east	Miesbach
KOP1	east	Eastern Flachgau/Attersee
KUC1	east	Salzach valley region
LAN1	east	Salzach valley region
LAU1	east	Salzach valley region
MAR1	west	Westernmost populations
MOO1	east	Miesbach
NUS1	west	Westernmost populations
PAL1	east	Salzach valley region
SCH1	east	Salzach valley region
STI1	east	Eastern Flachgau/Attersee
UNT1	east	Salzach valley region
UNT2	east	Salzach valley region
UNT3	east	Salzach valley region
VIE1	east	Salzach valley region
WOE1	east	Eastern Flachgau/Attersee

Table 5. Individuals assigned to a STRUCTURE cluster, which does not predominate in the geographical region. Individuals with Q-values < 75% are treated as admixed.

	Individuals (code)	Q-value
Population located in cluster 2, individuals assigned to cluster 1	KOE1_15	> 90%
	FEN1_01	> 75%
	BER5_12	> 75%
	LAU1_18	< 75%
	LAU1_19	> 90%
	SCH1_03	> 75%
Population located in cluster 1, individuals assigned to cluster 2	AMM2_10	< 75%
	AMM3_05	< 75%
	HAM1_07	> 75%

Table 6. Correlations and regressions calculated for Q-values of different STRUCTURE and BAPS analyses with longitude and achene indumentum. Abbreviations: N, number of comparisons; n.s., not significant (P-value >0.05); ρ , Spearman's (1904) rank correlation coefficient; *, P-value < 0.001.**

Analysis	Comparison	N	ρ	P-value	Linear regression line fit	R	R ²	Adjusted R ²	P-value
STRUCTURE (independent allele frequencies)	Cluster 1 - longitude	28	-0.891	0.000 ***	$y = -0.938x + 3.377$	0.938	0.880	0.875	0.000 ***
	Cluster 2 - longitude	28	0.897	0.000 ***	$y = 0.937x - 2.372$	0.937	0.878	0.873	0.000 ***
	Cluster 1 - achene indumentum	28	0.827	0.000 ***	$y = 0.823x + 0.014$	0.823	0.677	0.665	0.000 ***
	Cluster 2 - achene indumentum	28	0.827	0.000 ***	$y = -0.824x + 0.981$	0.824	0.680	0.667	0.000 ***
STRUCTURE (correlated allele frequencies)	Cluster 1 - longitude	28	0.909	0.000 ***	$y = -0.943x + 2.946$	0.943	0.889	0.885	0.000 ***
	Cluster 2 - longitude	28	0.893	0.000 ***	$y = 0.809x - 2.091$	0.809	0.654	0.641	0.000 ***
	Cluster 3 - longitude	28	0.114	0.562 n.s.	$y = 0.057x + 0.145$	0.057	0.003	-0.035	0.772 n.s.
	Cluster 1 - achene indumentum	28	0.841	0.000 ***	$y = 0.821x + 0.066$	0.821	0.674	0.661	0.000 ***
	Cluster 2 - achene indumentum	28	0.778	0.000 ***	$y = -0.856x + 0.727$	0.856	0.733	0.722	0.000 ***
	Cluster 3 - achene indumentum	28	0.119	0.546 n.s.	$y = 0.203x + 0.206$	0.203	0.041	0.004	0.300 n.s.
BAPS (spatial admixture)	Cluster 1 - longitude	28	0.827	0.000 ***	$y = -0.886x + 4.420$	0.886	0.785	0.777	0.000 ***
	Cluster 2 - longitude	28	0.827	0.000 ***	$y = 0.886x - 3.420$	0.886	0.785	0.777	0.000 ***
	Cluster 1 - achene indumentum	28	0.827	0.000 ***	$y = 0.889x - 0.082$	0.889	0.790	0.782	0.000 ***
	Cluster 2 - achene indumentum	28	0.827	0.000 ***	$y = -0.889x + 1.083$	0.889	0.790	0.782	0.000 ***
BAPS (non-spatial admixture)	Cluster 1 - longitude	28	0.827	0.000 ***	$y = -0.901x + 3.440$	0.901	0.812	0.804	0.000 ***
	Cluster 2 - longitude	28	0.827	0.000 ***	$y = 0.901x - 2.440$	0.901	0.812	0.804	0.000 ***
	Cluster 1 - achene indumentum	28	0.827	0.000 ***	$y = 0.717x - 0.073$	0.717	0.514	0.495	0.000 ***
	Cluster 2 - achene indumentum	28	0.827	0.000 ***	$y = -0.717x + 1.073$	0.717	0.514	0.495	0.000 ***
	Longitude - achene indumentum	28	0.827	0.000 ***	$y = -0.815x + 3.850$	0.815	0.663	0.651	0.000 ***

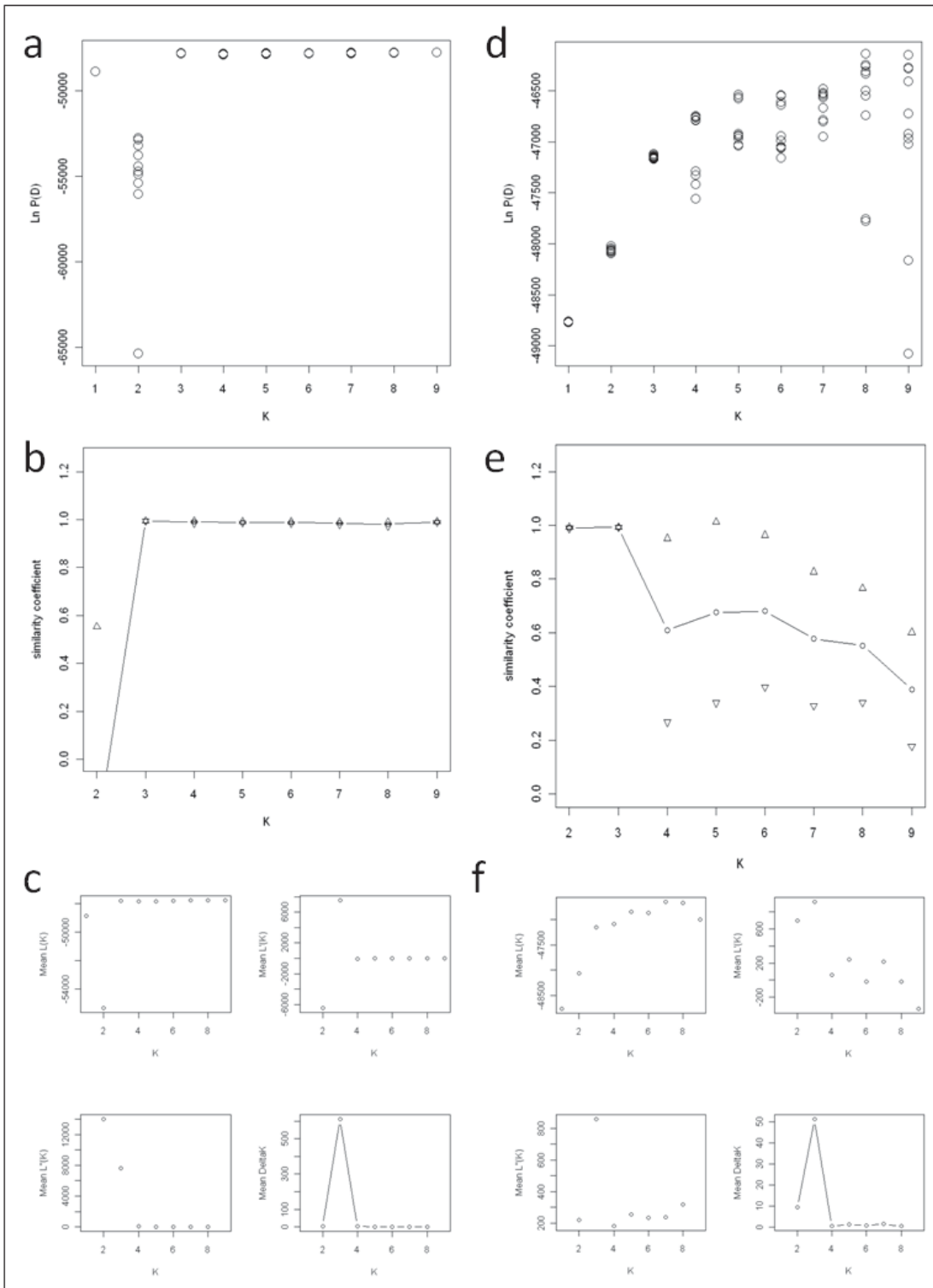


Figure 9. Likelihoods (a-b), similarities (c-d) and DeltaK (e-f) for STRUCTURE analyses using the recessive allele and the admixture model (independent allele frequency model: left side; correlated allele frequency model: right side) with K=1 to K=9.

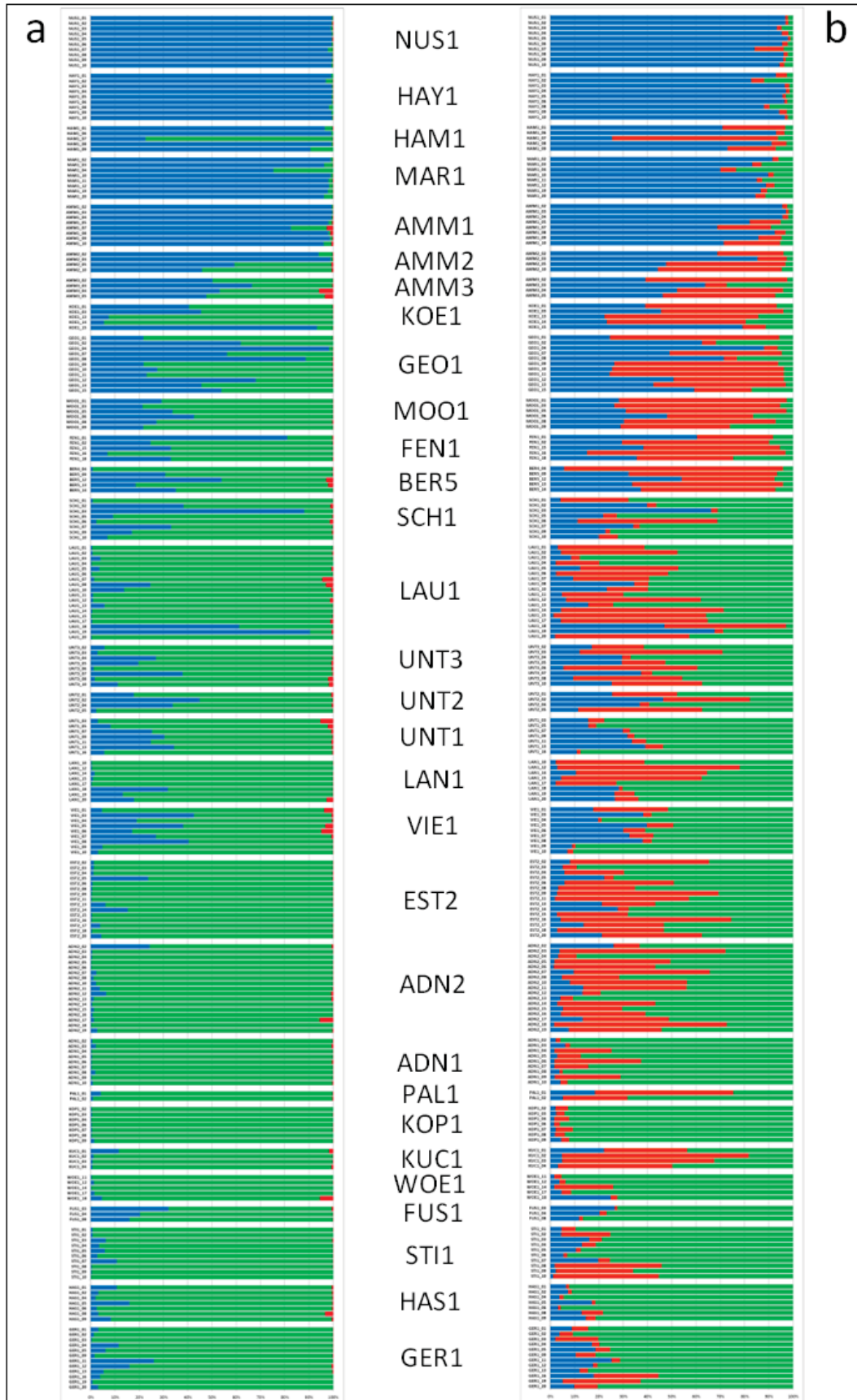


Figure 10. Bar plots displaying the Q-values of individuals for STRUCTION analyses with (a) the independent allele frequency model, and (b) the correlated allele frequency model. The blue color signs cluster 1, the green color cluster 2, and the red color cluster 3. Populations are sorted according to longitude i.e., the uppermost population is the most westerly.

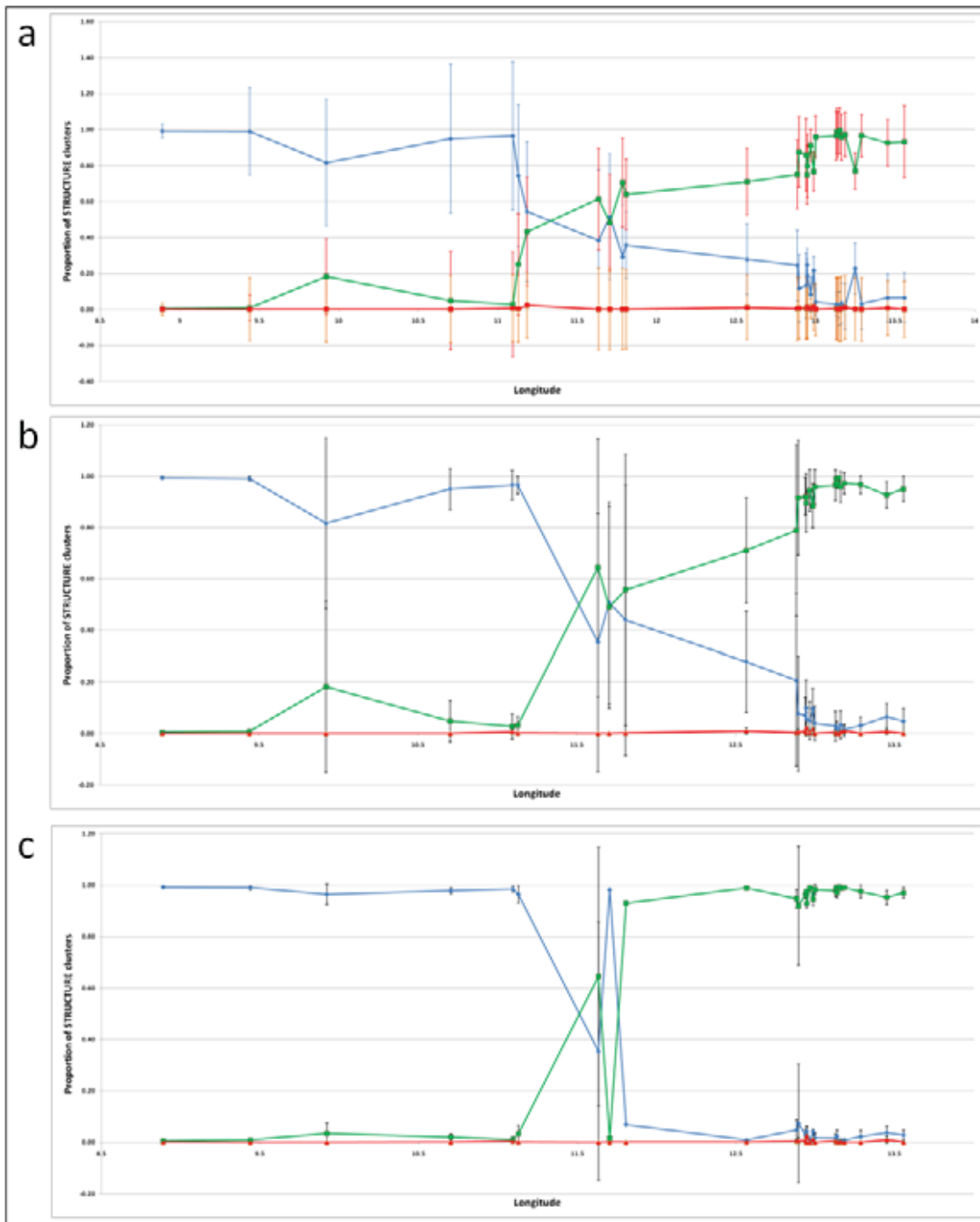


Figure 11. Line plots displaying the mean proportions (Q-values) of STRUCTURE clusters (independent allele frequency model) for each of the 29 *Tephroses helenitis* populations. They are sorted according to longitude (horizontal axis). The blue color signs cluster 1, the green color cluster 2, and the red color cluster 3. Standard deviations are displayed as vertical bars. Line plots are depicted for (a) all individuals, as well as individuals with Q-values >75% (b) and Q-values >90% (c).

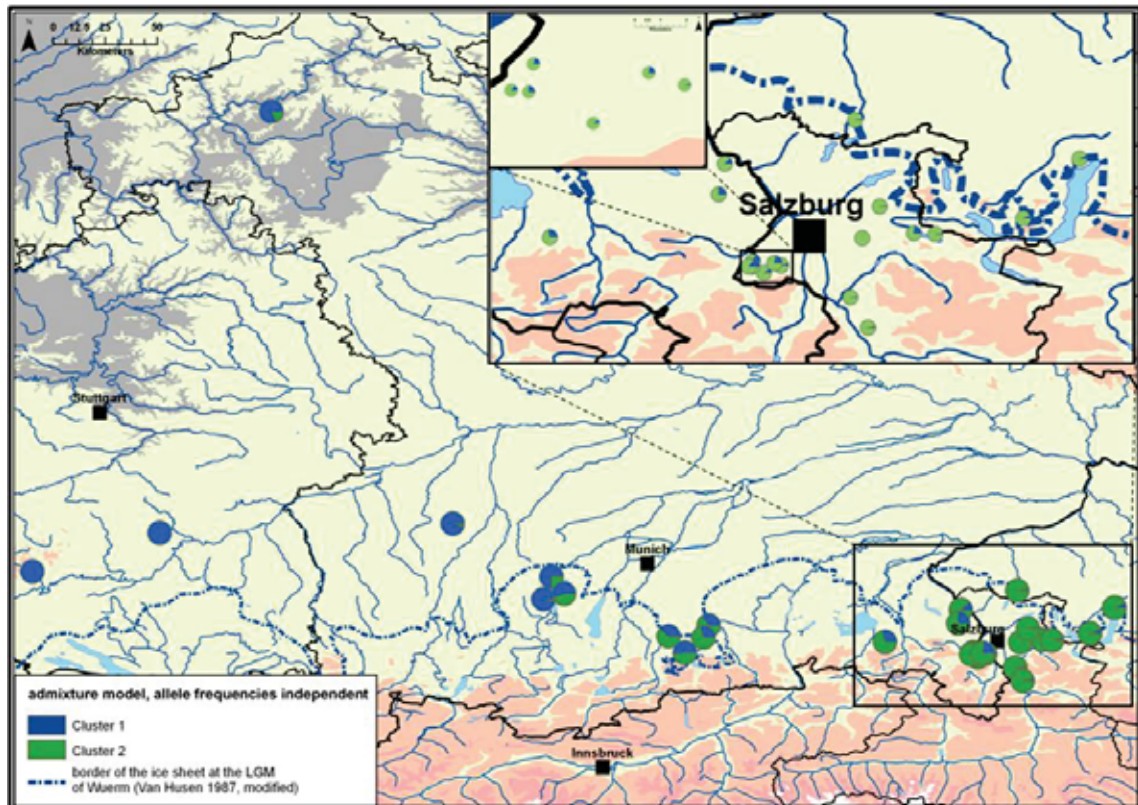


Figure 12. Spatial pattern of mean proportions (Q-values) of STRUCTURE clusters 1 vs. 2 (independent allele frequency model) for each of the 29 *Tephroses helenitis* populations.

3.2.2. STRUCTURE assignment tests using correlated allele frequencies

As shown in Figure 9d the likelihoods steadily increased until $K=9$, but the likelihoods of replications at $K=4$ to $K=9$ were scattered. From $K=1$ to $K=3$ the scatter was low and thus, favored an estimation of the best K . Similarity coefficients (Fig. 9e) showed their highest similarities at $K=2$ and $K=3$. Since estimates of mean ΔK (Fig. 9f) showed a peak at $K=3$, this number of clusters was taken as the best number of K .

Examinations of the bar plots at $K=3$ (Fig. 10b) showed results comparable to the model using independent allele frequencies. However, in contrast to the latter analysis, the third cluster was not negligible. As shown in Figures 13 and 14, the westernmost populations and population AMM1 were assigned to cluster 1 as in the independent allele frequencies model. Populations AMM2 and AMM3 showed higher values of cluster 3, which predominated in the populations of the adjacent Miesbach region (Q-values of about 50-60%) and the Chiemsee region (61%). Population GEO1 was intermediate between cluster 1 and cluster 3. Eastwards of the Chiemsee region proportions of cluster 1 and 3 decreased rapidly. Proportions of the two latter clusters were still noticeably higher in the Salzach valley region than in the more eastern Flachgau/Attersee region. As an exception population KUC1 comprised a higher proportion of cluster 3 (55%) than cluster 2 (36%), even though being situated in the Salzach valley region, where cluster 2 predominated. The line chart (Fig. 13a) displays the distribution of the three clusters in relation to longitude. Cluster 1 predominated from the Ammersee region westwards, cluster 2 in populations eastwards of the Chiemsee, and cluster 3 in-between the

latter two regions (Miesbach and Chiemsee). The exclusion of admixed individuals (< 75% and < 90% in Fig 13b and 13c, respectively) made that pattern even more distinct. Putative migrants among the three clusters were frequently found, whereas many of them were between cluster 2 and 3. Most of these migrants were admixed (Q-values of each cluster <75%). Only two individuals with a genotype of cluster 1 (Q-value >75%) were found in the region where cluster 3 predominates (GEO1_04, KOE1_15), and another two individuals with a cluster 3 genotype were found in the region where cluster 2 predominates (KUC1_02, LAN1_12). All of these putative migrants were assigned to one of the clusters with Q-values <90%.

Correlations of mean proportions of the STRUCTURE clusters in populations with longitude or mean proportion of pubescent achenes of populations using SPEARMAN'S (1904) rho showed high correlation coefficients for clusters 1 and 2 with high significances (Table 6). Correlations of cluster 3 showed weak correlation coefficients, which were not significant. Linear regressions revealed the highest regression coefficient when proportions of cluster 1 were correlated with longitude. It was lower for the regression of cluster 2 and longitude as well as the comparison of the latter two clusters with mean proportion of pubescent achenes.

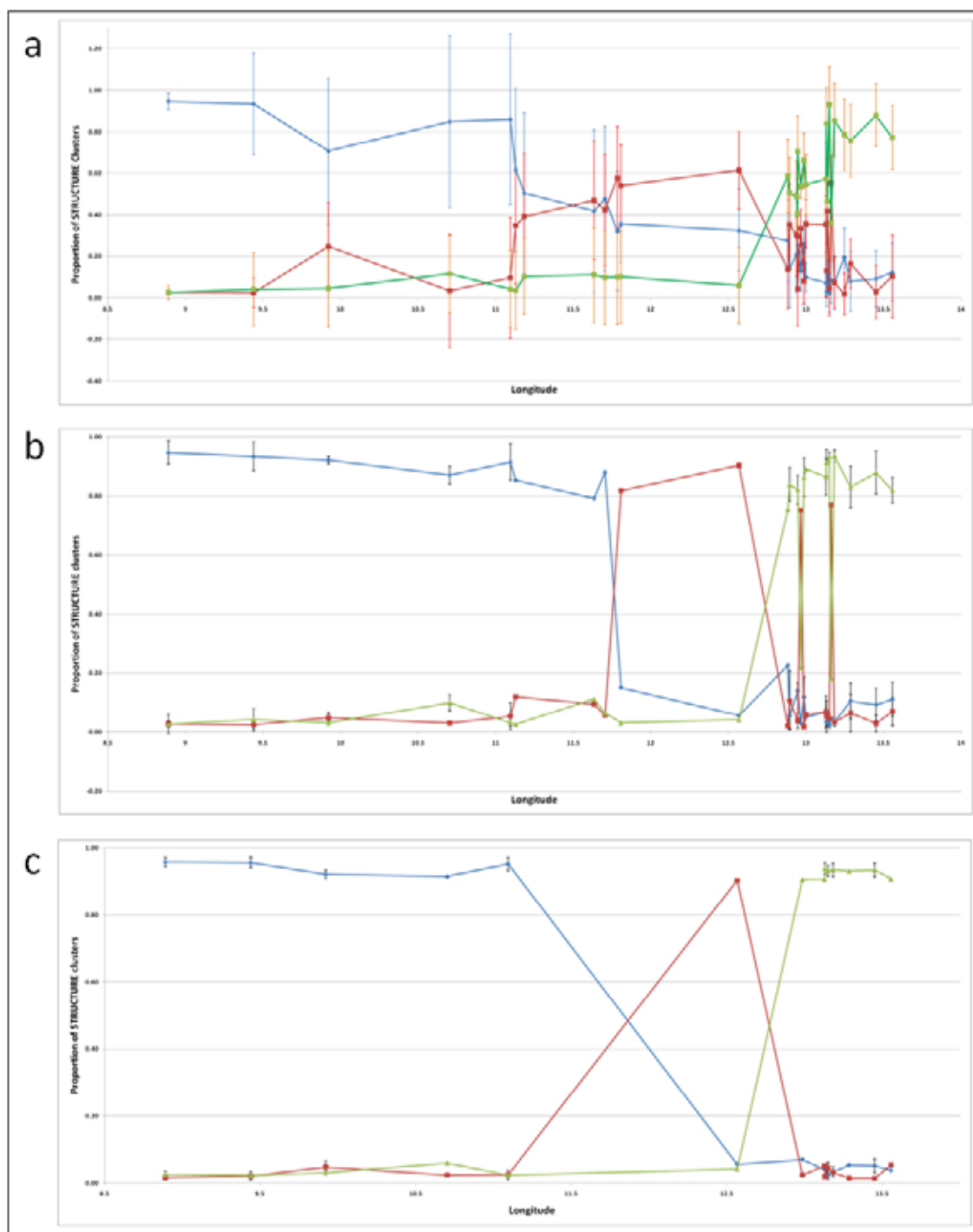


Figure 13. Line plots displaying the mean proportions (Q-values) of STRUCTURE clusters (correlated allele frequency model) for each of the 29 *Tephroses helenitis* populations according to longitude (horizontal axis). The blue color signs cluster 1, the green color cluster 2 and the red color cluster 3. Standard deviations are displayed as vertical bars. Line plots are depicted for (a) all individuals, as well as individuals with Q-values >75% (b) and Q-values >90% (c).

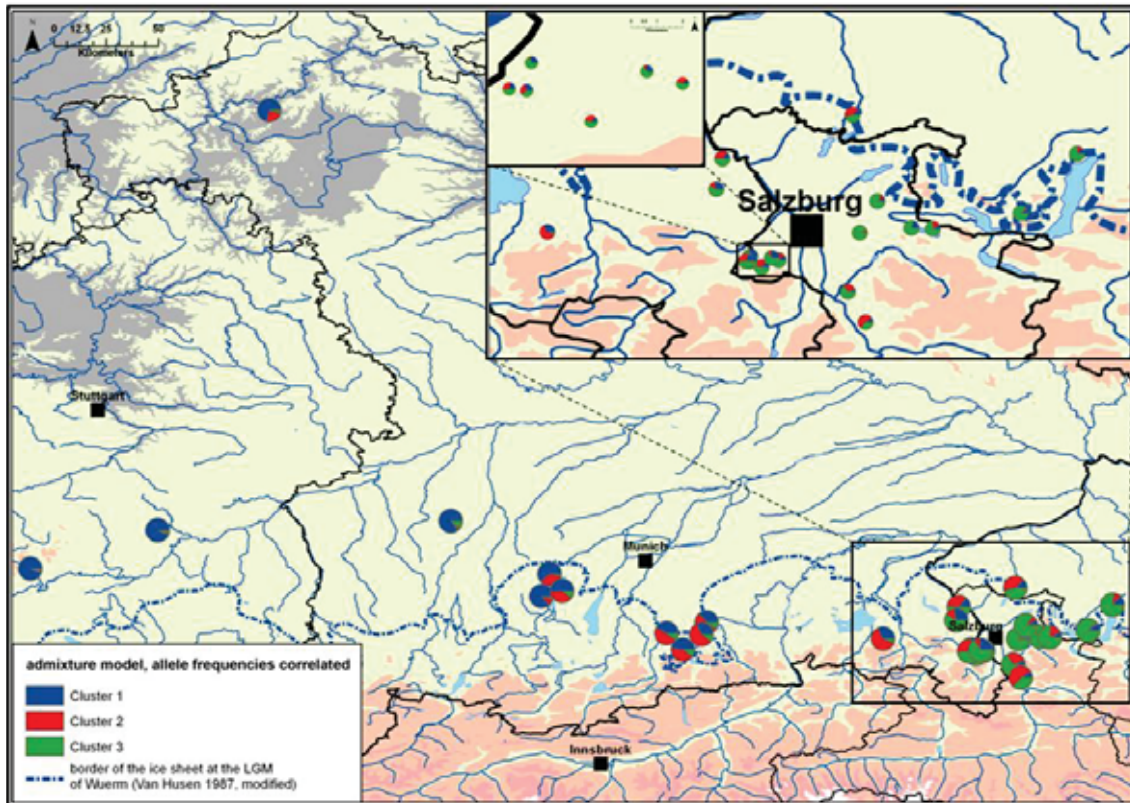


Figure 14. Spatial pattern of mean proportions (Q-values) of the three STRUCTURE clusters (correlated allele frequency model) for each of the 29 *Tephrosieris helenitis* populations.

3.2.3. BAPS non-spatial clustering

As shown in the bar plots (Fig. 15a-b) and the map (Fig. 16) the mixture clustering as well as the admixture clustering using the program BAPS was similar to results of STRUCTURE using the independent allele frequency model. The non-spatial analyses resulted in two clusters, whereby cluster 1 was distributed in the westernmost populations and in population AMM1. Under the admixture clustering model populations AMM2 and AMM3 were admixed between the two clusters, whereby AMM2 had a Q-value of 68% for cluster 1 compared to 18% in population AMM3. In the adjacent Miesbach region cluster 2 predominated (74-80%; population MOO1: 100%). From the Chiemsee region eastwards populations were exclusively ascribed to cluster 2; only two individuals were admixed (BER5_12, LAU1_18) and two individuals were assigned to cluster 1 (LAU1_19, SCH1_03). All of them had been identified in the STRUCTURE analysis using the independent allele frequencies model, too. Considering the proportions of BAPS clusters in populations depending on their longitude (Fig. 17a) revealed an unclear separation of the two clusters in the Ammersee region.

Correlations of mean proportions of the BAPS clusters in populations were performed with longitude or mean proportions of pubescent achenes of populations using SPEARMAN's (1904) rho. High correlation coefficients with high significance were found in the comparison with longitude and moderate values in the comparison with achene indumentum (Table 6). Linear regressions also showed high values for the comparison with longitude and moderate values for the comparison with achene indumentum. All of them were highly significant.

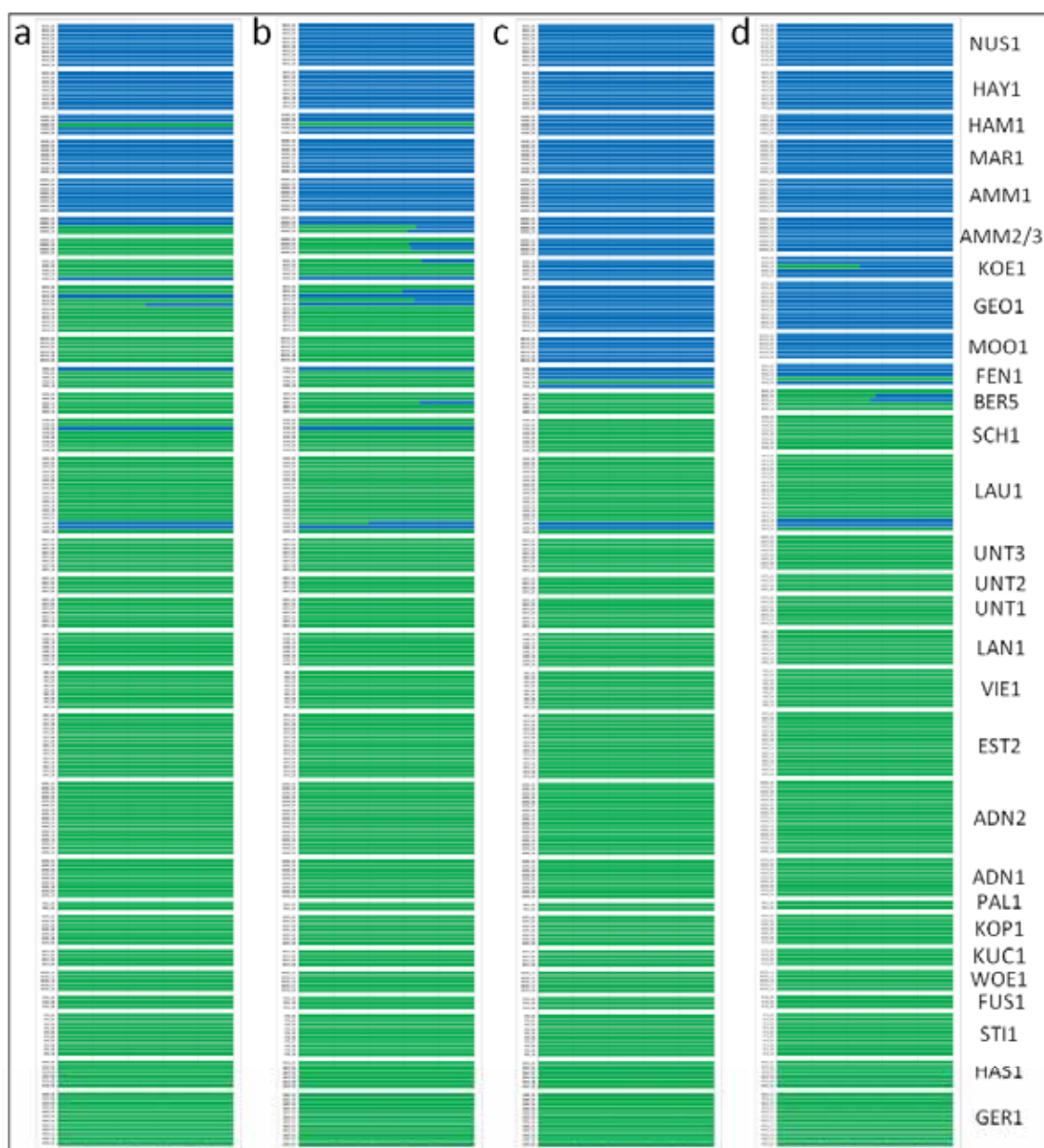


Figure 15. Bar plots displaying the assignment of individuals to BAPS clusters. The figure displays results obtained under (a) the non-spatial mixture model, (b) the admixture model based on the non-spatial mixture model, (c) the spatial mixture model and (d) the admixture model based on the spatial mixture model. The blue color signs cluster 1 and the green color cluster 2. Populations are sorted according to longitude, i.e. the uppermost population is the most westerly.

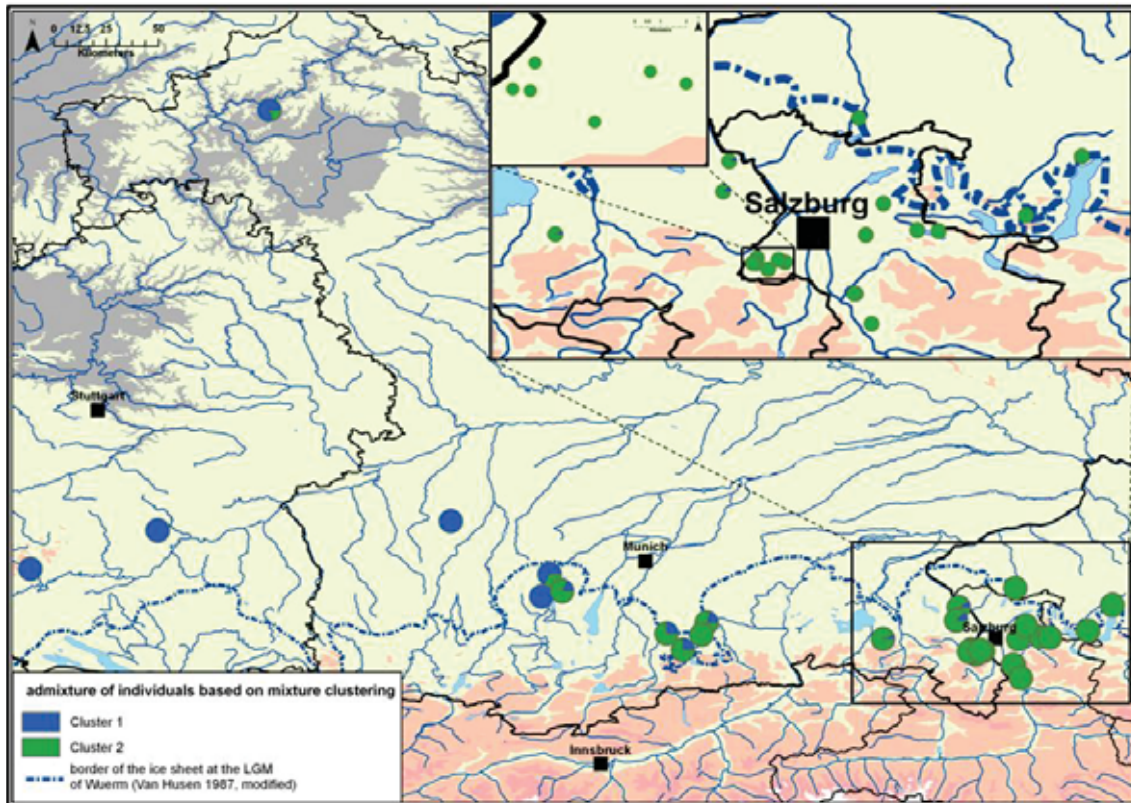


Figure 16. Spatial pattern of mean proportions of BAPS clusters 1 vs. 2 (admixture model based on the non-spatial mixture model) for each of the 29 *Tephroses helenitis* populations.

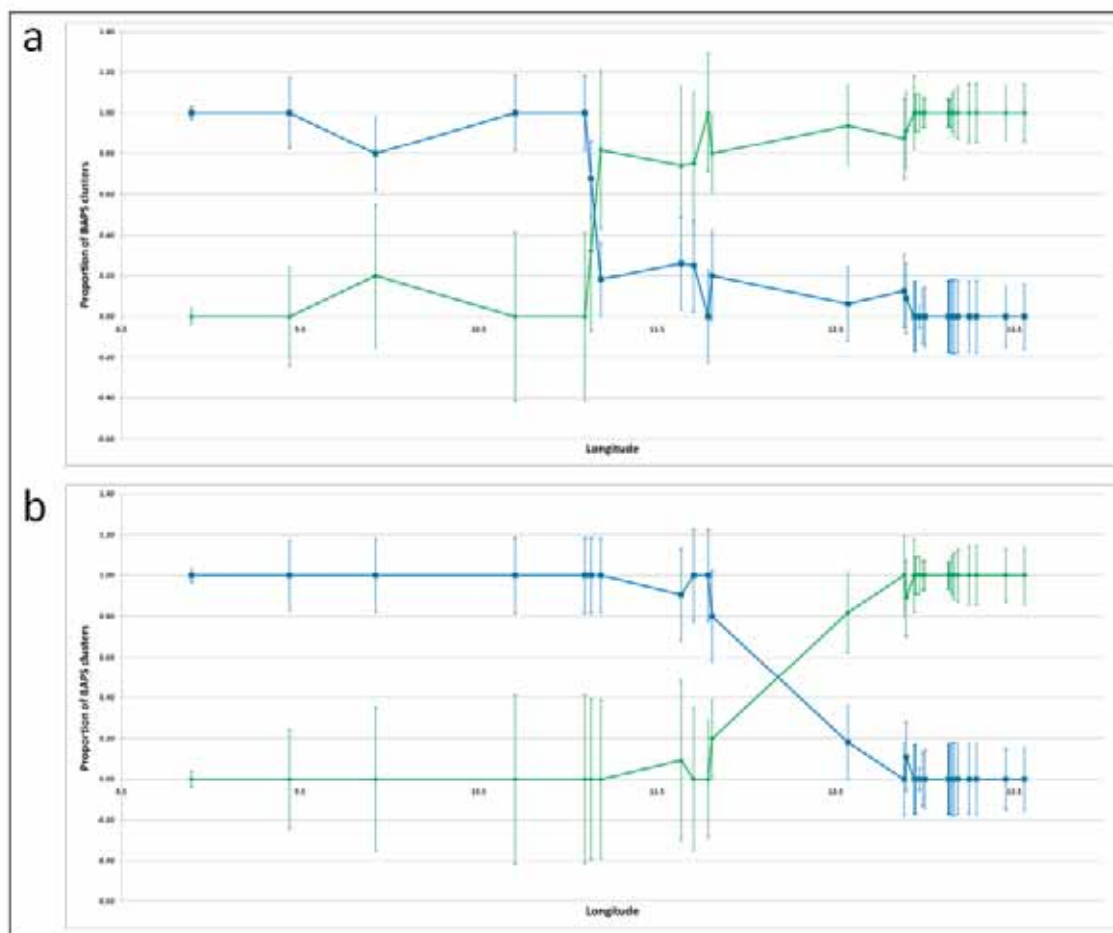


Figure 17. Line plots displaying the mean proportions of BAPS clusters for each of the 29 *Tephroses helenitis* populations according to longitude (horizontal axis). Line plots are depicted for admixture models based on (a) the non-spatial mixture model, and (b) the spatial mixture model. The blue color signs cluster 1 and the green color cluster 2. Standard deviations are displayed as vertical bars.

3.2.4. BAPS spatial clustering

Results of the BAPS analyses of spatial mixture and admixture clustering were nearly identical to those of the non-spatial approach revealing two clusters (Fig. 15c-d). Only three individuals were identified as admixed (BER5_09, BER5_12 and KOE1_13). As shown in Figures 18 and 19, cluster 1 predominated in the westernmost populations, i.e., the whole Ammersee and Miesbach region. From the Chiemsee region eastwards, cluster 2 predominated. Putative migrants between the two clusters were FEN1_16, LAU1_18 and LAU1_19. Individuals BER5_09 and BER5_12 showed admixed genotypes. The line chart (Fig. 17b) shows a very clear separation of the two clusters in relation to longitude.

Correlations of mean proportions of the BAPS clusters in populations were performed with longitude or mean proportion of pubescent achenes of populations using SPEARMAN'S (1904) rho. High correlation coefficients with high significance were found in all comparisons (Table 6), and the same was true for the linear regressions.

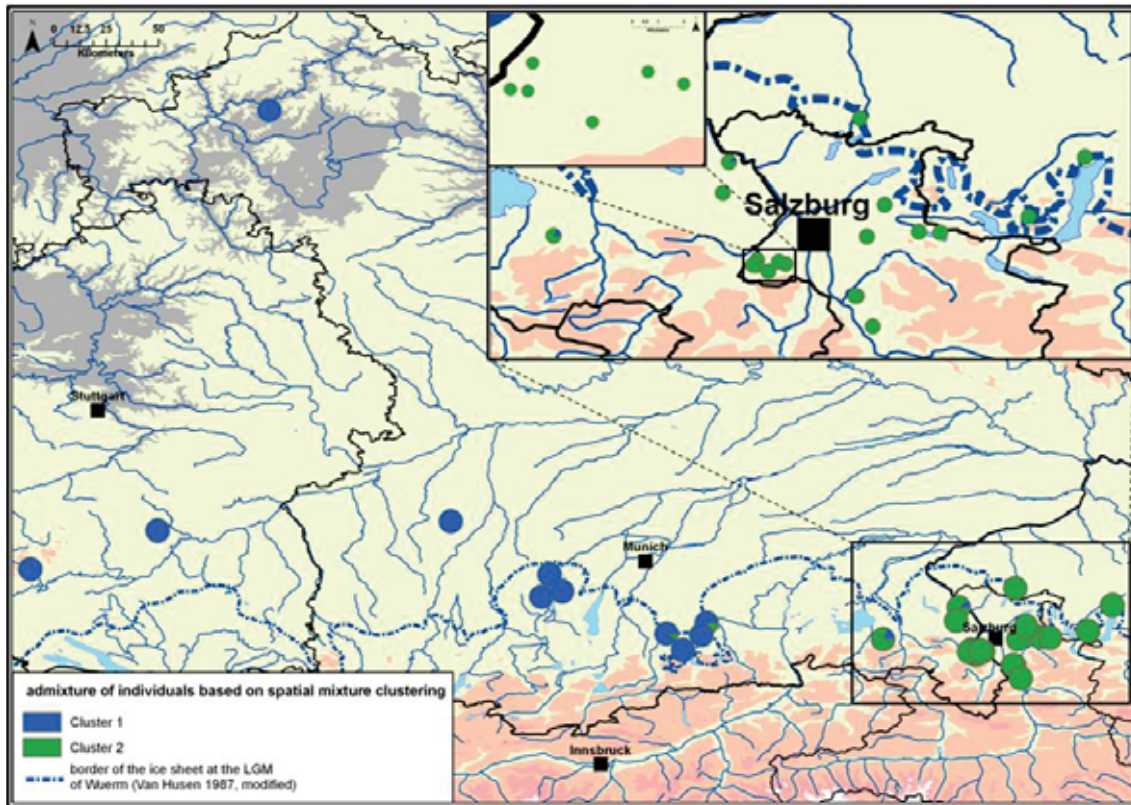


Figure 18. Spatial pattern of mean proportions of BAPS clusters 1 vs. 2 (admixture model based on the spatial mixture model) for each of the 29 *Tephroses helenitis* populations.

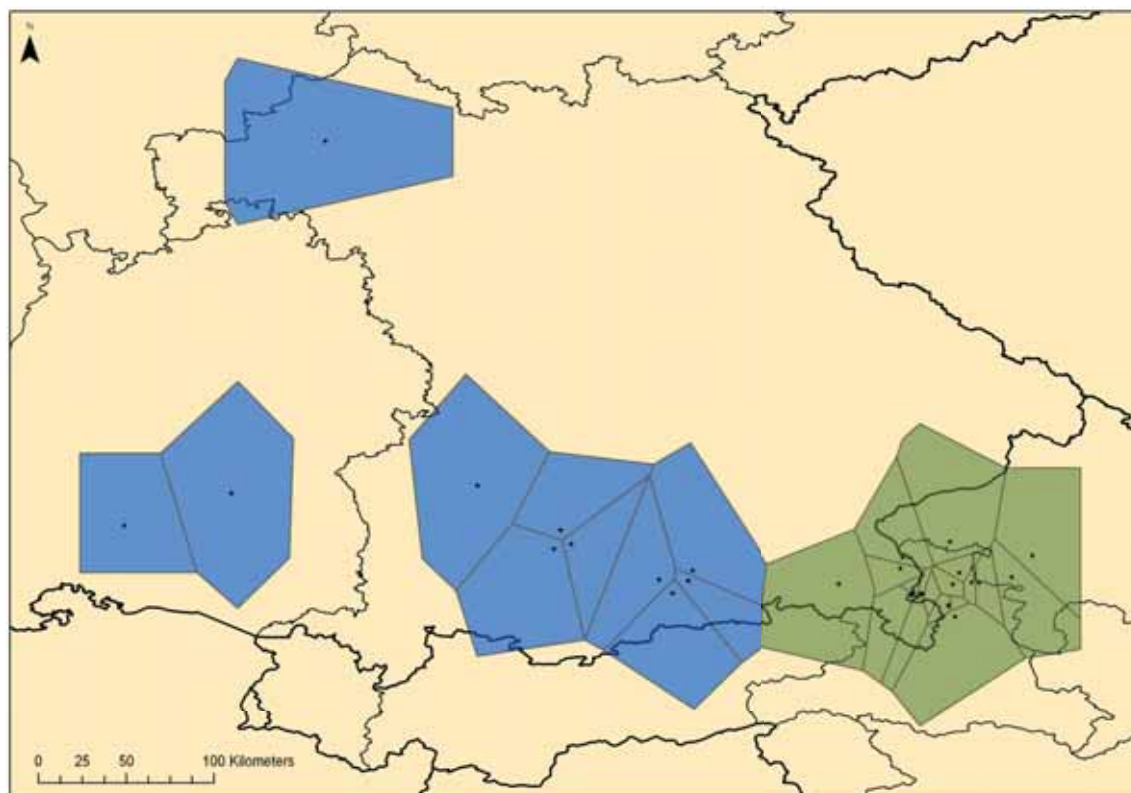


Figure 19. Spatial pattern of Voronoi tessellations of single populations resulting from BAPS (non-spatial mixture model) for 29 *Tephroses helenitis* populations. The blue color signs cluster 1 and the green color cluster 2.

3.3. Genetic relationships

3.3.1. Individual-based relationships

An individual-based NJ tree (Fig. 20) was calculated for 250 individuals (including 17 outgroup individuals) using the genetic distance of NEI & LI (1979). In comparison to the four outgroup species, *T. helenitis* formed a monophyletic group with a bootstrap support of 91%. The individuals generally showed only weak differentiation. Bootstrap values higher than 70% for groups with three or more individuals were nearly absent. Only three small groups of individuals were supported with moderate bootstrap values (86% for HAY1_01, HAY1_03 and HAY1_04; 70% for MOO1_03, MOO1_05, MOO1_06, MOO1_08 and MOO1_09; 86% for MOO1_03, MOO1_05 and MOO1_06).

Individuals were mainly grouped to their assignment of populations, but only rarely formed groups consisting exclusively of individuals of one population. Frequently, one or more individuals of other populations were nested within these groups; only the four westernmost populations (HAM1, HAY1, MAR1 and NUS1) formed exclusive groups.

The two clusters resulting from the STRUCTURE analysis (see section 3.2) were distinguished in the NJ-analysis, too. Population GEO1 could not be ascribed to any of these clusters and was treated as intermediate. The clusters could be substructured into smaller geographical regions (Table 4). The western cluster was subdivided into the “westernmost populations” (four populations) and the Ammersee region (three populations). The eastern cluster was separated into the Chiemsee region (one population), the Salzach valley region (eleven populations) and the “eastern Flachgau/Attersee” (six populations). The region “Miesbach” consisted of the population of the intermediate cluster (GEO1) and three populations of the eastern cluster.

Five individuals of populations, which are geographically located in the area of the eastern cluster, were nested within the western cluster in the NJ tree. Four individuals were from Miesbach (FEN1_02, KOE1_01, KOE1_13 and KOE1_15), which was geographically closest to the western cluster (Ammersee) and one individual from the Salzach valley region (LAU1_18). Vice versa one individual (AMM2_10) from a western cluster population was nested within the eastern cluster in the NJ-Tree.

The two subspecies of *T. helenitis* could not be differentiated in the NJ-Tree, even though the western and intermediate clusters consisted exclusively of individuals with pubescent achenes (inclusively the five above-mentioned individuals of the populations in the eastern cluster), while two third of the eastern cluster consisted of individuals with glabrous achenes (without Miesbach and Chiemsee: three quarters showed glabrous achenes). As shown in Figure 20 the individuals of the eastern cluster did not form a cohesive group in terms of achene indumentum type. Among individuals with pubescent achenes only these from Miesbach and the Chiemsee region formed cohesive groups, which were not supported by bootstrap values, however.

Results of the NeighborNet-tree (Fig. 21) generally agreed with results of the NJ tree. Individuals formed a “star-like pattern”, which did not demonstrate clear clusters and only weak genetic differentiation, where only the outgroup samples formed separate groups. Despite the weak differentiation STRUCTURE clusters were visible as in the NJ analysis. The

eastern cluster was subdivided into two parts through the outgroup samples. Herein, the “Salzach valley region” was divided into three parts.

Three individuals of eastern cluster populations (FEN_02, LAU1_18 and LAU1_19) were nested within the western cluster and one individual of the western cluster populations (AMM2_10) was nested in the eastern cluster. AMM2_10, LAU1_18 and FEN1_02 were also “mismatched” in the NJ-analysis, but LAU1_19 only in the NeighborNet-analysis. In contrast to the NJ tree, three individuals of population KOE1 were not nested in the western cluster.

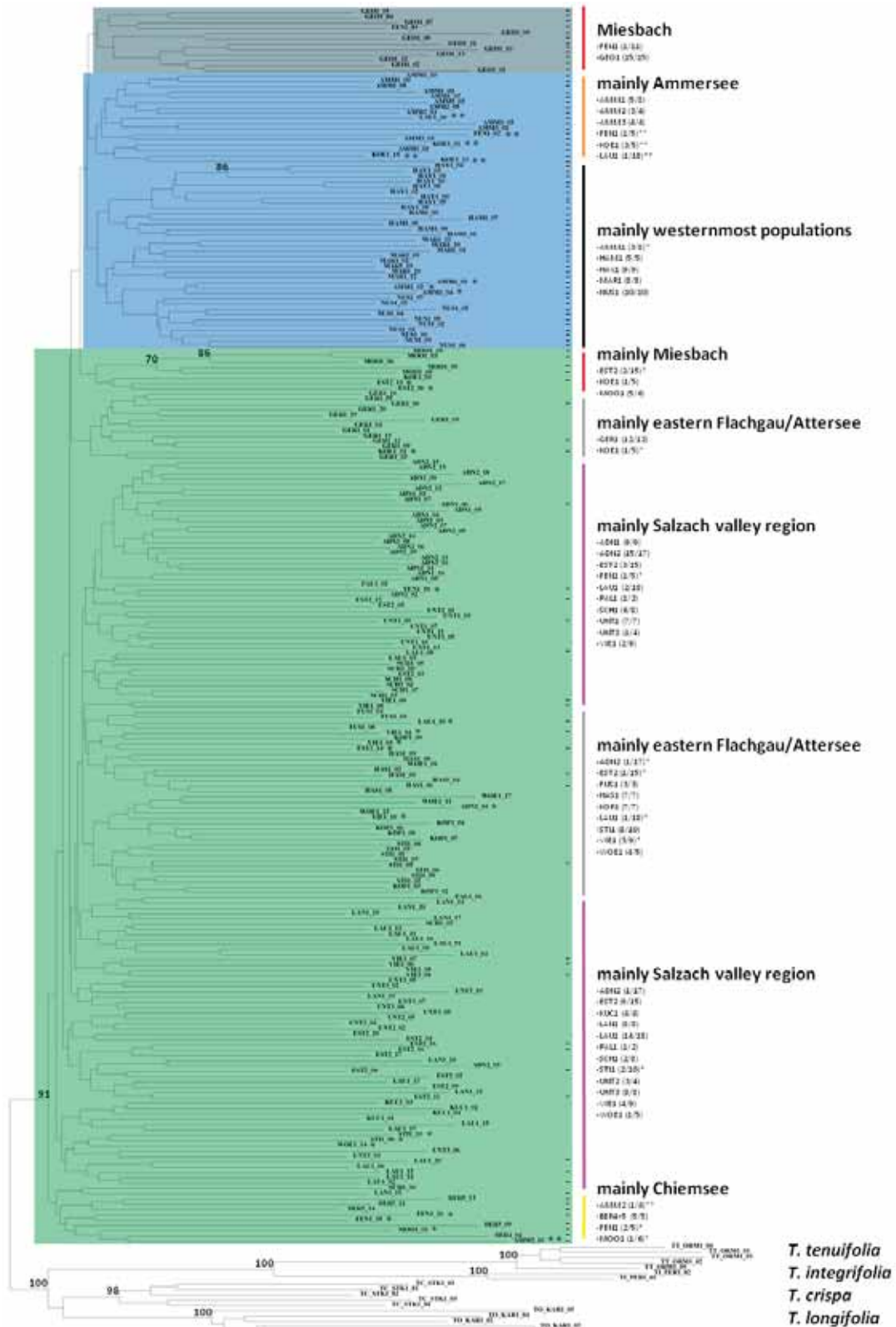


Figure 20. Individual-based NJ tree of 233 *Tephrosieris helenitis* individuals based on AFLP data, rooted with four outgroup populations. Bootstrap values >70% are shown along branches. The background color separates the clusters resulting from the program STRUCTURE (independent allele frequency model), whereby the blue color marks cluster 1, the green color cluster 2 and the grey color the intermediate population GEO1. An asterisk indicates individuals, which are not from the region described on the right side of the tree. Two asterisks indicate individuals, which belong to populations of the other STRUCTURE cluster. Dashes on the right margin of the colored background indicate individuals with pubescent achenes. The brackets next to population names (below the region names) show the number of individuals within this region, defined by vertical bars, compared to the total number of individuals for this population.

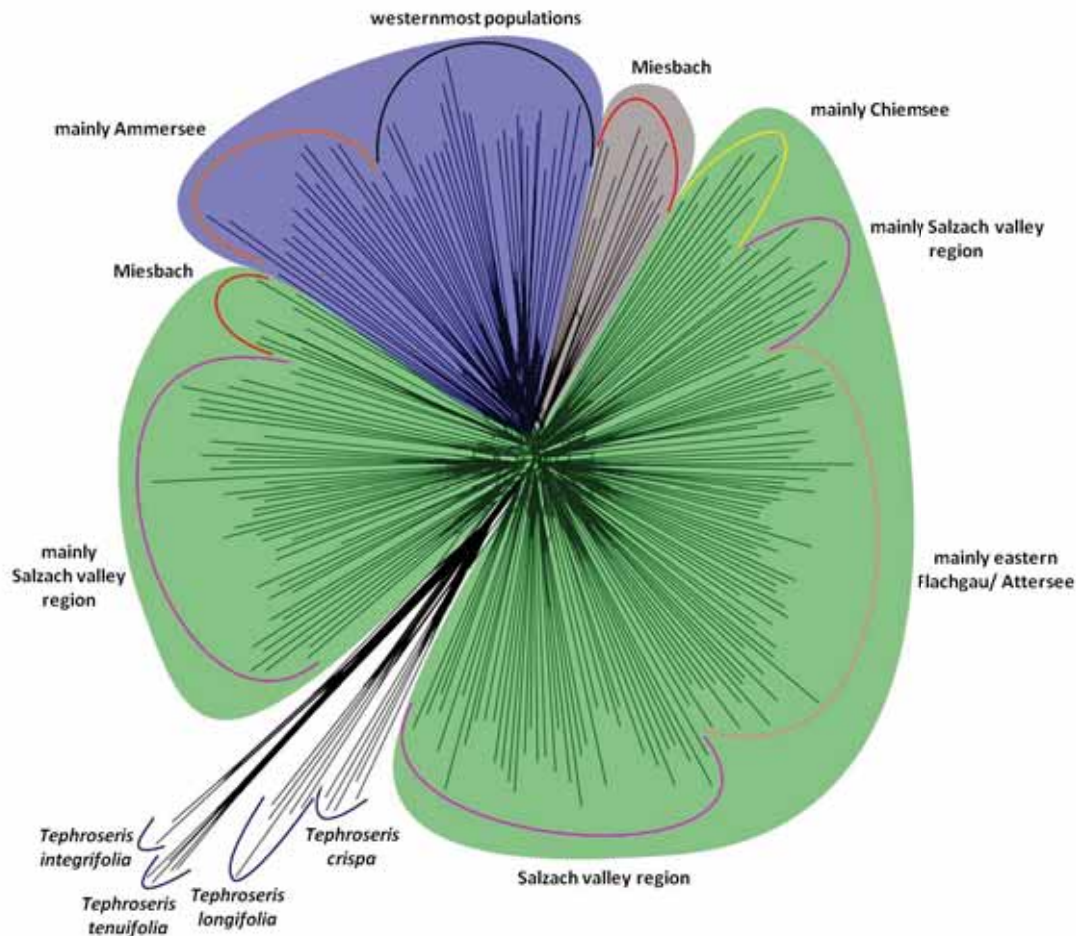


Figure 21. Individual-based NeighborNet graph of 233 *Tephroservis helenitis* individuals and four outgroup populations based on AFLP data. The background color separated the clusters resulting from the program STRUCTURE (independent allele frequency model), whereas the blue color marks cluster 1, the green color cluster 2 and the grey color the intermediate population GEO1. Region names are displayed next to the brackets.

3.3.2. Population-based relationships

All calculations were performed for populations with five or more individuals, only. Populations with four or less individuals were excluded.

A rooted NJ-Tree based on Nei & Li's (1979) genetic distance was calculated for 27 populations (including four outgroup populations; Fig. 22). The ingroup (*T. helenitis*), as well as all outgroup species formed groups, which were supported with 100% bootstrap values. Within the ingroup the only bootstrap values higher than 70% as found for the branch subtending the two subpopulations ADN1 and ADN2 (92%).

It was possible to visualize the clusters, which were formed by STRUCTURE, in the population-based NJ-analysis (like for the individual-based analyses). The western populations formed a monophyletic group, except population HAM1, which was nested within the eastern populations. A geographic structure within these clusters could be identified with the latter mentioned exception, too. Genetic differentiation was better displayed than in the individual-based NJ tree. The populations of the Miesbach region, which were ascribed to the eastern cluster, formed a group, as well as the Chiemsee region population and the populations of the Flachgau and adjacent areas.

An unrooted population-based NJ-analysis based on the genetic distance of Nei (1972) was performed for 23 populations of *T. helenitis* (Fig. 23). Two major clusters were identified, which fit to STRUCTURE results. The western cluster was strongly supported (90% bootstrap values) and was not found in the other analyses of genetic relationships. However, the eastern cluster was not supported by any bootstrap values higher than 70%. Like regions within the clusters could be identified in the unrooted NJ tree as in the rooted NJ tree, the unrooted NJ tree was structured along a west-east-direction, starting from the westernmost populations at one end of the tree across Ammersee, Miesbach/Chiemsee, and Salzach valley region to the eastern Flachgau/Attersee at the other end of the tree. Population GEO1, which was not ascribed to a cluster, even nested within the eastern cluster and grouped with populations from the regions Miesbach and Chiemsee, to which GEO1 geographically belongs to. Within these regions there was a 73% bootstrap support between the populations FEN1 and BER5. This group was not found in other analyses of genetic relationships. Populations from the Miesbach and Chiemsee region tended to group together, like these from the eastern Flachgau/Attersee and the Salzach valley region (except SCH1 and VIE1). The Salzach valley region was only weakly differentiated from the eastern Flachgau/Attersee region. Only subpopulations ADN1 and ADN2 (98% bootstrap support) were genetically more distant to the remaining populations from the Salzach valley region.

The population-based NeighborNet-Tree was calculated for 27 populations (including the four outgroup populations; Fig. 24). The outgroup was well separated from the *T. helenitis* populations. A tentative differentiation of groups was visible in the tree, comparable to the population-based NJ-analysis. The outgroup was again nested within the eastern cluster. While the populations of the Salzach valley and the eastern Flachgau/Attersee region formed a group, the populations of the geographically more western Miesbach and Chiemsee region grouped with populations of the west.

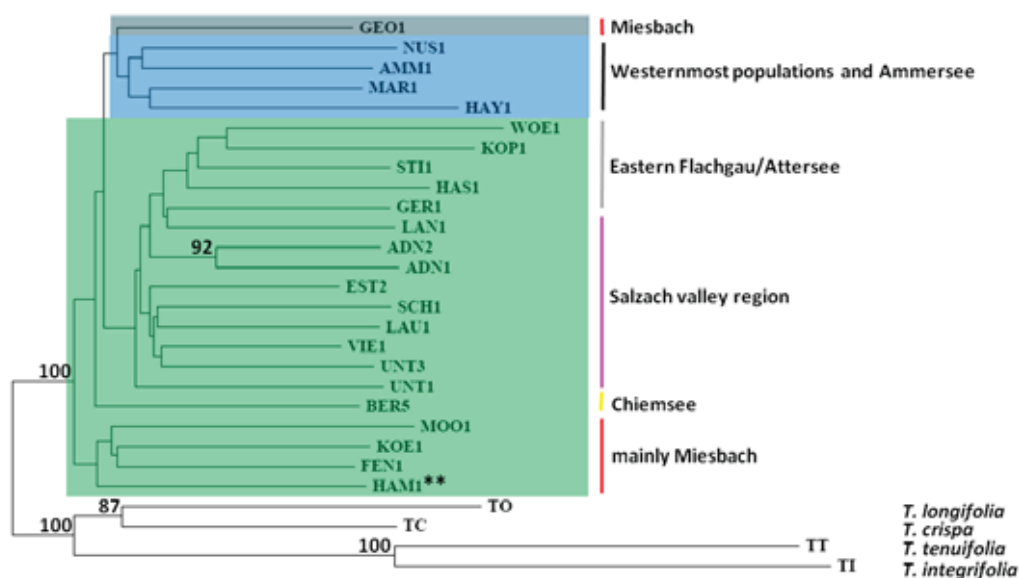


Figure 22. Population-based NJ-tree of 23 *T. helenitis* populations based on AFLP data (the two subpopulations ADN1+2 are counted as one population) and four outgroup populations. Only populations ≥ 5 individuals were taken into account. Bootstrap values $>70\%$ are shown along branches. The background color separate the clusters resulting from the program STRUCTURE (independent allele frequency model), whereas the blue color marks cluster 1, the green color cluster 2 and the grey color the intermediate population GEO1. Two asterisks indicate individuals, which belong to populations of the other STRUCTURE cluster. Region names are displayed next to the vertical bars.

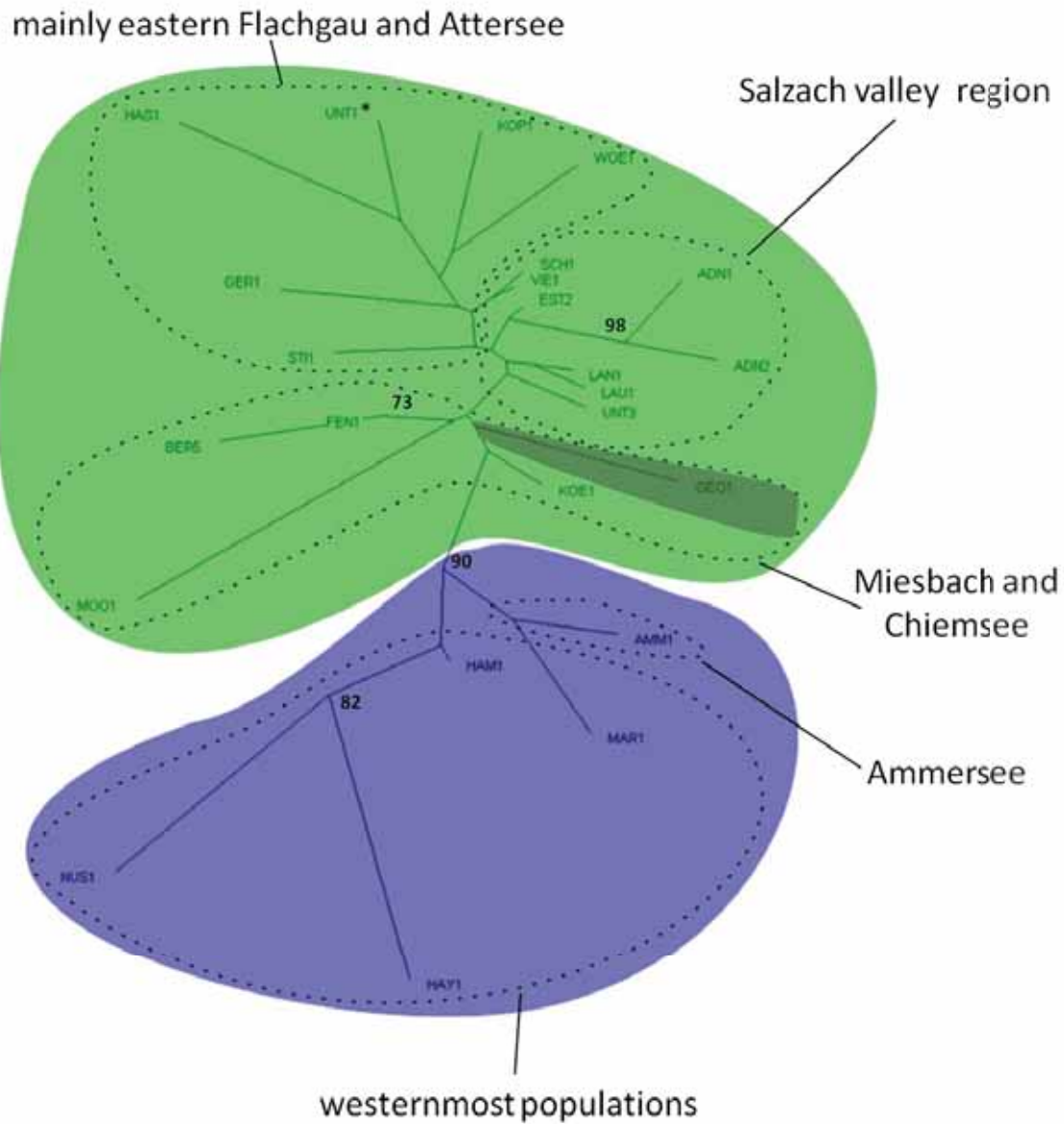


Figure 23. Unrooted population-based NJ-network of 23 *T. helenitis* populations based on AFLP data (the two subpopulations ADN1+2 are counted as one population). Only populations ≥ 5 individuals were taken into account. Bootstrap values $>70\%$ are shown along branches. The background color separates the clusters resulting from the program STRUCTURE (independent allele frequency model), whereby the blue color marks cluster 1, the green color cluster 2 and the grey color the intermediate population GEO1. An asterisk indicates individuals, which are not from the region described on the right side of the tree. Regions are defined by dotted lines.

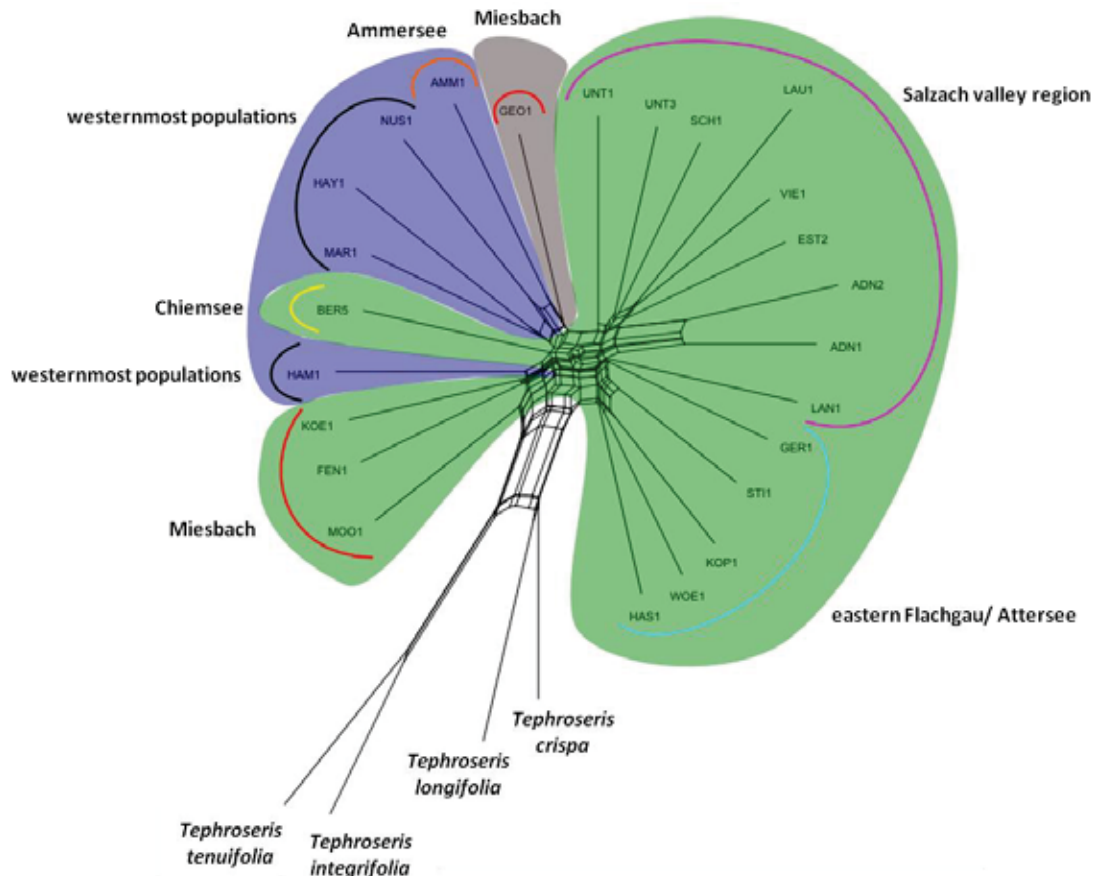


Figure 24. Population-based NJ-tree of 23 *T. helenitis* populations based on AFLP data (the two subpopulations ADN1+2 are counted as one population) and four outgroup populations. Only populations ≥ 5 individuals were taken into account. The background color separates the clusters resulting from the program STRUSTRUCTURE (independent allele frequency model), whereby the blue color marks cluster 1, the green color cluster 2 and the grey color the intermediate population GEO1. Region names are displayed next to the brackets.

3.4. Principal coordinates analysis (PCoA)

The individual-based PCoA based on DICE' (1945) similarity coefficient was performed for 233 individuals of *T. helenitis*. As shown in Figure 25, individuals were only weakly differentiated. Only the subpopulations ADN1 and ADN2 (blue ring) were separated from the remaining individuals along axis 3 (Ax3). Referring to the results of STRUSTRUCTURE (see section 3.2), the two clusters (independent allele frequency model; Fig. 25a-b) and three clusters (correlated allele frequency model; Fig. 25c-d) were utilized to label the individuals in the PCoA. The two clusters of the independent allele frequency model were separated along the first axis (Ax1). If individuals with admixed genotypes (<75% ascribed to one of the clusters) were not taken into account, then the two clusters could be separated along Ax1 very well. Taking the three STRUSTRUCTURE clusters into account (correlated allele frequency model), the PCoA plot showed more admixed individuals. The first axis mainly separated cluster 1 from clusters 2 and 3, while the second axis mainly separated cluster 2 from cluster 3. Excluding admixed individuals, the groups became more distinct.

Scores of individuals along Ax1 were also plotted against the longitude (Fig. 26). This revealed that the individuals were distributed clinally along the longitudinal axis with an R^2 of

0.581 (Fig. 26a). A separation of individuals due to their achene type was not possible through the scores of the Ax1 (Fig. 26b). The scores of the individual-based Ax1 are highly significant ($P < 0.001$) and slightly correlated with longitude (Spearman's $\rho = 0.596$). The linear regression was also highly significant ($P < 0.001$) with a line fit of " $y = 0.762x - 0.512$ ".

Figure 27 displays the population-based PCoA, which was performed for 29 populations (the two subpopulations ADN1 and ADN2 were presented as separate samples) based on Dice' similarity coefficient. The differentiation among the populations was weak, except for population PAL1 (represented by only two individuals in the dataset), which was separated by Ax2. Referring to the results of STRUCTURE (independent allele frequency model; Fig. 27a-b) there was no clear separation of the two clusters. About four populations of the eastern distributed cluster 2 grouped with cluster 1 populations. Considering the three clusters of the correlated frequency model (Fig. 27c-d), the four populations could be unraveled as populations from the Miesbach and Chiemsee region (cluster 3). Therefore, it was possible to separate cluster 2 by Ax1 and clusters 1 and 3 by Ax2. The first axis of the PCoA is plotted against the longitudinal position of the populations (Fig. 28). The trend line showed a high R^2 (0.84), which means that the clinal distribution along this axis was highly supported. The scores of the population-based PCoA-Ax1 were highly significant ($P < 0.001$) and strongly negatively correlated with longitude (Spearman's $\rho = -0.907$).

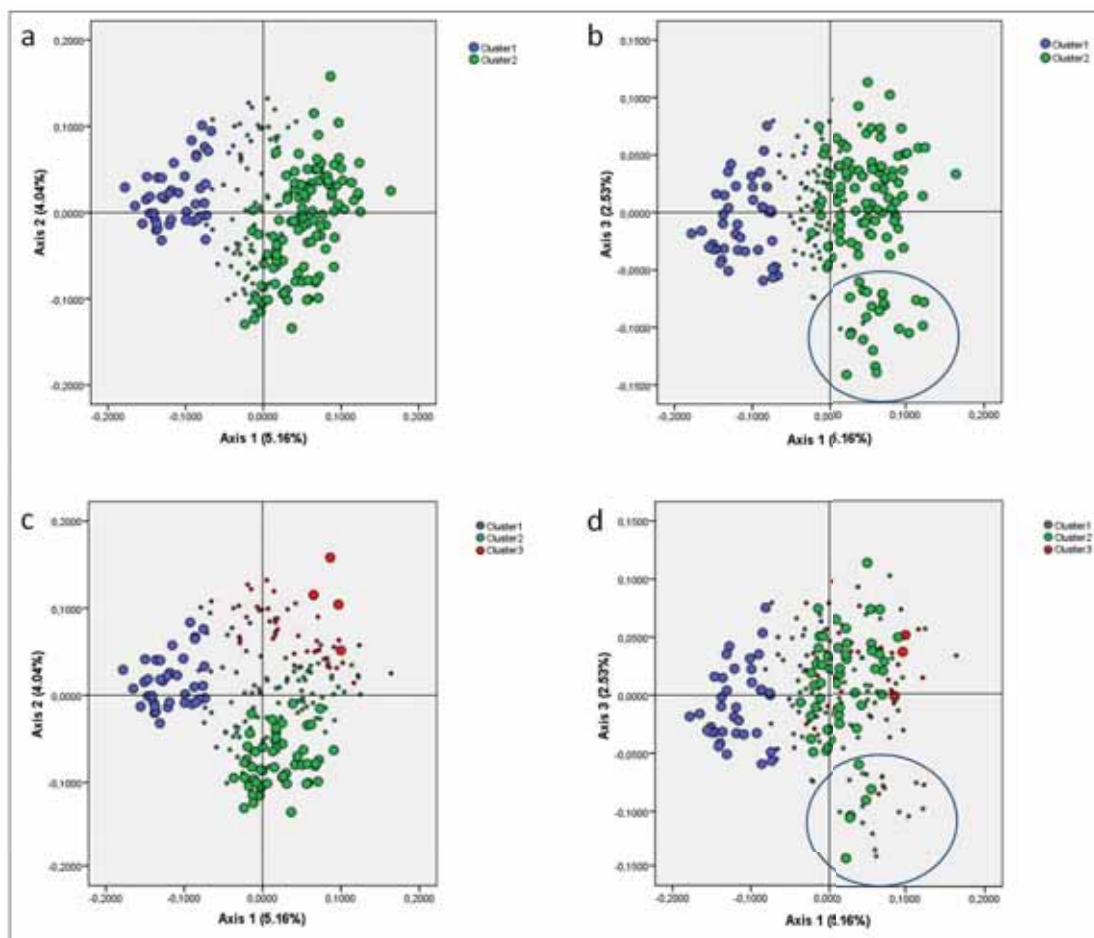


Figure 25. Principal coordinates analysis (PCoA) of 233 *T. helentis* individuals based on their AFLP profiles. Individuals are labeled according to their assignment to STRUCTURE clusters under (a-b) the independent allele frequency model, and (c-d) to the correlated allele frequency model. The blue ring signs individuals of the subpopulations ADN1 and ADN2.

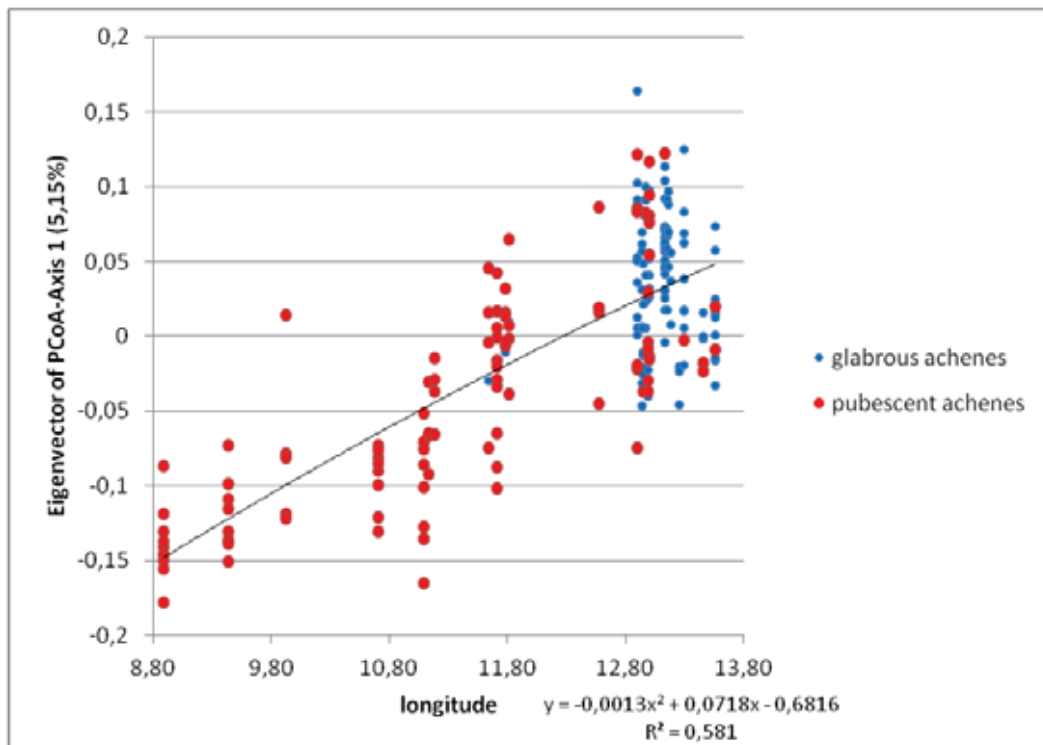


Figure 26. Individual scores of AFLP-based PCoA Axis 1 plotted against longitude with individuals labeled according to their achene type.

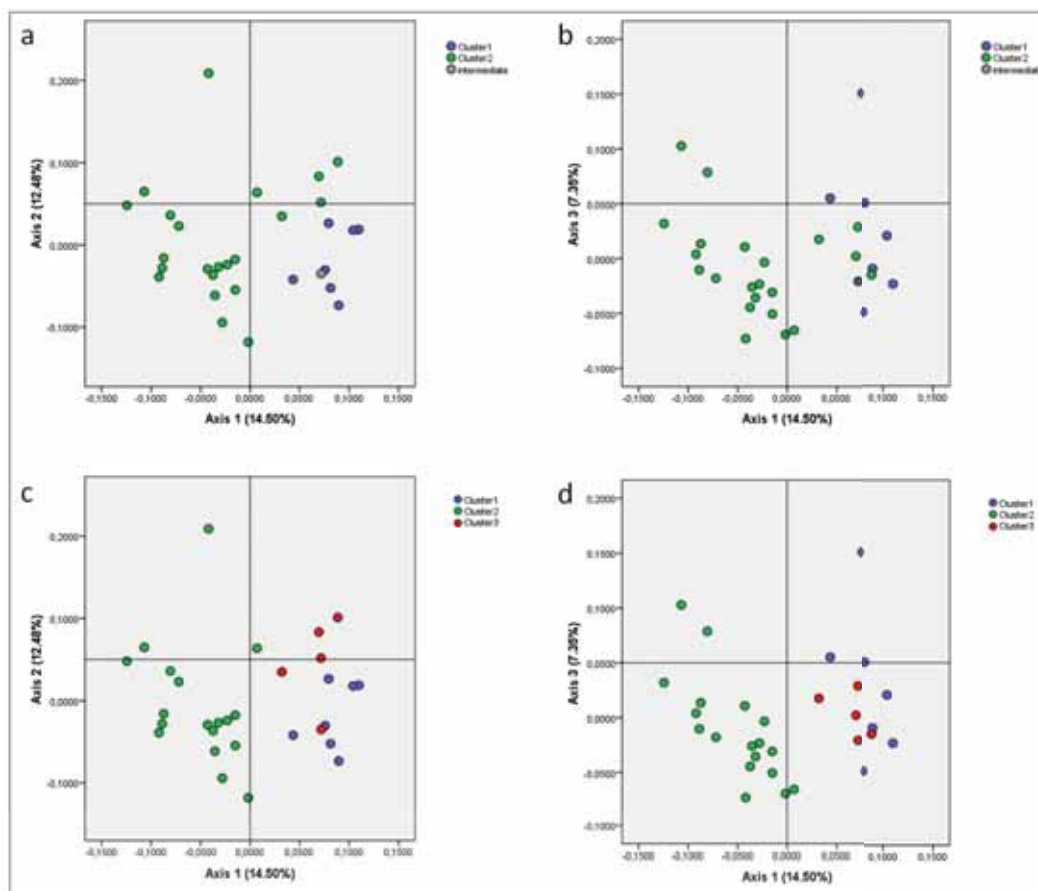


Figure 27. AFLP-based principal coordinates analysis (PCoA) of 23 *T. helenitis* populations (with two subpopulations, ADN1+2, counted as one population). Populations are labeled according to their assignment to STRUCLURE clusters under (a-b) the independent allele frequency model, and (c-d) to the correlated allele frequency model.

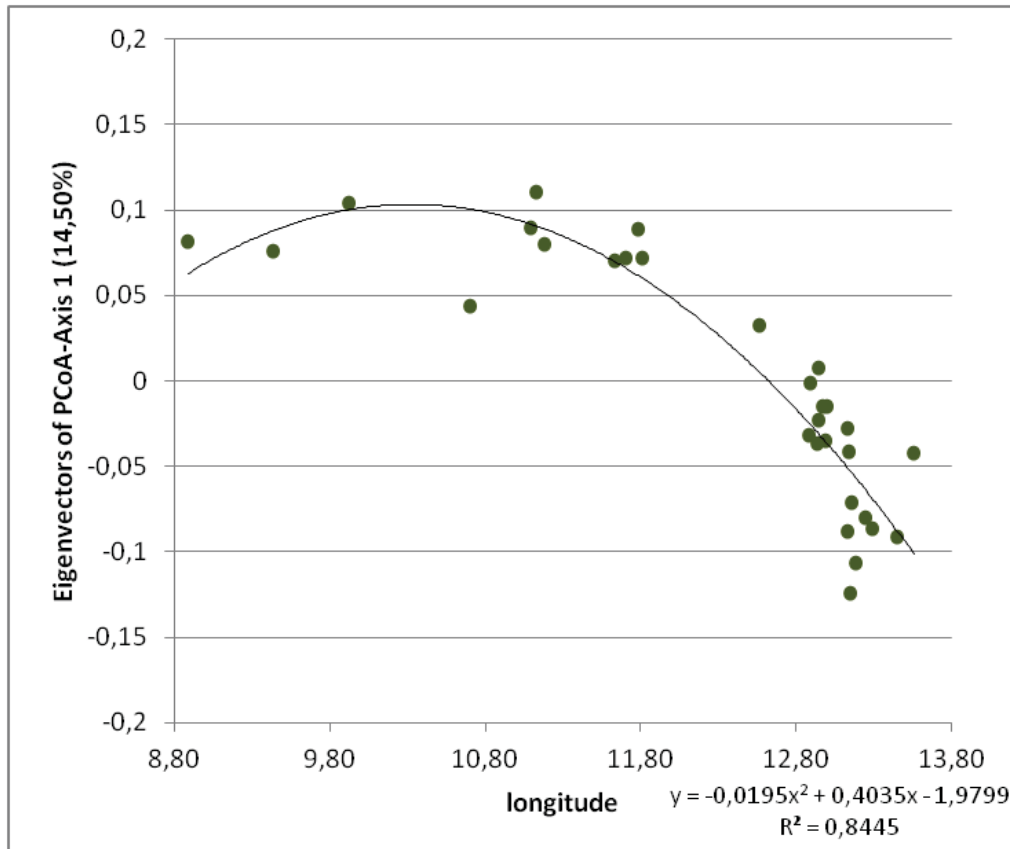


Figure 28. Population scores of AFLP-based PCoA-Axis 1 plotted against longitude.

3.5. Analyses of molecular variance (AMOVAs)

3.5.1. Non-hierarchical AMOVAs

Non-hierarchical AMOVAs (Table 7) were performed to test the partitioning of molecular variance within selected groups. The total dataset of *T. helenitis* revealed 15.36% of the total variation residing among populations. Based on the results of STRUCTURE (correlated and independent allele frequency model, respectively) and BAPS (spatial admixture model) populations were assigned to groups and tested for non-hierarchical AMOVAs.

The two clusters identified by STRUCTURE (allele frequencies independent) were analyzed separately, excluding population GEO1, which could not be assigned clearly to any of these clusters. The westernmost distributed cluster 1 showed 16.26% variation among the populations, whereas the more eastern distributed cluster 2 had 12.51% variation among populations. Therefore, populations of cluster 1 were more differentiated from each other than those of cluster 2.

Based on the results of the correlated allele frequency model (STRUCTURE), three clusters were formed. Cluster 1 (from Ammersee westwards) was examined including and excluding (identical to the independent allele frequency model) the admixed population GEO1, respectively. The AMOVAs showed 16.57% and 16.26% variation among populations, respectively, which did not differ significantly. Population GEO1 has therefore no role of

influencing among-population variation in cluster 1. The easternmost populations (cluster 2) revealed 11.59% (incl. the admixed population KUC1) and 11.43% (excl. population KUC1) variation among populations. There was thus no large difference, whether or not KUC1 was included. However, among-population variation was much lower than in cluster 1. The predominating cluster in the Miesbach and Chiemsee region (cluster 3) was analyzed including/excluding populations GEO1 and/or KUC1. The among-population variation varied from 12.57% (excl. both populations) to 14.48% (incl. both populations), which was in-between the variation of cluster 1 and cluster 2.

Spatial admixture analysis of the program BAPS resulted in two clusters, whereby cluster 1 included the whole Miesbach region (in contrast to the STRUCTURE results). Cluster 1 showed 17.08% among-population variation and “cluster 2” 11.80%. The variation among populations of cluster 2 was much lower than the variation in cluster 1, concordant with the results of the STRUCTURE-based grouping.

The two subspecies of *Tephrosieris helenitis* (viz. through their achene indumentum) were ascribed to two different populations (one population containing all individuals of one subspecies) to determine the proportion of variance, which was present between the two subspecies. The analysis showed 3.58% among-population variation. Excluding the westernmost populations and the Ammersee region, which were pure ssp. *helenitis* populations, the amount of variation drops to 0.37%, which was also not significant.

Table 7. Non-hierarchical AMOVAs based on AFLPs of *T. helenitis* (with two subpopulations, ADN1+2, counted as one population). The first column lists the analyses, which results were used for the formation of AMOVA groups. Abbreviations: d.f., degrees of freedom; n.s., not significant (P-value >0.05); *, P-value < 0.001.**

Non-hierarchical AMOVAs	Investigated group	Source of variation	D.f.	Sum of squares	Variance component	% variation	P-value	
	All populations	Among populations	29	2777.89	7.25	15.36	0.00000 ± 0.00000	***
		Within populations	203	8109.55	39.95	84.64		
	<i>Ssp. salisburgensis</i> - <i>ssp. helenitis</i> (treated as 2 populations)	Among populations	1	233.93	1.71	3.58	0.00000 ± 0.00000	***
		Within populations	219	10088.39	46.07	96.42		
	<i>Ssp. salisburgensis</i> - <i>ssp. helenitis</i> (excl. pop. from Ammersee westwards)	Among populations	1	52.20	0.17	0.37	0.08504 ± 0.00904	n.s.
		Within populations	140	6302.26	45.02	99.63		
STRUCTURE (allele frequencies independent)	Cluster 1 (excl. GEO1)	Among populations	6	546.48	7.67	16.26	0.00000 ± 0.00000	***
		Within populations	41	1619.17	39.49	83.74		
	Cluster 2 (excl. GEO1)	Among populations	21	1782.34	5.74	12.51	0.00000 ± 0.00000	***
		Within populations	152	6096.56	40.11	87.49		
STRUCTURE (allele frequencies correlated)	Cluster 1 (incl. GEO1)	Among populations	7	674.06	7.84	16.57	0.00000 ± 0.00000	***
		Within populations	51	2012.99	39.47	83.43		
	Cluster 1 (excl. GEO1)	Among populations	6	546.48	7.67	16.26	0.00000 ± 0.00000	***
		Within populations	41	1619.17	39.49	83.74		
	Cluster 2 (incl. KUC1)	Among populations	17	1434.23	5.28	11.59	0.00000 ± 0.00000	***
		Within populations	135	5432.06	40.24	88.41		
	Cluster 2 (excl. KUC1)	Among populations	16	1359.83	5.19	11.43	0.00000 ± 0.00000	***
		Within populations	132	5309.06	40.22	88.57		
	Cluster 3 (incl. GEO1 and KUC1)	Among populations	5	391.02	6.67	14.48	0.00000 ± 0.00000	***
		Within populations	30	1181.32	39.38	85.52		
	Cluster 3 (incl. GEO1; excl. KUC1)	Among populations	4	310.12	6.20	13.65	0.00000 ± 0.00000	***
		Within populations	27	1058.32	39.20	86.35		
Cluster 3 (incl. KUC1; excl. GEO1)	Among populations	4	281.94	6.25	13.69	0.00000 ± 0.00000	***	
	Within populations	20	787.50	39.38	86.31			
Cluster 3 (excl. GEO1 and KUC1)	Among populations	3	205.60	5.62	12.57	0.00000 ± 0.00000	***	
	Within populations	17	664.50	39.09	87.43			
BAPS (spatial admixture)	Cluster 1 (incl. GEO1)	Among populations	10	929.26	8.02	17.08	0.00000 ± 0.00000	***
		Within populations	64	2491.49	38.93	82.92		
	Cluster 2	Among populations	18	1524.35	5.41	11.80	0.00000 ± 0.00000	***
		Within populations	139	5618.06	40.42	88.20		

3.5.2. Hierarchical AMOVAs

Hierarchical AMOVAs (Table 8) were performed to test the partitioning of molecular variance residing within and among the above-mentioned groups. Based on the results of STRUCTURE using the independent allele frequency model the populations were divided into two clusters (see non-hierarchical AMOVAs). Population GEO1 was excluded as for the non-hierarchical AMOVAs. The among-group variation was 6.38%. After excluding admixed populations from the Ammersee and Miesbach regions (AMM2, AMM3, FEN1, MOO1, and KOE1) the variation among groups increased to 7.56%.

Using the correlated allele frequency model in STRUCTURE, three clusters were found. Populations GEO1 and KUC1 could not be assigned to any of these clusters clearly, or were assigned to a cluster, which was not predominate in their geographical region. Therefore,

these populations were included in each of the “ambiguous” clusters in separate AMOVA runs. The among-group variation was about 1% lower than using the independent allele frequency model within two clusters (see above). The highest value (5.47%) was found after ascribing the admixed population KUC1 to cluster 2 and the admixed population GEO1 to cluster 3, i.e. according to these clusters predominating in their geographic region of origin. The lowest value (5.09%) was found after ascribing both populations to the other cluster. Anyhow, the difference between these proportions was very low (0.38%).

Based on the spatial admixture analysis of BAPS (two groups), the among-group variation was 1.69% lower compared to the grouping based on the independent allele frequency model of STRUCTURE, and even lower (about 0.6%) compared to the correlated allele frequency model.

Table 8. Hierarchical AMOVAs based on AFLPs of *T. helentis* (with two subpopulations, ADN1+2, counted as one population). The first column presents the analysis which is the base of group construction (second column). Abbreviations: d.f., degrees of freedom; *, P-value between 0.01 and 0.05; **, P-value between 0.001 and 0.01; *, P-value < 0.001.**

Hierarchical AMOVAs	Groups	Source of variation	D.f.	Sum of squares	Variance component	% variation	P-value	
STRUCTURE (allele frequencies independent)	Cluster 1 (excl. GEO1) - cluster 2 (excl. GEO1)	Among groups	1	326.17	3.14	6.38	0.00000 ± 0.00000	***
		Among populations	27	2328.82	6.12	12.43		
		Within populations	193	7715.73	39.98	81.20		
	Cluster 1 - cluster 2 (both excl. AMM2, AMM3, FEN1, GEO1, MOO1, KOE1)	Among groups	1	330.30	3.74	7.56	0.00000 ± 0.00000	***
		Among populations	22	1924.48	5.84	11.79		
		Within populations	174	6949.98	39.94	80.65		
STRUCTURE (allele frequencies correlated)	Cluster 1 (incl. GEO1) - cluster 2 - cluster 3 (incl. KUC1)	Among groups	2	462.06	2.46	5.09	0.00000 ± 0.00000	***
		Among populations	27	2315.83	5.93	12.27		
		Within populations	203	8109.55	39.95	82.65		
	Cluster 1 (incl. GEO1) - cluster 2 (incl. KUC1) - cluster 3	Among groups	2	464.00	2.57	5.30	0.00000 ± 0.00000	***
		Among populations	27	2313.89	5.92	12.22		
		Within populations	203	8109.55	39.95	82.47		
	Cluster 1 - cluster 2 - cluster 3 (incl. GEO1 and KUC1)	Among groups	2	480.57	2.52	5.21	0.00000 ± 0.00000	***
		Among populations	27	2297.32	5.87	12.15		
		Within populations	203	8109.55	39.95	82.64		
	Cluster 1 - cluster 2 (incl. KUC1) - cluster 3 (incl. GEO1)	Among groups	2	487.06	2.65	5.47	0.00000 ± 0.00000	***
		Among populations	27	2290.82	5.85	12.07		
		Within populations	203	8109.55	39.95	82.46		
BAPS (spatial admixture)	Cluster 1 (incl. GEO1) - cluster 2	Among groups	1	324.28	2.27	4.69	0.00000 ± 0.00000	***
		Among populations	28	2453.61	6.22	12.84		
		Within populations	203	8109.55	39.95	82.48		

3.6. Genetic diversity and rarity

To estimate patterns of within-population genetic diversity, three parameters were calculated: percentage of polymorphic loci (“PLP”), NEI’s (1987) genetic diversity (H_E) and Shannon’s information index (SI; LEWONTIN 1972). Additionally, further parameters were estimated (total

number of loci, number of loci found in 50% or fewer populations and number of loci found in 25% or fewer populations). As seen in Table 9 the number of polymorphic loci was highest in population LAU1, which was also the population with the largest sample size. Higher values were also found in populations from the southern Salzach valley region, while lowest values were present in the Miesbach region and particularly in the eastern Flachgau region. Estimates of PLP were highly correlated with the sample size, Shannon's information index and total number of loci (P-values: <0.001, <0.001 and 0.024, respectively). Therefore, the latter mentioned parameters will not be considered in detail. The geographic distribution pattern of H_E is displayed in Figure 29, which shows regional patches of higher diversities but no clinal distribution pattern. Highest levels were found in the Ammersee region and the region between the Chiemsee in the west and the Untersberg region in the east (also seen in Fig. 30a). Lowest levels of genetic diversity were present in the Miesbach region, the eastern Flachgau/Attersee region and population HAY1. The overall level of genetic diversity in *T. helenitis* populations is low (mean: 0.18) and ranges from 0.14 (pop. HAY1) to 0.22 (pop. AMM2).

The distribution of rare markers was estimated using two parameters: number of private markers (p.m.) and "frequency-down-weighted marker values" (rarity, DW). Private markers (see Table 9) were only rarely found. The westernmost population NUS1 was the only population with more than one private marker, i.e. three private markers. One private marker each was found in populations HAY1, AMM1, FEN1, BER5, UNT2, VIE1 and EST2. The only region where no private markers were found is the eastern Flachgau/Attersee region. Concerning the rarity index, higher values were generally found in the two westernmost populations, NUS1 and HAY1, as well as in the Ammersee region (see also in Figs. 29 and 30b). The eastwards situated populations showed generally low values of rarity. Exceptions were two populations of the Untersberg region (UNT1 and VIE1) and HAS1 from the eastern edge of the species' range. Populations from the Miesbach region and the eastern Flachgau/Attersee had generally lower values than those from the Chiemsee and Salzach valley region, comparable to the genetic diversities. Values of the rarity index ranged from 1.27 (KOP1) to 2.75 (AMM1) with an overall mean of 1.95.

Correlations (using SPEARMAN's (1904) rho) and linear regressions of genetic diversity with longitude or sample size were both not significant (Table 10). Nonetheless, genetic diversity slightly increased towards the east (Fig. 31a) and even decreased with higher sample sizes (Fig. 32a). Correlating the rarity index with longitude (Fig. 31b), a negative significance was found, despite weak correlation and regression coefficients ($R = 0.428$; $R^2 = 0.183$; $P = 0.018$). The correlation and linear regression of genetic diversity with sample size (Fig. 32b) was not significant. When genetic diversity was correlated with rarity (Fig. 33), a highly significant and positive correlation was found ($R = 0.602$; $R^2 = 0.368$; $P < 0.001$).

Table 9. Genetic diversity and rarity indices of 29 *T. helenitis* populations (two subpopulations, ADN1 and ADN2, are treated separately). Diversity and rarity measures are divided by a black line. The cluster classification is based on the independent allele frequency model of STRUCTURE. The populations are sorted by longitude, starting with the westernmost population. DW, frequency-down-weighted marker values; H_E , Nei's (1987) gene diversity; Lb, lower bound of the 95% confidence interval of Nei's (1987) gene diversity; N, number of individuals; N loci, number of bands with frequency >5% in the dataset; N loci $\leq 25\%$, number of bands (frequency >5%) found in $\leq 25\%$ of the populations; N loci $\leq 50\%$, number of bands (frequency >5%) found in $\leq 50\%$ of the populations; p.m., number of private markers; PLP (%), percentage of polymorphic loci; pop., population code; SD, standard deviation; SI, Shannon's information index; Ub, upper bound of the 95% confidence interval of Nei's (1987) gene diversity; x, longitude.

Cluster	Pop.	x	N	PLP (%)	N loci	N loci $\leq 50\%$	N loci $\leq 25\%$	H_E	Lb	Ub	SI	SD	P.m.	DW
1	NUS1	8.89	10	44.79	268	75	25	0.17	0.15	0.18	0.21	0.01	3	2.64
1	HAY1	9.44	9	37.25	230	57	18	0.14	0.13	0.16	0.18	0.01	1	2.24
1	HAM1	9.92	5	36.14	219	42	10	0.17	0.15	0.20	0.19	0.01	0	1.69
1	MAR1	10.70	8	41.69	247	58	13	0.17	0.15	0.19	0.20	0.01	0	1.77
1	AMM1	11.09	8	49.00	287	86	31	0.20	0.18	0.22	0.23	0.01	1	2.75
1	AMM2	11.13	4	39.47	234	56	17	0.22	0.19	0.24	0.21	0.01	0	2.57
1	AMM3	11.18	4	38.14	235	58	20	0.21	0.18	0.23	0.20	0.01	0	2.59
2	KOE1	11.63	5	33.92	212	38	7	0.16	0.14	0.19	0.17	0.01	0	1.54
1/2	GEO1	11.70	11	49.00	260	66	18	0.17	0.16	0.19	0.22	0.01	0	1.65
2	MOO1	11.78	6	31.71	203	45	10	0.14	0.12	0.16	0.16	0.01	0	1.66
2	FEN1	11.81	5	38.36	228	47	14	0.19	0.17	0.21	0.19	0.01	1	2.09
2	BER5	12.57	5	41.91	235	49	12	0.21	0.18	0.23	0.21	0.01	1	2.16
2	SCH1	12.88	8	48.56	271	72	18	0.19	0.17	0.21	0.22	0.01	0	2.01
2	LAU1	12.89	18	65.41	327	119	39	0.20	0.18	0.21	0.25	0.01	0	2.00
2	UNT3	12.94	8	50.33	278	76	21	0.20	0.18	0.22	0.23	0.01	0	2.07
2	UNT2	12.95	4	32.37	216	43	10	0.18	0.15	0.20	0.17	0.01	1	2.07
2	UNT1	12.95	7	46.34	267	68	23	0.20	0.18	0.22	0.22	0.01	0	2.36
2	LAN1	12.97	8	46.34	255	61	15	0.19	0.17	0.21	0.21	0.01	0	1.66
2	VIE1	12.99	9	52.99	291	80	18	0.20	0.18	0.22	0.24	0.01	1	2.23
2	EST2	13.00	15	54.11	282	71	12	0.17	0.16	0.19	0.22	0.01	1	1.41
2	ADN2	13.13	17	56.32	295	91	25	0.18	0.16	0.19	0.22	0.01	0	1.69
2	ADN1	13.13	9	45.23	254	62	16	0.18	0.16	0.20	0.21	0.01	0	1.84
2	PAL1	13.14	2	18.40	169	23	5	0.18	0.15	0.22	0.11	0.01	0	1.85
2	KOP1	13.15	7	34.81	208	34	7	0.14	0.13	0.17	0.17	0.01	0	1.27
2	KUC1	13.16	4	32.37	210	44	9	0.18	0.16	0.21	0.17	0.01	0	1.91
2	WOE1	13.18	5	31.49	199	32	11	0.16	0.14	0.18	0.17	0.01	0	1.56
2	FUS1	13.25	3	25.06	211	31	4	0.17	0.14	0.20	0.14	0.01	0	1.96
2	STI1	13.29	10	43.46	239	48	11	0.16	0.14	0.18	0.20	0.01	0	1.47
2	HAS1	13.45	7	41.46	249	61	16	0.17	0.15	0.19	0.20	0.01	0	2.24
2	GER1	13.56	12	44.57	248	55	9	0.16	0.14	0.18	0.20	0.01	0	1.48
MEAN		12.26	7.77	41.70	244.23	58.27	15.47	0.18	0.16	0.20	0.20	0.01	0.33	1.95
SD		1.24	3.84	9.57	33.94	20.02	7.62	0.02	0.02	0.02			0.65	0.38

3. Results

Table 10. Correlations and regressions of genetic diversity and rarity with longitude and sample size. Abbreviations: N, number of comparisons; n.s., not significant (P-value >0.05); ρ , SPEARMAN'S (1904) rank correlation coefficient; *, P-value between 0.05 and 0.01; **, P-value between 0.001 and 0.01; ***, P-value < 0.001.

Comparison	N	ρ	P-value		Linear regression line fit	R	R ²	Adjusted R ²	P-value	
Genetic diversity – longitude	30	-0.206	0.275	n.s.	$y = 0.073x + 0.164$	0.073	0.005	-0.030	0.701	n.s.
Genetic diversity - sample size	30	-0.185	0.329	n.s.	$y = -0.092x + 0.182$	0.092	0.008	-0.027	0.629	n.s.
Rarity - longitude	30	-0.432	0.017	*	$y = -0.428x + 3.572$	0.428	0.183	0.154	0.018	*
Rarity - sample size	30	-0.230	0.221	n.s.	$y = -0.220x + 2.117$	0.220	0.048	0.014	0.243	n.s.
Genetic diversity - rarity	30	0.594	0.001	**	$y = 0.602x + 0.119$	0.602	0.363	0.340	0.000	***
PLP (%) – sample size	30	0.530	0.003	**	$y = 0.412x + 47.341$	0.412	0.170	0.140	0.024	*
PLP (%) – Shannon's Information index	30	0.852	0.000	***	$y = 0.853x + 17.726$	0.853	0.728	0.718	0.000	***
PLP (%) – total number of loci	30	0.865	0.000	***	$y = 0.831x + 15.266$	0.831	0.690	0.679	0.000	***

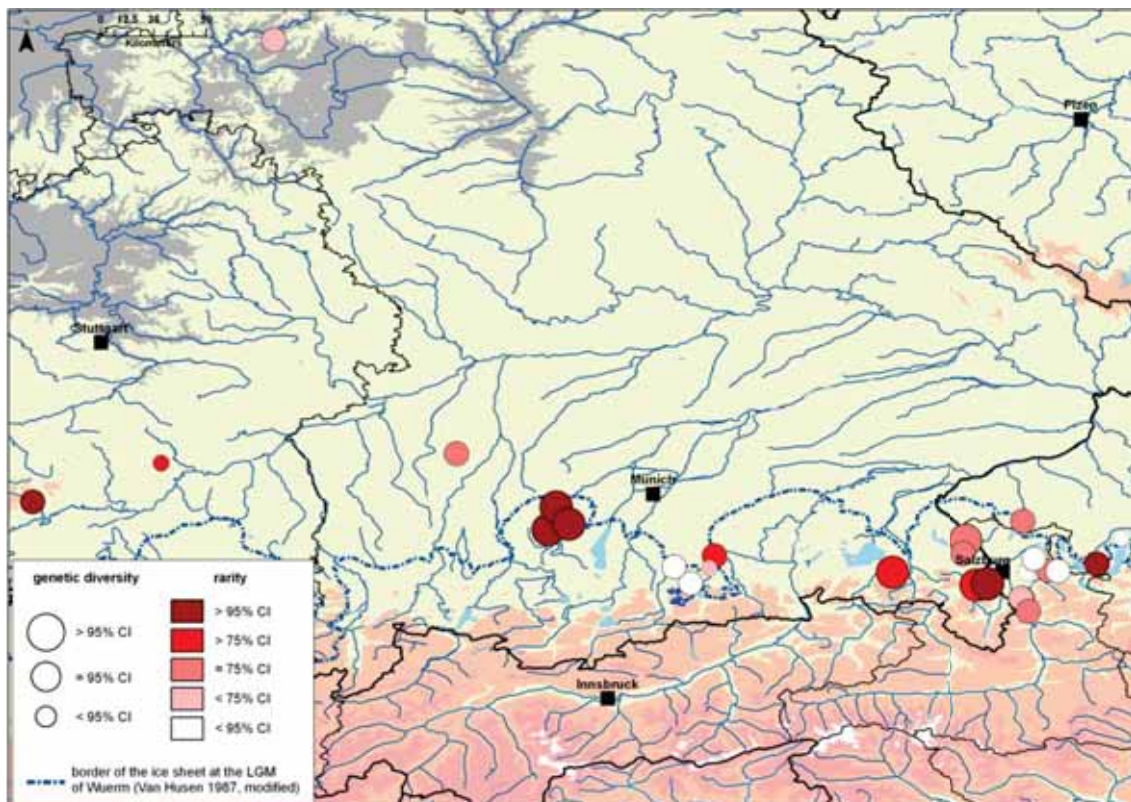


Figure 29. Spatial pattern of within-population genetic diversity (circle size) and rarity (circle color) of 29 *T. helenitis* populations.

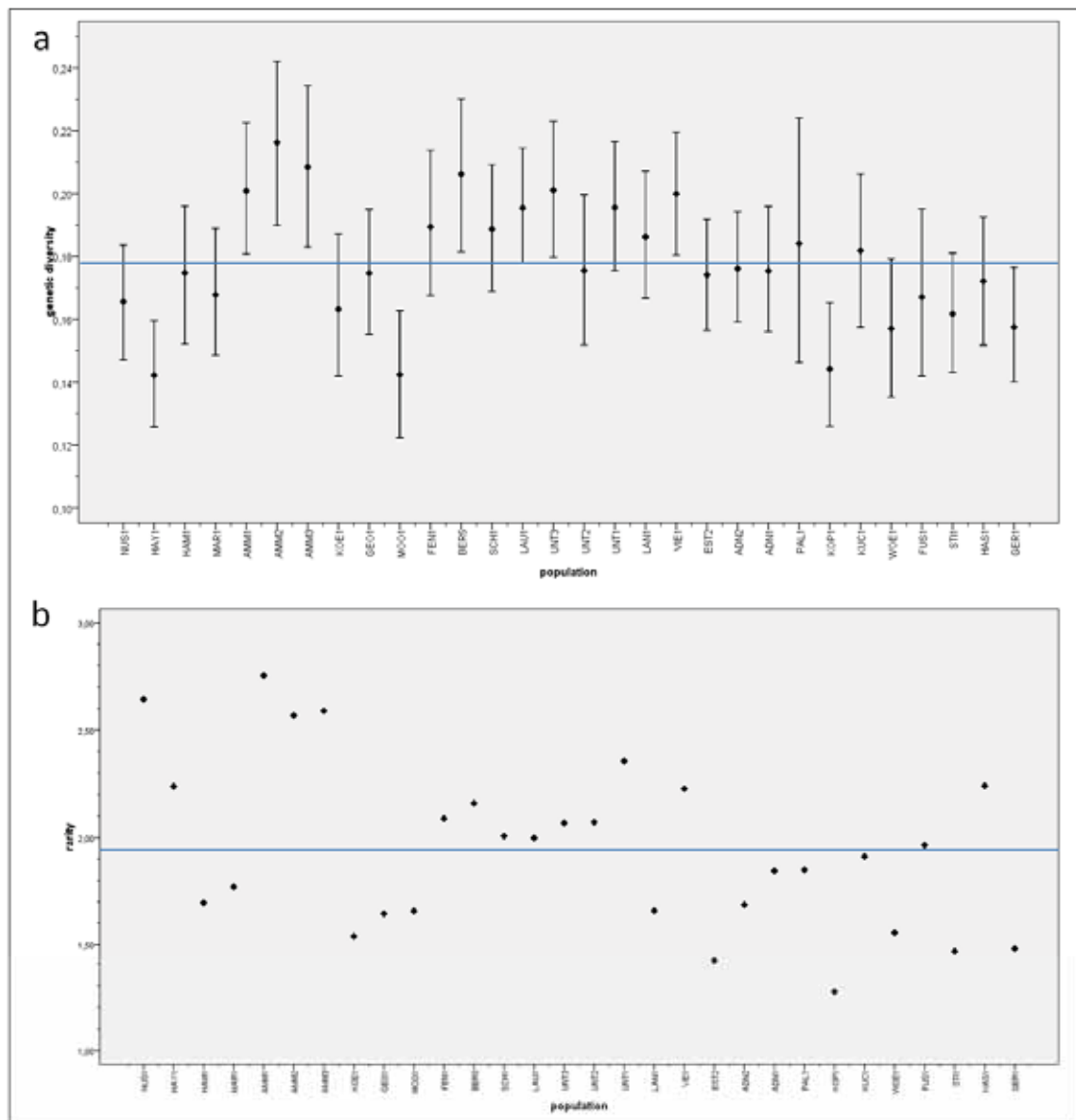


Figure 30. (a) Mean genetic diversity (\pm SD) and (b) mean rarity for 29 *T. helenitis* populations (two subpopulations, ADN1 and ADN2, are treated separately). Populations are sorted by longitude, whereby the leftmost population is the westernmost. The blue horizontal bar shows the average value across all populations.

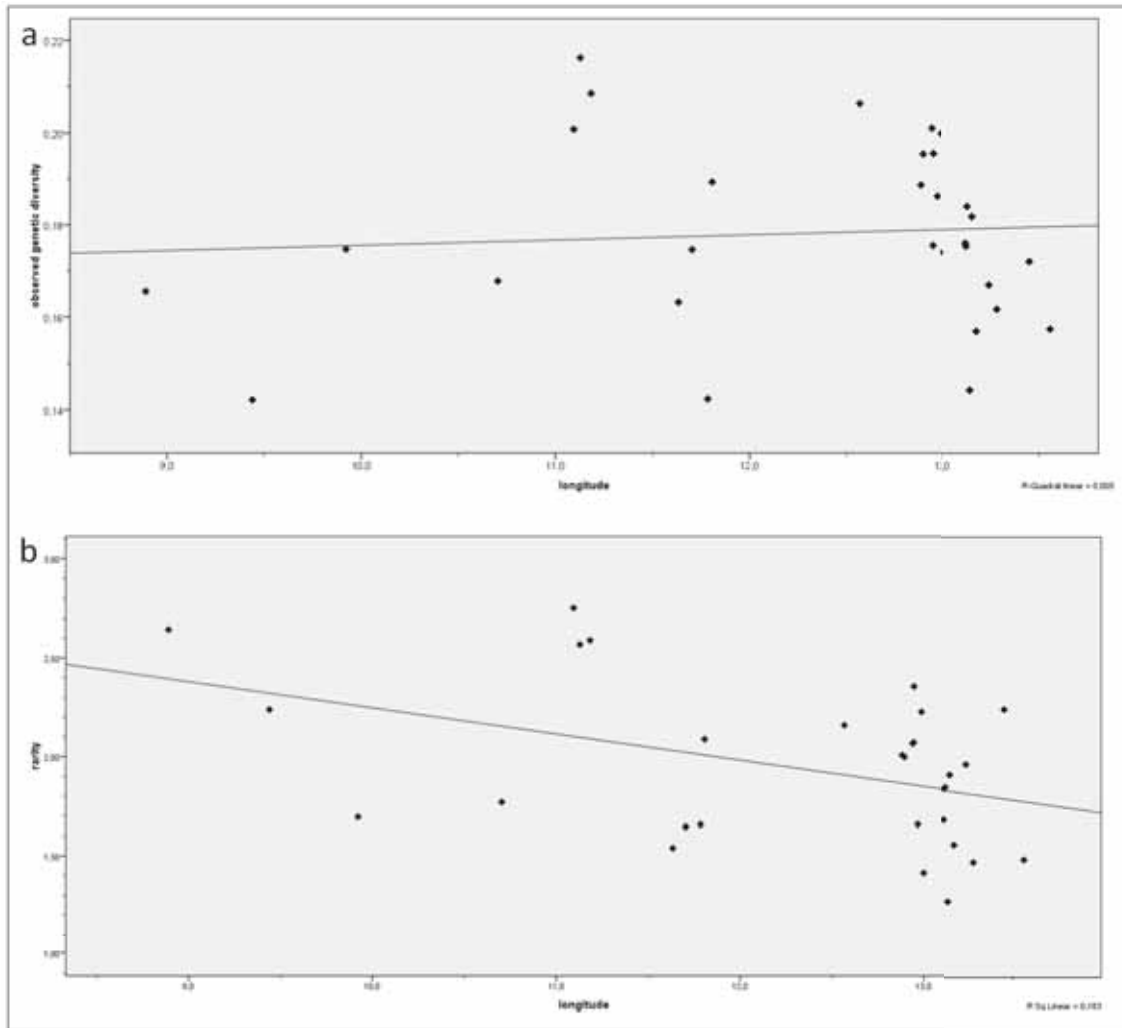


Figure 31. Means of (a) genetic diversity, and (b) rarity for 29 *T. helenitis* populations plotted against their longitudes. The black line displays the regression line.

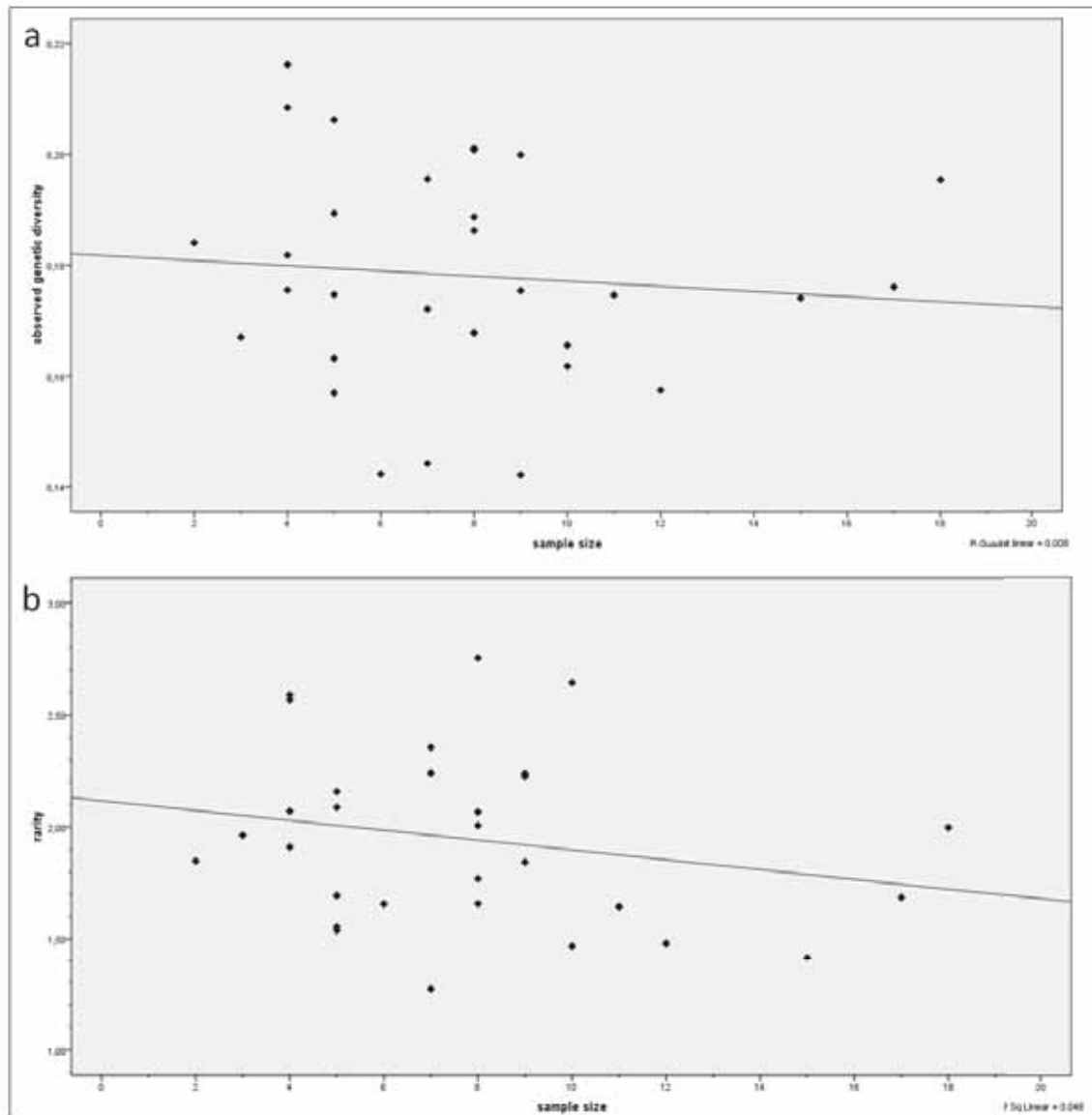


Figure 32. Means of (a) genetic diversity, and (b) rarity for 29 *T. helentis* populations plotted against to their sample sizes. The black line displays the regression line.

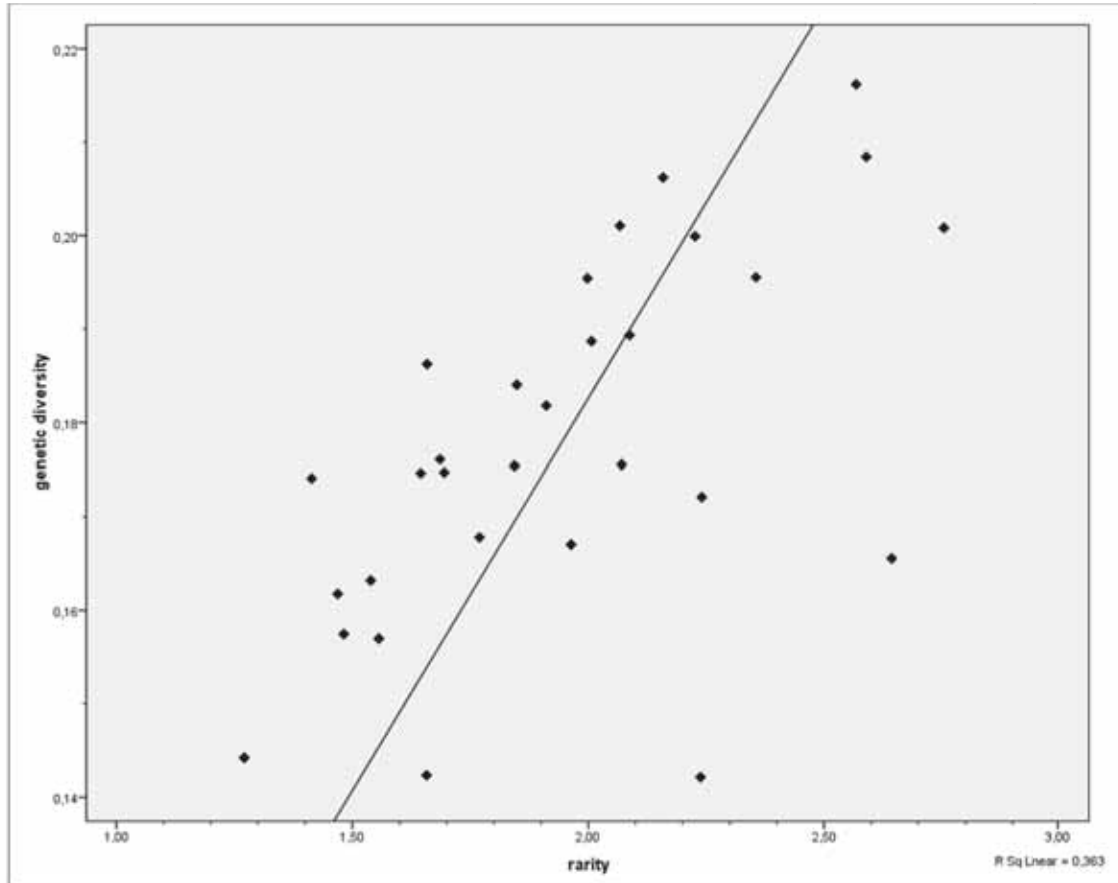


Figure 33. Relationship between genetic diversity and rarity in 29 *T. helenitis* populations. The black line displays the regression line.

3.7. AMOVA-derived F_{ST} values (Φ_{ST}) and patterns of isolation by distance (IBD)

The calculation of pairwise Φ_{ST} values among 30 (sub-) populations (incl. two subpopulations ADN1 and ADN2) of *T. helenitis* resulted in a symmetric matrix, which was utilized for the correlation with geographic distances among these populations using a Mantel test (see Table 11).

For the total dataset the correlation coefficient was high and positively significant ($rY1 = 0.619$; $P < 0.001$), indicating a strong IBD-pattern. The matrix was split into clusters resulting from STRUCTURE (independent and correlated allele frequencies, respectively) to compute Mantel tests for these clusters separately. For the independent allele frequency model (Fig. 34a), the correlation of cluster 1 was not significant ($rY1 = 0.355$; $P = 0.114$), while cluster 2 showed a moderate and significant correlation ($rY1 = 0.430$; $P = 0.004$) of Φ_{ST} s and geographic distances. Using the correlated allele frequency model as a base for cluster-construction, three clusters were taken into account, which all resulted in non-significant Mantel tests. Nevertheless, cluster 1 (identical to cluster 1 of the independent allele frequency model) and cluster 2 revealed moderate correlation coefficients ($rY1 = 0.355$; $P = 0.114$ and $rY1 = 0.228$; $P = 0.055$, respectively), while cluster 3 showed no correlation ($rY1 = 0.001$; $P = 0.526$).

To test for IBD in the core region (i.e. the putative hybrid zone of the two examined subspecies), populations west of the Ammersee region and east of Salzburg city were excluded from the dataset. As for the entire Φ_{ST} matrix, the dataset was split into either two or three clusters, resulting from the independent and correlated allele frequency model of STRUCTURE. In comparison to the whole dataset, the Mantel test of all populations in this core region displayed only a moderately high (positive) correlation coefficient, which was nonetheless highly significant ($rY1 = 0.399$; $P < 0.001$). Using the independent allele frequency model for group-construction (Fig. 35b), the westernmost distributed cluster 1 consisted of 3 populations only. There was a negative and significant correlation ($rY1 = -0.119$; $P = 0.014$). The Mantel test of cluster 2 was significant, too, and showed a moderately high (positive) correlation coefficient ($rY1 = 0.472$; $P = 0.003$). In the correlated allele frequency model, cluster 1 displayed similar results as under the independent allele frequency model ($rY1 = -0.119$; $P = 0.014$). Cluster 2 showed a negative correlation coefficient and was not significant ($rY1 = -0.224$; $P = 0.791$). In contrast to that, cluster 2 showed a moderate correlation, when the whole Φ_{ST} matrix was used (see above). Cluster 3 displayed no correlation as for the whole Φ_{ST} matrix (see above).

Table 11. Mantel correlation analyses of AMOVA-derived F_{ST} values (Φ_{ST}) between 29 *T. helenitis* populations (two subpopulations ADN1 and ADN2 are treated separately) and their geographic distances. Mantel tests have been performed for either for the entire dataset or for each cluster resulting from the STRUCTURE analyses (independent and correlated allele frequency model, respectively). Additionally, the “core region” has been analyzed separately including populations between AMM1 as the westernmost and EST2 as the easternmost population (16 populations). Abbreviations: N, number of comparisons; n.s., not significant (P-value >0.05); rY1, Mantel correlation coefficient; *, P-value between 0.01 and 0.05; **, P-value between 0.001 and 0.01; ***, P-value < 0.001.

Analysis		Comparison	N	rY1	P value	
Total dataset	independent allele frequencies	All populations	435	0.619	0.000	***
		Cluster 1	21	0.355	0.114	n.s.
		Cluster 2	232	0.430	0.004	**
	correlated allele frequencies	Cluster 1	21	0.355	0.114	n.s.
		Cluster 2	153	0.228	0.055	n.s.
		Cluster 3	10	0.001	0.526	n.s.
Core region	independent allele frequencies	All populations	120	0.399	0.000	***
		Cluster 1	3	-0.119	0.014	*
		Cluster 2	66	0.472	0.003	**
	correlated allele frequencies	Cluster 1	3	-0.119	0.014	*
		Cluster 2	31	-0.224	0.791	n.s.
		Cluster 3	7	0.001	0.560	n.s.

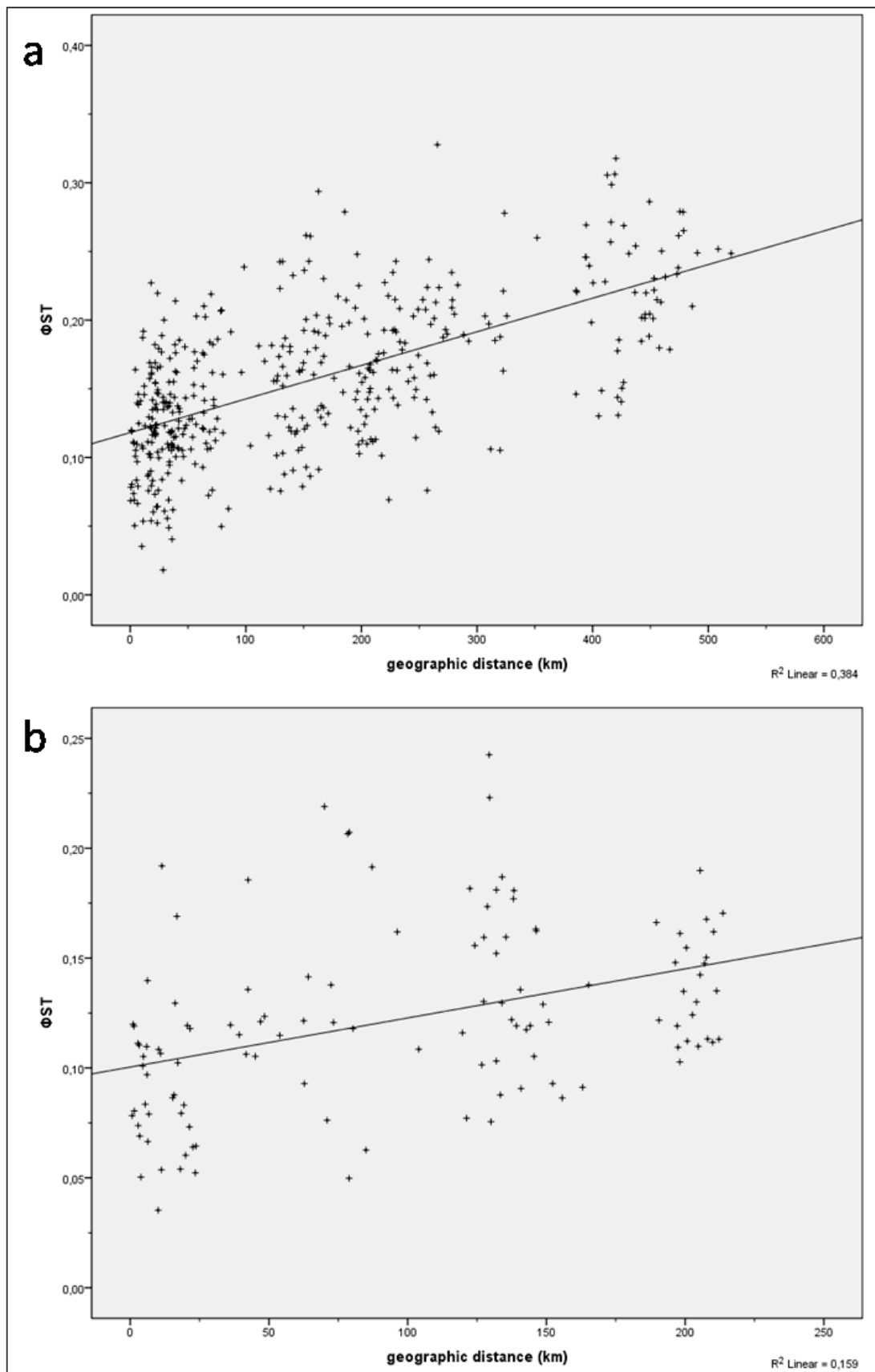


Figure 34. Φ_{ST} values plotted against their geographic distance among (a) 29 *Tephroseris helenitis* populations of the whole sampling area and (b) 16 *Tephroseris helenitis* populations of the "core region".

3.8. Detection of F_{ST} outlier loci and clinal distribution of allele frequencies at single AFLP loci

The MCEZA analysis (based on DFDIST) resulted in 13 outlier loci (36 outliers, including the loci, which were pruned due to the false discovery rate; Fig. 35), while BAYESCAN calculated 19 loci (Fig. 36; the F_{ST} posterior distribution is shown in Fig. 37). In total, 29 candidate loci out of 451 AFLP loci (6.4%) were found in MCEZA and/or BAYESCAN (Table 12). Only three of these loci (10.3%) have been found with both programs (N183.3, N203.1 and N269.1).

The allele frequencies of the F_{ST} outliers were checked for significant clines along the longitudinal axis. Three out of the 29 outlier loci (10.3%) showed significant clines for the models II or III of HUISMAN et al. (1993). More than one third of the loci showed a distribution without any spatial trend (39.9%: model I), while the remaining loci showed a spatial trend (19.3%: model II, 5.5%: model III, 17.1% model IV, 16.6%: model V). The clines under models II and III were significant in 34.8% (39 of 112). Only three outlier loci show significant clines (N183.3, N269.1, V325.8; Fig. 38), whereby the first two loci were found with both programs (MCEZA and BAYESCAN) and the last one only by BAYESCAN. The loci N183.3 and V325.8 were significant under model II of HUISMAN et al. (1993) (“an increasing or decreasing trend where the maximum is equal to the upper bound”), while N269.1 was significant for model III (“an increasing or decreasing trend where the maximum is below to the upper bound”).

The densities of inflection points for the clines of all loci significant for models II or III are displayed in Figure 39. The highest density of inflection points (more than 0.4) was found at about 13°E longitude. Quite high densities (about 0.2) were also found westwards up to 12°E and eastwards up to 14°E, which is also the eastern limit of the species’ range. From 11°E westwards inflection points were only found at a few loci. If only outlier loci were taken into account the inflection points ranged from 11.70°E (N269.1) to 12.90°E (N183.3). The third outlier locus showing significant clines (V325.8) had its inflection point between the first ones (11.92°E).

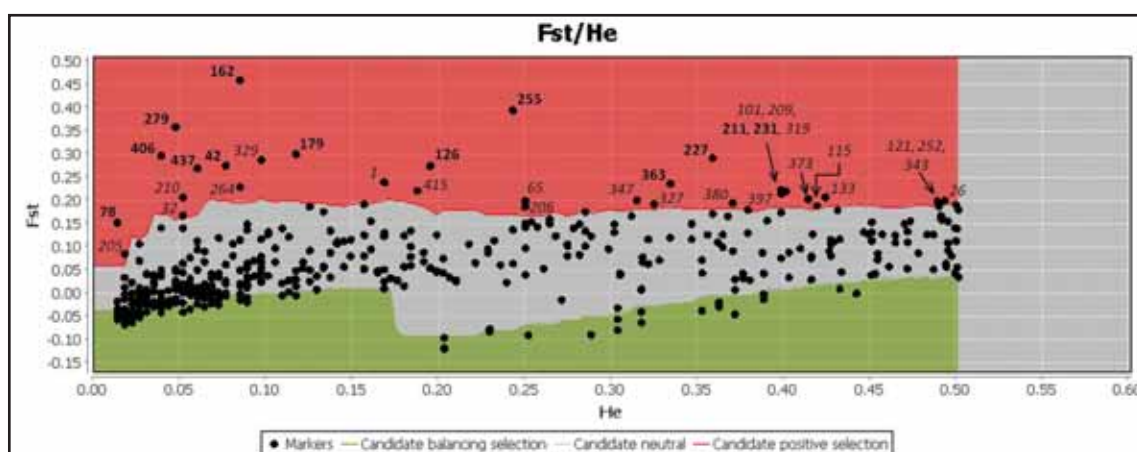


Figure 35. Graphical output of MCEZA (modified). The calculated F_{ST} values (vertical axis) are plotted against their heterozygosity (He, horizontal axis). The green background displays outlier loci under balancing selection, while the red background displays F_{ST} outlier loci under divergent selection.

Table 12. F_{ST} outlier loci determined by MCHEZA and BAYESCAN. Loci showing a significant cline (sign. HOF) for the models II and III ($P < 0.05$) of HUISMAN et al. (1993) are also included. Outlier loci identified in both programs are in bold. Abbreviations: n.s., not significant.

locus	MCHEZA	BAYESCAN	sign. HOF
42 F174.7	x		n.s.
74 F225.7		x	n.s.
78 F232	x		n.s.
101 F263.6		x	n.s.
104 F271.1		x	n.s.
121 F308.8		x	n.s.
126 F317.9	x		n.s.
130 F333		x	n.s.
133 F336.4		x	n.s.
153 F396.2		x	n.s.
162 F424.3	x		n.s.
170 F450.5		x	n.s.
179 F477.1	x		n.s.
180 F479.6		x	n.s.
194 F536.9		x	n.s.
211 N120.1	x		n.s.
227 N183.3	x	x	Model II
231 N203.1	x	x	n.s.
255 N269.1	x	x	Model III
279 N348.2	x		n.s.
330 V163.1		x	n.s.
350 V199.6		x	n.s.
363 V237.8	x		n.s.
397 V325.8		x	Model II
400 V334.9		x	n.s.
406 V347.5	x		n.s.
412 V365.7		x	n.s.
437 V453.2	x		n.s.
442 V481.7		x	n.s.
total	13	19	3

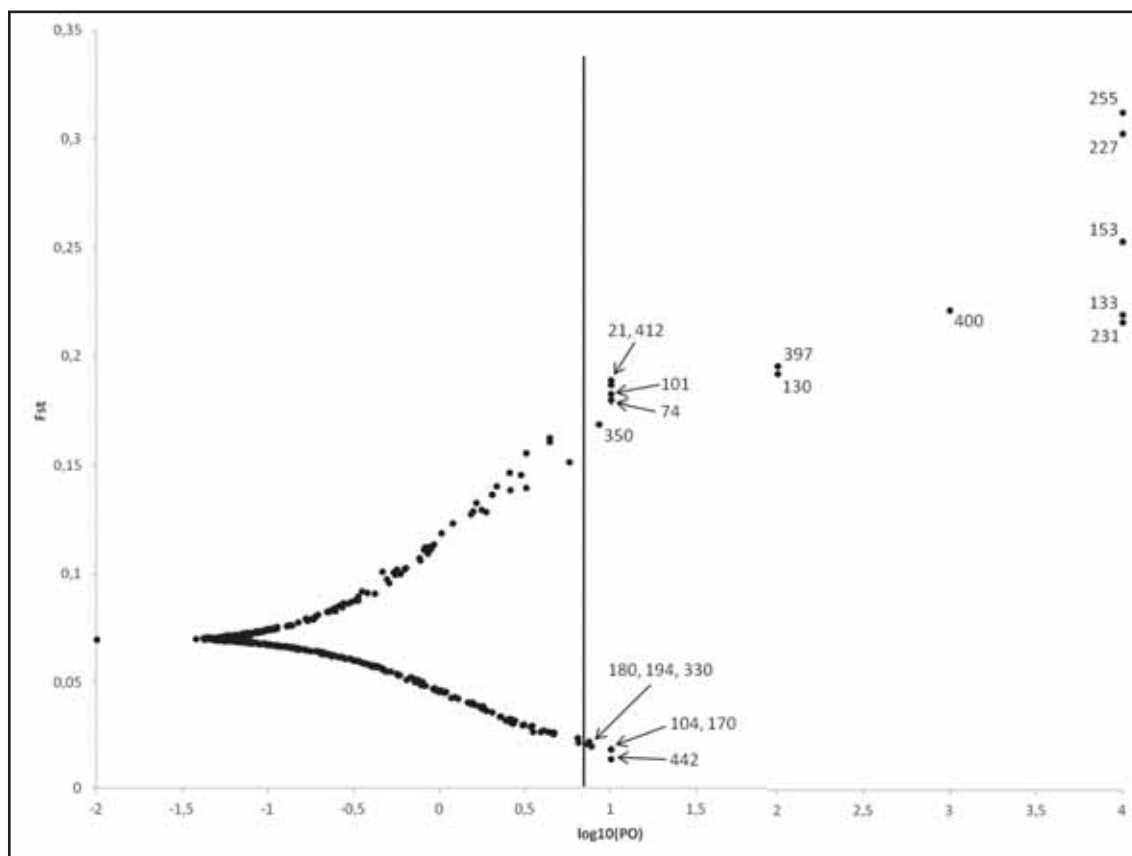


Figure 36. Graphical output of BAYESCAN (modified). The calculated F_{ST} values (vertical axis) are plotted against the logarithm of their Posterior Odds (PO) to the base of 10 (horizontal axis). The vertical line shows the PO threshold of the false discovery rate (0.87918).

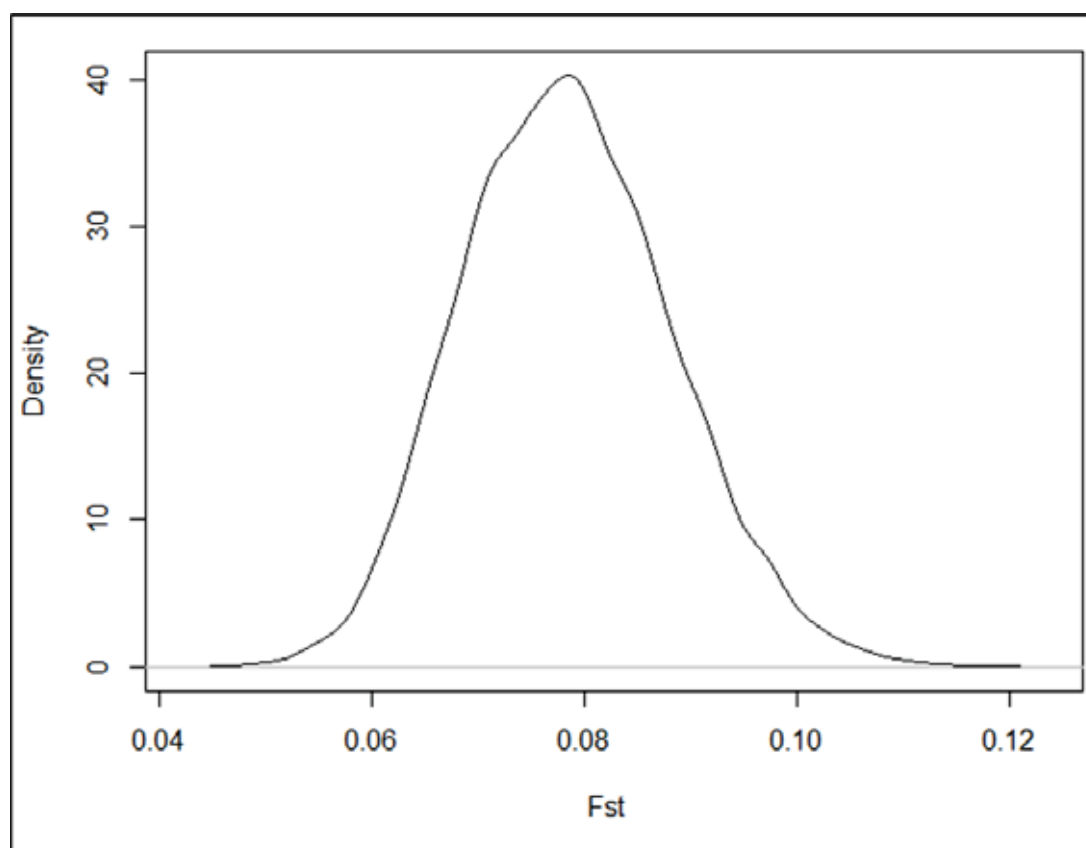


Figure 37. Posterior distribution of F_{ST} in BAYESCAN (451 loci).

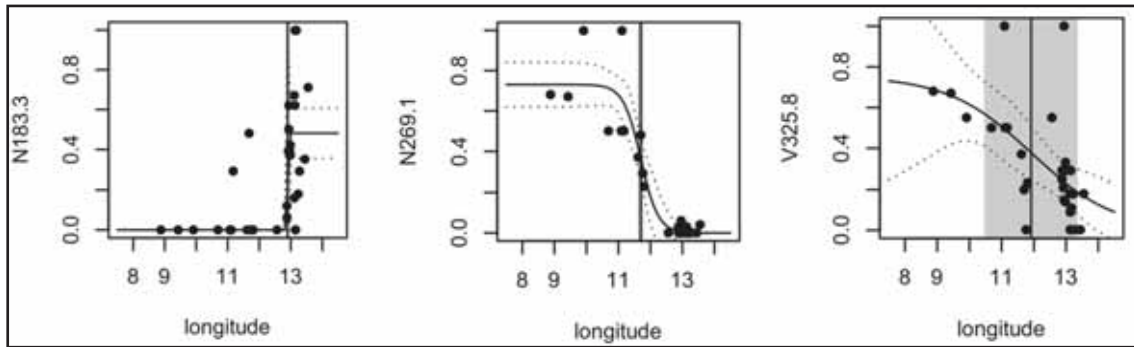


Figure 38. F_{ST} outlier loci showing a significant cline under models II and III of HUISMAN et al. (1993). The vertical axis shows the allele frequencies of populations, the horizontal axis represents their longitude. The vertical line displays the inflection point of the curve calculated with the nonlinear least square model; the gray background represents its standard error, the stippled lines indicate confidence intervals of the regression fit.

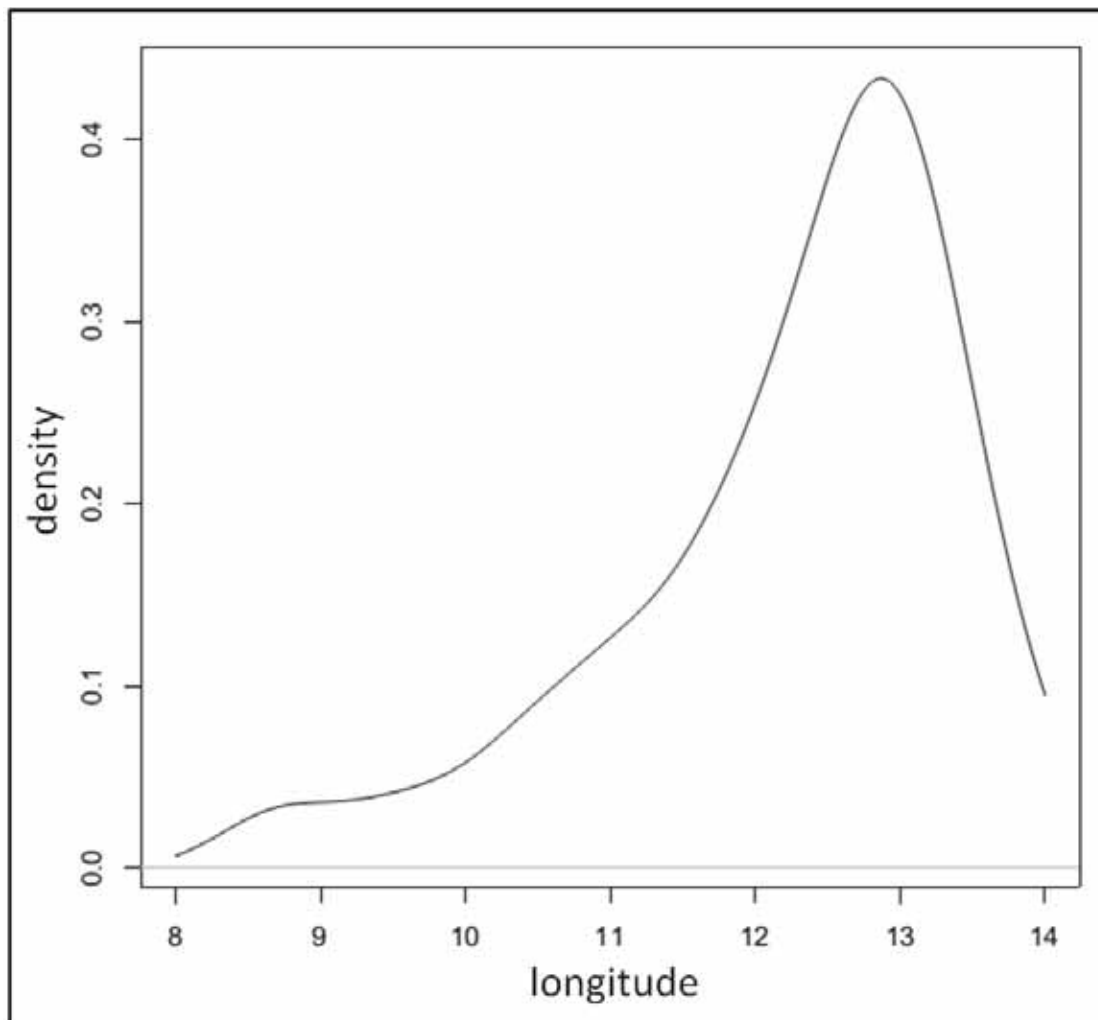


Figure 39. Densities of inflection points using the non-linear least squares (NLS) model (vertical axis) plotted against their position on the longitudinal axis (horizontal axis).

3.9. Morphological analyses

Achene indumentum (achenes glabrous, pubescent or sparsely hairy) was recorded for 561 individuals in 27 populations (including the two subpopulations ADN1 + ADN2, EST1 + EST2 and the three subpopulations BER1, BER4 + BER5). Twenty-five of these populations were also analyzed for AFLPs, thus excepting populations BER1 and EST1. The proportions of the three states of achene indumentum type are shown in Table 13 and as pie charts on a map (Fig. 40). Populations from the Ammersee region westwards exclusively had pubescent achenes, while a few individuals in the Miesbach region also showed glabrous or sparsely hairy achenes in addition to pubescent ones. As displayed in the line chart, where achene type is plotted against longitude (Fig. 41), glabrous achenes predominated in populations from the Chiemsee eastwards (except in population VIE1). The proportion of glabrous achenes increased towards east. In populations UNT2, FUS1 and WOE1 (all Flachgau) all individuals showed glabrous or sparsely hairy achenes, which were therefore thought as pure *ssp. salisburgensis* populations.

SPEARMAN's (1904) rank correlations were performed to compare the proportion of achene indumentum state with longitude. Highly significant correlation coefficients were found for glabrous and pubescent achenes ($\rho = 0.893$, P-value <0.001 and $\rho = -0.869$, P-value <0.001, respectively). No significant correlation with longitude was found for the proportion of sparsely hairy achenes in populations ($\rho = 0.341$, P = 0.082. Assigning the 220 individuals (analyzed for AFLPs) to STRUCTURE and BAPS clusters (see Table 14), respectively, revealed that the westernmost cluster 1 had >96% individuals with pubescent achenes across the four analyses (STRUCTURE: independent and correlated allele frequency model, BAPS: spatial and non-spatial admixture model). In the easternmost cluster 2 60% to 73% of the individuals had glabrous achenes and 17% to 29% pubescent achenes, while sparsely hairy achenes were found in around 10%. Cluster 3, which was found under the correlated allele frequency model of STRUCTURE only, showed 63% pubescent and 29% glabrous achenes.

Six morphological characters ("achenes pubescent", "ray flowers present", "stem red colored", "bract tips red colored", "rosette leaf lamina abruptly narrowed to the petiole", "upper surface of rosette leaves glabrous or with short hair" and "rosette leaves crenate or dentate") were recorded as present or absent in 105 individuals of six populations, which were also analyzed for AFLPs and achene indumentum. A cross tabulation was computed to associated the morphological traits among themselves (Table 17). High percentages of common morphological character states throughout the individuals ($\geq 80\%$) were found in the following comparisons: 83.7% of the individuals with glabrous achenes showed red stems whereas only 63.2% of the individuals with red stems showed glabrous achenes; 88.9% of the individuals without ray flowers showed red stems (opposite case: 60.4%); 83.3% of the individuals without red stems showed pubescent achenes (opposite case: 30.0%); 80% and 84.4% of the individuals with red bracts showed glabrous achenes and red stems, respectively (opposite case: 69.6% and 70.4%, respectively); individuals with rosette leaf laminae gradually narrowed to the petiole showed in 81.5% red stems (opposite case: 44.9%); 82.4% of the individuals with glabrous upper basal leaf surfaces showed red stems (opposite case: 28.6%). Many high percentages were found for red stems, which is presumably due to the high number of individuals with red stems in the dataset (73.0%). In two associations of morphological characters both character states and the opposite cases were high (>50%), which could indicate a "correlation of the characters": glabrous and pubescent achenes with

red and green/brownish bract tips, respectively; upper surface of basal leaves glabrous and arachnoid with (nearly) entire and crenate/dentate basal leaf margins. Nevertheless, the values are partially quite low, so a high correlation between any of morphological characters can be excluded.

Proportions of individuals exhibiting certain morphological characters in populations (Table 16) were correlated with longitude using SPEARMAN's (1904) rank correlation coefficient in SPSS (see Table 18 and Fig. 42). These correlations were not significant in all analyses.

Table 13. Proportions of different achene types in 27 populations of *Tephrosieris helenitis*. Populations are sorted by longitude, starting with the westernmost population. N, number of achenes checked for indumentum type; s., achenes were only sporadically checked for achene indumentum in the field.

Population code	N	Achene type		
		Glabrous	Pubescent	Sparsely hairy
NUS1	s.	0.00	1.00	0.00
HAY1	s.	0.00	1.00	0.00
HAM1	5	0.00	1.00	0.00
MAR1	s.	0.00	1.00	0.00
AMM1	20	0.00	1.00	0.00
AMM2	17	0.00	1.00	0.00
AMM3	20	0.00	1.00	0.00
KOE1	21	0.05	0.86	0.10
GEO1	15	0.00	1.00	0.00
MOO1	20	0.15	0.80	0.05
FEN1	22	0.00	0.82	0.18
BER1-5	54	0.61	0.30	0.09
LAU1	20	0.50	0.35	0.15
UNT3	14	0.71	0.21	0.07
UNT2	7	0.60	0.00	0.40
UNT1	31	0.55	0.26	0.19
LAN1	20	0.75	0.15	0.10
VIE1	35	0.35	0.56	0.09
EST1-2	50	0.60	0.26	0.14
ADN1-2	41	0.86	0.04	0.10
KOP1	32	0.91	0.03	0.06
KUC1	33	0.62	0.23	0.15
WOE1	20	1.00	0.00	0.00
FUS1	33	0.94	0.00	0.06
STI1	32	0.66	0.21	0.14
HAS1	10	0.80	0.20	0.00
GER1	20	0.90	0.10	0.00

Table 14. Proportions of different achene types in the total dataset and in clusters according to different analyses of STRUCTURE and BAPS. Abbreviations: Allele freq. corr., Allele frequencies correlated; Allele freq. ind., Allele frequencies independent; Cl., Cluster; Spatial adm., Spatial admixture; Non-spatial adm., Non-spatial admixture.

Achene type	Total	STRUCTURE						BAPS			
		Allele freq. ind.		Allele freq. corr.				Spatial adm.		Non-spatial adm.	
		Cl. 1	Cl.2	Cl.1	Cl.2	Cl.3	Cl.1	Cl.2	Cl.1	Cl.2	
Glabrous	0.45	0.00	0.60	0.02	0.73	0.29	0.03	0.67	0.00	0.68	
Pubescent	0.47	1.00	0.29	0.96	0.17	0.63	0.96	0.22	1.00	0.21	
Sparsely hairy	0.08	0.00	0.10	0.02	0.11	0.08	0.01	0.11	0.00	0.11	

Table 15. Number of morphological character states recorded in six populations.

Character	Character state	ADN2	EST2	GEO1	GER1	HAS1	LAU1	Total
Achene type	Pubescent	0	9	15	2	2	7	35
	Glabrous and sparsely hairy	19	11	0	18	8	13	69
Capitulum type	Ray flowers present	10	7	14	11	7	6	55
	Ray flowers absent	9	13	0	9	3	14	48
Stem color	Red	16	17	6	-	-	15	54
	Green or brownish	4	3	8	-	-	5	20
Bract tip color	Red	16	15	0	5	10	14	60
	Green or brown	3	5	15	15	0	6	44
Basal leaf shape	Rosette leaf lamina abruptly narrowed to the petiole	14	9	7	12	7	11	60
	Rosette leaf lamina gradually narrowed to the petiole	6	10	4	8	3	7	38
Basal leaf indumentum	Upper surface of rosette leaves glabrous or with short hairs	6	7	2	12	2	3	32
	Upper surface of rosette leaves arachnoid	14	12	9	8	8	15	66
Rosette leaf margin	Crenate to dentate	15	12	9	13	9	7	65
	Entire or slightly crenate	5	7	2	7	1	11	33

Table 16. Mean proportions of different states of six morphological characters in six populations (and standard deviations in parentheses). Within-population sample sizes of each morphological character are given in Table 15. Abbreviations: achenes, achenes pubescent; basal leaf indumentum, upper surface of rosette leaves glabrous or with short hair; basal leaf margin, rosette leaves crenate to dentate; basal leaf shape, rosette leaf lamina abruptly narrowed to the petiole; bract tips, bract tips red colored; Pop., Population code; ray flowers, ray flowers present; stem, stem red colored.

Pop.	Achenes	Ray flowers	Stem	Bract tips	Basal leaf shape	Basal leaf indumentum	Basal leaf margin
ADN2	0.00 (±0.00)	0.53 (±0.51)	0.80 (±0.41)	0.84 (±0.37)	0.70 (±0.47)	0.30 (±0.47)	0.75 (±0.44)
EST2	0.45 (±0.51)	0.35 (±0.49)	0.85 (±0.37)	0.75 (±0.44)	0.47 (±0.51)	0.37 (±0.50)	0.63 (±0.50)
GEO1	1.00 (±0.00)	1.00 (±0.00)	0.43 (±0.51)	0.00 (±0.00)	0.64 (±0.50)	0.18 (±0.40)	0.82 (±0.40)
GER1	0.10 (±0.31)	0.55 (±0.51)	-	0.25 (±0.44)	0.60 (±0.50)	0.60 (±0.50)	0.65 (±0.49)
HAS1	0.20 (±0.42)	0.70 (±0.48)	-	1.00 (±0.00)	0.70 (±0.48)	0.20 (±0.42)	0.90 (±0.32)
LAU1	0.35 (±0.49)	0.30 (±0.47)	0.75 (±0.44)	0.70 (±0.47)	0.61 (±0.50)	0.17 (±0.38)	0.39 (±0.50)

Table 17. Cross table of the seven morphological traits recorded in six populations of *Tephroses helenitis*. The lines represent the investigated individuals; the rows show the percentage of the character states within these aliquots. Percentages $\geq 80\%$ are displayed in bold. Abbreviations: 0, no; 1, yes; bas. leaf lamina a. narrowed, basal leaf lamina abruptly narrowed to the petiole; bas. leaves cren. to dent., basal leaves crenate to dentate; u. surf. of bas. leaves glab., upper surface of basal leaves glabrous or with short hairs.

Morphological character state	N	Achenes pubescent		Ray flowers present		Stem red colored		Bract tips red colored		Bas. leaf lamina a. narrowed		U. surf. of bas. leaves glab.		Bas. leaves cren. to dent.		
		0	1	0	1	0	1	0	1	0	1	0	1	0	1	
Achenes pubescent	0	69	-	52.2	47.8	16.3	83.7	30.4	69.6	33.8	66.2	64.7	35.3	30.9	69.1	
	1	35	-	35.3	64.7	40.0	60.0	65.7	34.3	51.7	48.3	72.4	27.6	41.4	58.6	
Ray flowers present	0	48	75.0	25.0	-	11.1	88.9	35.4	64.6	37.8	62.2	77.8	22.2	37.8	62.2	
	1	55	60.0	40.0	-	41.7	58.3	47.3	52.7	41.2	58.8	56.9	43.1	31.4	68.6	
Stem red colored	0	20	36.8	66.7	21.1	78.9	-	-	63.2	36.8	27.8	72.2	83.3	16.7	27.8	72.2
	1	54	63.2	33.3	60.4	39.6	-	-	29.6	70.4	44.9	55.1	71.4	28.6	38.8	61.2
Bract tips red colored	0	44	47.7	52.3	39.5	60.5	42.9	57.1	-	-	43.6	56.4	64.1	35.9	35.9	64.1
	1	60	80.0	20.0	51.7	48.3	15.6	84.4	-	-	36.2	63.8	69.0	31.0	32.8	67.2
Bas. leaf lamina a. narrowed	0	38	60.5	39.5	44.7	55.3	18.5	81.5	44.7	55.3	-	-	71.1	28.9	42.1	57.9
	1	60	76.3	23.7	48.3	51.7	32.5	67.5	37.3	62.7	-	-	65.0	35.0	28.3	71.7
U. surf. of bas. leaves glab.	0	66	67.7	32.3	54.7	45.3	30.0	70.0	38.5	61.5	40.9	59.1	-	-	24.2	75.8
	1	32	75.0	25.0	31.2	68.8	17.6	82.4	43.8	56.2	34.4	65.6	-	-	53.1	46.9
Bas. leaves cren. to dent.	0	33	63.6	36.4	51.5	48.5	20.8	79.2	42.4	57.6	48.5	51.5	48.5	51.5	-	-
	1	65	73.4	26.6	44.4	55.6	30.2	69.8	39.1	60.9	33.8	66.2	76.9	23.1	-	-

Table 18. Correlations and regressions of mean proportions of morphological characters states with longitudes. Within-population sample sizes of each morphological character are given in Table 15. Abbreviations: N, number of comparisons (=populations); n.s., not significant (P-value >0.05); ρ , SPEARMAN'S (1904) rank correlation coefficient; *, P-value between 0.05 and 0.01; **, P-value between 0.001 and 0.01; *, P-value < 0.001 .**

Source	Morphological character (mean proportions)	N	ρ	P-value	
Populations recorded for achene indumentum	Achenes glabrous	27	0.893	0.000	***
	Achenes pubescent	27	-0.869	0.000	***
	Achenes sparsely hairy	27	0.341	0.082	n.s.
Populations recorded for morphological characters	Achenes pubescent	6	-0.771	0.072	n.s.
	Ray flowers present	6	0.086	0.872	n.s.
	Stem red colored	4	0.800	0.200	n.s.
	Bract tips red colored	6	0.429	0.397	n.s.
	Rosette leaf lamina abruptly narrowed to the petiole	6	0.058	0.913	n.s.
	Upper surface of rosette leaves glabrous or with short hair	6	0.714	0.111	n.s.
	Rosette leaves crenate or dentate	6	0.200	0.704	n.s.

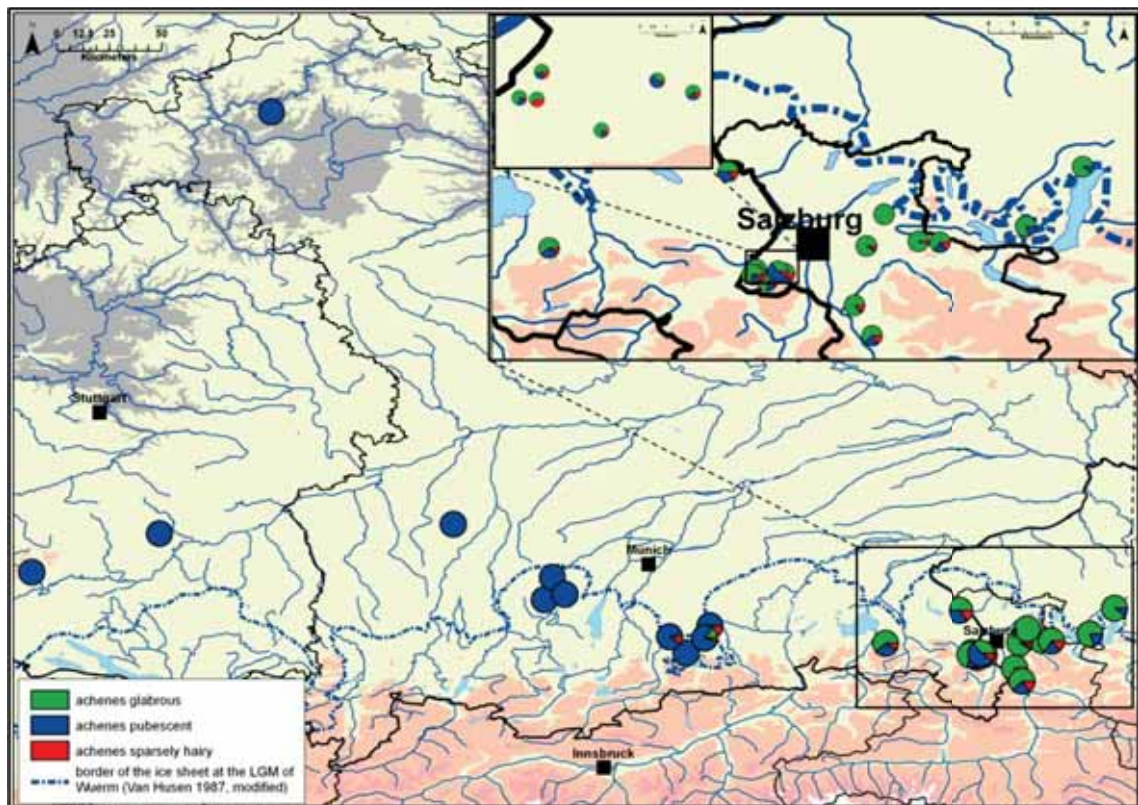


Figure 40. Spatial pattern of achene types in 27 *Tephroseris helenitis* populations.

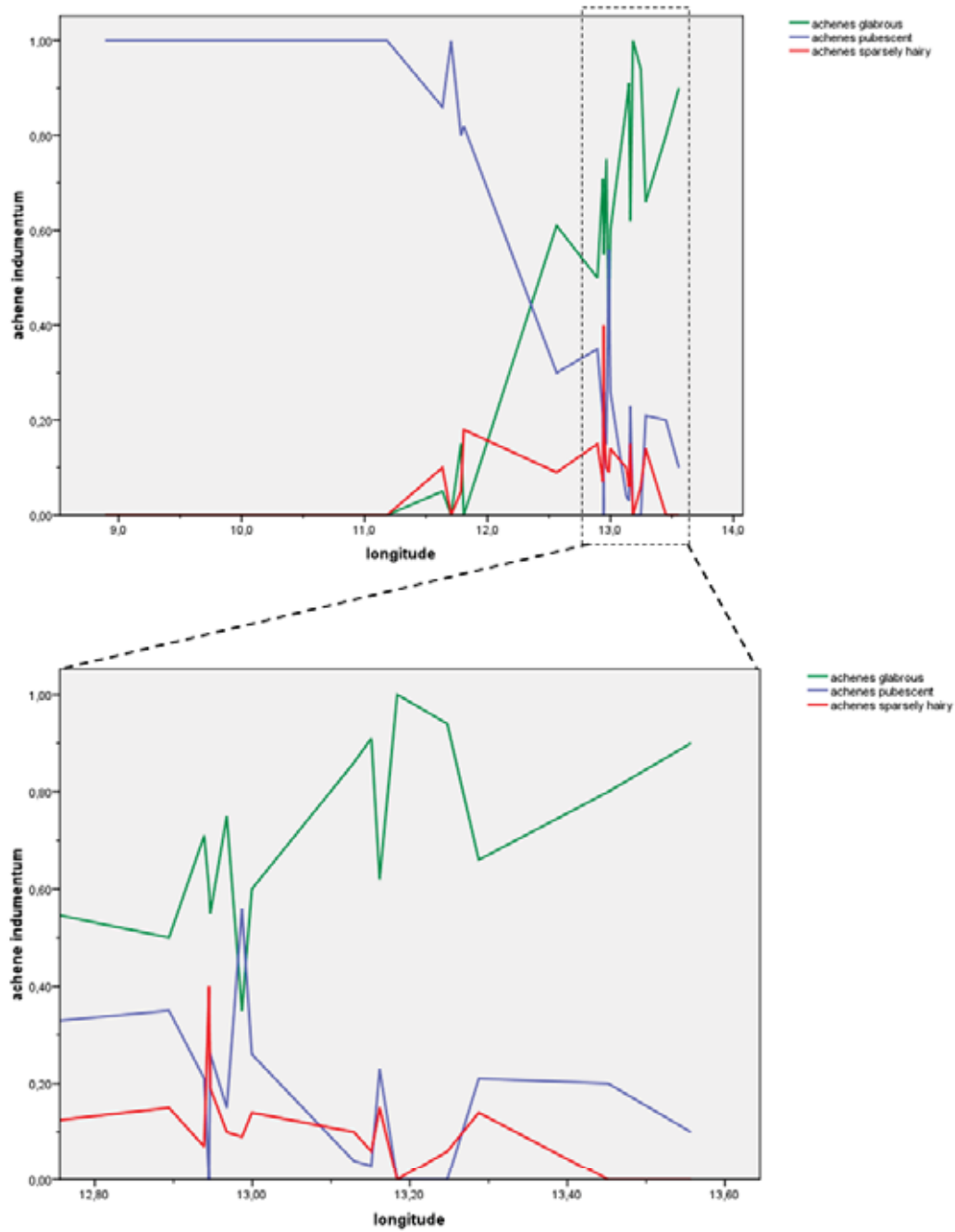


Figure 41. Line plot displaying the mean proportions of achene indumentum states in 27 *Tephroseris helenitis* populations against their longitude.

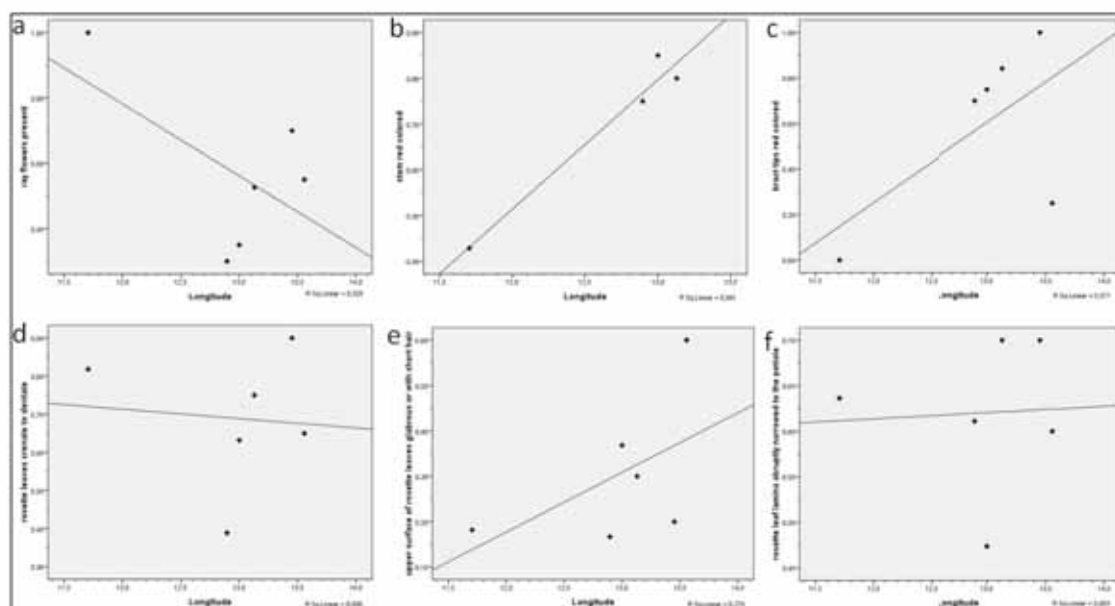


Figure 42. Mean proportions of six morphological character states in six *Tephrosieris helenitis* populations plotted against their longitude for (a) present ray flowers, (b) red colored stems, (c) red colored bracts tips, (d) crenate to dentate rosette leaves, (e) glabrous or short haired upper surfaces of rosette leaves and (f) rosette leaves with abruptly to the petiole narrowed lamina.

3.10. Vegetation data analyses

In four *T. helenitis* populations (ADN2, EST2, GEO1 and LAU1) associated vascular plant species were surveyed in altogether 68 plots (ADN2: 19 plots, EST2: 16 plots, GEO1: 13 plots, LAU1: 20 plots). In total, 105 species were recorded (64 species in ADN2, 49 species in EST2, 36 species in GEO1 and 51 species in LAU1) as present or absent in the plot. The data matrix was used to perform a principal component analysis (PCA) in the program PAST. Eigenvalues and the percentages of variation of the first seven components are shown in Table 19. Loadings $>|0.25|$ of the PCA variables (viz. species) for the first three components are presented in Table 20. Five species, *Anemone nemorosa* L., *Colchicum autumnale* L., *Laserpitium prutenicum* L., *Phragmites australis* (CAV.) TRIN. ex STEUD. and *Stachys officinalis* (L.) TREVIS., were negatively correlated with the first axis with loadings $>|0.25|$. *Carex flacca* SCHREB. was highly negatively correlated with the second axis, while *Deschampsia cespitosa* (L.) P.BEAUV. and *Lysimachia vulgaris* L. were positively correlated with this axis. *Carex elata* ALL., *Carex panicea* L., *Filipendula ulmaria* (L.) MAXIM. and *Selinum carvifolia* (L.) L. showed negative correlation with the third axis.

The PCA-scores of the plots, which were labeled either by population or morphological character states, are displayed as scatter plots in Figure 43a-i. Labeling the plots by population (Fig. 43a-b) revealed a clear separation of groups. The first axis separated population LAU1 from the remaining three populations. Axis 2 separated these remaining populations moderately, while Axis 3 separated population ADN2 clearly. When samples were labeled by achene type (Fig. 43c-d) or six other recorded morphological characters recorded (Fig. 44a-f) there was no clear separation of groups. Therefore, the plots entirely cluster according to their geographic origin and not according to their achene type (viz. subspecies) or other

morphological characters. Using only data of the two admixed populations for achene type (EST2 and LAU1) the results were similar. Also in the case, there was no clear distinction of groups due to achene indumentum or other morphological characters (data not shown).

Figure 45 presents mean Ellenberg's indicator values (EIV) for each of the four populations, which were calculated using the EIV of the recorded species of each plot. Population GEO1 showed about 1.5 lower levels of soil humidity (F) than the remaining three populations. The level of continentality (K) was also lowest in this population, while the highest value was found in population EST2. No separation of the populations was indicated for light (L) and soil reaction (R). The level of nutrients (N) was highest in population GEO1, while temperature (T) was higher in populations EST2 and LAU1 than in ADN2 and GEO1.

Table 19. Eigenvalues and percentages of variance for seven components with the highest Eigenvalues resulting from the PCA analysis of four populations surveyed for associated vegetation of *Tephrosieris helenitis* individuals.

Component	Eigenvalue	% of variance
1	1.931	17.598
2	1.116	10.172
3	1.079	9.834
4	0.488	4.450
5	0.455	4.146
6	0.410	3.739
7	0.396	3.613

Table 20. PCA-scores of associated vascular plant species with loadings >|0.25| for at least one of the first three components of the PCA.

Recorded species	Loadings		
	Axis 1	Axis 2	Axis 3
<i>Anemone nemorosa</i> L.	-0.270	-0.084	-0.028
<i>Carex elata</i> ALL.	0.128	-0.017	-0.272
<i>Carex flacca</i> SCHREB.	-0.042	-0.335	0.163
<i>Carex panicea</i> L.	-0.124	-0.028	-0.349
<i>Colchicum autumnale</i> L.	-0.273	-0.110	-0.082
<i>Deschampsia cespitosa</i> (L.) P.BEAUV.	0.039	0.322	0.198
<i>Filipendula ulmaria</i> (L.) MAXIM.	-0.114	-0.211	-0.254
<i>Laserpitium prutenicum</i> L.	-0.271	0.231	0.157
<i>Lysimachia vulgaris</i> L.	-0.080	0.287	0.165
<i>Phragmites australis</i> (CAV.) TRIN. ex STEUD.	-0.278	0.236	0.161
<i>Selinum carvifolia</i> (L.) L.	0.174	0.114	-0.316
<i>Stachys officinalis</i> (L.) TREVIS.	-0.285	-0.040	-0.041

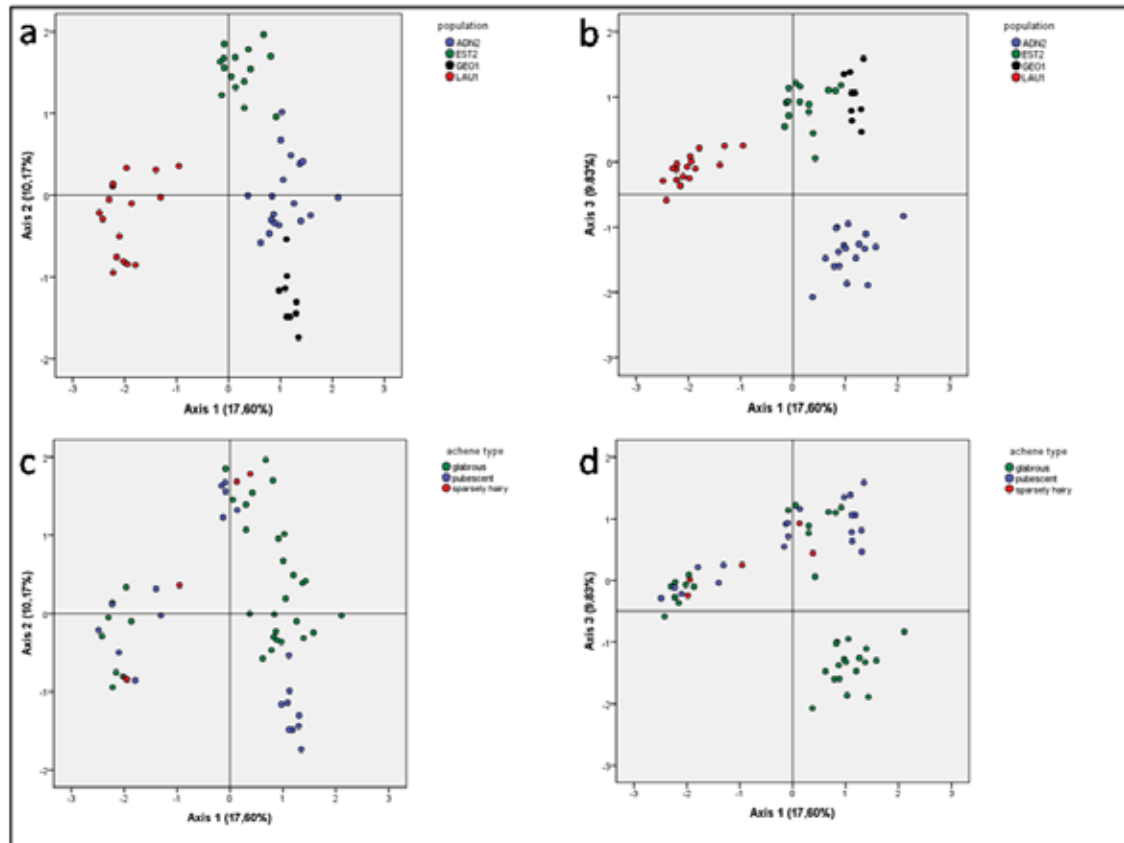


Figure 43. Principal component analysis (PCA) of 68 vegetation plots. Plots are labeled according to (a-b) their population origin and (c-d) the achene indumentum state of the *Tephroservis helenitis* individual, which was at the center of the plot.

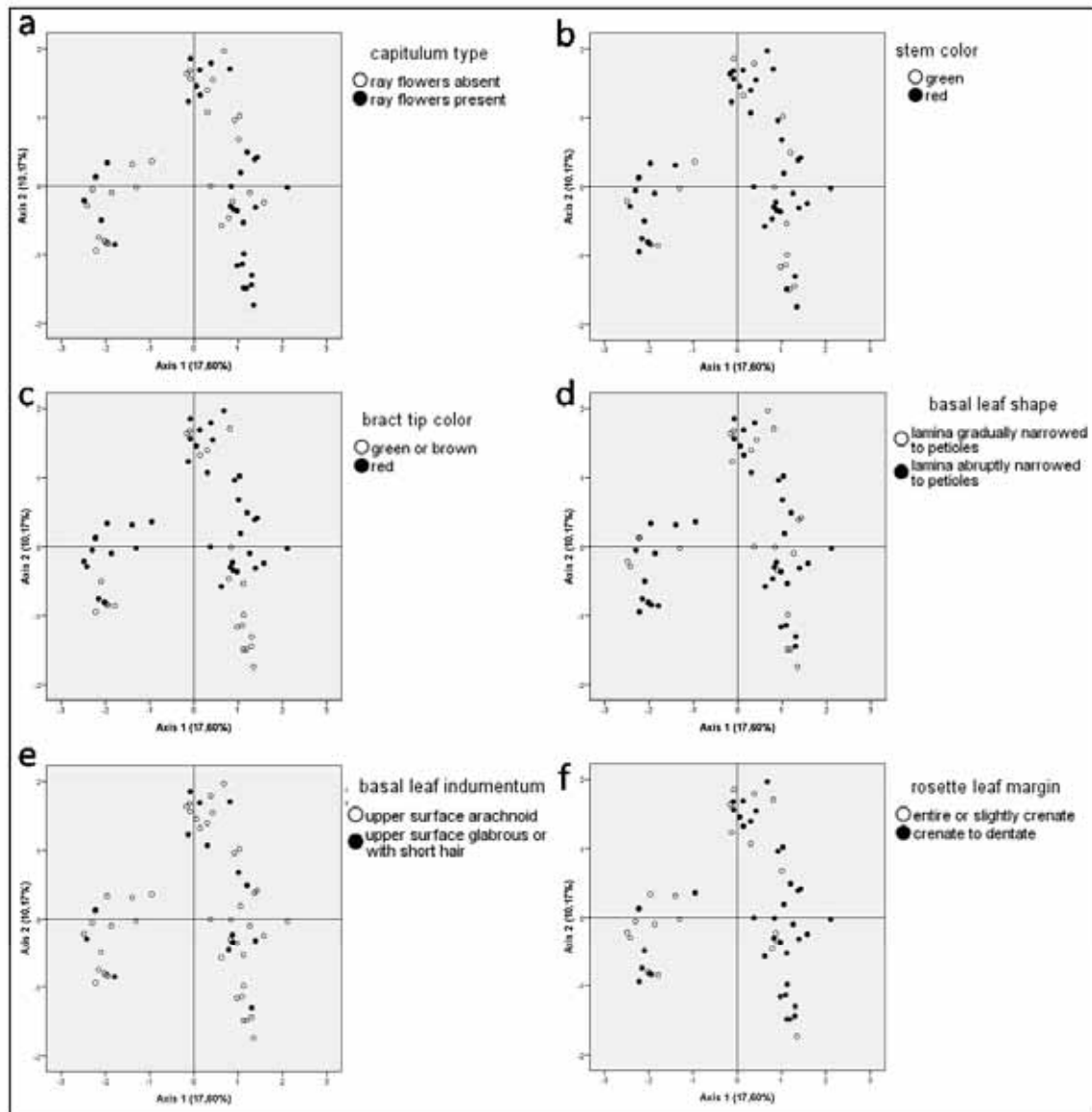


Figure 44. Principal component analysis (PCA) of 68 vegetation plots. Plots are labeled according to the states of six morphological characters of the *Tephrosia helenitis* individual, which was at the center of the plot: (a) capitulum type, (b) stem color, (c) bract tip color, (d) basal leaf shape, (e) basal leaf indumentum and (f) basal leaf margin.

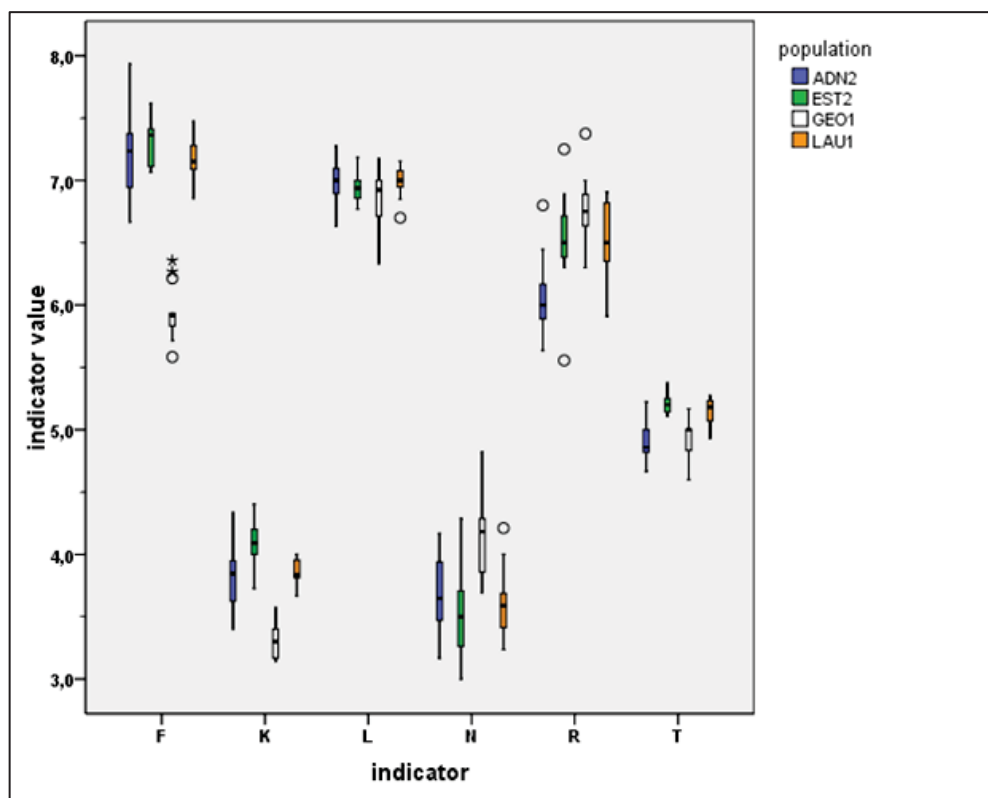


Figure 45. Average Ellenberg's indicator values of populations ADN2, EST2, GEO1 and LAU1 in a box plot diagram. Abbreviations: F, soil humidity; K, continentality; L, light; N, nutrients; R, soil reaction; T, temperature.

3.11. Association of morphological characters and vegetation data with genetic data

3.11.1. Mapping of morphological characters onto the genetic data

Tests of association between genetic and morphological data were performed for 68 individuals in six populations (ADN2, EST2, GEO1, GER1, HAS1 and LAU1) using a PCA in the program CANOCO with the genetic data, taken as the primary matrix for the PCA. The morphological data was utilized as a secondary matrix and was superimposed on the PCA afterwards. As shown in Figure 46a-b, the first axis separated the populations only weakly. Population ADN2 and the two easternmost populations (GER1 and HAS1) were separated from the remaining populations. Axis 2 separated the two latter mentioned populations and population LAU1. The third axis separated population GEO1 from the remaining populations. Considering the morphological characters, which were correlated with the PCA axes (also displayed in Table 21), the red stem color was highly negatively correlated with the first axis (-0.526). Red colored bract tips were negatively correlated to the first axis as well as to the third axis. The remaining four characters were only weakly correlated to the three axes. Labeling the individuals with their states of morphological characters (including achene type), no pattern of separation could be observed in any of them (Fig. 46c-d and Fig. 47a-f). Thus, genetic variation

of the first three PCA components was mainly associated with population origin rather than any of the morphological characters.

Table 22 presents the mean proportions of individuals exhibiting certain morphological character states for each cluster as identified by STRUCTURE (independent and correlated allele frequency model) and BAPS (non-spatial and spatial admixture model). Pubescent achenes were found in 100% of the individuals of cluster 1 in all analyses. Cluster 2 contained only 20-30% individuals with pubescent achenes (cluster 3: 52%). Present ray flowers were found in 75-92% of the individuals of cluster 1, while cluster 2 only contained 44-51% (cluster 3: 57%). Individuals with red colored stems and glabrous upper surfaces of rosette leaves were slightly commoner in cluster 2 than in cluster 1 (and cluster 3). Red bract tips were clearly commoner in cluster 2 (about 60-70%) than in cluster 1 (about 10-25%), whereas cluster 3 was intermediate (48%). Rosette leaves with laminae abruptly narrowed to the petiole and a crenate to dentate margin presented slightly higher proportions in cluster 1 (compared to cluster 2). The highest value of crenate to dentate rosette leaves was found in cluster 3.

Binary logistic regressions were used to compare binary data with continuous data (Table 23). Comparisons of the morphological characters with individuals scores of the PCoA-Ax1 based on the AFLP data and longitude generally showed low levels of correlation. Chi-square levels were low (0.0 to 12.15), except for achene indumentum compared with PCoA-Ax1 (78.43; P-value < 0.001) and longitude (142.88; P-value < 0.001). These high values are due to the larger number of individuals surveyed for achene indumentum (220 samples in both analyses). Nevertheless, despite the low chi-square levels, the Omnibus tests of model coefficients were also significant for comparing capitulum type with PCoA-Ax1 (P-value = 0.009) and longitude (P-value = 0.010), stem color with longitude (P-value = 0.007), bract tip color with PCoA-Ax1 (P-value = 0.002) and longitude (P-value < 0.001) and basal leaf indumentum with longitude (P-value = 0.038). The Cox & Snell R^2 (0.30 and 0.48, respectively) and Nagelkerke R^2 (0.40 and 0.68, respectively) tests generally show low levels, except the comparison of achene indumentum and longitude showed moderate levels (0.68).

Table 21. Scores of six morphological character states for the first three components of the AFLP-based PCA.

Morphological character	Component 1	Component 2	Component 3
Achenes pubescent	-0.016	0.193	0.267
Ray flowers present	-0.064	-0.193	0.179
Stem red colored	-0.526	0.175	-0.132
Bract tips red colored	-0.280	-0.048	-0.552
Rosette leaf lamina abruptly narrowed to the petiole	0.015	-0.096	-0.009
Upper surface of rosette leaves glabrous or with short hair	0.170	0.026	-0.036
Rosette leaves crenate to dentate	-0.115	-0.298	0.126

Table 22. Proportions of different states of six morphological characters in genetic (AFLP) clusters identified in different analyses using STRUCTURE and BAPS. Within-population sample sizes of each morphological character are given in Table 15. Abbreviations: Allele freq. corr., Allele frequencies correlated; Allele freq. ind., Allele frequencies independent; Cl., Cluster; Spatial adm., Spatial admixture; Non-spatial adm., Non-spatial admixture.

Morphological character	STRUCTURE					BAPS			
	Allele freq. ind.		Allele freq. corr.			Spatial adm.		Non-spatial adm.	
	Cl. 1	Cl.2	Cl.1	Cl.2	Cl.3	Cl.1	Cl.2	Cl.1	Cl.2
Achenes pubescent	1.00	0.28	1.00	0.20	0.52	1.00	0.23	1.00	0.32
Ray flowers present	0.88	0.48	0.86	0.45	0.57	0.92	0.44	0.75	0.51
Stem red colored	0.57	0.75	0.50	0.82	0.67	0.50	0.79	0.50	0.75
Bract tips red colored	0.13	0.62	0.14	0.67	0.48	0.08	0.67	0.25	0.59
Rosette leaf lamina abruptly narrowed to the petiole	0.86	0.61	0.83	0.63	0.59	0.70	0.63	1.00	0.62
Upper surface of rosette leaves glabrous or with short hair	0.29	0.33	0.33	0.35	0.24	0.20	0.34	0.00	0.34
Rosette leaves crenate or dentate	0.71	0.64	0.67	0.61	0.76	0.70	0.64	0.67	0.65

Table 23. Binary logistic regressions of achene indumentum and morphological characters states with scores of the PCoA-Axis1 based on AFLP data and longitude. Abbreviations: ach. i., achene indumentum; b.l. ind., basal leaf indumentum; b.l. margin, basal leaf margin; b.l. shape, basal leaf shape; bract tip c., bract tip color; cap. t., capitulum type; cren. to dent., crenate to dentate; lamina a. narr., lamina abruptly narrowed to the petiole; N, number of samples included in analysis; n.s., not significant (P-value >0.05); O. tests of model coeff., Omnibus tests of model coefficients; pred. perc., predicted percentage; sig., significance; stem c., stem color; u. surf. glab., upper surface glabrous or with short hairs; *, P-value between 0.05 and 0.01; **, P-value between 0.001 and 0.01; ***, P-value < 0.001.

Comparison	Character state	N	Pred. perc.	O. tests of model coeff.			Cox & Snell R ²	Nagelkerke R ²	Classification table		
				χ^2	df	sig.			no	yes	total
Ach. i. - PCoA-Ax1	Pubescent	220	52.70	78.34	1	0.000 ***	0.30	0.40	80.20	70.20	75.50
Ach. i. - longitude	Pubescent	220	52.70	142.88	1	0.000 ***	0.48	0.64	97.41	74.04	86.36
Cap. t. - PCoA-Ax1	Present	79	51.90	6.79	1	0.009 **	0.08	0.11	57.89	60.98	59.49
Cap. t. - longitude	Present	103	53.40	6.57	1	0.010 *	0.06	0.08	25.00	67.27	47.57
Stem c. - PCoA-Ax1	Red	60	73.33	2.99	1	0.084 n.s.	0.05	0.07	12.50	97.73	75.00
Stem c. - longitude	Red	74	72.97	7.32	1	0.007 **	0.09	0.14	40.00	88.89	75.68
Bract tip c. - PCoA-Ax1	Red	79	56.96	9.79	1	0.002 **	0.12	0.16	50.00	77.78	65.82
Bract tip c. - longitude	Red	104	57.69	12.15	1	0.000 ***	0.11	0.15	34.09	100.00	72.12
B.l. shape - PCoA-Ax1	Lamina a. narr.	74	63.51	0.18	1	0.668 n.s.	0.00	0.00	0.00	100.00	63.51
B.l. shape - longitude	Lamina a. narr.	98	61.22	0.00	1	0.954 n.s.	0.00	0.00	0.00	100.00	61.22
B.l. ind. - PCoA-Ax1	U. surf. glab.	74	67.57	1.72	1	0.189 n.s.	0.02	0.03	98.00	0.00	66.22
B.l. ind. - longitude	U. surf. glab.	98	67.35	4.28	1	0.038 *	0.04	0.06	100.00	0.00	67.35
B.l. margin - PCoA-Ax1	Cren. to dent.	74	64.86	0.09	1	0.768 n.s.	0.00	0.00	0.00	100.00	64.86
B.l. margin - longitude	Cren. to dent.	98	66.33	0.05	1	0.826 n.s.	0.00	0.00	0.00	100.00	66.33

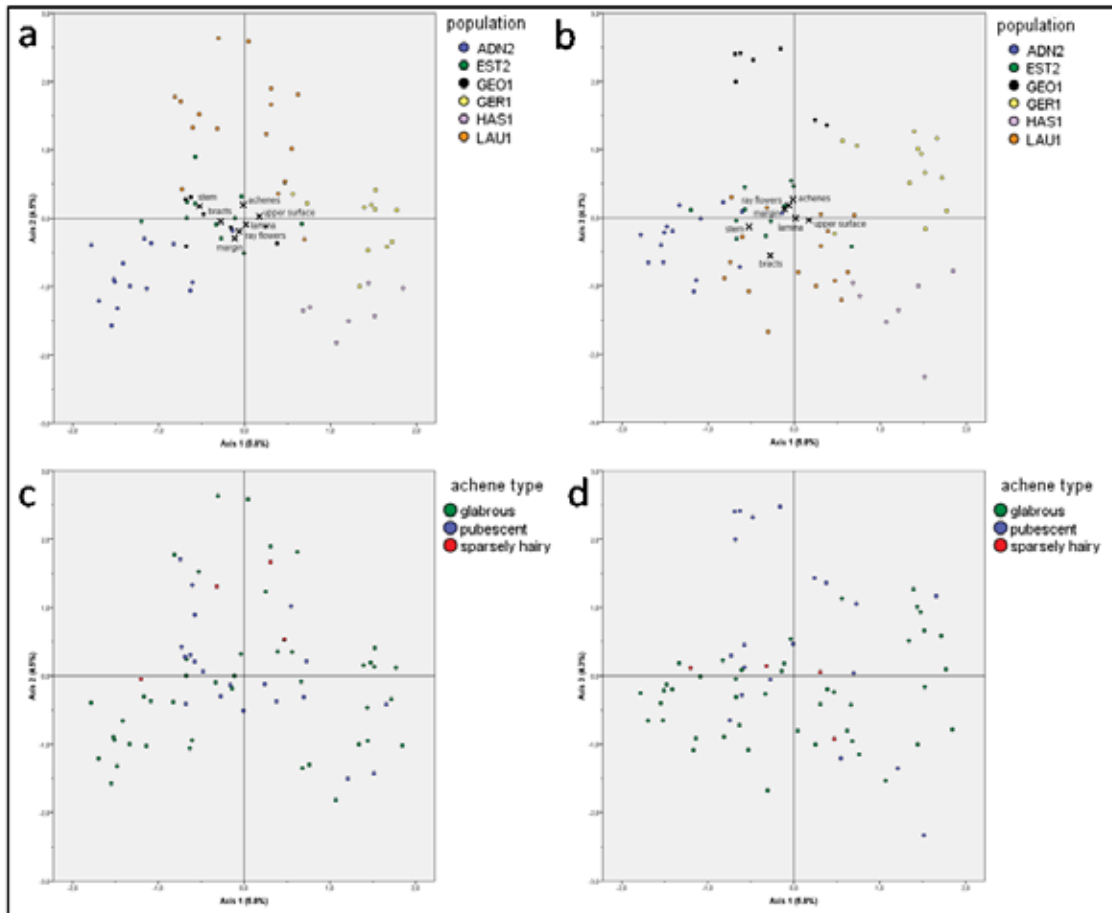


Figure 46. PCA based on AFLP profiles of 68 *Tephrosia helenitis* individuals. Associated morphological character states were correlated with this PCA and were displayed as loadings (a-b). Samples are labeled by (a-b) their population origin and (c-d) their achene indumentum type.

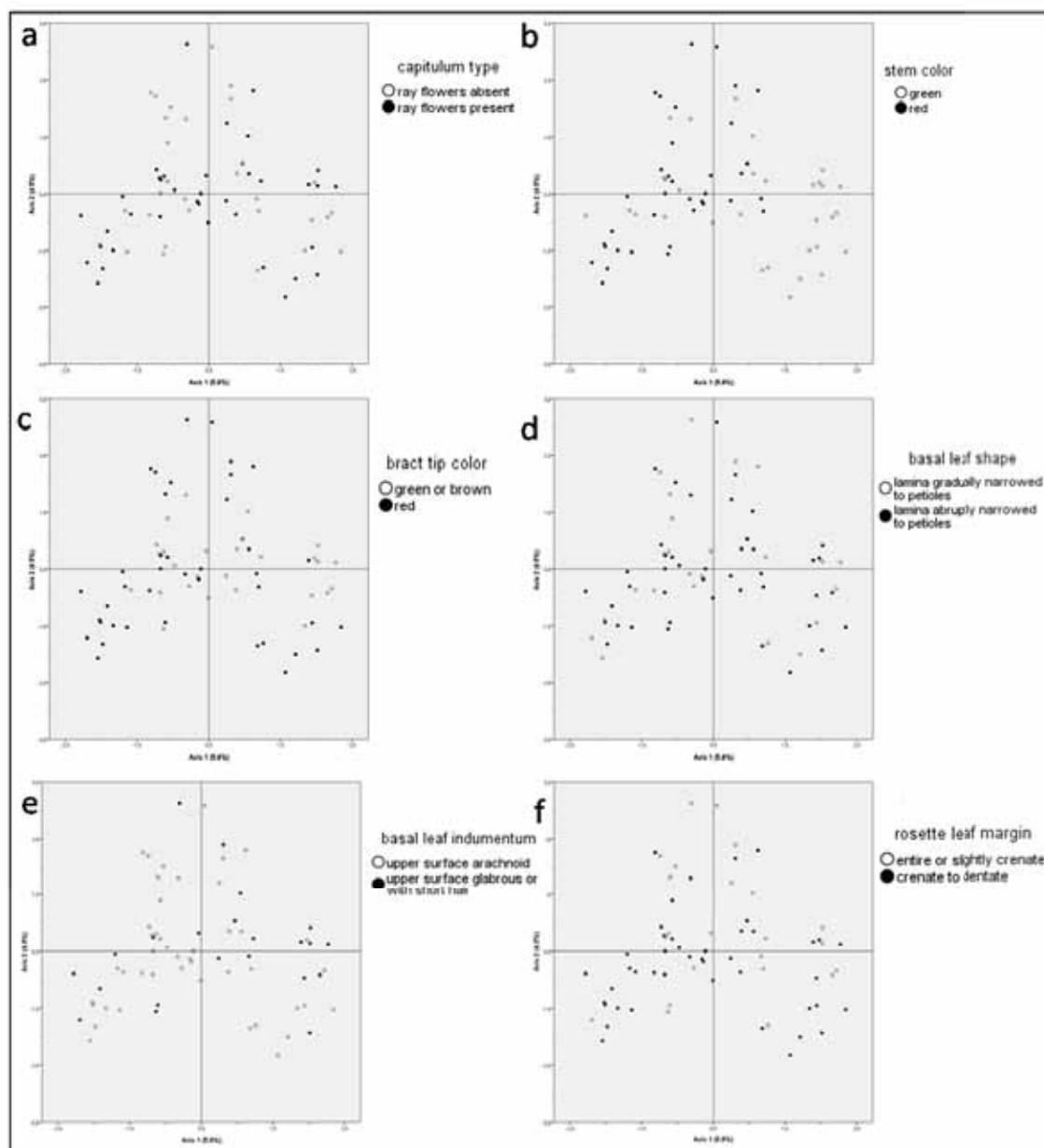


Figure 47. PCA based on AFLP profiles of 68 *Tephrosia helenitis* individuals. Samples are labeled by their states of six morphological characters: (a) capitulum type, (b) stem color, (c) bract tip color, (d) basal leaf shape, (e) basal leaf indumentum and (f) basal leaf margin.

3.11.2. Mapping of vegetation data onto the genetic data

An AFLP-based PCA was performed for 56 individuals in four populations (ADN2, EST2, GEO1 and LAU1) as described in section 3.11.1, using the vegetation data matrix as secondary matrix in CANOCO. As shown in Figure 49, populations were separated very well. The first axis separated ADN2 and GEO1 from EST2 and LAU1, and the two latter populations were separated along the second axis. Axis 3 had no effect. Associated plant species of *T. helenitis* with loadings $>|0.5|$ are listed in Table 24 and shown in Figure 48. *Carex panicea* and *Selinum carvifolia* were negatively correlated with the first axis, while *Carex flacca*, *Phyteuma orbiculare* and *Scabiosa columbaria* were positively correlated. A negative correlation with axis

2 was given for *Prunella vulgaris*, *Selinum carvifolia* and *Vicia cracca*. Six species were found, which were positively correlated with the second axis - *Anemone nemorosa*, *Carex hartmanii*, *Colchicum autumnale*, *Laserpitium prutenicum*, *Mentha aquatica* and *Phragmites australis*. No species had loadings $>|0.5|$ for the third axis.

As a secondary approach, the matrix of six Ellenberg indicator variables (EIVs) was used as the secondary matrix. As shown in Figure 49 and Table 25, continentality and soil humidity were negatively correlated with the first axis, while soil acidity and nutrients were positively correlated. Temperature was positively correlated with the second axis.

Table 24. Scores of associated vascular plant species with loadings $>|0.5|$ in at least one of the first three components of the AFLP-based PCA. Loadings $>|0.5|$ are in bold.

Recorded species	Component 1	Component 2	Component 3
<i>Anemone nemorosa</i> L.	-0.096	0.725	-0.094
<i>Carex flacca</i> SCHREB.	0.633	0.111	-0.080
<i>Carex hartmanii</i> CAJANDER	-0.102	0.799	-0.200
<i>Carex panicea</i> L.	-0.619	0.105	-0.099
<i>Colchicum autumnale</i> L.	-0.193	0.693	-0.114
<i>Laserpitium prutenicum</i> L.	-0.136	0.732	0.250
<i>Mentha aquatica</i> L.	-0.041	0.532	-0.098
<i>Phragmites australis</i> (CAV.) TRIN. ex STEUD.	-0.122	0.776	0.218
<i>Phyteuma orbiculare</i> L.	0.529	-0.143	0.147
<i>Prunella vulgaris</i> L.	0.272	-0.613	-0.117
<i>Scabiosa columbaria</i> L.	0.678	-0.174	0.046
<i>Selinum carvifolia</i> (L.) L.	-0.594	-0.578	-0.013
<i>Stachys officinalis</i> (L.) TREVIS.	-0.189	0.658	-0.119
<i>Valeriana dioica</i> L.	-0.228	0.503	-0.192
<i>Vicia cracca</i> L.	-0.159	-0.517	-0.338
<i>Vicia tetrasperma</i> (L.) SCHREB.	-0.092	0.715	-0.113

Table 25. Scores of Ellenberg indicators variables with loadings $>|0.5|$ in at least one of the first three components of the AFLP-based PCA. Loadings $>|0.5|$ are in bold.

Indicator	Component 1	Component 2	Component 3
Continentality	-0.580	0.248	0.199
Light	-0.226	-0.027	0.017
Nutrients	0.444	-0.175	-0.049
Soil acidity	0.330	0.112	-0.051
Soil humidity	-0.776	0.242	0.002
Temperature	-0.019	0.524	0.228

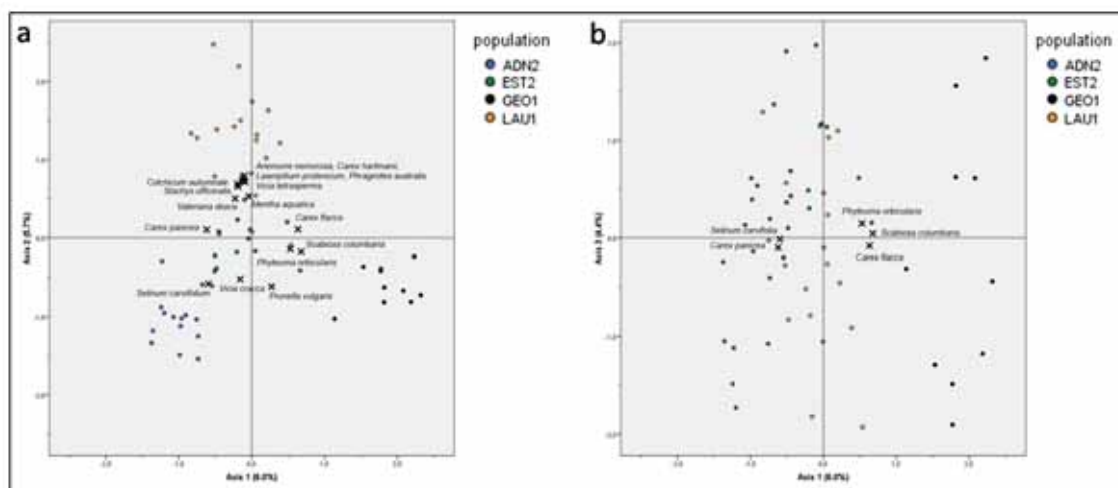


Figure 48. PCA based on AFLP profiles of 56 *Tephrosieris helenitis* individuals. Associated vascular plant species of single *Tephrosieris helenitis* individuals with loadings $>|0.5|$ for at least one of the shown axes are shown. Samples are labeled by their assignment to populations.

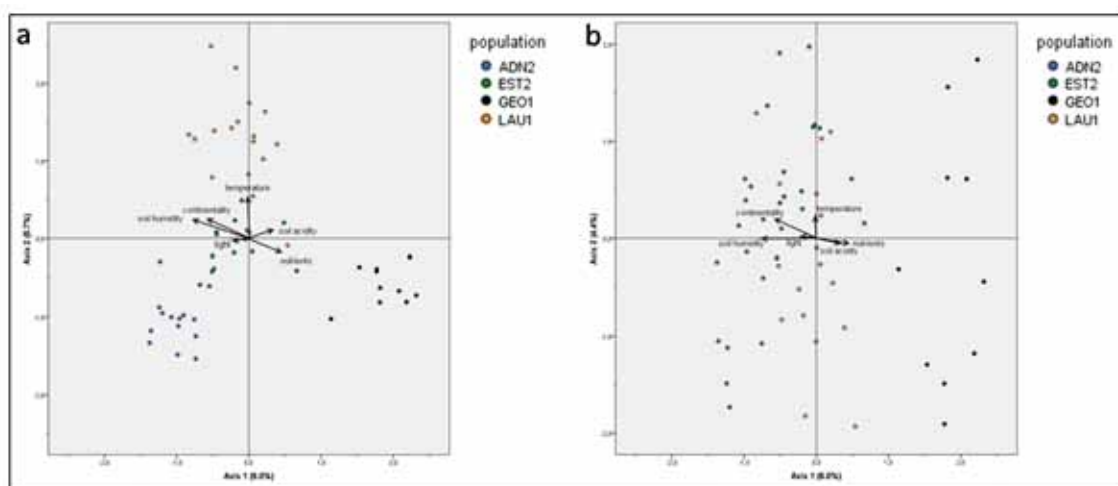


Figure 49. PCA based on AFLP profiles of 56 *Tephrosieris helenitis* individuals. Associated means of six indicator values of single plots were correlated with this PCA and are displayed as arrows. Samples are labeled by their population origin.

3.12. Self-incompatibility tests

Bagging-tests were performed at two sites (field vs. botanical garden) in a total of 19 plants. Five individuals showed pubescent achenes (viz. ssp. *helenitis*), 13 and one individuals had glabrous and sparsely hairy achenes, respectively (viz. ssp. *salisburgensis*). At the time of fruiting (see Fig. 50a), achenes were examined for their state of maturity. In bagged capitula or inflorescences, only undeveloped achenes (see Fig. 50b as an example) were found, except for one individual (Nr. 7) of the field site, which had < 5% mature (and pubescent) achenes upon bagging of its whole inflorescence with a paper bag (see Fig. 50c as example). By contrast, the control individuals (4 individuals at the field site and 2 individuals at the botanical garden) generally had 50-70% mature and well developed achenes under conditions of open pollination (mean: $59\% \pm 25\%$; min. 15%, max. 100%).

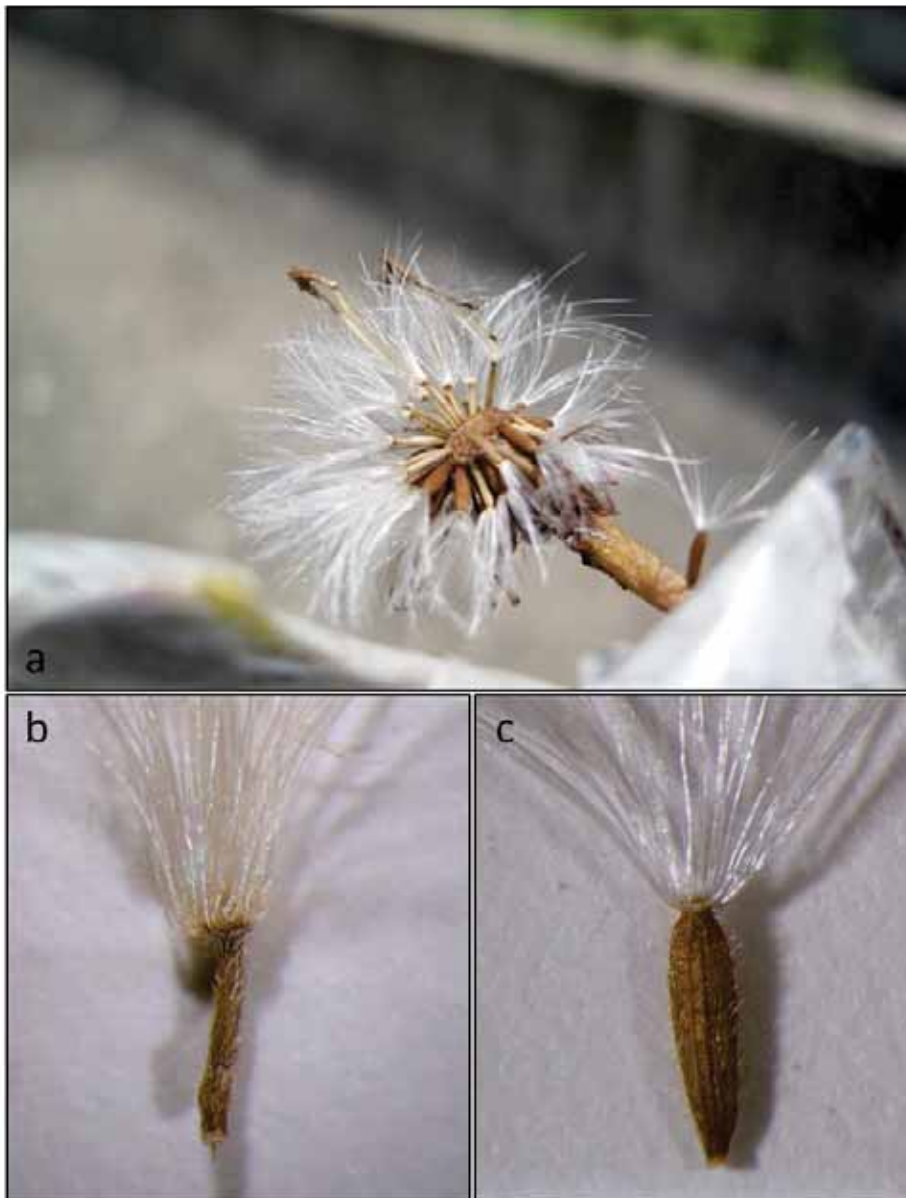


Figure 50. Fruiting capitulum of a control (open-pollinated) individual showing both mature and undeveloped achenes (a), an undeveloped achene found in a bagged capitulum (b) and a mature achene found in a non-bagged capitulum (c).

4. Discussion

4.1. Taxonomical aspects

4.1.1. Distribution patterns of *Tephroseris helenitis* subsp. *helenitis* and *salisburgensis* at the northern fringe of the Alps

Field observations of achene indumentum, which is the taxonomically most relevant trait for this purpose, were conducted between 2006 and 2010 across 30 populations to investigate the distribution pattern of *T. helenitis* subsp. *helenitis* and *salisburgensis* at the northern fringe of the Alps. Subspecies *helenitis* (showing pubescent achenes) was found throughout the whole study area (from the westernmost population NUS1 in Baden-Wuerttemberg to the easternmost population GER1 in Upper Austria), while ssp. *salisburgensis* (showing glabrous or sparsely hairy achenes) occurs exclusively east of the Munich area. However, there are only three populations and one subpopulation that entirely consist of individuals with glabrous and/or sparsely hairy achenes: STI1, UNT2, WOE1 and ADN2. All of them are located in the Salzburg area (in the Salzach valley and the eastern Flachgau /Attersee region). All 20 sampled individuals of subpopulation ADN2 showed glabrous achenes. By contrast, individuals showing only pubescent achenes were found in eight populations. Seven of those are distributed west of the Munich area, while only one population (GEO1) is located just east of Munich. Mixed stands exhibiting both achene types, however, comprised the majority of all populations studied, in fact 15 populations and the subpopulation ADN1.

My own observations can be compared with information retrieved from unpublished floristic databases (FLORISTISCHE KARTIERUNG ÖSTERREICHS unpubl. data, SABOTAG unpubl. data), distribution maps (BIB 2010, FLORAWEB 2010) and the taxonomic/systematic literature (HEGI 1928, CUFODONTIS 1933, OBERDORFER 1983, SCHUBERT & VENT 1988, KRACH 2000, SEYBOLD 2006, FISCHER et al. 2008). However, detailed accounts of the distribution patterns of ssp. *salisburgensis* are rarely found (HEGI 1928, CUFODONTIS 1933, KRACH 2000, BIB 2010, FLORAWEB 2010). According to CUFODONTIS (1933), ssp. *salisburgensis* occurs at the southeastern range limit of *T. helenitis*, i.e. in the region of Salzburg and adjacent areas in Bavaria. Individuals with achenes, which are “becoming more or less bald” (i.e. glabrous), are described as var. *pratensis* KOCH in HEGI (1928) for the alpine foothills of Salzburg and Upper Bavaria. In this reference individuals of Upper Bavaria with glabrous and pubescent achenes are mentioned as well as transitional forms between them. KRACH (2000) claims that “pure” ssp. *salisburgensis* plants (with glabrous achenes) occur in the region of Salzburg, southwestern Upper Austria, Lower Austria and rarely in southeastern Bavaria, while transitional forms are more common in the latter region. My own observations show that ssp. *helenitis* is much more frequent in populations of Salzburg than thought previously. In the floristic databases of the FLORISTISCHE KARTIERUNG ÖSTERREICHS (unpubl. data) and SABOTAG (unpubl. data) most *T. helenitis* data are without subspecies designation (see also STÖHR 2003). Most of the remaining entries refer to ssp. *salisburgensis*, while only a few or even none are ascribed to ssp. *helenitis*. In fact, the latter subspecies is entirely absent in the FLORISTISCHE KARTIERUNG ÖSTERREICHS (unpubl. data) and recorded only nine times in SABOTAG (unpubl. data), compared to 10 and 58 records of ssp. *salisburgensis*, respectively. Nevertheless, ssp. *salisburgensis* clearly predominates in the

eastern part of the area. But why has ssp. *helenitis* been recorded so rarely in the Salzburg area? Possibly older herbarium specimens were ascribed to ssp. *salisburgensis* because other than achene indumentum characters were used for subspecies identification in the older literature, such as the balding lower leaf surfaces (HEGI 1928, CUFODONTIS 1933). Another possibility is that ssp. *salisburgensis* was simply expected as a local form of *T. helenitis*, which occurs in Salzburg and adjacent areas. So, only ssp. *salisburgensis* was presumed there and ssp. *helenitis* was just not taken into account.

In the present study, the frequency of achene types of *T. helenitis* populations was plotted against longitude, resulting in a clinal pattern (Fig. 41). That is, pubescent achenes decrease towards the east, while glabrous ones increase. Sparsely hairy achenes are always in the minority within populations but show highest proportions in the central region (from the Miesbach region in the west to the eastern Flachgau region in the east), which might indicate a hybrid zone (see below). As stated above, HEGI (1928) but also KRACH (2000) report transitional forms between individuals of different achene types viz. subspecies. FISCHER et al. (2008), however, ascribe these sparsely hairy achenes to ssp. *salisburgensis*.

4.1.2. Association of achene type with genetic, morphological and vegetation data

Individual-based AFLP data neither separate the subspecies according to their achene indumentum (Figs. 26b, 43c-d) nor any other morphological character (Fig. 44). Although logistic regressions of achene type with individual scores of the AFLP-based PCoA-Ax1 resulted in low regression coefficients of 0.30 to 0.40, these were highly significant with P-values < 0.001 (Table 23). When logistic regressions of PCoA-Ax1 and further morphological characters were performed, the coefficients were still low and non-significant, ranging from 0.00 to 0.12, but the regressions with capitulum type and bract tip color were significant (P-values = 0.009 and 0.002, respectively). The two subspecies are not separated according to achene indumentum and the other surveyed morphological characters. Nevertheless, clinal variation in genetic data is recognizable, i.e. in population scores of AFLP-based PCoA-Ax1 (Fig. 28), which is probably not depending on subspecies status (achene indumentum), but on the geographic distances among the populations. This also fits the “isolation by distance” (IBD) pattern found in *T. helenitis* at the northern edge of the Alps (Fig. 34). Stem and bract color show similar clinal trends as achene indumentum when plotted against longitude (Fig. 42). While individuals with glabrous achenes often have red stems and bract tips, individuals with pubescent achenes generally have green or brownish ones (Table 16). Nevertheless, a high concordance of these characters was not found and it is not supposed that stem and bract tip color are diagnostic characters. Presumably the red color is a modification to high humidity of the habitats (see section 4.4.1).

Another character of considerable interest is the presence or absence of ray flowers. These are presumed to be important for the attraction of pollinators, which is strengthened due to the fact that they are pistillate (female, without stamens). STUESSY et al. (1986) revealed that the visitation frequency of pollinators of *Helianthus grosseserratus* is 61% lower in rayless populations compared to rayed populations. Besides, the diversity of pollinators dropped sharply. The seed-set of rayless populations was found to be 64% lower than for rayed

populations. In *Senecio vulgaris* similar results have been found in natural populations of rayed and rayless variants (MARSHALL & ABBOTT 1982). These authors also mention the lower outcrossing rate of rayless individuals (1%) compared to rayed individuals (13-20%). A small contribution of ray flowers to seed set (15%) has been reported for *Senecio integrifolius* (syn. *Tephrosieris integrifolia*), a close relative of *Tephrosieris helenitis* (ANDERSSON & WIDEN 1993), whereby the number of capitula per plant was negatively correlated with seed set. The presence vs. absence of ray flowers in Asteraceae has often a simple genetic basis with one or two major genes and several modifiers (GILLIES et al. 2002). For example, in *Gerbera hybrida* the CYCLOIDEA-like (CYC-like) homolog GhCYC2 is only expressed in ray flowers but not in the disk flowers (BROHOLM et al. 2008). In *Senecio* the RAY locus generally controls the presence/absence of ray flowers as shown by ABBOTT et al. (1992), COMES (1998) and ANDERSSON (2001). In the literature (SEYBOLD 2006, FISCHER et al. 2008) it is mentioned that ray flowers can be absent in both subspecies of *Tephrosieris helenitis*, but more often lack in ssp. *salisburgensis* than in ssp. *helenitis*. This cannot be supported by the present study, if the subspecies are designated by achene indumentum (Table 17). However, own observations have shown that ray flowers are often absent in the populations of the eastern part of the study area, while they are rarely absent in the western part (even in the Miesbach region, Fig. 42a). Contradictory information stems from T. MEYER (pers. comm), who reports that ray flowers are often absent (at a rough frequency estimate of 50%) in the westernmost part of the sampling area (population MAR1). So, this character seems to be unsuitable for subspecies designation, notwithstanding its biological significance. An accumulation of rayless individuals in the eastern part of the study area, however, is not associated with achene indumentum (Table 17) or genetic data (Fig. 47a).

Besides the presence or absence of ray flowers, the number of ray flowers is mentioned as a diagnostic character of subspp. *salisburgensis* and *helenitis* (SEYBOLD 2006, FISCHER et al. 2008). While ssp. *helenitis* is thought to have 13 ray flowers, ssp. *salisburgensis* is supposed to have 15-17 ray flowers. Morphological investigations of F. HÖGLINGER (unpubl. data) in 1995 and 2010 contradicted this assertion. There was no clear difference in the proportion of glabrous (ssp. *salisburgensis*) vs. pubescent (ssp. *helenitis*) achenes in relation to the number of ray flowers. Observations of 81 individuals in 1995 showed that individuals with pubescent achenes tend to have slightly more ray flowers; the observations of 133 individuals in 2010 were to the contrary. Nevertheless, there was no clear signal for subspecies differentiation due to the number of ray flowers. Most of the ray-flowered individuals surveyed by F. HÖGLINGER showed (15-) 20-21 (-22) ray flowers, while the lowest number was 11 and the highest 39. Some ray flower counts were found for only one achene type: four individuals with higher numbers than 30 and four individuals with 12 ray flowers had only glabrous achenes, whereas three individuals with 23 ray flowers had only pubescent achenes. While in 1995 individuals without ray flowers were preponderant with pubescent achenes, in 2010 glabrous achenes prevailed. These patterns do not indicate an association of presence or absence of ray flowers and achene indumentum. Besides, both subspecies show an average ray flower number between 19 and 19.5, which is more than the values reported in the literature (13; 15-17).

Indumentum, margin and the transition zone of lamina and petiole of basal leaves do not seem to be relevant for subspecies differentiation either. These characters are mentioned in OBERDORFER (1983) and SCHUBERT & VENT (1988), but as the present results show, they are neither associated with achene indumentum (Table 17) nor with the genetic data (Fig. 47d-f) or longitude (Fig. 42). The inappropriateness of basal leaf indumentum for subspecies

differentiation is also claimed by PILSL et al. (2002) and STÖHR (2009). As shown in Table 17, the indumentum of basal leaves is often concordant with the leaf margin. While leaves with arachnoid upper surfaces often show crenate to dentate margins, leaves with glabrous upper surfaces or short hairs show (nearly) entire margins.

A potential factor accounting for the lack of a clear separation of the subspecies based on their achene type (and other morphological characters) could be gene introgression, which might have resulted in the transfer of alleles for, e.g., pubescent achenes into ssp. *salisburgensis* populations, and vice versa (see below).

Vegetation characteristics clearly differentiated the four populations studied (Fig. 43), but they did not allow distinguishing the two subspecies in terms of different microhabitat requirements. The differences in vegetation were mainly due to some indicator species, which were only present in a given population: *Carex hostiana*, *C. umbrosa*, *Crepis mollis*, *Festuca arundinacea*, *Galium album*, *Picea abies*, *Sesleria varia* and *Valeriana officinalis* in population ADN2; *Galium verum* and *Solidago gigantea* in population EST2; *Ajuga reptans*, *Phyteuma orbiculare*, *Plantago lanceolata*, *Scabiosa columbaria* and *Trifolium pratense* in population GEO1; *Anemone nemorosa*, *Carex hartmanii*, *Hypericum tetrapterum*, *Mentha aquatica* and *Vicia tetrasperma* in population LAU1. A comparison of genetic data and vegetation data was performed to obtain potential microhabitat differences between the two subspecies. It was hypothesized that the two subspecies may have different (micro-habitat) requirements, as indicated by different associated plant species in the direct neighborhood (1m distance to the *Tephrosia helenitis* individuals). Therefore, the individual-based AFLP matrix was used as a primary matrix for a PCA and the vegetation data as a secondary matrix (Fig. 48). The PCA did not show any differentiation of subspecies (according to their achene type and/or further morphological characters). Instead, the genetic data clustered according to population origin but according to differences in indicator species or indicator values that may represent microhabitat differences within populations (Fig. 48 and Fig. 49). However, the separation of populations in the PCA based on genetic data was not as clear as that in the PCA from vegetation data (Fig. 43). Nevertheless, some of the associated species were correlated with the PCA-axes (Table 24). In sum, these species are not associated with the named subspecies of *T. helenitis* but rather characterize single populations.

4.1.3. Is the taxonomic rank of “subspecies” for individuals with glabrous achenes justifiable?

According to MERXMÜLLER (1949), subspecies are closely related intra-specific groups, which are geographically separated, regardless of the degree of morphological differences, while MAYR (1969) defined a subspecies as “an aggregate of phenotypically similar populations of a species inhabiting a geographic subdivision of the range of that species and differing taxonomically from other populations of that species”. Currently, genetic and/or ecological traits are frequently involved to recognize and differentiate subspecies (A. TRIBSCH, pers. comm). As to a close relation of such groups, this is clearly supported by the present analyses. Individuals and populations of both *T. helenitis* subspecies are genetically closely related (Figs. 10, 15, 20-24). However, it is not possible to differentiate individuals with glabrous vs. pubescent achenes by their genetic AFLP profiles (Fig. 46c-d). Likewise, other morphological characters surveyed

cannot be correlated with the genetic data (Fig. 47). Also, there is no geographical isolation between the two groups (Fig. 40). Individuals with pubescent achenes (ssp. *helenitis*) are found in all populations, except three populations and one subpopulation in Salzburg. Nearly all populations within the alleged ssp. *salisburgensis*' range are in fact mixed stands of both subspecies, which means that ssp. *salisburgensis* only occurs in sympatry with ssp. *helenitis*. Nevertheless, individuals with glabrous achenes (ssp. *salisburgensis*) show a clearly delimited, endemic distribution. As pointed out by MAYR (1969), the term "subspecies" should not be used when several subspecies of one species occur in the same locality. Besides, no differences in ecological factors were found, which could have at least supported the status of subspecies (see Fig. 43c-d). Thus, it seems more plausible that individuals with glabrous achenes are a variety (also claimed in STÖHR 2009). HOHLA et al. (2009) also considers the rank "subspecies" as set too high. HEGI (1928) already describes individuals of *T. helenitis* with achenes, which are "becoming more or less bald" as var. *pratensis* KOCH (see section 4.1.1)

This is similar to, e.g., *Filipendula ulmaria*, where the subspp. *denudata* (J. & C. PRESL) HAY. and *ulmaria* are almost completely sympatrically distributed, and morphologically and ecologically barely distinguishable. Therefore it was recommended to treat ssp. *denudata* as forma only (KURTTO et al. 2004). As to another example, in Svalbard, two subspecies of *Saxifraga oppositifolia*, subspp. *reptans* (ANDERSS. & HESSELM.) RØNNING and *pulvinata* (ANDERSS. & HESSELM.) RØNNING, were surveyed for variation in morphology, ecology, and pollen size and stainability (BRYSTING et al. 1996). Both taxa differ in growth form being either prostrate (ssp. *reptans*) or cushion-formed (ssp. *pulvinata*). Despite high levels of genetic variation observed for *Saxifraga oppositifolia* (ABBOTT et al. 1995, GABRIELSEN et al. 1997), it was not possible to recognize distinct groups. Also, other examined morphological characters could not be used to separate the two growth forms, which is similar to *Tephroses helenitis* in this study.

4.2. Population history of *Tephroses helenitis* at the northern fringe of the Alps

Intra-population genetic diversity measures were used to determine the direction of postglacial recolonization of *Tephroses helenitis* populations at the northern edge of the Alps. In general, such recolonization of populations can be inferred by a gradual decrease of genetic diversity along a geographic gradient. High diversities are expected for ancient, stable and/or refugial populations (HEWITT 1996, HEWITT 2000, PETIT et al. 2003, WINKLER et al. 2010). Low diversities generally characterize populations, which recently (re-)colonized an area, whereby the direction of spread is inferred from populations with high diversities to populations with low diversities. It was hypothesized that genetic diversities decrease from west to east due to the direction of postglacial recolonization. The easterly distributed populations of *T. helenitis* are entirely found in formerly glaciated areas (Fig. 7). However, this expected pattern could not be observed in *T. helenitis* at the northern edge of the Alps. Rather, the populations surveyed within this area show a mosaic-like ("patchy") pattern of genetic diversities (Table 9 and Figs. 29, 30a, 31a). Diversities with high, intermediate or low levels were distributed within the same local area. Hence, it can be assumed that these populations did not persist in these places during, e.g., the last glaciated maximum (LGM, ca. 18,000 yrs ago) but rather (re-)colonized them postglacially. However, the genetic diversities were not correlated with

longitude (Table 10), as would be expected under the leading edge hypothesis of recolonization (HEWITT 2000).

As mentioned in a review of 134 studies by ECKERT et al. (2008) a decline of within-population genetic diversities towards range margins was found in 64.2% of these studies, of those an increase of among-population differentiation was found in 70.2%. Nevertheless, there were no large differences in genetic diversity levels in most cases. Decreasing genetic diversities were found by DURKA (1999) and LAMMI et al. (1999), whereas an increase of genetic differentiation was reported by ECKSTEIN et al. (2006). VIEJO et al. (2010) also describe drastic reductions in reproductive traits (percentage of reproductive individuals, reproductive allocation, and reproductive capacity) and plant size of *Fucus serratus* in marginal populations. A fine-scale-study by PARISOD & BONVIN (2008) showed that genetic diversity decreases from the core part of a single population to its isolated marginal patches. A positive correlation of latitude and body size has been found in isolated populations of *Metrioptera roeselii*, while the correlation was weak or absent in continuously distributed populations (CASSEL-LUNDHAGEN et al. 2010). No correlation with range periphery was found in GARNER et al. (2004). HOBAN et al. (2010) studied populations of *Juglans cinerea*, which declined due to a fungal pathogen in the 20th century. However, this had a lower impact on the genetics of the populations than their postglacial recolonization history. PAUN et al. (2008) mention that rarity measures (frequency-down-weighted marker values) “appear to be a much better indicator of historical processes and are correlated with refugia” than genetic diversity. Rare markers accumulate in populations over time and indicate old populations (SCHÖNSWETTER & TRIBSCH 2005). In *Tephrosieris helenitis*, the patchy distribution patterns of both genetic diversity and rarity (Fig. 29) better fit to the theory that populations survived the Ice Ages in local refugia outside the ice shield and (re-)colonized new, ice-free terrain from nearby source populations. Therefore, only little genetic variation got lost over these short distances, and thus populations showing relatively high variation might signify (nearby) refugia. The populations of the Ammersee and Untersberg region show higher genetic diversities than the remaining populations. Similar patterns are found for frequency-down-weighted markers, which also have high values in the westernmost (formerly unglaciated) populations. High values of rarity in the latter populations could indicate the proximity to refugia or that *T. helenitis* even survived the Ice Ages at these stands. In the Ammersee region both genetic diversities and rarities are very high, even though the area was glaciated at the LGM. Nevertheless, these populations are close to the border of the ice shield and perhaps represent refugia at glacial-like conditions after the LGM (e.g. Older and Younger Dryas). Effects of these cold periods are likely displayed in the distribution ranges of *Conioselinum tataricum*, *Oxytropis campestris*, *Pulsatilla vernalis* and *Tephrosieris integrifolia* (MEUSEL & JÄGER 1992). These species are absent from large areas of Scandinavia, which were covered by an ice shield at the LGM. However, the distribution margins of these species are not congruent with the borders of the ice shield, but with the borders of the ice shield at later glacial-like periods (A. TRIBSCH, pers. comm). The regions of Miesbach and the eastern Flachgau are adjacent to the Ammersee and Untersberg regions, respectively, and show quite low levels of diversity and/or rarity in *Tephrosieris helenitis* (Fig. 29). This could be due to a later recolonization and therefore a younger age of these populations. The significant negative correlation of rarity and longitude (Table 10) is a possible result of higher gene flow in the eastern populations, which are geographically adjacent and were sampled at higher densities, possibly resulting in a lower number of rare markers.

Pairwise F_{ST} values between populations are significantly positively correlated with their geographic distance (Table 11, Fig. 34). This indicates a so called „isolation by distance“-pattern (HUTCHISON & TEMPLETON 1999). A positive correlation of pairwise F_{ST} values with geographic distances among populations means that gene flow and genetic drift are in equilibrium. It can be assumed that populations are stable and have not experienced a range expansion very recently. So, it seems feasible that populations of *T. helenitis* recolonized the formerly glaciated areas postglacially and attained an equilibrium of gene flow and genetic drift afterwards. However, the direction of postglacial recolonization could not clearly be inferred. Nonetheless, there is evidence to suggest that *T. helenitis* survived the Ice Ages in refugia close to the Ammersee and possibly the Untersberg region.

4.3. Hybrid zone between subspp. *helenitis* and *salisburgensis*

4.3.1. Do the two subspecies form a hybrid zone?

It is difficult to prove that there is a hybrid zone between the two subspecies at the northern edge of the Alps. Each putatively diagnostic character of subspp. *helenitis* and *salisburgensis* proved to be uninformative, even though achene indumentum is frequently mentioned as the taxonomically most relevant trait. Considering achene indumentum, hybrids may show intermediate states between pubescent (ssp. *helenitis*) and glabrous (ssp. *salisburgensis*), which would indicate genetically “additive” traits. Intermediate variants with sparsely hairy achenes were found for about 8% of the surveyed individuals, usually ranging from 0 – 20% per population (only population UNT2 has 40%; Table 13). These intermediate achene types are found more frequently in the central part of the sampling area, i.e. between Miesbach in the west and the central Flachgau in the east (Figs. 40-41). Besides their intermediate achene indumentum these individuals also show achenes that are also intermediate in shape. While pubescent (ssp. *helenitis*) achenes have a torpedo-like shape with narrowed endings, the glabrous achenes (ssp. *salisburgensis*) show an oblong shape with nearly parallel margins and slightly narrowed endings. The sparsely hairy achenes are intermediate in shape (Figs. 6a-c). Nevertheless, an intermediate state of these individuals could not be inferred from the genetic data (Figs. 46c-d). As mentioned above, individuals with sparsely hairy achenes were treated as ssp. *salisburgensis* by CUFODONTIS (1933) or as transitional forms by KRACH (2000) and HEGI (1928). Due to the low genetic differentiation between the subspecies (Figs. 20-21, 25) there is a high likelihood that they hybridize and form a hybrid zone. Clustering algorithms have been used to estimate the number of genetic groups and levels of admixture. Several analyses with different settings were performed in the two programs STRUCTURE (Figs. 10-14) and BAPS (Figs. 15-19). Especially the analyses of STRUCTURE show high admixture at a broad geographical scale. Two clusters were formed based on a model using independent allele frequencies, and which form a cline in the central part of the sampling area (Fig. 11). Thus, the populations from the Miesbach region in the west to the “Salzach valley and Untersberg” region in the east are highly admixed. Populations further west or east show lower levels of admixture and could often be clearly ascribed to one genetic cluster. When allele frequencies were treated as “correlated” in STRUCTURE, a third cluster was identified, which has its

highest proportions in the same regions of the central part of the sampling area. In particular, the third cluster predominates in the regions of Miesbach and Chiemsee, whereas the two other clusters predominate west and east of these regions, respectively. PRITCHARD et al. (2007) mention that the model with correlated allele frequencies often overestimates the number of clusters, but has a “better power to detect subtle population structure”. The program BAPS uses a Bayesian clustering algorithm as well. In contrast to STRUCTURE it shows much less admixture of individuals and more or less clear cluster borders. However, the location of these borders differed, depending on whether the spatial-(ad)mixture model (Figs. 15a-b) or the non-spatial-(ad)mixture model (Figs. 15c-d) was used. Furthermore, these borders were not congruent to the “breaks” in STRUCTURE (Fig. 10). So, it seems that the central part of the sampling area cannot really be ascribed to one of the two major groups. The high levels of admixture also indicate a low genetic differentiation between the two subspecies and/or geographic population groups, suggesting a hybrid zone of subspp. *helenitis* and *salisburgensis* in the region between Miesbach and the Chiemsee.

In addition to the clustering algorithms, distance-based analyses were used to confirm these assumptions. At first, an individual-based NJ-tree using NEI & LI's (1979) genetic distance measure was calculated (Fig. 20). However, a bootstrap support for branches in this tree can be found only in its basal part. The outgroup (*T. integrifolia*, *T. longifolia* and *T. tenuifolia*) as well as the ingroup *T. helenitis* show high support (98-100% and 91%, respectively). Within *T. helenitis*, bootstrap values >70% could only be found between two pairs of individuals (and two times for groups of three individuals). This supports the results of STRUCTURE and BAPS, indicating a weak differentiation within *T. helenitis*. The rooted population-based NJ-network (Fig. 22) shows a similar picture as the individual-based tree, whereas the unrooted population-based NJ-tree (Fig. 23) presents some support for genetic clusters. The branch connecting the westerly located populations (from the Ammersee westwards) and the central and easterly located populations (from the Miesbach region eastwards) shows a bootstrap support of 90%, which indicates a differentiation of these two clusters. This result, however, should be treated with caution since populations <5 individuals were excluded from the population-based analyses. So, for instance, two populations of the Ammersee region (AMM2 and AMM3) were excluded. These populations are genetically very close to the populations of the eastern part and thus would have lowered the bootstrap value. Besides the NJ-analyses, a NeighborNet analysis was performed using the program SPLITSTREE. The advantage of this method is that genetic relationships are shown as split networks, which do not form hierarchies and may therefore provide a better picture of relations. Both the individual-based (Fig. 21) and the population-based (Fig. 24) network show a star-like pattern which indicates a low differentiation, as in the NJ-analyses. Only the outgroup samples were distinct from those of the ingroup.

In sum, genetic differentiation is low within *T. helenitis* and individuals in the central and eastern parts of the sampling area show high levels of admixture. Therefore, a hybrid zone is (highly) likely to be present in these regions. Further estimation of the centre and width of the hybrid zone was attempted by using the program CFIT (GAY et al. 2008). Unfortunately, it failed due to the high amount of loci in the AFLP dataset. So, the centre and width of the hybrid zone was inferred from genetic clustering (programs: STRUCTURE and BAPS), the density of inflection points (the curvature of functions change at these points) of single loci and the distribution of achene types. Hybrid zones can be inferred from the presence of admixture in

individuals/populations. As shown in Figures 10-19, admixture is prevalent in the Ammersee region (populations AMM2 and AMM3) in the west and extends to the easternmost populations. Here, high amounts of admixture can be found between the Miesbach region in the west and the Untersberg region in the east. Based on the STRUCTURE analysis using correlated allele frequencies (Fig. 14), the “Salzach valley” populations (Table 4) show high levels of admixture due to the third cluster, which is formed in the centre, too. This cluster shows its highest proportions in the populations of the Miesbach and Chiemsee region, where the centre of the hybrid zone is hypothesized. This is also supported by the distribution of achene types. The intermediate achene type, which is thought as an indicator of hybrids (see Fig. 6b), is most frequently observed in the region between Miesbach and the Untersberg region. The Untersberg region is also characterized by the highest density of inflection points of single AFLP loci, which show significant clines along the longitudinal axis (Fig. 39). So, the hybrid zone probably extends from the Ammersee region eastwards to the distribution border of *T. helenitis* in the east (Attersee region). If the hybrid zone is considered more stringently, it reaches from the Miesbach region to the Untersberg/Salzach valley region. In this zone, the centre of the hybrid zone is to be expected, even though it cannot be determined more precisely at present.

4.3.2. Is the hybrid zone a primary or secondary one?

Distinguishing between primary and secondary hybrid zones (explanations in section 1.1) is notoriously difficult (ENDLER 1977). Somewhat surprisingly, this topic has received only sparse interest from plant evolutionary biologists. Hence, methods for distinguishing these hybrid zones are mainly found in the animal literature. According to FUTUYMA (2007, p.373f), different selection pressures along a geographical cline can be inferred from varying allele frequencies at single loci along this gradient. In a primary hybrid zone, the clines are expected at different geographic positions among the loci, while in a secondary one, clines should occur at similar positions (Fig. 51). The first step is the observation of loci, which are under divergent selection. Therefore, the programs BAYESCAN and MCHEZA were used. A comparison of three programs (BAYESCAN, DETSELD, DFDIST) resulted in BAYESCAN as the most efficient program (PEREZ-FIGUEROA et al. 2010), which determines the highest percentage of true selective “outlier” loci (COLLIN & FUMAGALLI 2011, FITZPATRICK et al. 2011, NUNES et al. 2011, BUCKLEY et al. 2012). The second program that has been used for outlier loci detection is MCHEZA, which is based on the algorithm of DFDIST (WILDING et al. 2001, MINDER & WIDMER 2008, GAGNAIRE et al. 2009, RYMER et al. 2010, KUCHMA & FINKELDEY 2011, NUNES et al. 2011, BUCKLEY et al. 2012), a modification of FDIST (BEAUMONT & NICHOLS 1996) for the usability of dominant markers (COLLIN & FUMAGALLI 2011).

The detection of outlier loci is based on “identifying loci (molecular markers) that present population differentiation (F_{ST}) coefficients that are ‘distinct’ (called outlier loci) from those under neutral expectations” (PEREZ-FIGUEROA et al. 2010). For the present dataset of 451 loci, BAYESCAN and MCHEZA detected 19 (4.2% of the total loci) and 13 (2.9%) outlier loci, respectively. In total, 29 (6.4%) candidate outlier loci were found. Surprisingly, only three of these loci (10.3%; 0.7% of all loci) were detected in both programs. Furthermore, three out of the 29 candidate loci (10.3%), as well, show a significant fit for the models II and III of HUISMAN et al. (1993), both indicating an increasing or decreasing sigmoid trend. Two of those loci were

detected in both programs (N183.3 and N269.1), and one locus was detected in BAYESCAN (V325.8). The inflection points of these loci were calculated to compare their positions along the longitudinal axis. They resulted in different positions within a distance of 1.20° (90 km) between the Miesbach and the Untersberg region. This is strongly suggestive of a primary hybrid zone, even though the amount of loci supporting this inference is low. The region between Miesbach and the Untersberg is also that region, where the achene indumentum has its transition zone (Figs. 40-41), and the same applies to the genetic data, represented through the PCoA-Axis1 (Fig. 28). Furthermore, this region is the zone of highest admixture in STRUCTURE (Figs. 12, 14). Besides, scanning the overall AFLP loci for significant fits to models II and III resulted in 32 loci. The remaining 29 loci, which were not F_{ST} outliers are considered as false positives. They possibly form a clinal pattern through genetic drift without an influence of selection and restricted gene flow by distance. Nevertheless, the inflection points of all 32 loci had their highest density in the region between the Chiemsee and eastern Flachgau. The majority of selectively neutral loci show clines like in Fig. 51 (cline: d), whereas the allele frequencies are commonly scattered and do not form significant clines (Fig. 51a). This also supports the presence of a primary hybrid zone.

Besides above methods considering clines in allele frequencies there is another possibility to test for the existence of (at least) secondary hybrid zones. Thus, in a secondary hybrid zone, highest diversities are expected in the centre of the zone (related to PETIT et al. 2003). However, in the present study system, the levels of diversities are distributed in patches (see section 4.2). Although there are two regions that show high levels of genetic diversity, i.e. the Ammersee and the Untersberg region (Fig. 29), the former is outside the otherwise inferred hybrid zone and exclusively has individuals with pubescent achenes. The Untersberg region shows lower diversities than the Ammersee region, but is within the hybrid zone or slightly outside. The Untersberg region is quite interesting, showing a high percentage of potential hybrids (showing sparsely hairy achenes; Fig. 40). Hence, the centre of the hybrid zone might be situated in the Untersberg region (see section 4.3.1). However, the Untersberg region does not show genetic diversities which are obviously higher than in the surrounding populations. Therefore, in conclusion, there is no strong evidence for a secondary hybrid zone and a primary hybrid zone is inferred.

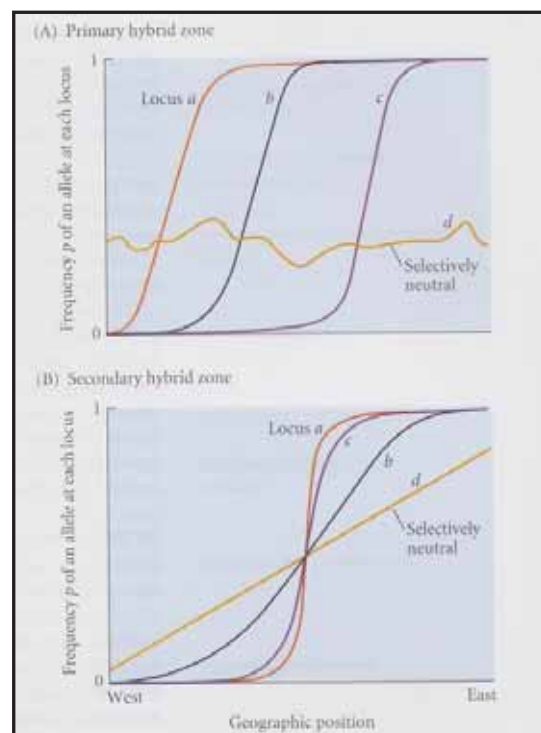


Figure 51. Distinguishing primary and secondary hybrid zones based on the geographic position of clines in allele frequencies (from FUTUYAMA 2007)

4.3.3. Origin and maintenance of characters varying along the cline

Based on the above, there is a primary hybrid zone of *T. helenitis* at the northern fringe of the Alps, showing AFLP loci under selection as well as a clinal pattern of achene types. So, why is there any selective pressure along this gradient? As mentioned in section 4.1.2, the cause could not be found in the habitat parameters measured. So, why did the clinal patterns, especially in achene type, evolve? Trichomes on achene surfaces are thought to have effects on dispersal and germination. Two achene types are described in *Senecio jacobaea* L.: achenes of disc flowers are more numerous, lighter, equipped with a pappus and rows of trichomes in contrast to achenes of ray flowers. The trichomes are supposed to increase the dispersability of the achenes, because of aiding attachment to passing animals and/or by increasing the resistance to the air (MCEVOY 1984, MCEVOY & COX 1987). Germination rates of achenes of disc flowers in *Senecio jacobaea* are higher than those of ray flower achenes due to a thinner pericarp (MCEVOY 1984). MAYEUX (1989) supposes that trichomes could act as an anchor for the achenes and therefore enhance soil penetration. It is also presumed that the trichomes draw and retain water next to the pericarp, hence facilitating higher germination rates. According to these assumptions, it can be supposed that glabrous achenes of *Tephrosieris helenitis* ssp. *salisburgensis*, which also show a more slender shape than pubescent achenes, have lower dispersal attributes and lower germination rates than pubescent ones. Possibly the lack of trichomes arose spontaneously before the LGM. While individuals with glabrous achenes postglacially occupied the eastern part of the area, they could not establish in the western part due to restricted dispersability and the competition with individuals having pubescent achenes. Afterwards, the pubescent variants may have dispersed into the eastern populations and formed a cline (see in section 4.4.2).

An alternative hypothesis is the introgression of *T. crispa* genes into *T. helenitis*, resulting in glabrous achenes in ssp. *salisburgensis*. The similar morphological characters (as *Senecio helenitis* ssp. *salisburgensis* and *Senecio rivularis* var. *schkührii*, respectively) and the parapatric distribution ranges of both taxa are mentioned in CUFODONTIS (1933). It is possible that gene flow between the two taxa in adjacent populations (especially in the Tennengau region southerly the city of Salzburg) resulted in the origin of glabrous achenes in ssp. *salisburgensis*. Gene introgression from *T. crispa* into *T. helenitis* was also supposed by KRACH (2000) according to some herbarium specimens of *T. helenitis* (ssp. *salisburgensis*) with sharply serrated leaf margins. Nevertheless, frequent gene flow between both species can be (safely) excluded, because they form well separated genetic groups and extant populations are well geographically separated (Figs. 20-22).

Additional morphological and genetic characters need to be investigated in more populations and individuals to infer potential patterns of clinal variation in the study area. Moreover, ecological parameters should be obtained in these populations and compared with morphological and genetic traits. The indumentum of leaves might be associated with soil humidity (CUFODONTIS 1933), which potentially differs between populations in the western and the eastern parts of the sampling area. The two populations not collected in fens or wet meadows are from less humid habitats (HAM1: road embankment and HAY1: deciduous forest) and are exclusively comprised of ssp. *helenitis*, while individuals of ssp. *salisburgensis* exclusively grow in humid habitats (fens and wet meadows). Furthermore, the habitat of population GEO1 (Miesbach region) seemed to be drained, as also indicated by vegetation surveys (Fig. 45). Interestingly, this population exclusively shows individuals with pubescent

achenes, although adjacent populations also contain some individuals with non-pubescent achenes. Possibly, individuals of ssp. *helenitis* are better adapted to less humid conditions.

4.4. Miscellaneous aspects

4.4.1. Red bract/stem color and anthocyanin synthesis

CUFODONTIS (1933) mentions that individuals of *Senecio helenitis* (syn. *Tephroseris helenitis*) with red bracts and sometimes also red stems are found in moister habitats. These character states are associated with tenuous and large leaves and reduced leaf hairiness. He also mentions that ssp. *salisburgensis* quite often shows red bracts (see Fig. 6f), especially when plants do not show a floccose indumentum. A floccose indumentum is generally regarded as a transpiration protection and, as well as the red color, a thermal absorber. The environmental significance of anthocyanins in plant stress responses is well documented (CHALKER-SCOTT 1999). Their adaptive advantages in non-reproductive tissues are not yet clear, but they are induced by several factors, such as visible and UVB radiation, cold temperature, and water stress. ANDERSEN et al. (1984) report that flooded *Malus* and *Pyrus* trees showed a higher anthocyanin synthesis in leaves. This was interpreted as a reaction to secondary drought in leaves due to depressed root function. CHALKER-SCOTT (1999) and references therein mention deficiencies in nitrogen and phosphorous, lowered pH, wounding, pathogen infections or fungal elicitors as additional causes for anthocyanin induction. Own observations can exclude at least the lowered pH as a cause for higher anthocyanin content in *Tephroseris helenitis* plants. Population GEO1 exclusively shows green stems and bracts, but has an even lower pH than the remaining populations (Fig. 45). The content of nutrients, however, is higher in this population. Nevertheless, there is no reason to suggest that a lower nutrient content is the reason for higher anthocyanin synthesis in certain *T. helenitis* plants, because at least in the present study area this species mainly occurs in wet meadows, which are generally nutrient poor.

4.4.2. Replacement of “glabrous individuals” by “pubescent” ones

It is tempting to speculate that individuals with glabrous achenes (ssp. *salisburgensis*) will become replaced over time by individuals with pubescent achenes (ssp. *helenitis*). One argument is that populations of both subspecies (plus mixed stands) are longitudinally oriented and thus can be influenced by the Westerlies due to the fact that achenes are wind dispersed. Therefore, the westerly distributed group with pubescent achenes might infiltrate the easterly distributed group with glabrous achenes, because the west winds cause a stronger dispersal from west to east than contrariwise. This hypothesis is supported by the absence of a pure wider area of ssp. *salisburgensis*, whereas ssp. *helenitis* has pure populations across the whole western part (from Ammersee eastwards). That process might be expected to occur over relatively short time scales. However, observations of achene type frequencies in population GER1, the easternmost population of *T. helenitis*, from 1995 and 2010 run counter

these expectations (HÖGLINGER, unpubl. data) as the proportion of pubescent achenes actually decreased from 72% (1995) to 28% (2010).

In populations of the eastern part of the sampling area, the proportion of the western STRUCTURE-cluster was higher than contrariwise (Figs. 10-11). Hence, an influx of alleles from west to east seems much stronger than from east to west. Furthermore, there were five individuals showing a “west-genotype” (AFLP data, Q-values of the western STRUCTURE-cluster >75%) in eastern populations (KOE1_15, FEN1_01, BER5_12, LAU1_19, SCH1_03; Table 5) in contrast to only one individual showing an “east-genotype” in western populations (HAM1_07; Table 5).

4.4.3. Conservation aspects

Tephroseris helenitis is listed in the red lists of Salzburg (WITTMANN et al. 1996), Upper Austria (HOHLA et al. 2009) and Austria (NIKLFIELD & SCHRATT-EHRENDORFER 1999) as “endangered” (red list status: 2), while it is listed as “vulnerable” (and more threatened in at least one region; red list status: 3 r!) in Germany (KORNECK et al. 1996). In Bavaria, both subspecies considered here are also listed as “vulnerable” (SCHEUERER & AHLMER 2003). Baden-Wuerttemberg lists *T. helenitis* as “endangered” (BREUNIG & DEMUTH 1999). However, this species is not listed in the red list of the “International Union for Conservation of Nature and Natural Resources” (IUCN 2012).

The above treatments of *T. helenitis* as “vulnerable” or even “endangered” in the red lists primarily reflects the loss of its habitats as mentioned in section 1.1. In the Austrian red list of the 1980's *T. helenitis* was listed as “vulnerable” (NIKLFIELD et al. 1986), but this changed to “endangered” 13 years after. Factors promoting this loss of habitat involve intensification of agriculture, fertilization, succession or reforestation, as well as natural scarcity (STÖHR 2009). This can be also recognized in the distribution map (Fig. 1), where most records in the northern part of the species' range in Germany date from before 1950 (white circles). Only a few quadrants have been confirmed after 1980, especially in the lower Franconia/Thuringia region (black circles). The southern region near the Alps seems to have suffered less from habitat loss, because nearly all observations have been confirmed after 1950. In Switzerland, most of the quadrants have not been confirmed after 1982 and only a few recent populations are mentioned. Based on the newly compiled map of ssp. *salisburgensis* populations and mixed stands (Fig. 7), it appears that populations in the central Flachgau went extinct, which in particular relates to populations in Salzburg City and the Ursprunger Moor. These regions have been heavily urbanized during the last centuries and/or have a high proportion of intensively used grasslands. Many populations of *T. helenitis* recorded at the border of Salzburg province and Upper Austria have also been confirmed after 1980 (and in the present study). “Hot spots” of *T. helenitis* in Austria are the Untersberg region and areas just north of the Fuschlsee.

The genetic data, however, do not reflect the loss of habitats. The “isolation of distance” pattern found at the broad regional scale (Fig. 34a) shows that populations are at an equilibrium between gene flow and genetic drift, implying they are stable and not genetically isolated (also at smaller geographic scales, Fig. 34b). Furthermore, population genetic differentiation is low throughout the whole sampling area (Figs. 10, 20), suggesting ongoing or only recently interrupted gene flow. Nevertheless, probably the time since habitat

fragmentation had started (60 to 70 years ago) has not been long enough to shape the genetic pattern (AGUILAR et al. 2008, YUAN et al. 2012).

4.4.4. Self-incompatibility tests

There are contradicting reports in the literature regarding the breeding (compatibility) system of *T. helenitis*. While KRACH (2000) mentions that *T. helenitis* is self-incompatible, like the other *Tephroses* species, KLOTZ et al. (2002) asserts that *T. helenitis* is self-compatible for the same reasons. However, recent surveys of the breeding system of *T. integrifolia* have shown that this species is self-incompatible (ISAKSSON 2009, paper II). Therein it is also mentioned that the self-incompatibility (SI) system of *T. integrifolia* is assumed to be sporophytic, because all SI systems of the Asteraceae family are sporophytic. Own observations of 19 *T. helenitis* plants at two sites (field and botanical garden) have shown that this species is clearly self-incompatible, too. Only one bagged individual of the field site formed <5% mature achenes, but which is still much less than observed in reference individuals grown under conditions of open-pollination (usually 50-70% mature achenes; min. 15%, max. 100%).

4.5. Outlook

The above mentioned morphological and genetic characters (as well as additional ones) potentially differentiating the subspecies (besides the achene indumentum) need to be investigated in more populations and ideally under common garden conditions. Especially the presence or absence of ray flowers should be investigated in several populations throughout the whole hybrid zone and adjacent areas. Soil samples have already been taken from six populations (ADN1, AMM1, AMM2, FEN1, GEO1, LAU1), whereby two populations are from the western part of the sampling area (AMM1, AMM2), two are from the central part (FEN1, GEO1) and another two are from the eastern part (ADN1, LAU1). Based on these and possibly additional samples, differences in edaphic habitat preferences might become apparent with the prediction of a clinal pattern that fits the clinal pattern of achene type and genetic data. This should be complemented by an analysis of climatic factors across the study area.

Clearly, more analytical work is also needed concerning those AFLP loci, which show a clinal distribution of allele frequencies. There are programs available to infer the centre and width of a hybrid zone such as CFIT (GAY et al. 2008) and which are increasingly used for inferring properties of such hybrid zones. CFIT is cited 30 times in the Web of Science (<http://wokinfo.com>; 10.04.2012) with 20 publications in 2011. Most of them focused on hybrid zones in birds (IRWIN et al. 2009, BARROWCLOUGH et al. 2011, TOEWS et al. 2011) and insects (GOMPERT et al. 2010, VEDENINA 2011, WITTKOPP et al. 2011), while only one such publication dealt with plants (BRENNAN et al. 2009). Another interesting topic would be the reconstruction of the potential range of *T. helenitis* at the LGM using “ecological niche modelling” (PHILLIPS et al. 2006, WALTARI et al. 2007, QI et al. 2012, SAKAGUCHI et al. 2012).

Conclusions

Individuals with pubescent achenes (ssp. *helenitis*) were found throughout the whole study area, while individuals with glabrous or sparsely hairy achenes (ssp. *salisburgensis*) occur only east of the Munich area. The majority of populations in the common distribution range are mixed stands exhibiting both achene types. Subspecies *helenitis* is much more frequent in populations in Salzburg province than expected from the literature. Possibly older herbarium specimens were ascribed to ssp. *salisburgensis* because of other characters than achene indumentum or ssp. *salisburgensis* was expected as a local form of *T. helenitis* and ssp. *helenitis* was simply not taken into account. Nevertheless, ssp. *salisburgensis* predominates in this region and was found only east of the Munich area, which conforms to the literature.

Genetic data (individual-based AFLP data) neither separates subspp. *helenitis* and *salisburgensis* according to their achene indumentum nor any other morphological character. It can be presumed that the subspecies are not reproductively isolated, and achene indumentum as well as other supposedly diagnostic morphological characters proved to be unsuitable for subspecies designation. Furthermore, no other morphological character was found to be associated with achene indumentum and could be used as a further reliable character for subspecies differentiation. Differences in microhabitat requirements between the two subspecies were not found according to associated plant species in the direct neighborhood of *T. helenitis* individuals. Instead, the vegetation data clearly separated the four populations surveyed.

Due to the fact that subspp. *salisburgensis* and *helenitis* cannot be separated by their AFLP profiles, their occurrence in sympatry (nearly all populations within the alleged distribution range of ssp. *salisburgensis* are mixed stands exhibiting both achene types viz. subspecies), and the lack of possible ecological differences, it is considered that the rank “subspecies” is set too high at least for ssp. *salisburgensis* and that it should be classified as “variety”.

The population genetic history of *T. helenitis* was inferred by intra-population genetic diversity measures. A gradual decrease of genetic diversity along a geographic gradient from western populations, which occupy formerly unglaciated terrain at the LGM, to eastern populations, which occur in formerly glaciated areas, could not be observed ruling out a broad-scale postglacial recolonization scenario from west to east. Instead, genetic diversity measures show a mosaic-like pattern, suggesting postglacial small-scale recolonization from (multiple) local refugia, which could be located close to regions currently exhibiting high genetic diversities and rarities, such as the Ammersee and Untersberg region. Nonetheless, populations of *T. helenitis* form an “isolation by distance” pattern, implying an equilibrium of gene flow and genetic drift and thus fairly stable population demographics in recent history.

The existence of a hybrid zone between subspp. *salisburgensis* and *helenitis* is supported by (i) high genetic admixture according to Bayesian clustering programs; (ii) low genetic differentiation obtained by genetic distance approaches; (iii) a high density of inflection points of single AFLP loci; and (iv) intermediate types of achene indumentum in the central and eastern parts of the study area. The putative hybrid zone extends from the Ammersee region in the west to the easternmost populations in the Attersee region. The centre of the hybrid zone was inferred to be situated between the Miesbach region in the west and the Untersberg

region in the east. Within this zone, genetic admixture, the density of inflection points and the proportion of intermediate (sparsely hairy) achene types were highest.

Distinguishing between a primary and secondary hybrid zone mainly followed the reasoning of FUTUYMA (2007), whereby single AFLP loci under selection are expected to show clines either at different positions (primary hybrid zone) or at close positions (secondary hybrid zone) along a geographic gradient. AFLP loci under divergent selection of *T. helenitis* were identified with programs detecting F_{ST} outlier loci (BAYESCAN, MCEZA). For three F_{ST} outlier loci a significant cline was found, with their inflection points located within a longitudinal range of 90 km (1.20°). This is taken as evidence for a primary hybrid zone. The existence of a secondary hybrid zone was tested using intra-population genetic diversities, where a peak of genetic diversity would be expected at the centre of the secondary hybrid zone. However, the genetic diversities of *T. helenitis* populations are distributed in mosaic-like patches, with “diversity hotspots” occurring in the Ammersee and Untersberg regions. These regions are located at the border or outside the hybrid zone (Ammersee region) or do not present clear peaks of genetic diversity compared to surrounding populations (Untersberg region). Therefore, these (genetic diversity) data do not support the existence of a secondary hybrid zone.

Acknowledgements

At first, I want to thank my supervisor Prof. Dr. Hans-Peter Comes of the University of Salzburg for the scientific support of this Master thesis, especially for helpful discussions, taking care to keep the thread of the thesis and for the very precise and time-consuming corrections and hints of the manuscript.

Sincerely thanks also go to my second supervisor Dr. Andreas Tribsch of the University of Salzburg, who supported me with sacrificing encouragement in many parts of this thesis. Especially, I want to thank him for providing excursions to collect plant material, support in the field, the lab and particularly with computer programs. He always had a sympathetic ear for minor and major problems.

This Master thesis was funded by the University of Salzburg (Department of Organismic Biology), whereas the Faculty of Natural Sciences also awarded a scholarship (Förderstipendium) at the beginning of this project.

For their help in the molecular lab I want to thank Dr. Michaela Eder and Dr. Georg Brunauer, as well as the Division of Plant Physiology for the possibility to use the Nanodrop ND-1000. Very special thanks go to Dr. Matthias Affenzeller, who aided in the lab elaborately and made the AFLPs working.

I am also thankful for all field collectors: special thanks go to Dr. Christian Eichberger, for his help with vegetation plots, the collection of samples and providing morphological data, Dipl.-Ing. Franz Höglinger, for exhausting and detailed field observations of morphological characters of *T. helenitis* at the “Gerlhamer Moor” and the collection of samples, Wolfgang Riedel and Georg Pangerl for guiding my collection trip to the Swabian Jura and making this excursion to a nice and successful journey and Dipl.-Biol. Peter Sturm and the ANL (Bayerische Akademie für Naturschutz und Landschaftspflege) for organizing and assisting a collection trip and vegetation plots in the “Berchtesgadener Land”. My thank goes to Christian Niederbichler and the District Government of Upper Bavaria for collecting plant material of the Ammersee region and the Bergener Moos, whereas I also want to thank the latter for providing an approval for the collection of plant material at the Ammersee region, Prof. Dr. Lenz Meierott for sending leave samples of the distant population in Franconia and Thomas Meyer for assisting the tour to Bavarian Swabia.

Further thanks for providing data of ancient and recent populations of *T. helenitis* in Salzburg go to Mag. Peter Pilsl and the Sabotag (Salzburger Botanische Arbeitsgemeinschaft), Mag. Günther Nowotny and Isolde Althaler (both “Government of Salzburg”) for offering the biotope charting data in Salzburg, Dr. Oliver Stöhr and Dr. Helmut Wittmann for the access to the herbarium “SZB” at the “Haus der Natur Salzburg” for revisions of *Tephroses* specimens, Dipl.-Biol. Gabriela Schneider, Josef Faas, Jürgen Adler, Jürgen Sandner and Elisabeth Pleyl for population and distribution data in Bavaria, Dr. Arno Wörz and Thomas Breunig for population data in Baden-Wuerttemberg and Prof. Dr. Harald Niklfeld for floristic data in Austria.

To Mag. Roland Kaiser I want to express very special thanks. His help in GIS, statistics and the program „R“ were unsurpassable, whereas unsolvable problems were resolved in exhausting computer sessions with programming in “R”. Further thanks for statistical support go to Mag. Roman Fuchs, Mag. Albin Blaschka and my sister Sybille Pflugbeil, BSc.

For providing digital photos of *T. helenitis* I want to thank Martin Kletzander, BSc, Mag. Günther Nowotny and Ursula Jaros, MA rer.nat. For the photographs of achene surfaces and the pappus of *T. helenitis* using the confocal laser microscope I want to thank Patric Schmölder, who unfortunately had a too early death, and the Division of Plant Physiology.

Finally I want to thank my parents Rudolf and Barbara Pflugbeil for their encouragement and support, wherever it was needed. I also want to thank my grandfather Dr. Albert Zeilinger for the field trip to Miesbach, which exposed as very important samples for this study. I am also very thankful for all my friends and colleagues, especially Karin Moosbrugger, MSc, Ursula Jaros, MA rer.nat. and Judith Schistek, B.rer.nat, for their encouragement and assistance.

References

- ABBOTT RJ, ASHTON PA, FORBES DG (1992) Introgressive Origin of the radiate Groundsel, *Senecio vulgaris* L var. *hibernicus* SYME - AAT-3 Evidence. *Heredity* **68**, 425-435.
- ABBOTT RJ, CHAPMAN HM, CRAWFORD RMM, FORBES DG (1995) Molecular Diversity and Derivations of Populations of *Silene acaulis* and *Saxifraga oppositifolia* from the High Arctic and More Southerly Latitudes. *Molecular Ecology* **4**, 199-207.
- AFZELIUS K (1949) Chromosome numbers in *Senecio* and some allied genera. *Acta Horti Bergiani* **15**, 65-77.
- AGUILAR R, QUESADA M, ASHWORTH L, HERRERIAS-DIEGO Y, LOBO J (2008) Genetic consequences of habitat fragmentation in plant populations: susceptible signals in plant traits and methodological approaches. *Molecular Ecology* **17**, 5177-5188.
- ANDERSEN PC, LOMBARD PB, WESTWOOD MN (1984) Leaf Conductance, Growth, and Survival of Willow and Deciduous Fruit Tree Species under Flooded Soil-Conditions. *Journal of the American Society for Horticultural Science* **109**, 132-138.
- ANDERSSON S (2001) The genetic basis of floral variation in *Senecio jacobaea* (Asteraceae). *Journal of Heredity* **92**, 409-414.
- ANDERSSON S, WIDEN B (1993) Pollinator-Mediated Selection on Floral Traits in a Synthetic Population of *Senecio integrifolius* (Asteraceae). *Oikos* **66**, 72-79.
- ANTAO T, BEAUMONT MA (2011) Mchaza: a workbench to detect selection using dominant markers. *Bioinformatics* **27**, 1717-1718.
- ARAFEH RMH, SAPIR Y, SHMIDA A, et al. (2002) Patterns of genetic and phenotypic variation in *Iris haynei* and *I. atrofusca* (*Iris* sect. *Oncocyclus* = the royal irises) along an ecogeographical gradient in Israel and the West Bank. *Molecular Ecology* **11**, 39-53.
- BARROWCLOUGH GF, GUTIERREZ RJ, GROTH JG, LAI JE, ROCK DF (2011) The Hybrid Zone between Northern and California Spotted Owls in the Cascade-Sierran Suture Zone. *Condor* **113**, 581-589.
- BARTISH IV, KADEREIT JW, COMES HP (2006) Late Quaternary history of *Hippophae rhamnoides* L. (Elaeagnaceae) inferred from chalcone synthase intron (Chsi) sequences and chloroplast DNA variation. *Molecular Ecology* **15**, 4065-4083.
- BARTON NH, HEWITT GM (1985) Analysis of hybrid zones. *Annual Review of Ecology and Systematics* **16**, 113-148.
- BEAUMONT MA, BALDING DJ (2004) Identifying adaptive genetic divergence among populations from genome scans. *Molecular Ecology* **13**, 969-980.
- BEAUMONT MA, NICHOLS RA (1996) Evaluating loci for use in the genetic analysis of population structure. *Proceedings of the Royal Society B-Biological Sciences* **263**, 1619-1626.
- BENJAMINI Y, HOCHBERG Y (1995) Controlling the False Discovery Rate - a Practical and Powerful Approach to Multiple Testing. *Journal of the Royal Statistical Society Series B-Methodological* **57**, 289-300.
- BERNATCHEZ L, WILSON CC (1998) Comparative phylogeography of nearctic and palearctic fishes. *Molecular Ecology* **7**, 431-452.
- BIB BOTANISCHER INFORMATIONSKNOTEN BAYERN (2010). http://www.bayernflora.de/de/info_pflanzen.php?taxnr=23949&suchtext=&g=&de=&prev=prev, Retrieved 09.08.2010.
- BONIN A, BELLEMAIN E, BRONKEN EIDEN P, et al. (2004) How to track and assess genotyping errors in population genetics studies. *Molecular Ecology* **13**, 3261-3273.
- BONIN A, EHRLICH D, MANEL S (2007) Statistical analysis of amplified fragment length polymorphism data: a toolbox for molecular ecologists and evolutionists. *Molecular Ecology* **16**, 3737-3758.
- BRENNAN AC, BRIDLE JR, WANG AL, HISCOCK SJ, ABBOTT RJ (2009) Adaptation and selection in the

- Senecio* (Asteraceae) hybrid zone on Mount Etna, Sicily. *New Phytologist* **183**, 702-717.
- BREUNIG T, DEMUTH S (1999) Rote Liste der Farn- und Blütenpflanzen Baden-Württembergs. *Naturschutz-Praxis, Artenschutz* **2**. Landesanstalt für Umweltschutz Baden-Württemberg, Karlsruhe: 161.
- BROHOLM SK, TAHTIHARJU S, LAITINEN RAE, et al. (2008) A TCP domain transcription factor controls flower type specification along the radial axis of the *Gerbera* (Asteraceae) inflorescence. *Proceedings of the National Academy of Sciences of the United States of America* **105**, 9117-9122.
- BRYSTING AK, GABRIELSEN TM, SORLIBRATEN O, YTREHORN O, BROCHMANN C (1996) The Purple Saxifrage, *Saxifraga oppositifolia*, in Svalbard: Two taxa or one? *Polar Research* **15**, 93-105.
- BUCKLEY J, BUTLIN RK, BRIDLE JR (2012) Evidence for evolutionary change associated with the recent range expansion of the British butterfly, *Aricia agestis*, in response to climate change. *Molecular Ecology* **21**, 267-280.
- CASSEL-LUNDHAGEN A, KANUCH P, LOW M, BERGGREN Å (2011) Limited gene flow may enhance adaptation to local optima in isolated populations of the Roesel's bush cricket (*Metrioptera roeselii*). *Journal of Evolutionary Biology* **24**, 381-390.
- CHALKER-SCOTT L (1999) Environmental significance of anthocyanins in plant stress responses. *Photochemistry and Photobiology* **70**, 1-9.
- CHATER AO, WALTERS SM (1976) *Senecio* L. In: *Flora Europaea* (eds. TUTIN TG, HEYWOOD VH, BURGESS NA, et al.): **4**. Cambridge: 191-205.
- COLLIN H, FUMAGALLI L (2011) Evidence for morphological and adaptive genetic divergence between lake and stream habitats in European minnows (*Phoxinus phoxinus*, Cyprinidae). *Molecular Ecology* **20**, 4490-4502.
- COMES HP (1998) Major gene effects during weed evolution: Phenotypic characters cosegregate with alleles at the ray floret locus in *Senecio vulgaris* L. (Asteraceae). *Journal of Heredity* **89**, 54-61.
- COMES HP, KADEREIT JW (1998) The effect of Quaternary climatic changes on plant distribution and evolution. *Trends in plant science* **3**, 432-438.
- CORANDER J, MARTTINEN P (2006) Bayesian identification of admixture events using multilocus molecular markers. *Molecular Ecology* **15**, 2833-2843.
- CORANDER J, MARTTINEN P, MANTYNIEMI S (2006) A Bayesian method for identification of stock mixtures from molecular marker data. *Fishery Bulletin* **104**, 550-558.
- CORANDER J, MARTTINEN P, SIREN J, TANG J (2008b) Enhanced Bayesian modelling in BAPS software for learning genetic structures of populations. *Bmc Bioinformatics* **9**.
- CORANDER J, SIREN J, ARJAS E (2008a) Bayesian spatial modeling of genetic population structure. *Computational Statistics* **23**, 111-129.
- COYNE JA, ORR HA (2004) Speciation. *Sinauer*, Sunderland: 545.
- CRUZ R, VILAS C, MOSQUERA J, GARCIA C (2004) Relative contribution of dispersal and natural selection to the maintenance of a hybrid zone in *Littorina*. *Evolution* **58**, 2734-2746.
- CUFODONTIS G (1933) Kritische Revision von *Senecio* Section Tephroseris. *Feddes Repertorium novarum specierum regni vegetabilis* **70**, 1-266.
- DARWIN C (1859) On the Origin of Species by Means of Natural Selection, or the Preservation of Favoured Races in the Struggle for Life. *John Murray*, London.
- DAVIS JC (1986) Statistics and Data Analysis in Geology. 2 edn., *John Wiley & Sons*, New York: 656.
- DICE LR (1945) Measures of the amount of ecologic association between species. *Ecology* **26**, 297-302.
- DOBZHANSKY TG (1970) Genetics of the Evolutionary Process. *Columbia University Press*: 505.
- DURKA W (1999) Genetic diversity in peripheral and subcentral populations of *Corrigiola litoralis* L. (Illecebraceae). *Heredity* **83**, 476-484.
- EASTWOOD R, HUGHES JM (2003) Phylogeography of the rare myrmecophagous butterfly *Acrodipsas cuprea* (Lepidoptera : Lycaenidae) from pinned museum specimens.

- Australian Journal of Zoology* **51**, 331-340.
- ECKERT CG, SAMIS KE, LOUGHEED SC (2008) Genetic variation across species' geographical ranges: the central-marginal hypothesis and beyond. *Molecular Ecology* **17**, 1170-1188.
- ECKSTEIN RL, O'NEILL RA, DANIHELKA J, OTTE A, KOHLER W (2006) Genetic structure among and within peripheral and central populations of three endangered floodplain violets. *Molecular Ecology* **15**, 2367-2379.
- EHRICH D (2006) AFLPDAT: a collection of R functions for convenient handling of AFLP data. *Molecular Ecology Notes* **6**, 603-604.
- EHRICH D, GAUDEUL M, ASSEFA A, et al. (2007) Genetic consequences of Pleistocene range shifts: contrast between the Arctic, the Alps and East African mountains. *Molecular Ecology* **16**, 2542-2559.
- ELLENBERG H, WEBER HE, DÜLL R, et al. (1992) Zeigerwerte von Pflanzen in Mitteleuropa. *Scripta Geobotanica* **18**.
- ENDLER JA (1977) Geographic variation, speciation, and clines. *Monographs in Population Biology*: **10**. Princeton University Press, Princeton: 262.
- ESRI INC. (2006) ArcMap, Redlands, vers. 9.2.
- EVANNO G, REGNAUT S, GOUDET J (2005) Detecting the number of clusters of individuals using the software STRUCTURE: a simulation study. *Molecular Ecology* **14**, 2611-2620.
- EXCOFFIER L, LAVAL LG, SCHNEIDER S (2005) Arlequin ver. 3.0: An integrated software package for population genetics data analysis. *Evolutionary Bioinformatics Online* **1**, 47-50.
- EXCOFFIER L, SMOUSE PE, QUATTRO M (1992) Analysis of molecular variance inferred from metric distances among DNA haplotypes: application to human mitochondrial DNA restriction data. *Genetics* **131**, 479-491.
- FALUSH D, STEPHENS M, PRITCHARD JK (2003) Inference of population structure using multilocus genotype data: linked loci and correlated allele frequencies. *Genetics* **164**, 1567-1587.
- FELSENSTEIN J (2005) PHYLIP (Phylogeny Inference Package), *Distributed by the author*. Department of Genome Sciences, University of Washington, Seattle, vers. 3.6.
- FISCHER MA, OSWALD K, ADLER W (2008) Exkursionsflora für Österreich, Liechtenstein und Südtirol. 3 edn., *Biologiezentrum der Oberösterreichischen Landesmuseen*, Linz: 1391.
- FITZPATRICK JM, CARLON DB, LIPPE C, ROBERTSON DR (2011) The West Pacific diversity hotspot as a source or sink for new species? Population genetic insights from the Indo-Pacific parrotfish *Scarus rubroviolaceus*. *Molecular Ecology* **20**, 219-234.
- FLANN C (2009 onwards) Global Compositae Checklist. <http://compositae.landcareresearch.co.nz/>, Retrieved 01.05.2011.
- FLORAWEB (2010). <http://www.floraweb.de/>, Retrieved 03.04.2010.
- FLORAWEB (2011). <http://www.floraweb.de/>, Retrieved 20.05.2011.
- FOLL M (2010) BayeScan v2.0 user manual
- FOLL M, GAGGIOTTI O (2008) A Genome-Scan Method to Identify Selected Loci Appropriate for Both Dominant and Codominant Markers: A Bayesian Perspective. *Genetics* **180**, 977-993.
- FUTUYMA DJ (2005) Evolution. *Sinauer Associates*, Sunderland: 603.
- GABRIELSEN TM, BACHMANN K, JAKOBSEN KS, BROCHMANN C (1997) Glacial survival does not matter: RAPD phylogeography of Nordic *Saxifraga oppositifolia*. *Molecular Ecology* **6**, 831-842.
- GAGNAIRE PA, ALBERT V, JONSSON B, BERNATCHEZ L (2009) Natural selection influences AFLP intraspecific genetic variability and introgression patterns in Atlantic eels. *Molecular Ecology* **18**, 1678-1691.
- GARNER TWJ, PEARMAN PB, ANGELONE S (2004) Genetic diversity across a vertebrate species' range: a test of the central-peripheral hypothesis. *Molecular Ecology* **13**, 1047-1053.
- GAY L, CROCHET PA, BELL DA, LENORMAND T (2008) Comparing Clines on Molecular and Phenotypic Traits in Hybrid Zones: A Window on Tension Zone Models. *Evolution* **62**, 2789-2806.
- GBIF (2009). <http://www.gbif.org/>, Retrieved 11.06.2009.

- GILLIES ACM, CUBAS P, COEN ES, ABBOTT RJ (2002) Making rays in the Asteraceae: Genetics and evolution of radiate versus discoid flower heads. In: *Developmental Genetics and Plant Evolution* (eds. CRONK QCB, BATEMAN RM, HAWKINS JA), Taylor & Francis, London: 233-246.
- GOLLMANN G (1984) Allozymic and Morphological Variation in the Hybrid Zone between *Bombina bombina* and *Bombina variegata* (Anura, Discoglossidae) in Northeastern Austria. *Zeitschrift Fur Zoologische Systematik Und Evolutionsforschung* **22**, 51-64.
- GOMPERT Z, LUCAS LK, FORDYCE JA, FORISTER ML, NICE CC (2010) Secondary contact between *Lycaeides idas* and *L. melissa* in the Rocky Mountains: extensive admixture and a patchy hybrid zone. *Molecular Ecology* **19**, 3171-3192.
- HAMMER O, HARPER DAT, RYAN PD (2001) PAST: Paleontological Statistics software package for education and data analysis. *Palaeontologia Electronica* **4**, 9.
- HAZEN SP, LEROY P, WARD RW (2002) AFLP in *Triticum aestivum* L.: patterns of genetic diversity and genome distribution. *Euphytica* **125**, 89-102.
- HEGI G (1928) Illustrierte Flora von Mittel-Europa: **6/2**. A. Pichler's Witwe & Sohn, Wien: 740-742.
- HEB HE, LANDOLT E, HIRZEL R (1972) Flora der Schweiz: **3**. Birkhäuser Verlag, Basel: 876.
- HEWITT GM (1996) Some genetic consequences of ice ages, and their role in divergence and speciation. *Biological Journal of the Linnean Society* **58**, 247-276.
- HEWITT GM (2000) The genetic legacy of the Quaternary ice ages. *Nature* **405**, 907-913.
- HOBAN SM, BORKOWSKI DS, BROSI SL, et al. (2010) Range-wide distribution of genetic diversity in the North American tree *Juglans cinerea*: a product of range shifts, not ecological marginality or recent population decline. *Molecular Ecology* **19**, 4876-4891.
- HOHLA M, STÖHR O, BRANDSTÄTTER G, et al. (2009) Katalog und Rote Liste der Gefäßpflanzen Oberösterreichs. *Stapfia* **91**, 1-324.
- HOLUB J (1973) New Names in Phanerogamae 2. *Folia Geobotanica & Phytotaxonomica* **8**, 155-179.
- HUISMAN J, OLFF H, FRESCO LFM (1993) A Hierarchical Set of Models for Species Response Analysis. *Journal of Vegetation Science* **4**, 37-46.
- HUSON DH, BRYANT D (2006) Application of Phylogenetic Networks in Evolutionary Studies. *Molecular Biology and Evolution* **23**, 254-267.
- HUTCHISON DW, TEMPLETON AR (1999) Correlation of pairwise genetic and geographic distance measures: Inferring the relative influences of gene flow and drift on the distribution of genetic variability. *Evolution* **53**, 1898-1914.
- IRWIN DE, BRELSFORD A, TOEWS DPL, MACDONALD C, PHINNEY M (2009) Extensive hybridization in a contact zone between MacGillivray's warblers *Oporornis tolmiei* and mourning warblers *O. philadelphia* detected using molecular and morphological analyses. *Journal of Avian Biology* **40**, 539-552.
- ISAKSSON K (2009) Self-incompatibility does not explain declining population sizes of *Tephroses integrifolia* (Asteraceae), paper II, *Doctor thesis, University of Lund, Faculty of Sciences, Department of Ecology*: 97.
- IUCN (2012) The IUCN Red List of Threatened Species, *Version 2012.1*. <http://www.iucnredlist.org>, last updated 19.06.2012.
- JOHANNESEN J, DRUEKE U, SEITZ A (2010) Parapatric diversification after post-glacial range expansion in the gall fly *Urophora cardui* (Tephritidae). *Journal of Biogeography* **37**, 635-646.
- JOHANNESSON K, ANDRE C (2006) Life on the margin: genetic isolation and diversity loss in a peripheral marine ecosystem, the Baltic Sea. *Molecular Ecology* **15**, 2013-2029.
- KERGUELEN M (1987) Données taxonomiques, nomenclaturales et chorologiques pour une révision de la Flore de France. *Lejeunea, nouv. sér* **120**.
- KLOTZ S, KÜHN I, DURKA W (2002) BIOLFLOR - Eine Datenbank zu biologisch-ökologischen Merkmalen der Gefäßpflanzen in Deutschland. *Schriftenreihe für Vegetationskunde* **38**.
- KNUTH P (1898) Handbuch der Blütenbiologie: **2/1**. Engelmann, Leipzig: 697.

- KOCH M (2002) Genetic differentiation and speciation in prealpine *Cochlearia*: Allohexaploid *Cochlearia bavarica* Vogt (Brassicaceae) compared to its diploid ancestor *Cochlearia pyrenaica* DC. in Germany and Austria. *Plant Systematics and Evolution* **232**, 35-49.
- KOLAR F, STECH M, TRAVNICEK P, et al. (2009) Towards resolving the *Knautia arvensis* agg. (Dipsacaceae) puzzle: primary and secondary contact zones and ploidy segregation at landscape and microgeographic scales. *Annals of Botany* **103**, 963-974.
- KONOLD W, HACKEL A (1990) Beitrag zur Geschichte der Streuwiesen und der Streuwiesenkultur im Alpenvorland. *Zeitschrift für Agrargeschichte und Agrarsoziologie* **38**, 176-191.
- KORNECK D, SCHNITTLER M, VOLLMER I (1996) Rote Liste der Farn- und Blütenpflanzen (Pteridophyta et Spermatophyta) Deutschlands. *Schriftenreihe für Vegetationskunde* **28**, 21-187.
- KRACH B (1988) *Tephroseris integrifolia* subsp. *vindellicorum*, eine neue Sippe vom Augsburger Lechfeld. *Mitteilungen der Botanischen Staatssammlung München* **27**, 73-86.
- KRACH B (2000) Charakterisierung des Salzburger Spatelblättrigen Greiskrautes (*Tephroseris helenitis* subsp. *salisburgensis*) im Rahmen des Artenhilfsprogrammes für endemische und stark bedrohte Gefäßpflanzen Bayerns. *Bayerisches Landesamt für Umweltschutz*: 1-12.
- KUCHMA O, FINKELDEY R (2011) Evidence for selection in response to radiation exposure: *Pinus sylvestris* in the Chernobyl exclusion zone. *Environmental Pollution* **159**, 1606-1612.
- KUMAR S, SKJAEVELAND A, ORR RJS, et al. (2009) AIR: A batch-oriented web program package for construction of supermatrices ready for phylogenomic analyses. *Bmc Bioinformatics* **10**.
- KURTTO A, LAMPINEN R, JUNIKKA L (eds.) (2004). *Atlas Florae Europaeae. Distribution of Vascular Plants in Europe: 13*. The Committee for Mapping the Flora of Europe & Societas Biologica Fennica Vanamo, Helsinki: 320.
- LAMMI A, SIIKAMAKI P, MUSTAJARVI K (1999) Genetic diversity, population size, and fitness in central and peripheral populations of a rare plant *Lychnis viscaria*. *Conservation Biology* **13**, 1069-1078.
- LESICA P, ALLENDORF FW (1995) When Are Peripheral Populations Valuable for Conservation. *Conservation Biology* **9**, 753-760.
- LYNCH M, MILLIGAN BG (1994) Analysis of Population Genetic-Structure with Rapid Markers. *Molecular Ecology* **3**, 91-99.
- MANTEL N (1967) Detection of Disease Clustering and a Generalized Regression Approach. *Cancer Research* **27**, 209-&.
- MARSHALL DF, ABBOTT RJ (1982) Polymorphism for Outcrossing Frequency at the Ray Floret Locus in *Senecio vulgaris* L. 1. Evidence. *Heredity* **48**, 227-235.
- MAYEUX HS (1989) Snakeweed seed characteristics and germination requirements. In: *Snakeweed: Problems and Perspectives* (eds. HUDDLESTON EW, PIEPER RD): **751**. New Mexico State University Agricultural Experiment Station Bulletin: 39-49.
- MAYR E (1942) Systematics and the origin of species. *Columbia University Press*, New York: 344.
- MAYR E (1969) Principles of Systematic Zoology. *McGraw-Hill*, New York: 428.
- MAYR E (1970) Populations, Species, and Evolution. *Harvard University Press*, Cambridge: 453.
- MCCUNE B, MEFFORD MJ (2006) PC-ORD Multivariate analysis of ecological data, *MJM Software*, Glendened Beach, vers. 5.
- MCVOY PB (1984) Dormancy and Dispersal in Dimorphic Achenes of Tansy Ragwort, *Senecio Jacobaea* L (Compositae). *Oecologia* **61**, 160-168.
- MCVOY PB, COX CS (1987) Wind Dispersal Distances in Dimorphic Achenes of Ragwort, *Senecio Jacobaea*. *Ecology* **68**, 2006-2015.
- MEINDL C (2006) *Tephroseris integrifolia* subsp. *vindellicorum*, eine Populationsgefährdungsanalyse, *Diploma thesis, University of Regensburg, Lehrstuhl für Botanik*: 153.
- MEINDL C, POSCHLOD P (2007) *Tephroseris integrifolia* ssp. *vindellicorum* - eine

- Populationsgefährdungsanalyse. Biologie und Ökologie einer endemischen Kalkmagerrasenart in Bayern. *Hoppea* **68**, 115-168.
- MERXMÜLLER H (1949) Fragen des Artbegriffes in der Botanik. *Naturwissenschaftliche Rundschau* **2**, 68.
- MEUSEL H, JÄGER EJ (1992) Vergleichende Chorologie der Zentraleuropäischen Flora: **3**. *Gustav Fischer Verlag*, Jena: 688.
- MILLAR CV (1983) A steep cline in *Pinus muricata*. *Evolution* **37**, 311-319.
- MINDER AM, WIDMER A (2008) A population genomic analysis of species boundaries: neutral processes, adaptive divergence and introgression between two hybridizing plant species. *Molecular Ecology* **17**, 1552-1563.
- MUELLER UG, WOLFENBARGER LL (1999) AFLP genotyping and fingerprinting. *Trends in Ecology and Evolution* **14**, 389-394.
- MURRAY MC, HARE MP (2006) A genomic scan for divergent selection in a secondary contact zone between Atlantic and Gulf of Mexico oysters, *Crassostrea virginica*. *Molecular Ecology* **15**, 4229-4242.
- NEI M (1972) Genetic distance between populations. *The American Naturalist* **106**, 283-292.
- NEI M (1987) *Molecular Evolutionary Genetics*. *Columbia University Press*, New York: 512.
- NEI M, LI W-H (1979) Mathematical model for studying genetic variation in terms of restriction endonucleases. *Proceedings of the National Academy of Science USA* **76**, 5269-5273.
- NIKL FELD H, KARRER G, GUTERMANN W, SCHRATT L (1986) Rote Liste gefährdeter Farn- und Blütenpflanzen (Pteridophyta und Spermatophyta) Österreichs. In: *Rote Listen gefährdeter Pflanzen Österreichs* (ed. NIKL FELD H): **5**. Grüne Reihe Bundesministerium für Gesundheit und Umweltschutz, Wien: 28-131.
- NIKL FELD H, SCHRATT-EHRENDORFER L (1999) Rote Liste gefährdeter Farn- und Blütenpflanzen Österreichs. In: *Rote Listen gefährdeter Pflanzen Österreichs*, 2 edn., (ed. NIKL FELD H): **10**. Grüne Reihe des Bundesministeriums für Umwelt, Jugend und Familie Graz: 33-151.
- NORDBORG M, HU TT, ISHINO Y, et al. (2005) The pattern of polymorphism in *Arabidopsis thaliana*. *Public Library of Science, Biology* **3**, e196.
- NORDENSTAM B (1978) Taxonomic studies in the tribe Senecioneae (Compositae). *Opera Botanica* **44**, 1-83.
- NUNES VL, BEAUMONT MA, BUTLIN RK, PAULO OS (2011) Multiple approaches to detect outliers in a genome scan for selection in ocellated lizards (*Lacerta lepida*) along an environmental gradient. *Molecular Ecology* **20**, 193-205.
- OBERDORFER E (1983) *Pflanzensoziologische Exkursionsflora*. 5 edn., *Eugen Ulmer*, Stuttgart: 1051.
- OKSANEN J (2011) *gravy: Gradient Analysis of Vegetation*, vers. 0.2-0/r1760, <http://R-Forge.R-project.org/projects/vegan/>.
- OKSANEN J, BLANCHET FG, KINDT R, et al. (2011) *vegan: Community Ecology Package*, vers. 2.0-2, <http://CRAN.R-project.org/package=vegan>.
- OKSANEN J, MINCHIN PR (2002) Continuum theory revisited: what shape are species responses along ecological gradients? *Ecological Modelling* **157**, 119-129.
- PAGE RDM (1996) TreeView: An application to display phylogenetic trees on personal computers. *Computer Applications in the Biosciences* **12**, 357-358.
- PARISOD C, BONVIN G (2008) Fine-scale genetic structure and marginal processes in an expanding population of *Biscutella laevigata* L. (Brassicaceae). *Heredity* **101**, 536-542.
- PAUN O, SCHÖNSWETTER P, WINKLER M, CONSORTIUM I, TRIBSCH A (2008) Historical divergence vs. contemporary gene flow: evolutionary history of the calcicole *Ranunculus alpestris* group (Ranunculaceae) in the European Alps and Carpathians. *Molecular Ecology* **17**.
- PEAKALL R, SMOUSE PE (2006) GENALEX 6: Genetic Analysis in Excel. Population genetic software for teaching. *Molecular Ecology Notes* **6**, 288-295.
- PELSER PB, NORDENSTAM B, KADEREIT JW, WATSON LE (2007) An ITS phylogeny of tribe Senecioneae (Asteraceae) and a new delimitation of *Senecio* L. *Taxon* **56**, 1077-1104.

- PEREZ-FIGUEROA A, GARCIA-PEREIRA MJ, SAURA M, ROLAN-ALVAREZ E, CABALLERO A (2010) Comparing three different methods to detect selective loci using dominant markers. *Journal of Evolutionary Biology* **23**, 2267-2276.
- PETIT RJ, AGUINALDE I, DE BEAULIEU J-L, et al. (2003) Glacial refugia: hotspots but not melting pots of genetic diversity. *Science* **300**, 1563-1565.
- PFEIFER M, SCHATZ B, PICO FX, et al. (2009) Phylogeography and genetic structure of the orchid *Himantoglossum hircinum* (L.) Spreng. across its European central-marginal gradient. *Journal of Biogeography* **36**, 2353-2365.
- PHILLIPS SJ, ANDERSON RP, SCHAPIRE RE (2006) Maximum entropy modeling of species geographic distributions. *Ecological Modelling* **190**, 231-259.
- PILSL P, WITTMANN H, NOWOTNY G (2002) Beiträge zur Flora des Bundeslandes Salzburg III. *Linzer Biologische Beiträge* **34**, 5-165.
- PINHEIRO J, BATES D, DEBROY S, SARKAR D, R DEVELOPMENT CORE TEAM (2012) nlme: Linear and Nonlinear Mixed Effects Models, vers. 3.1-103.
- POLATSCHEK A (1997) Flora von Nordtirol, Osttirol und Vorarlberg: **1**. *Tiroler Landesmuseum Ferdinandeum*, Innsbruck: 1024.
- PRITCHARD JK, STEPHENS M, DONNELLY P (2000) Inference of population structure using multilocus genotype data. *Genetics* **155**, 945-959.
- PRITCHARD JK, WEN X, FALUSH D (2007) Documentation for structure software: Version 2.2: 36.
- QI X-S, CHEN C, COMES HP, et al. (2012) Molecular data and ecological niche modelling reveal a highly dynamic evolutionary history of the East Asian Tertiary relict *Cercidiphyllum* (Cercidiphyllaceae). *New Phytologist* **196**, 617-630.
- R DEVELOPMENT CORE TEAM (2009) R: a language and environment for statistical computing, R Foundation for Statistical Computing, Vienna, vers. 2.9.2.
- REMINGTON CL (1968) Suture-zones of hybrid interaction between recently joined biotas. In: *Evolutionary biology* (eds. DOBZHANSKY T, HECHT MK, STEERE WC), Plenum Press, New York: 321-428.
- RYMER PD, MANNING JC, GOLDBLATT P, POWELL MP, SAVOLAINEN V (2010) Evidence of recent and continuous speciation in a biodiversity hotspot: a population genetic approach in southern African gladioli (*Gladiolus*; Iridaceae). *Molecular Ecology* **19**, 4765-4782.
- SAITOU N, NEI M (1987) The Neighbor-joining Method: A new method for reconstructing phylogenetic trees. *Molecular Biology and Evolution* **4**, 406-425.
- SAKAGUCHI S, QIU Y-X, LIU Y-H, et al. (2012) Climate oscillation during the Quaternary associated with landscape heterogeneity promoted allopatric lineage divergence of a temperate tree *Kalopanax septemlobus* (Araliaceae) in East Asia. *Molecular Ecology* **21**, 3823-3838.
- SCHUEERER M, AHLMER W (2003) Liste gefährdeter Gefäßpflanzen Bayerns mit regionalisierter Florenliste. *Schriftenreihe des Bayerischen Landesamt für Umweltschutz* **165**, 372.
- SCHMICKL R, KOCH MA (2011) *Arabidopsis* hybrid speciation processes. *Proceedings of the National Academy of Sciences of the United States of America* **108**, 14192-14197.
- SCHÖNSWETTER P, STEHLIK I, HOLDEREGGER R, TRIBSCH A (2005) Molecular evidence for glacial refugia of mountain plants in the European Alps. *Molecular Ecology* **14**, 3547-3555.
- SCHÖNSWETTER P, TRIBSCH A (2005) Vicariance and dispersal in the alpine perennial *Bupleurum stellatum* L. (Apiaceae). *Taxon* **54**, 725-732.
- SCHUBERT R, VENT W (1988) Exkursionsflora für die Gebiete der DDR und der BRD, Kritischer Band, begründet von ROTHMALER W: **4**. 7 edn., *Volk und Wissen Volkseigener Verlag*, Berlin: 811.
- SCHWARTZ MK, MILLS LS, ORTEGA Y, RUGGIERO LF, ALLENDORF FW (2003) Landscape location affects genetic variation of Canada lynx (*Lynx canadensis*). *Molecular Ecology* **12**, 1807-1816.
- SEYBOLD S (2006) Schmeil-Fitschen Flora von Deutschland und angrenzender Länder. 93 edn., *Quelle & Meyer*, Wiebelsheim: 863.
- SHANNON CE (1948) A Mathematical Theory of Communication. *The bell system technician*

- journal* **27**, 379-423, 623-656.
- SHERWIN WB, JABOT F, RUSH R, ROSSETTO M (2006) Measurement of biological information with applications from genes to landscapes. *Molecular Ecology* **15**, 2857-2869.
- SPEARMAN C (1904) The proof and measurement of association between two things. *American Journal of Psychology* **15**, 72-101.
- SPSS INC. (2008) SPSS 16.0 for Windows, Chicago, vers. 16.0.2.
- STEVENS PF (2001 onwards) Angiosperm Phylogeny Website, Version 12. <http://www.mobot.org/MOBOT/research/APweb/>, last updated July 2012.
- STÖHR O (2003) Vegetationskundliche Untersuchungen an Streuwiesen im Vorfeld des Untersberges bei Großmain (Salzburg, Österreich) und Marzoll (Bayern, BRD). *Stapfia* **81**, 1-231.
- STÖHR O (2009) *Tephrosieris helenitis* (L.) B. Nord. subsp. *salisburgensis* (Cufod.) B. Nord. 1978. In: *Endemiten - Kostbarkeiten in Österreichs Pflanzen- und Tierwelt* (eds. RABITSCH W, ESSL F), Naturwissenschaftlicher Verein für Kärnten und Umweltbundesamt GmbH, Klagenfurt und Wien: 246-247.
- STREISFELD MA, KOHN JR (2005) Contrasting patterns of floral and molecular variation across a cline in *Mimulus aurantiacus*. *Evolution* **59**, 2548-2559.
- STUESSY TF, SPOONER DM, EVANS KA (1986) Adaptive Significance of Ray Corollas in *Helianthus Grosse serratus* (Compositae). *American Midland Naturalist* **115**, 191-197.
- SZYMURA JM, FARANA I (1978) Inheritance and Linkage Analysis of 5 Enzyme Loci in Interspecific Hybrids of Toadlets, Genus *Bombina*. *Biochemical Genetics* **16**, 307-319.
- TABERLET P, FUMAGALLI L, WUST-SAUCY A-G, COSSON J-F (1998) Comparative phylogeography and postglacial colonization routes in Europe. *Molecular Ecology* **7**, 453-464.
- TER BRAAK CJF, ŠMILAUER P (2002) Canoco reference manual and CanoDraw for Windows user's guide: software for canonical community ordination (version 4.5), *Microcomputer Power*, Ithaca, vers. 4.55.
- TOEWS DPL, BRELSFORD A, IRWIN DE (2011) Hybridization between Townsend's *Dendroica townsendi* and black-throated green warblers *D. virens* in an avian suture zone. *Journal of Avian Biology* **42**, 434-446.
- TREMETSBERGER K, STUESSY TF, SAMUEL RM, BAEZA CM, FAY MF (2003) Genetics of colonization in *Hypochaeris tenuifolia* (Asteraceae, Lactuceae) on Volcan Lonquimay, Chile. *Molecular Ecology* **12**, 2649-2659.
- VAN DE PEER Y, DE WACHTER R (1994) TREECON for Windows: a software package for the construction and drawing of evolutionary trees for the Microsoft Windows environment. *Computer Applications in the Biosciences* **10**, 569-570.
- VAN HUSEN D (1987) Die Ostalpen in den Eiszeiten. Geologische Bundesanstalt, Wien.
- VAN MIERLO SOFTWARE CONSULTANCY (2006) DAX Data Acquisition and Data Analysis, Eindhoven, vers. 8.0.
- VEDENINA V (2011) Variation in complex courtship traits across a hybrid zone between grasshopper species of the *Chorthippus albomarginatus* group. *Biological Journal of the Linnean Society* **102**, 275-291.
- VIEJO RM, MARTÍNEZ B, ARRONTE J, ASTUDILLO C, HERNÁNDEZ L (2011) Reproductive patterns in central and marginal populations of a large brown seaweed: drastic changes at the southern range limit. *Ecography* **34**, 75-84.
- VOS P, HOGERS R, BLEEKER M, et al. (1995) AFLP: a new technique for DNA fingerprinting. *Nucleic Acid Research* **23**, 4407-4414.
- WALTARI E, HIJMANS RJ, PETERSON AT, et al. (2007) Locating Pleistocene Refugia: Comparing Phylogeographic and Ecological Niche Model Predictions. *Plos One* **2**.
- WIEDERMANN R (1995) Pflanzensoziologisches Datenmanagement mittels PC-Programm HITAB5. *Carinthia II* **53. Sonderheft**, 133-134.
- WILDING CS, BUTLIN RK, GRAHAME J (2001) Differential gene exchange between parapatric morphs of *Littorina saxatilis* detected using AFLP markers. *Journal of Evolutionary Biology* **14**, 611-619.

- WINKLER M, TRIBSCH A, PAUN O, et al. (2010) Pleistocene distribution range shifts were accompanied by breeding system divergence within *Hornungia alpina* (Brassicaceae) in the Alps. *Molecular Phylogenetics and Evolution* **54**, 571-582.
- WITTKOPP PJ, SMITH-WINBERRY G, ARNOLD LL, et al. (2011) Local adaptation for body color in *Drosophila americana*. *Heredity* **106**, 592-602.
- WITTMANN H, PILSL P, NOWOTNY G (1996) Rote Liste gefährdeter Farn- und Blütenpflanzen des Bundeslandes Salzburg. In: *Naturschutzbeiträge*, 5 edn., (eds. AMT DER SALZBURGER LANDESREGIERUNG, NATURSCHUTZREFERAT): **8/1996**. 1-83.
- YUAN N, COMES HP, MAO Y-R, QI X-S, QUI Y-X (2012) Genetic effects of recent habitat fragmentation in the Thousand-Island Lake region of southeast China on the distylous herb *Hedyotis chrysotricha* (Rubiaceae). *American Journal of Botany* **99**, 1715-1725.
- ZDSF (2010) *Tephrosia helenitis* (L.) B. Nord. <http://www.crsf.ch>, Retrieved 22.11.2010.
- ZELESNY H (1994) Vegetationskundliche und nährstoffökologische Untersuchungen im Übergangsbereich von Mehrschnitt-Wirtschaftsgrünland zu Streuwiese im Württembergischen Alpenvorland. *Dissertationes botanicae* **211**, 1-243.

A. Appendix

Table 26. Population numbers and codes, observed data, number of individuals, sampling sites, habitats, geographical coordinates, altitude, collectors and collection date for populations of *Tephroseris helenitis* at the northern fringe of the Alps and used outgroups. Abbreviations: A, Austria; AFLP, number of AFLP profiles used for genetic data analyses; B, Bavaria; BW, Baden-Wuerttemberg; DNA, samples for DNA Extraction; G, Germany; I, Italy; L, Lower Austria; N, total number of individuals for DNA samples and recorded for achene indumentum; P, Piedmont; S, Salzburg; SV, Slovenia; Tc, *Tephroseris crispa*, Ti, *T. integrifolia*, Th, *T. helenitis*; Thh, *T. helenitis* ssp. *helenitis*; Ths, *T. helenitis* ssp. *salisburgensis*; Tl, *Tephroseris* cf. *longifolia*; Tt, *T. cf. tenuifolia*; U, Upper Austria; UC, Upper Carniola.

population number	taxon	population code	samples for DNA extraction achenes recorded for indumentum	morphological traits observed	vegetation plots performed	N	individuals for DNA extraction	AFLP	country	province	locality	habitat	longitude (decimal degrees)	latitude (decimal degrees)	meters above mean sea level	leg., det.	date
01	Thh	NUS1	X			21	10	10	G	BW	2.7 km S Nusplingen	wet meadow	8.8903	48.1072	705	Andreas Tribsch & Georg Pflugbeil	10.05.2010
02	Thh	HAY1	x			10	10	9	G	BW	2.5km W Hayingen, close to the cave	steep, rocky deciduous wood and earthy rock steps	9.4392	48.2733	628	Andreas Tribsch, Georg Pflugbeil, Wolfgang Riedel & Georg Pangerl	09.05.2010
03	Thh	HAM1	x			5	5	5	G	B	3.4 km SSE Hammelburg, "Roederwald"	road embankment	9.9214	50.0853	329	Lenz Meierott	12.05.2010
04	Thh	MAR1	x			20	10	8	G	B	0.5km NW Margertshausen	wet meadow	10.7033	48.3133	509	Andreas Tribsch, Georg Pflugbeil & Thomas Meyer	09.05.2010
05	Thh	AMM1	x	x		20	10	8	G	B	3.4 km S Utting a. A., NSG Seeholz und Seewiese	fen meadow	11.0943	47.9885	540	Christian Niederbichler	08.06.2009
06	Thh	AMM2	x	x		17	10	4	G	B	1 km E Eching am Ammersee, NSG Ampermoos	fen	11.1288	48.0850	530	Christian Niederbichler	09.06.2009
07	Thh	AMM3	x	x		20	10	4	G	B	1.4 km N Herrsching am Ammersee	fen	11.1837	48.0116	535	Christian Niederbichler	12.06.2009
08	Thh + Ths	KOE1	x	x		21	10	5	G	B	Holzkirchen, 0.45 km NW Koegelsberg	wet meadow	11.6338	47.8293	719	Georg Pflugbeil	06.06.2009
09	Thh	GEO1	x	x	x	15	15	11	G	B	Waakirchen, 0.4 km N Georgenried	drained wet meadow	11.7043	47.7590	777	Georg Pflugbeil	06.06.2009
10	Thh + Ths	MOO1	x	x		20	10	6	G	B	Weyarn, 1.6 km W Gotzing	wet meadow	11.7849	47.8240	687	Georg Pflugbeil	06.06.2009
11	Thh + Ths	FEN1	x	x		22	10	5	G	B	Weyarn, 0.6 km SO Fentbach	wet meadow	11.8072	47.8764	648	Georg Pflugbeil	06.06.2009
12a	Ths	BER1	x			8	0	0	G	B	Bergener Moos, 1.5 km W Bergen	fen meadow	12.5728	47.8081	544	Andreas Tribsch	03.07.2006
12b	Th	BER2	x			20	0	0	G	B	Bergener Moos, 1.5 km W Bergen	fen meadow	12.5678	47.8047	544	Andreas Tribsch	03.07.2006

12c	Th	BER3	x	x				2	2	0	G	B	Bergener Moos, 1.5 km W Bergen	fen meadow	12.5700	47.8112	544	Christian Niederbichler	14.06.2006
12d	Thh + Ths	BER4	x	x				6	6	1	G	B	Bergener Moos, 1.5 km W Bergen	fen meadow	12.5624	47.8009	544	Christian Niederbichler	01.07.2006
12e	Thh + Ths	BER5	x	x				18	10	4	G	B	Bergener Moos, 1.5 km W Bergen	fen meadow	12.5676	47.8058	540	Christian Niederbichler	15.06.2009
13	Th	SUR1	x					6	6	0	G	B	Sagmeister, 3 km W Oberteisendorf	fen fallow	12.7415	47.8591	523	Georg Pflugbeil	25.05.2009
14	Th	SCH1	x					14	10	8	G	B	0.4 km NW Moosen, SO-edge of the Schönramer Filz	limy fen	12.8830	47.8856	420	Georg Pflugbeil	25.05.2009
15	Thh + Ths	LAU1	x	x	x	x		20	20	18	G	B	0.2 km W Straß, 2 km W Laufen	wet meadow	12.8943	47.9429	422	Georg Pflugbeil	25.05.2009
16	Thh + Ths	UNT3	x	x				14	10	8	A	S	Großgmain, Holzeck, 3.8 km NE Großgmain, 'Stoehr 34'	wet meadow, Schoenetum	12.9389	47.7514	471	Hans-Peter Comes & Andreas Tribsch	20.06.2006
17	Ths	UNT2	x	x				7	7	4	A	S	Großgmain, 4.1 km NE Großgmain, 'Stoehr 23'	wet meadow, Schoenetum	12.9450	47.7508	484	Hans-Peter Comes & Andreas Tribsch	20.06.2006
18	Thh + Ths	UNT1	x	x				31	10	7	A	S	Großgmain, 5.0 km NE Großgmain, 'Stoehr 18'	wet meadow	12.9467	47.7606	481	Hans-Peter Comes & Andreas Tribsch	20.06.2006
19	Thh + Ths	LAN1	x	x				20	10	8	A	S	Langwiesen 4.8 km ENE Großgmain, 'Stoehr 45'	wet meadow	12.9675	47.7400	610	Hans-Peter Comes	28.06.2006
20	Thh + Ths	VIE1	x	x				35	10	9	A	S	Viehhausen, Salzweg to Fuerstenbrunn, 'OENB-Wiese'	wet meadow	12.9869	47.7575	449	Hans-Peter Comes	23.06.2006
21a	Thh + Ths	EST1	x	x				30	0	0	A	S	Fuerstenbrunn, 0.3 km NE Restaurant Esterer	wet meadow	12.9994	47.7539	430	Hans-Peter Comes & Andreas Tribsch	20.06.2006
21b	Thh + Ths	EST2	x	x	x	x		20	20	15	A	S	Fuerstenbrunn, 0.3 km NE Restaurant Esterer	wet meadow	12.9994	47.7533	430	Georg Pflugbeil	20.05.2009
22a	Thh + Ths	ADN1	x	x				31	10	9	A	S	Adnet, 0.25 km S Adnet	wet meadow	13.1320	47.6941	469	Hans-Peter Comes & Christian Eichberger	22.06.2006
22b	Ths	ADN2	x	x	x	x		20	20	17	A	S	Adnet, 0.25 km S Adnet	wet meadow	13.1290	47.6942	469	Georg Pflugbeil	23.05.2009
23	Th	PAL1	x					2	2	2	A	U	1.2 km NNE Palting, Imsee	fen	13.1377	48.0245	506	Georg Pflugbeil	09.08.2009
24	Thh + Ths	KOP1	x	x				32	10	7	A	S	Eastern part of Koppler Moor, 0.6 km SW Koppl	wet meadow	13.1511	47.8044	756	Christian Eichberger	05.07.2006
25	Thh + Ths	KUC1	x	x				33	10	4	A	S	1.9 km NE Kuchl, Freimoos	wet meadow	13.1617	47.6375	466	Hans-Peter Comes & Christian Eichberger	22.06.2006
26	Ths	WOE1	x	x				20	10	5	A	S	Woerleemoos 0.8 km ESE Unzing, 5.5 km SE Seekirchen a. Wallersee	wet meadow	13.1839	47.8633	593	Christian Eichberger	29.06.2006
27	Ths	FUS1	x	x				33	10	3	A	S	Hof bei Salzburg, Baderluck, 0.8 km NW Schloss Fuschl	wet meadow	13.2475	47.8133	672	Andreas Tribsch	22.06.2006

28	Thh + Ths	STI1	x	x			32	10	10	A	S	Thalgau, Egg, "Stilles Tal" 2.2 km NW Fuschl am See	wet meadow	13.2875	47.8117	715	Christian Eichberger	29.06.2006
29	Thh + Ths	HAS1	x	x	x		10	10	7	A	U	3.1 km SSE Oberwang, close to the Haslau-Moos, 1,49km W Riedlbach	wet meadow	13.4517	47.8411	616	Georg Pflugbeil, Ursula Jaros & Franz Höglinger	22.05.2010
30	Thh + Ths	GER1	x	x	x		20	15	12	A	U	1.4 km W Seewalchen, Litzlberg, Gerlhamer Moor	wet meadow	13.5578	47.9522	512	Georg Pflugbeil, Ursula Jaros & Franz Höglinger	22.05.2010
31	Tt	ORM1	x				15	5	5	I	P	Colle caprauna, 2.6km E Ormea	forest glade, northern slope	7.9327	44.1286	1535	Georg Pflugbeil	27.06.2009
32	Ti	PER1	x				10	5	2	A	L	Perchtoldsdorfer Heide, 'Kleine Heide', 1.0 km WNW Perchtoldsdorf	dry grassland on carbonate	16.2519	48.1222	330	Andreas Tribsch	21.04.2007
33	Tl	KAR1	x				5	5	5	SV	UC	Preddvor, path from St. Jakob - Western slope of Javorov Vrh - Hudičev Borst	open grassland in an beech forest, on limestone	14.4417	46.3333	1000 - 1400	Andreas Tribsch	10.06.2006
34	Tc	STK1	x				5	5	5	A	S	St. Koloman, along the road to the Trattberg, near Kerzenbrunn	swampy, bright fen wood	13.2325	47.6367	960	Andreas Tribsch	19.05.2007

Table 27. Example of sample arrangement in a 48-well PCR plate.

	A	B	C	D	E	F	G	H
6	NUS1_04	NUS1_05	NUS1_06	NUS1_07	NUS1_08	WOE1_18_P	UNT3_07_R	B
5	HAY1_06	HAY1_07	HAY1_08	HAY1_09	HAY1_10	NUS1_01	NUS1_02	NUS1_03
4	MAR1_12	MAR1_19	MAR1_20	HAY1_01	HAY1_02	HAY1_03	HAY1_04	HAY1_05
3	PAL1_02	MAR1_01	MAR1_02	MAR1_03	MAR1_04	MAR1_05	MAR1_10	MAR1_11
2	STI1_04	STI1_05	STI1_06	STI1_07	STI1_08	STI1_09	STI1_10	PAL1_01
1	UNT3_06	UNT3_07	UNT3_08	UNT3_09	UNT3_10	STI1_01	STI1_02	STI1_03

Table 28. Adaptor names and sequences.

Adaptor name	Supplier	DNA sequence
EcoRI-1	Eurofins MWG Operon (Ebersberg, Germany)	5'-CTCGTAGACTGCGTACC-3'
EcoRI-2	Eurofins MWG Operon (Ebersberg, Germany)	5'-AATTGGTACGCAGTCTAC-3'
MseI-1	Eurofins MWG Operon (Ebersberg, Germany)	5'-GACGATGAGTCCTGAG-3'
MseI-2	Eurofins MWG Operon (Ebersberg, Germany)	5'-TACTCAGGACTCAT-3'

Table 29. Reaction mix for the Restriction/Ligation.

Reagent	Supplier	Volume [μ l]
double distilled H ₂ O		2.87
T4 DNA Ligase buffer (10x)	Promega	1.10
NaCl (0.5M)	Sigma Aldrich (St. Louis, USA)	1.10
Bovine Serum Albumine (1 mg/ ml)	Thermo Fisher Scientific	0.55
EcoRI adaptor pair (5 pmol/ μ l)	Eurofins MWG Operon	1.00
MseI adaptor pair (50 pmol/ μ l)	Eurofins MWG Operon	1.00
EcoRI (80 U/ μ l)	Promega	0.06
MseI (50 U/ μ l)	New England Biolabs (Ipswich, USA)	0.02
T4 DNA Ligase (3 U/ μ l)	Promega	0.30
Total		8.00

Table 30. Reaction mix for the preselective amplification.

Reagent	Supplier	Volume [μ l]
double distilled H ₂ O		5.10
GoTaq [®] reaction buffer, green (5x)	Promega	2.00
dNTP mix (10mM of each nucleotide)	Applied Biosystems	0.22
EcoRI+A primer (10 pmol/ μ l)	Eurofins MWG Operon	0.29
MseI+C primer (10 pmol/ μ l)	Eurofins MWG Operon	0.29
GoTaq [®] DNA Polymerase (5 U/ μ l)	Promega	0.10
Total		8.00

Table 31. Primer names and sequences used for preselective amplification.

Primer name (supplier: Eurofins MWG Operon)	DNA sequence
EcoRI+A	5'- GACTGCGTACCAATTCA-3'
MseI+C	5'- GATGAGTCCTGAGTAAC-3'

Table 32. PCR program for the preseleective amplification.

PCR step	Temperature [°C]	Duration [min]
Initial hold	72	2
30 cycles (ramp time: 90%)	94	0.5
	56	0.5
	72	1
Final holds	72	10
	4	∞

Table 33. Tested primer pairs for the selective amplification and the prior used preseleective primer pairs.

Primer number	Primer name (supplier: Eurofins MWG Operon)	DNA sequence	Presel. primer
FAM1	EcoRI+ACT	5'-GACTGCGTACCAATTCACT-3'	EcoRI+A
	MseI+CAG	5'-GATGAGTCCTGAGTAACAG-3'	MseI+C
FAM2	EcoRI+ACA	5'-GACTGCGTACCAATTCACA-3'	EcoRI+A
	MseI+CAC	5'-GATGAGTCCTGAGTAACAC-3'	MseI+C
FAM3	EcoRI+AGA	5'-GACTGCGTACCAATTCAGA-3'	EcoRI+A
	MseI+CAC	5'-GATGAGTCCTGAGTAACAC-3'	MseI+C
FAM4	EcoRI+AGA	5'-GACTGCGTACCAATTCAGA-3'	EcoRI+A
	MseI+CATT	5'-GATGAGTCCTGAGTAACATT-3'	MseI+CA
FAM5	EcoRI+ACA	5'-GACTGCGTACCAATTCACA-3'	EcoRI+A
	MseI+CAGC	5'-GATGAGTCCTGAGTAACAGC-3'	MseI+CA
FAM6	EcoRI+ACA	5'-GACTGCGTACCAATTCACA-3'	EcoRI+A
	MseI+CTCG	5'-GATGAGTCCTGAGTAACTCG-3'	MseI+CT
NED1	EcoRI+AGC	5'-GACTGCGTACCAATTCAGC-3'	EcoRI+A
	MseI+CAG	5'-GATGAGTCCTGAGTAACAG-3'	MseI+C
NED2	EcoRI+ACA	5'-GACTGCGTACCAATTCACA-3'	EcoRI+A
	MseI+CTA	5'-GATGAGTCCTGAGTAACTA-3'	MseI+C
NED3	EcoRI+ACC	5'-GACTGCGTACCAATTCACC-3'	EcoRI+A
	MseI+CAG	5'-GATGAGTCCTGAGTAACAG-3'	MseI+C
NED4	EcoRI+ACA	5'-GACTGCGTACCAATTCACA-3'	EcoRI+A
	MseI+CAGG	5'-GATGAGTCCTGAGTAACAGG-3'	MseI+CA
NED5	EcoRI+ACC	5'-GACTGCGTACCAATTCACC-3'	EcoRI+A
	MseI+CAGA	5'-GATGAGTCCTGAGTAACAGA-3'	MseI+CA
NED6	EcoRI+AGC	5'-GACTGCGTACCAATTCAGC-3'	EcoRI+A
	MseI+CTGA	5'-GATGAGTCCTGAGTAACTGA-3'	MseI+CT
VIC1	EcoRI+ACG	5'-GACTGCGTACCAATTCACG-3'	EcoRI+A
	MseI+CAT	5'-GATGAGTCCTGAGTAACAT-3'	MseI+C
VIC2	EcoRI+AGG	5'-GACTGCGTACCAATTCAGG-3'	EcoRI+A
	MseI+CAA	5'-GATGAGTCCTGAGTAACAA-3'	MseI+C
VIC3	EcoRI+AGG	5'-GACTGCGTACCAATTCAGG-3'	EcoRI+A
	MseI+CAT	5'-GATGAGTCCTGAGTAACAT-3'	MseI+C
VIC4	EcoRI+AGA	5'-GACTGCGTACCAATTCAGA-3'	EcoRI+A
	MseI+CTCA	5'-GATGAGTCCTGAGTAACTCA-3'	MseI+CT
VIC5	EcoRI+AAG	5'-GACTGCGTACCAATTC AAG-3'	EcoRI+A
	MseI+CTGA	5'-GATGAGTCCTGAGTAACTGA-3'	MseI+CT
VIC6	EcoRI+AGG	5'-GACTGCGTACCAATTCAGG-3'	EcoRI+A
	MseI+CAGT	5'-GATGAGTCCTGAGTAACAGT-3'	MseI+CA

Table 34. Selected primer pairs for the selective amplification.

Fluorescent label	Primer number	Primer name	DNA sequence
6-FAM	FAM3	EcoRI+AGA	5'-GACTGCGTACCAATTCAGA-3'
		MseI+CAC	5'-GATGAGTCCTGAGTAACAC-3'
NED	NED1	EcoRI+AGC	5'-GACTGCGTACCAATTCAGC-3'
		MseI+CAG	5'-GATGAGTCCTGAGTAACAG-3'
VIC	VIC1	EcoRI+ACG	5'-GACTGCGTACCAATTCACG-3'
		MseI+CAT	5'-GATGAGTCCTGAGTAACAT-3'

Table 35. Reaction mix for the selective amplification.

Reagent	Supplier	Volume [μ l]
double distilled H ₂ O		5.36
GoTaq [®] reaction buffer, green (5x)	Promega	2.00
dNTP mix (10mM of each nucleotide)	Applied Biosystems	0.22
EcoRI+ANN primer (10 pmol/ μ l)	Eurofins MWG Operon	0.05
MseI+CNN primer (10 pmol/ μ l)	Eurofins MWG Operon	0.27
GoTaq [®] DNA Polymerase (5 U/ μ l)	Promega	0.10

Table 36. PCR program for the selective amplification.

PCR step	Temperature [$^{\circ}$ C]	Duration [min]
initial hold	95	10
13 cycles (ramp time: 90%)	94	0.5
	65	1
	72	1
23 cycles (ramp time: 90%)	94	0.5
	56	1
	72	1
	72	1
final holds	72	10
	4	∞

Table 37. ET550-R-ROX-MegaBace[™]-Standard dilution.

Reagents	Supplier	Volume [μ l]
ET550-R-ROX-MegaBACE [™] -Standard	GE Healthcare Bio-Sciences	0.1
double distilled H ₂ O		12.9
total		13.0

Table 38. MegaBACE settings.

Parameter	Setting
sample injection voltage	4 kV
injection time	25 sec
running voltage	10 kV
running time	70 min
chemistry	GT Dye Set 2 (ET-ROX; FAM; NED; HEX)

Table 39. Color separation matrix used in DAX.

1.0000	0.0654	0.0978	0.0498
0.1118	1.0000	0.0019	0.0107
0.3993	0.0211	1.0000	0.5795
0.0075	0.0341	0.3820	1.000

Table 40. Settings for the automatic peak search in DAX.

Fluorescent color	Parameter	Setting
FAM	minimum area	0.004
	noise level	3.8
NED	minimum area	0.400
	noise level	10.0
VIC	minimum area	0.040
	noise level	3.8